STUDIES OF THE STRUCTURE AND WATER ABSORPTION PROPERTIES OF CELLULOSIC MATERIALS BY INFRA-RED SPECTROSCOPY.

A Thesis Presented to

The University of Leeds

By PAUL ROBERT GREEN.

For

The Degree of Doctor of Philosophy

Textile Physics Laboratory,

Department of Textile Industries,

The University of Leeds.

December 1975.

SUMMARY

The work presented in this thesis applies the high resolution derivative technique developed in this laboratory to a study of the structure and water absorption of viscose, dicel and tricel films, prepared in a pure form by techniques developed during the course of this work. These three materials provide a means of following how progressive acetylation (from 0% in viscose to 88.3% in dicel to 98.3% in tricel) influences structure and water absorption.

A controlled Temperature and Relative Humidity cell was developed to standardize experimental conditions and to enable reproducible spectra to be recorded, especially in spectral regions where temperature sensitive hydrogen bonding occurred. The use of the cell enabled structural and/or water absorption properties of these materials to be observed by changing the temperature or Relative Humidity at which spectra were recorded; or by observing annealed sample spectra at a standard temperature.

Experiments were undertaken to determine the existence of chain folding in viscose, dicel and tricel films.The results of these experiments support the existence of chain folding in viscose and the nature of the fold is discussed in detail.

A.T.R. absorption spectra of the film surfaces were recorded in an attempt to study water absorption at surfaces and these spectra were correlated where possible with stereoscan tracings of the surfaces of the films.

Evidence is presented from the results of the work in this thesis for the involvement of CH groups in hydrogen bonding.

DEDICATION

I would like to dedicate this thesis to my mother, the late Mrs. Laura Green.

CONTENTS

Page

CHAPTER I.
INTRODUCTION

CHAPTER 2
MATERIALS, METHODS AND EARLY EXPERIMENTS

CHAPTER 3
THE EFFECTS OF HEATING AND ANNEALING & COOLING ON THE SPECTRA OF VISCOSE (CELLULOSE II), CELLULOSE I, DICEL AND TRICEL.

Page

CHAPTER I

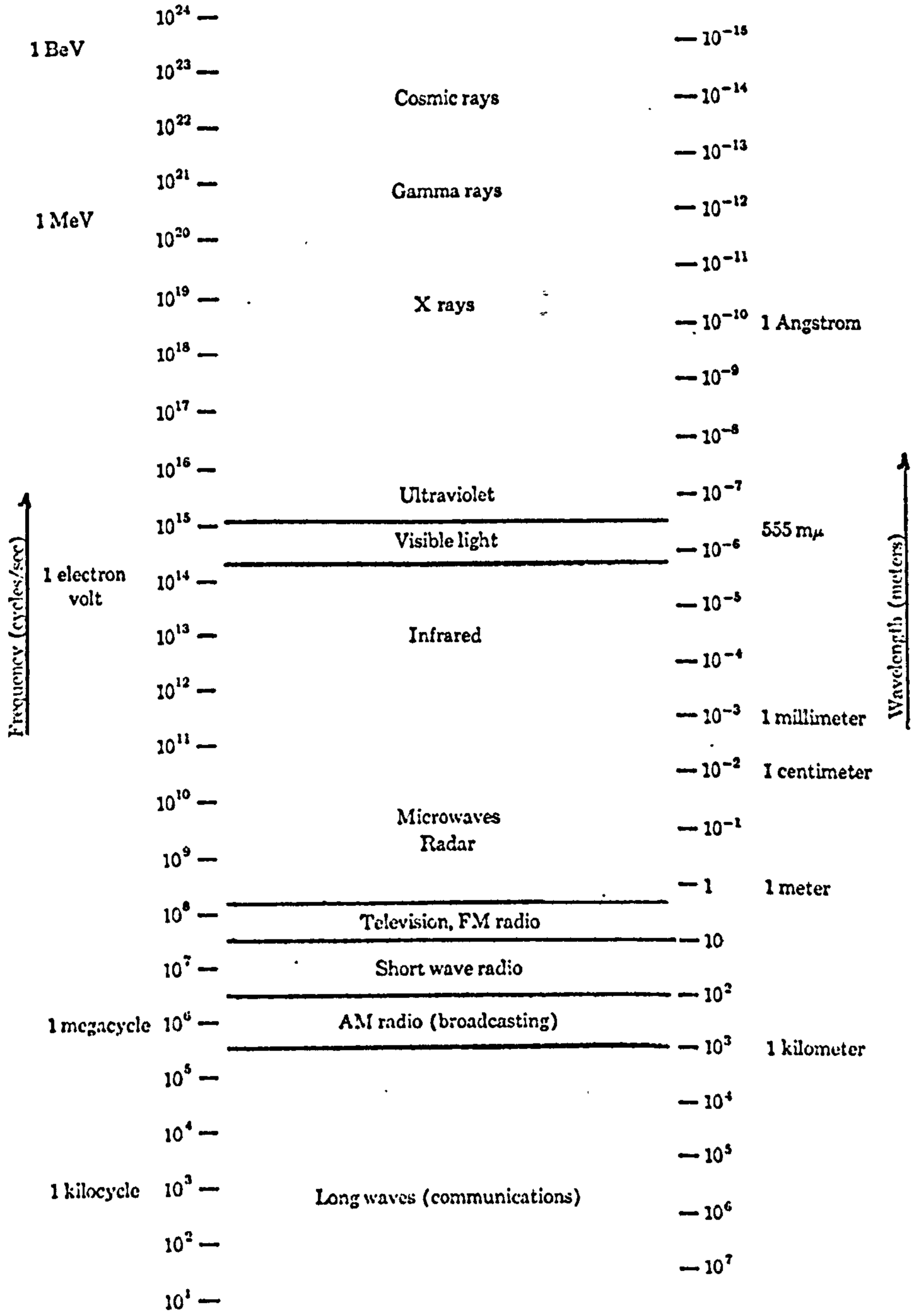
1 BeV
1 MeV
1 electron volt
1 megacycle
1 kilocycle
Frequency (cycles/sec)
Wavelength (meters)
Cosmic rays
Gamma rays
X rays
Ultraviolet
Visible light
Infrared
Microwaves
Radar
Television, FM radio
Short wave radio
AM radio (broadcasting)
Long waves (communications)
1 Angstrom
555 mμ
1 millimeter
1 centimeter
1 meter
1 kilometer

FIG. 1

CHAPTER 1

INTRODUCTION

1.1 Development of the Theory of Infra-red Absorption.

In 1800 Sir William Herschel detected infra-red radiation as an invisible 'heat' radiation beyond the visible red region of a spectrum produced from prismatically dispersed sunlight. It was later shown that this radiation did not differ fundamentally from visible light but formed part of the electromagnetic spectrum (Fig.1) between the visible and microwave regions and had a wavelength in the range 1 to 200 μm. (1 μm. or $1\mu = 10^{-6}$m.)

In general, absorption spectra may be determined in the ultraviolet, visible and infra-red regions, but a limited number of observations have been made in the microwave region. Spectra are obtained when a sample is exposed to radiation over a limited wavelength range and the amount of radiation absorbed is measured as a function of wavelength.

A significant development in theoretical physics arose in 1900 when Planck's quantum theory of energy distribution was introduced, in which he postulated that a vibrating body could only take up energy in discrete units, called quanta.

This is expressed mathematically as:-

$$E = h\nu \qquad \text{(Eq.1)},$$

where E = value of a quantum,

h = Planck's constant,

ν = frequency of radiation absorbed.

The quantum theory thus began as an atomic theory of energy, which assumed that atoms were vibrating bodies.

Einstein developed Planck's theory and showed that it held more

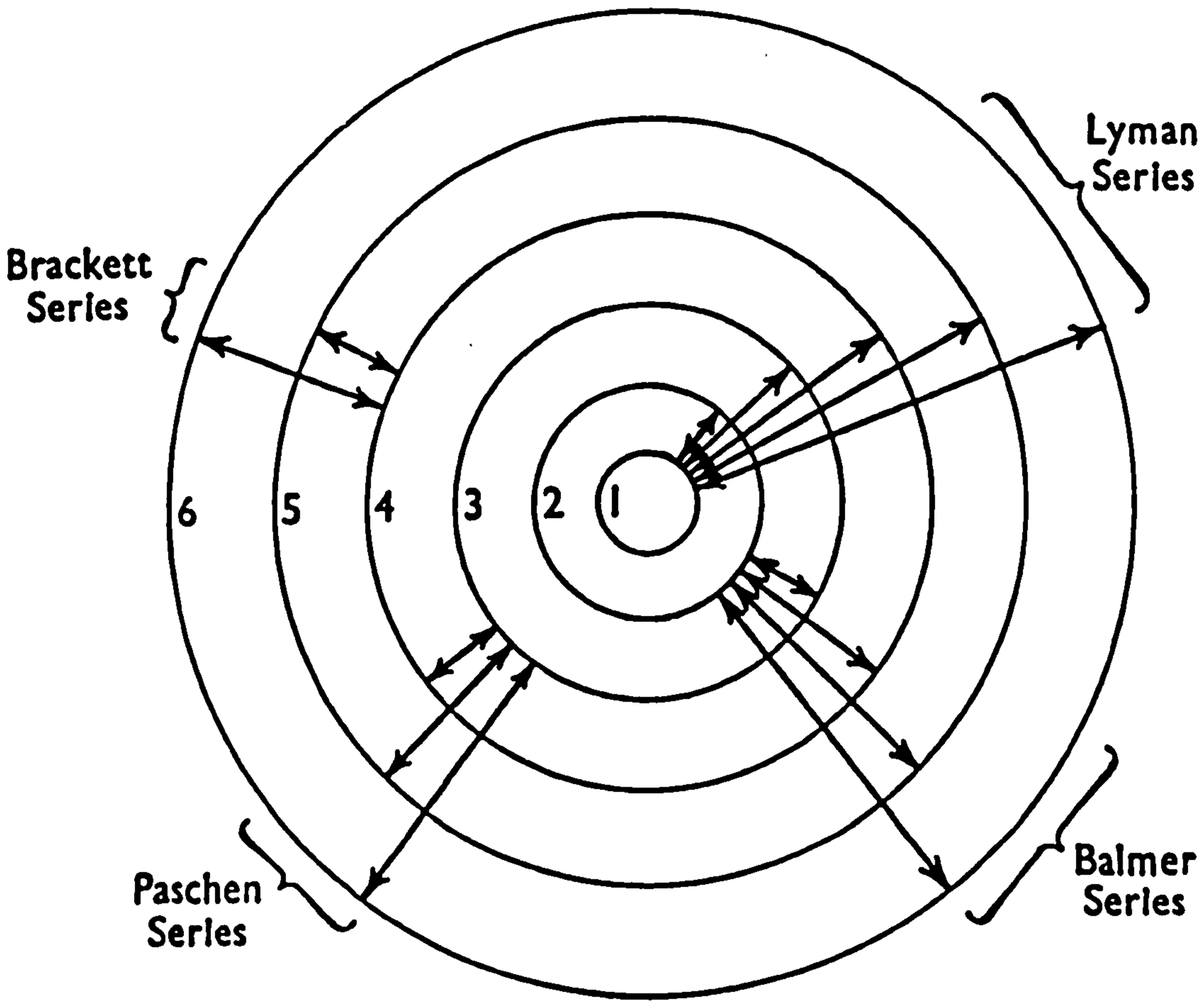

FIG. 2 Illustration of the energy changes which an electron can undergo in moving from one energy level to another in an atom. The diagram is not to scale, for the radii of the various stationary states shown are, in fact, proportional to the squares of the principal quantum numbers allotted to them.

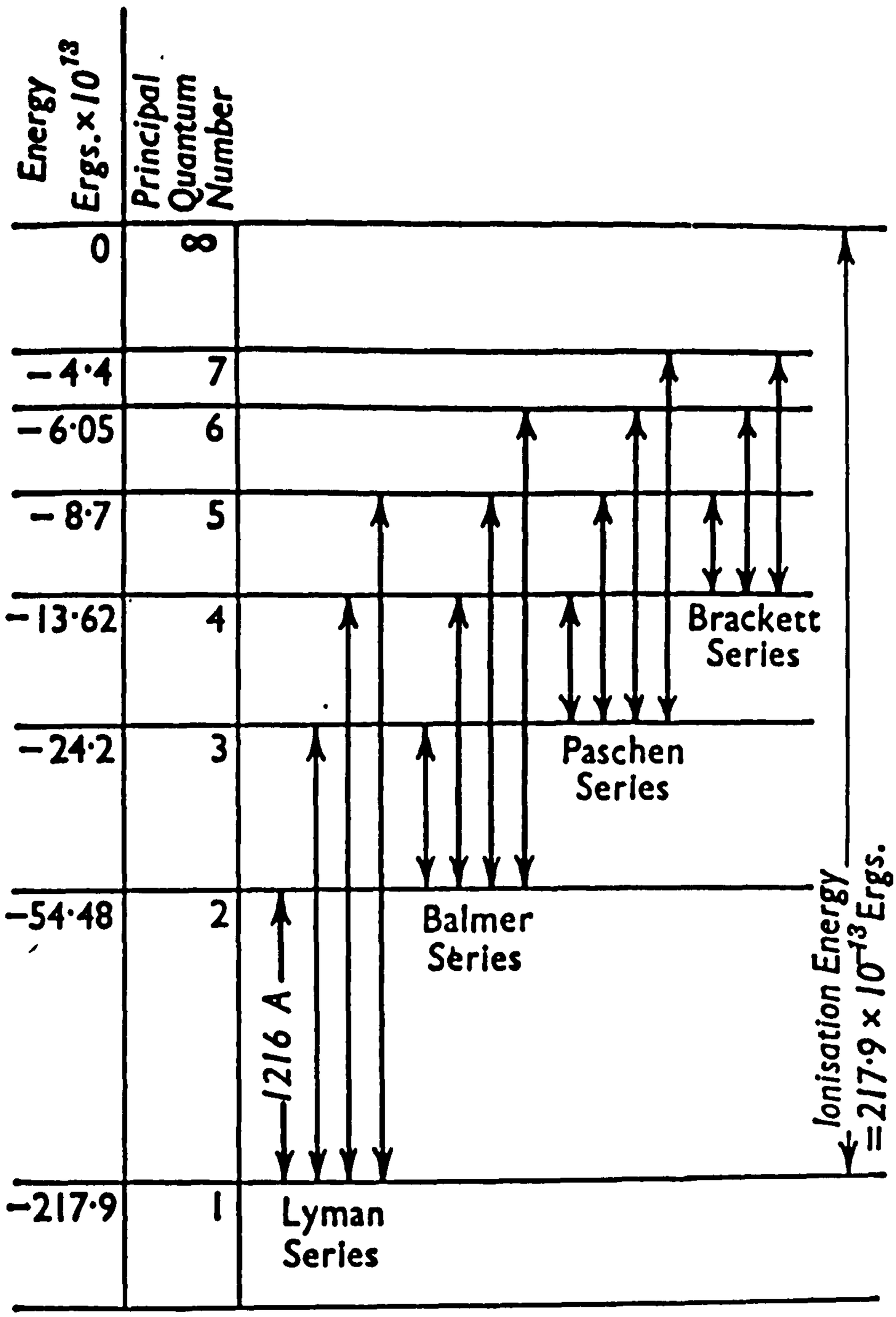

FIG. 3 The energy levels in the hydrogen atom.

generally for any body which emitted or absorbed radiation. For a body from an initial energy E_1 to a final energy E_2 it was shown that

$$E_1 - E_2 = nh\nu = \frac{nhc}{\lambda} \qquad \text{(Eq.2)},$$

where n is an integer.

Several attempts were made to apply Planck's theory to the large number of observed atomic spectra, but the first successful application was made by N. Bjerrum in 1912, in the field of molecular spectroscopy. It was possible to show that infra-red absorption by molecules arose from the uptake of rotational and vibrational energy in precise quanta.

However, in 1914 N. Bohr was able to interpret the atomic spectral series of hydrogen in terms of the Planck - Einstein equation (Eq.2). It was shown that extranuclear atomic electrons could only rotate in such stationary states as allowed no radiation to be emitted. Absorption or emission of radiation was described in terms of absorption or emission of a quantum of energy, with a concomitant transition of the electron from one energy state to another. The magnitude of the quantum absorbed or emitted, and hence the frequency of the radiation absorbed or emitted, was thus shown to correspond exactly to the energy difference between the two stationary states

Thus $\underline{E_u - E_\ell = h\nu}$ = energy of quantum absorbed or emitted (Eq.3)

where E_u = energy of upper stationary state

E_ℓ = energy of lower stationary state.

Bohr was thus able to account for the sharp spectral series of hydrogen (Fig. 2 & 3), but could not account for all the spectral lines observed, particularly in heavier atoms.

Another significant development in atomic theory was made in 1924

by De Broglie, who emphasised the wave-particle duality of matter. He stated that a moving electron had a definite wavelength which was expressed as :-

$$\lambda = \frac{h}{mc} \qquad \text{(Eq.4)}$$

where m = mass of electron,

h = Planck's constant,

c = velocity of electron

If p = momentum of electron = mc,

then :- $p\lambda = h$ (Eq.5),

so that the relationship between the particle-like property of an electron (i.e. its momentum) and its wave-like aspect (i.e. its wavelength) was established.

The work of De Broglie, Schrödinger and Dirac between 1925 and 1927 laid the basis for modern physics and led to the postulation of a mathematical theory based on the concept of a wave function and to its application to the wave pattern of an electron. The theory, now known as the theory of quantum mechanics is expressed mathematically as the Schrödinger wave equation and is given here for 3 dimensions as :-

$$\frac{d^2\psi}{dx^2} + \frac{d^2\psi}{dy^2} + \frac{d^2\psi}{dz^2} + \frac{8\pi^2 m}{h^2}(w-v) = 0 \qquad \text{(Eq.6)}$$

$$\text{or} \qquad \nabla^2\psi + \frac{8\pi^2 m}{h^2}(w-v) = 0 \qquad \text{(Eq.7)}$$

where $$\nabla^2 = \frac{d^2}{dx^2} + \frac{d^2}{dy^2} + \frac{d^2}{dz^2} \qquad \text{(Eq.8)},$$

ψ is the wave function,

w = total energy of system,

v = potential energy of system,

m = mass of electron,

h = Planck's constant,

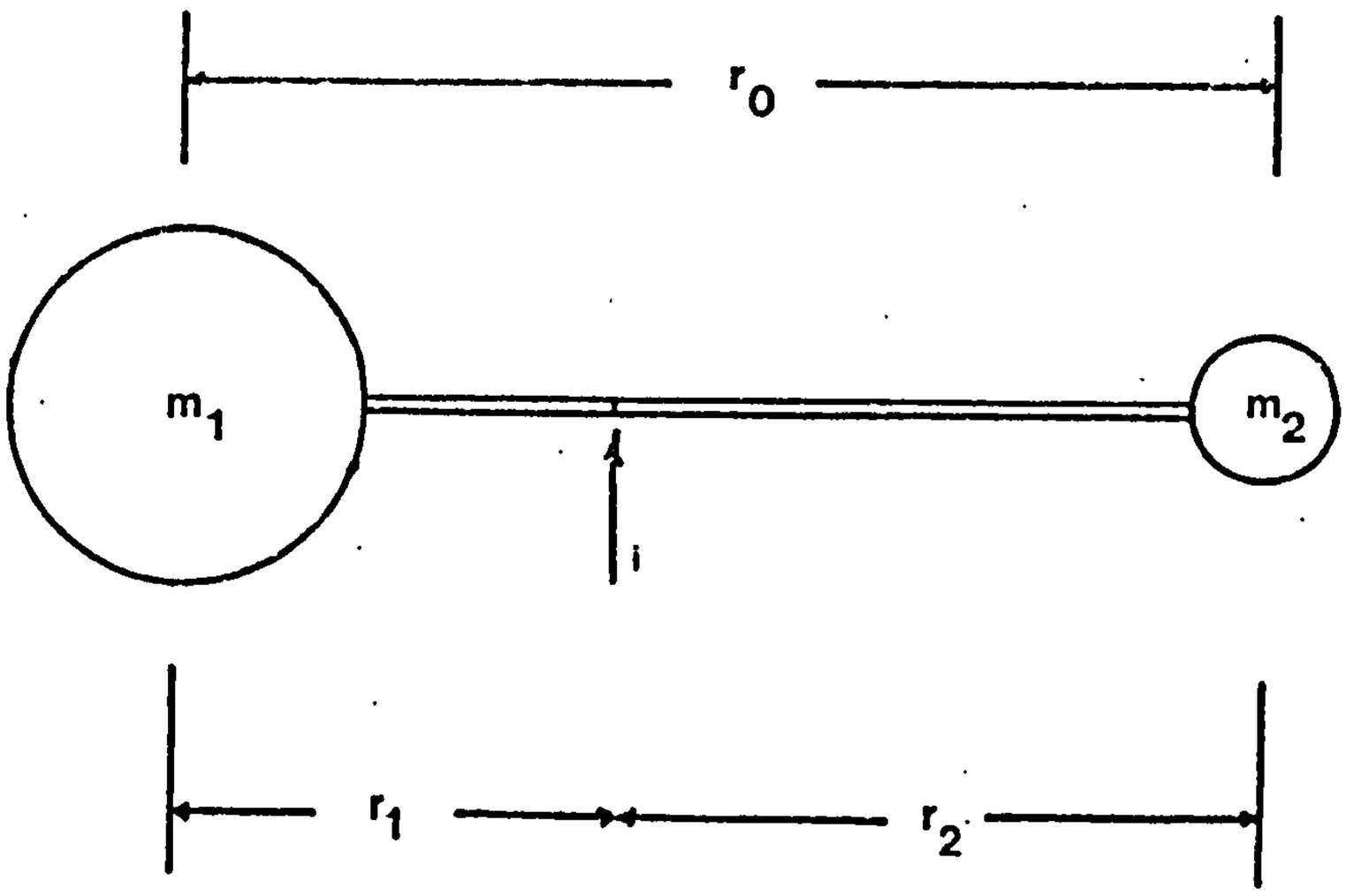

FIG. 4.

THE RIGID DIATOMIC MOLECULE

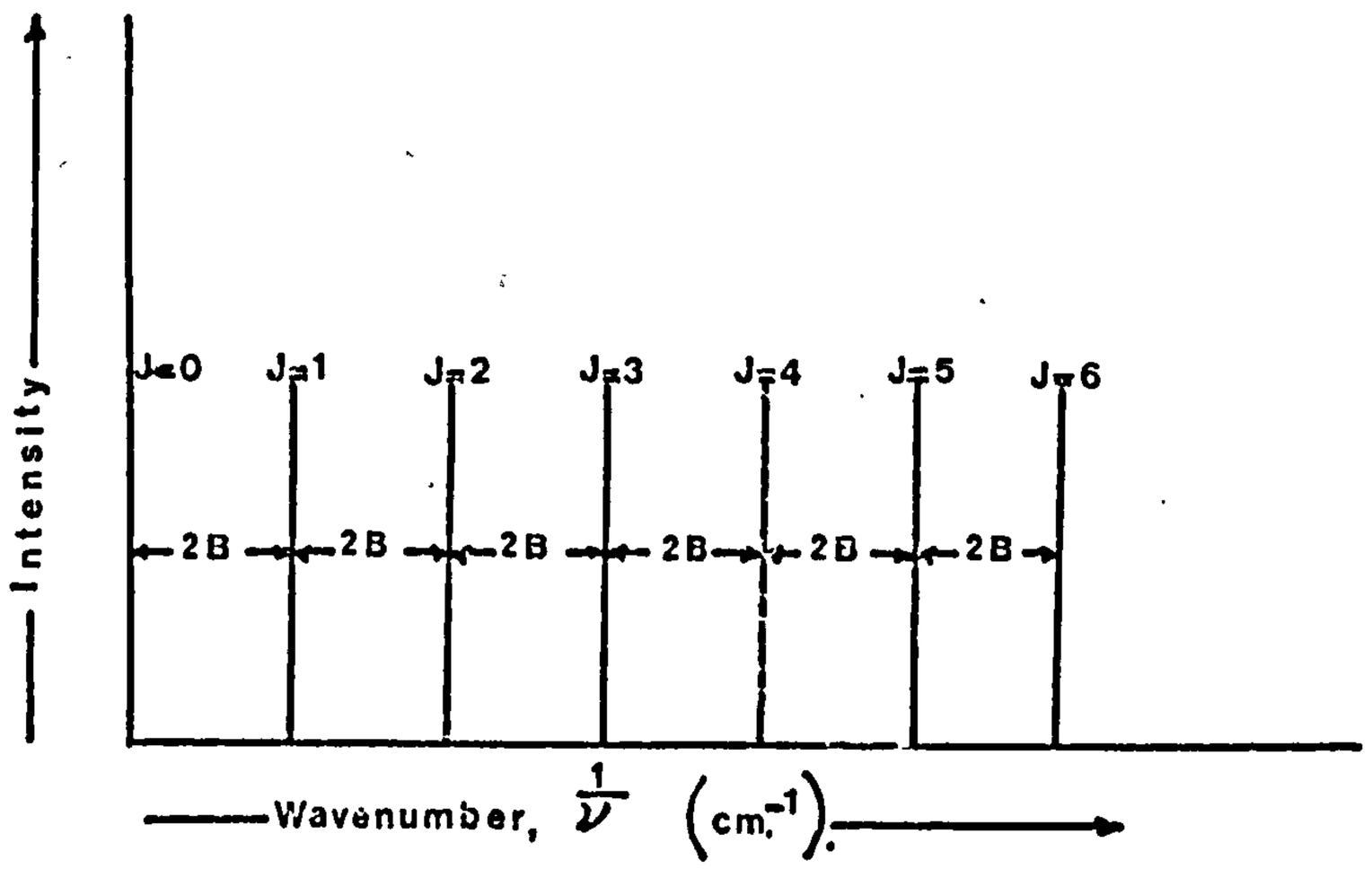

FIG. 5.

and x, y and z are the spatial co-ordinates of the system. The mathematical solution of the Schrödinger equation showed that three quantum numbers n, ℓ and m were required to characterise an electron, where n is the principal quantum number and corresponds to the principal orbit i.e. group of orbitals - within a primary shell; ℓ, the subsidiary quantum number, corresponds to the orbital, i.e. 's', 'p', 'd' or 'f', to which the electron belongs and m is the magnetic quantum number which arises from several orbitals which have the same energy. These orbitals of equal energy are depicted in several planes: for example, three planes in the case of p orbitals (p_x, p_y and p_z), according to the solution.

A further quantum number, the spin quantum number s, is required to exactly identify each electron, from Pauli's exclusion principal. This has a value s = +1 or s = -1 depending on the spin orientation. No two electrons in the same orbital have the same spin.

A systematic substitution into and solution of the Schrödinger wave equation gives a complete set of quantum numbers which are unique for every extranuclear electron and enables the electronic structure of all the elements in the periodic table to be elucidated.

The application of quantum mechanics to molecular spectra and in particular to infra-red spectra has also led to the prediction of the quantisation of energy, and this substantiates the earlier postulates of Bjerrum. The way in which quantum mechanics affects infra-red spectroscopy is considered in the following theory of rotational and vibrational spectra.

If we consider a rigid diatomic molecule (Fig.4) with a moment of inertia I, as given by:-

$$I = m_1 r_1^2 + m_2 r_2^2$$

On taking moments about i,

$$m_1 r_1 = m_2 r_2$$

and $$r_1 + r_2 = r_o$$

$$I = \frac{m_1 m_2}{m_1 + m_2} \quad r_e^2 = \mu r_e^2 \qquad \text{(Eq.9)},$$

where $$\mu = \frac{m_1 m_2}{m_1 + m_2} \qquad \text{(Eq.10) and}$$

is known as the reduced mass.

Applying the Schrödinger wave equation to rotational energy levels, it may be shown that the energy E_J of the rotational energy levels allowed for a rigid diatomic molecule is given by:-

$$E_J = h\nu = \frac{h^2}{8\pi^2 I} \; J(J+1) \text{ ergs.} \qquad \text{(Eq.11)}$$

where J, the rotational quantum number may only have discrete values, i.e. 0, 1, 2.....etc. When the rotational absorption spectrum of a particular molecular species is considered, the difference in energy between two rotational energy levels corresponds to the absorption of a quantum of energy of magnitude $h\nu_1$. The return of the molecules to the ground state on dispersion of their gained energy enables a continuous absorption of identical quanta to occur, which results in a spectral line at a frequency ν_1

i.e. at a wavelength $\lambda = \frac{c}{\nu_1}$

However, spectra are often discussed in terms of wavenumber $\bar{\nu}$,where $\bar{\nu} = \frac{1}{\lambda}$, hence equation 11 is modified, i.e. the energy ε_J of the rotational levels allowed in a rigid diatomic molecule is given in spectroscopic units ($cm.^{-1}$) by

$$\varepsilon_J = \bar{\nu} = \frac{E_J}{hc} = \frac{h}{8\pi^2 Ic} \; J(J+1) \; cm.^{-1}. \qquad \text{(Eq.12)}$$

$$= BJ(J+1) \; cm.^{-1} \qquad \text{(Eq.13)}$$

where $B = \frac{h}{8\pi^2 Ic}$ and is known as the rotational constant.

Substitution of increasing values of J in equation 13 results in an absorption spectrum consisting of lines at 2B, 4B, 6B $cm.^{-1}$ etc. when the rotational energy of molecules in the same ground state is increased.

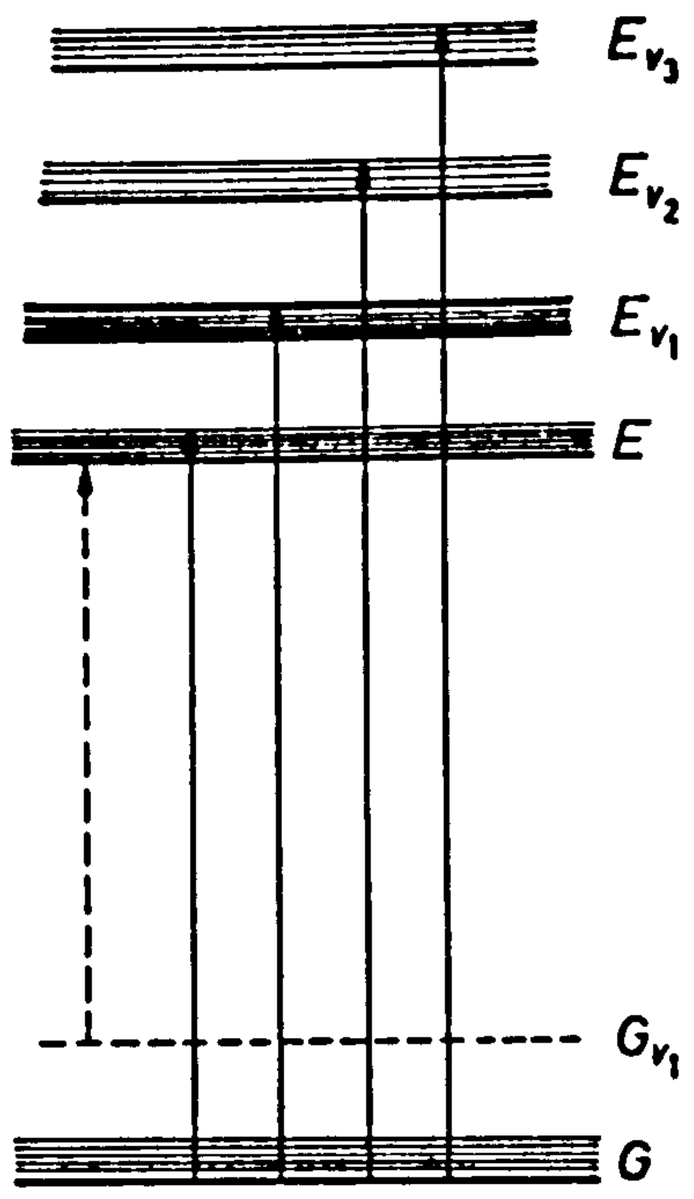

Figure 6 Energy levels for a polyatomic molecule and the origin of absorption lines. G, ground electronic state; E, excited electronic state; V_1, V_2, V_3, different vibrational states. The closely spaced lines represent rotational levels

Fig. 7

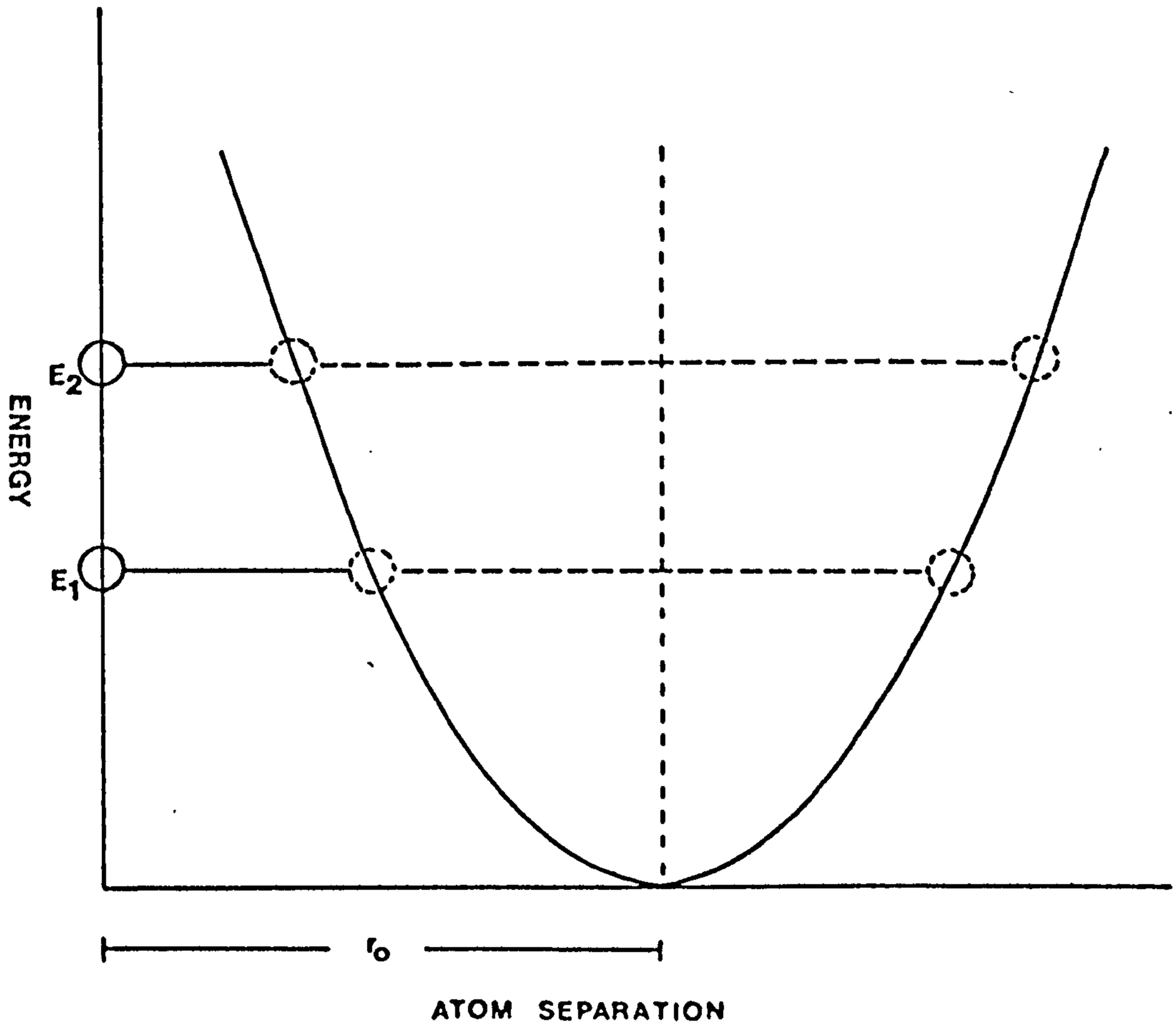

However, quantum mechanics predicts selection rules which only allow $J = \pm 1$ and requires the molecule to have a permanent dipole. Hence for a simple diatomic molecule, spectral lines are found at constant spacings of 2B $cm.^{-1}$ and are of equal intensities (Fig.5) for low values of J.

As J increases, however, the spectral line spacing decreases from 2B $cm.^{-1}$ due to bond vibration, which causes a change in bond length. Vibrational and rotational energy levels are thus inter-related (1,2) (Fig.6) and changes in one are reflected in the other. Vibrational levels thus form an integral part of infra-red spectra and these levels will be considered for a simple vibrating diatomic molecule.

For an 'idealised' diatomic molecule, the two atoms of the molecule may be considered as two spherical masses m_1 and m_2 connected by a Hookian spring and executing Simple Harmonic Motion. It can be shown for such a molecule that:-

$$f = -k\,(r-r_o) \qquad \text{(Eq.14)}$$

where f = the restoring force,

r = the atomic separation,

r_o = the atomic separation at equilibrium,

k = a constant.

Figure 7 shows that the energy distribution varies parabolically with atomic separation. The energy at any particular atomic separation r_p is given by:-

$$E = \tfrac{1}{2} k\,(r_p - r_o)^2 \qquad \text{(Eq.15)}$$

It has been shown, however, that the energy state does not affect the vibrational frequency of the idealised diatomic molecule. This vibrational frequency, denoted by the symbol ω, is given by:-

$$\omega = \frac{1}{2\pi}\sqrt{\frac{k}{\mu}} \quad \text{Hz.} \qquad \text{(Eq.16),}$$

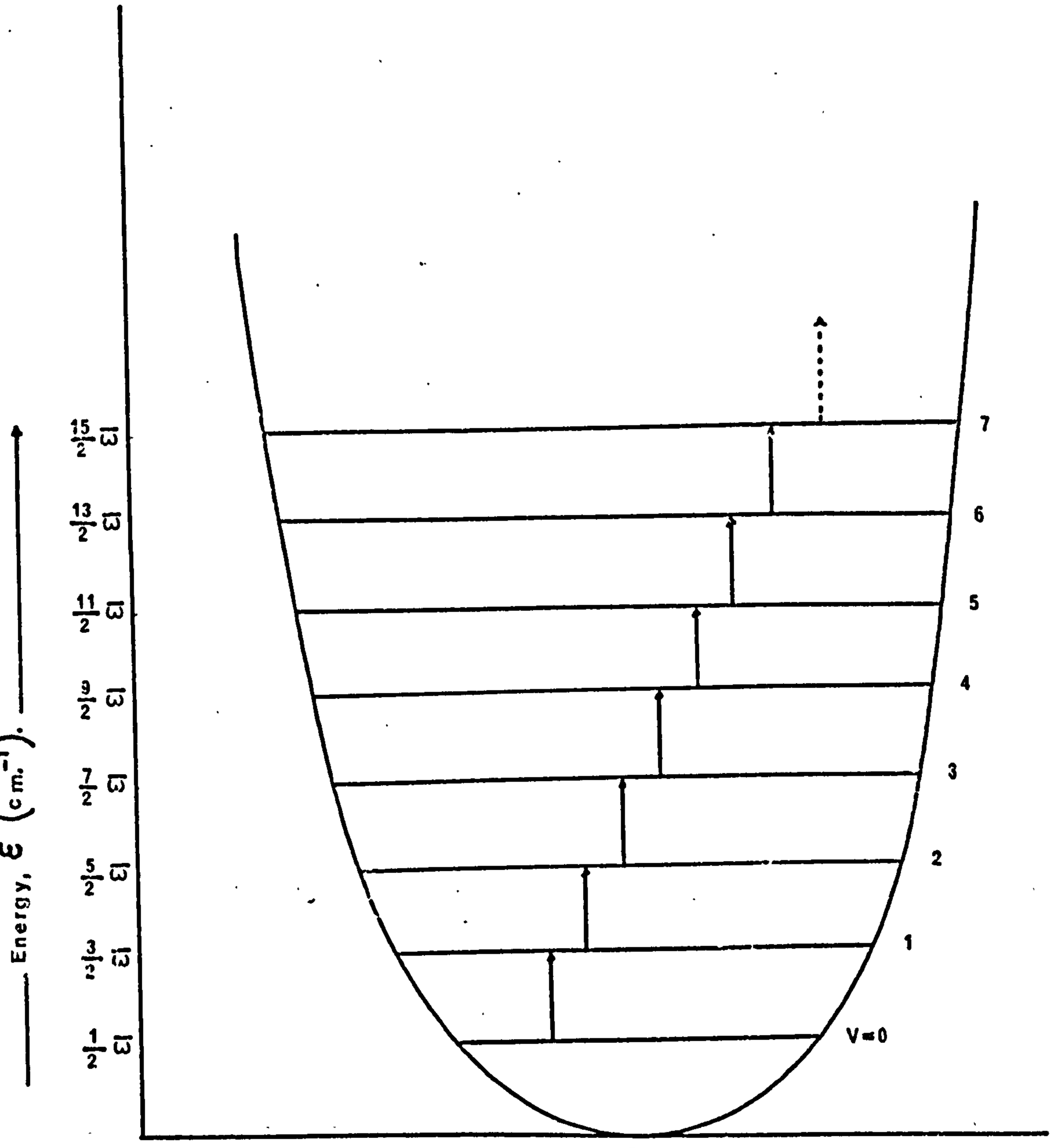

FIG. 8.

ALLOWED VIBRATIONAL ENERGY LEVELS OF THE SIMPLE HARMONIC OSCILLATOR (IDEALIZED DIATOMIC MOLECULE).

or for spectroscopic purposes as:-

$$\bar{\omega} = \frac{1}{2\pi c}\sqrt{\frac{k}{\mu}} \quad cm.^{-1} \qquad \text{(Eq.17)}$$

Wave mechanics shows that vibrational energies as all other energies, are quantised. The permitted vibrational energies (E_v) may be calculated from the Schrödinger wave equation. For the 'idealised' vibrating diatomic molecule, these are given by:-

$$E_v = (V + \tfrac{1}{2})\, h\omega \text{ ergs} \qquad \text{(Eq.18)}$$

where $V = 0, 1, 2.....etc.$

In spectroscopic units this becomes:-

$$\varepsilon_v = \frac{E_v}{hc} = (V + \tfrac{1}{2})\, \bar{\omega}\ cm.^{-1} \qquad \text{(Eq.19)}$$

Figure 8 illustrates some of the allowed vibrational levels of the Simple Harmonic Oscillator (idealised diatomic molecule). It is noted that the energy level may never have zero point energy, i.e. $V \neq 0$ so that $\varepsilon_o = \frac{1}{2}\bar{\omega}$. The minimum point energy is thus only dependent upon the vibrational frequency and strength of the chemical bond. Selection rules apply for vibrational modes such that $\Delta V = +1$ and the system must possess a changing dipole.

The Simple Harmonic Oscillator gives a good experimental approximation for diatomic gases at low temperatures, but at higher temperatures where the total energy of the system is large, the approximation becomes less accurate and anharmonic oscillations occur. At very high temperatures and energy levels, anharmonic oscillations predominate and finally molecular dissociation occurs.

When these concepts are extended to the infra-red spectra of polyatomic and polymeric systems, individual line spectra which correspond to specific bonds do not occur, since when one bond is in motion the rest of the molecule is involved. The resonant frequencies produced are thus characteristic of

the repeating polymer unit and are determined mainly by the masses of the individual atoms, their geometrical arrangement and bond strengths. Peak maxima for particular bonds of chemical groups such as C-C, C-O, C-H, O-H etc. do, however, occur within certain known frequency ranges (3,4,5). In addition, the effect of any coupling of groups, eg. in -COOH or $C\overset{H}{\underset{O}{=}}$, has been established. These facts enable tentative assignments of peaks in complex macromolecules to be undertaken. Such assignments are usually confirmed by reference to compounds of similar chemical composition and structure. Simple 'model compounds' are also often referred to in order to confirm assignments.

In the case of a molecule which has n atoms, there are n degrees of freedom, distributed as 3 translational, 3 rotational and (3n-6) vibrational modes. Those vibrational modes which possess a permanent dipole are 'Infra-red Active', that is, they absorb infra-red radiation at characteristic resonant frequencies producing characteristic peaks. However, those vibrational modes which do not possess a permanent dipole moment are not capable of absorbing infra-red radiation, although they are 'Raman Active'.

The total number of 'Infra-red Active' vibrational modes of a polymer molecule should thus determine the total number of peaks occurring in an absorption spectrum, but in an actual spectrum, further peaks occur due to:-

(i) Overtone Bands These are integral multiples of fundamental modes (i.e. transitions for which $\Delta V = \pm 2$; the so-called 'forbidden' transitions in which the selection rule $\Delta V = \pm 1$ is broken).

(ii) Combination Bands These arise from the sum or difference of two or more fundamental frequencies.

(iii) Bands due to Fermi Resonance These arise when an overtone of a vibration or a combination of two other vibrations occur near the fundamental of another vibration of the same symmetry class.

In addition to these factors, crystallinity, hydrogen bonding,

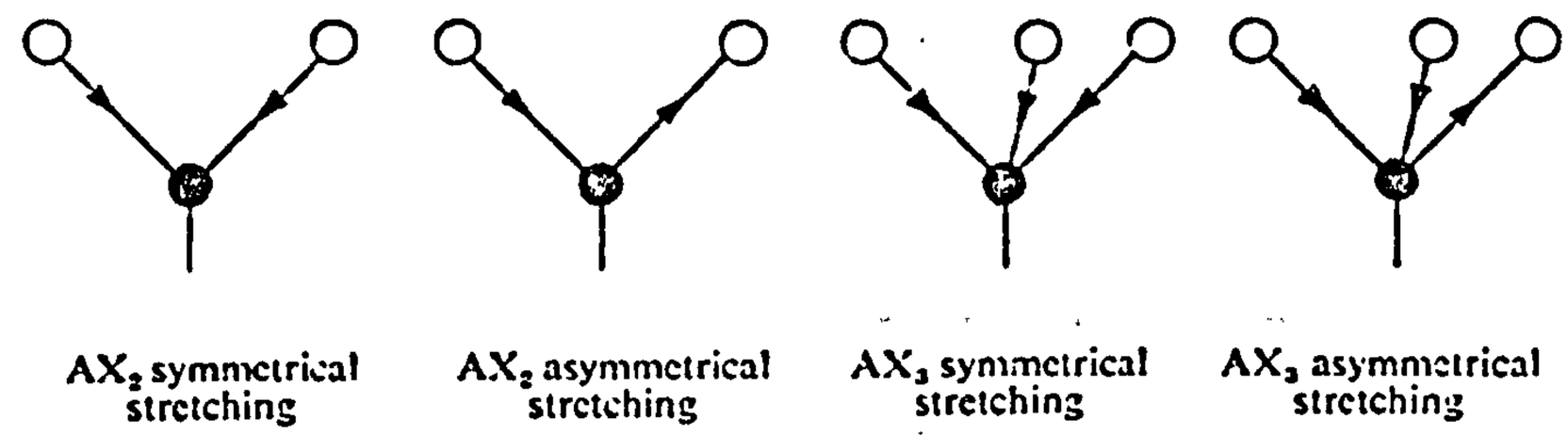

Figure 9 Deformation (bending) vibration modes

temperature, water content and physical state of a polymer may affect the total number of peaks which occur. These factors are discussed later in this chapter.

Vibrational modes are usually described and classified simply by the following terminology:- Vibrations occurring along valency bonds are known as stretching modes (ν), whilst disturbances perpendicular to bonds are known as bending modes (δ). In a triatomic system, in phase stretching results in symmetrical stretching absorptions and out of phase stretching results in asymmetrical stretching absorptions. Deformation vibrations occurring in a common plane are known as rocking motions, when in phase and scissoring motions, when out of phase. Motions perpendicular to their common plane are known as wagging and twisting modes when in and out of phase respectively. (Fig.9).

1.2 Symmetry, Group Theory and Their Application to Infra-red Spectra

At this point it is relevant to consider symmetry and group theory, which have been applied to polymers to predict the number and distribution of vibrational modes (6-10). In its simplest form, group theory has been applied to an isolated repeat unit of the polymer and assumes that the vibrations of this unit are characteristic of the whole molecule. In this case, the molecule is regarded as an infinite extension of the repeat unit in a stereo-regular pattern.

1.2.1 Symmetry Elements and Symmetry Operations

To apply symmetry considerations to a molecule, its component atomic nuclei must be regarded as points in a fixed co-ordinate system. If the system possesses one or more elements of symmetry, it is possible to transform it in such a way that the position of each atom appears unchanged.

Such a transformation is known as a symmetry operation. The following elements of symmetry must be considered for spectroscopic purposes:-

(i) A Plane of Symmetry

For a group or molecule to possess a plane of symmetry, reflection in that plane of all nuclei must produce a configuration identical to the original.

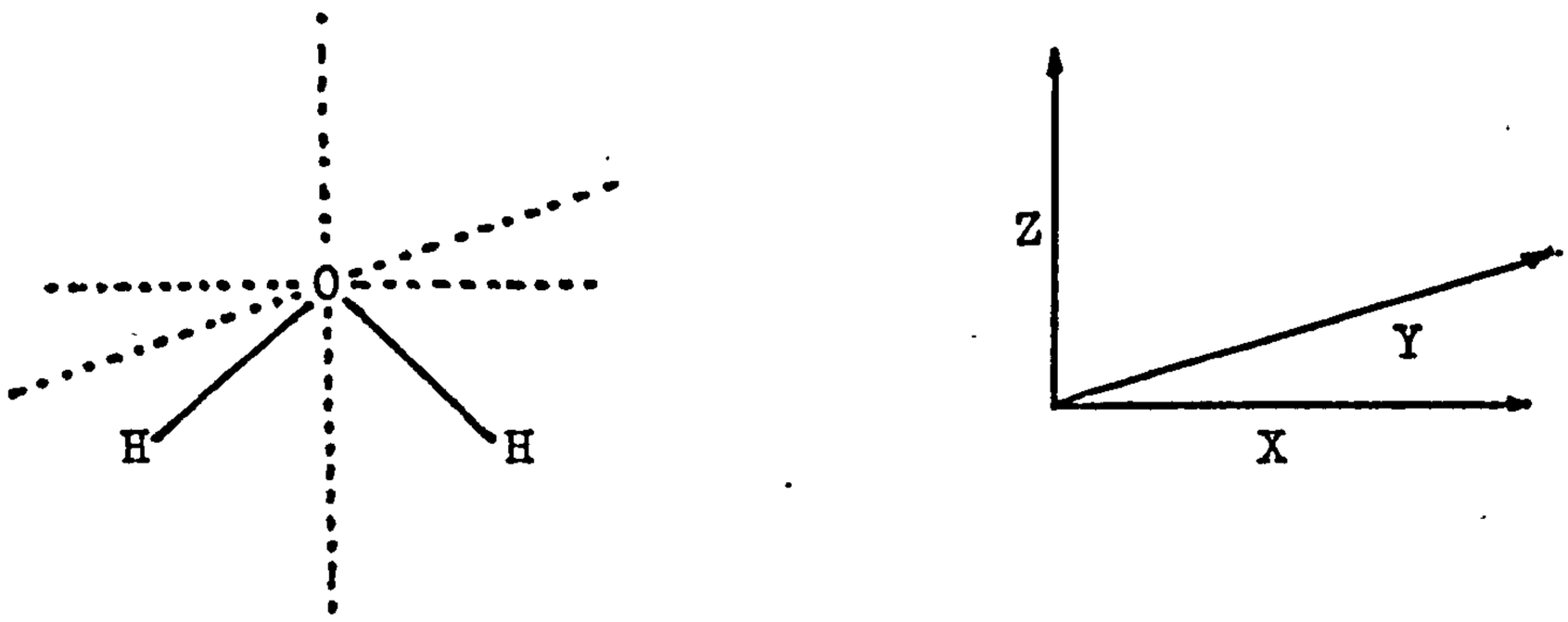

Fig.10. Mirror Planes (σ_{xz} σ_{xy}) of Water

Planes of symmetry are usually designated by σ , with subscripts h or v denoting horizontal and vertical planes respectively. The designation is, however, much more useful in terms of co-ordinate axes, x, y and z. Thus in the case of water molecules (Fig.10), there are two planes of symmetry, σ_{xz} and σ_{yz}.

(ii) A Centre of Symmetry

A molecule possesses a centre of symmetry, i, if a line drawn from each atom through this centre, intersects an identical atom on the other side of the centre in such a way that both atoms are equidistant from this centre. Thus trans dichloro-ethylene possesses a centre of symmetry i, whereas cis dichloro-ethylene does not (Fig.11).

Centre of Symmetry i

Trans Dichloro-ethylene Cis Dichloro-ethylene

FIG. 11

(iii) A p-fold Axis of Symmetry (p fold Rotation Axis, C_p)

The symmetry operation for C_p is a rotation of $\frac{360^o}{p}$ about an axis of the molecule, so that the original configuration is produced. Clearly p = 1 for all molecules, but in the case of water p = 2 since a rotation of $\frac{360^o}{2}$ produces the original configuration. The co-ordinate of the axis of rotation may also be specified in this symmetry element. Thus the water molecule in Fig.10 possesses a C_2 (z) symmetry element. Ammonia and methane are examples of molecules with C_3 symmetry elements.

(iv) A p-fold Rotation - Reflection Axis (S_p)

In a molecule with a p-fold rotation - reflection axis, the symmetry operation is a rotation by $\frac{360^o}{p}$ followed by reflection at a plane perpendicular to the original. Again, the co-ordinates of the axis may be specified, i.e. S_{p_x} S_{p_y} or S_{p_z}.

(v) The Identity, E

Every body possesses a trivial element E, in which the operation is to leave the molecule unchanged. For example, performing twice the symmetry

Table I Symmetry species for the point group D_{2h} and for the isomorphous line group of the polyethylene chain

Point group D_{2h}	E	$C_2(y)$	$C_2(x)$	$C_2(z)$	i	$\sigma(xz)$	$\sigma(yz)$	$\sigma(xy)$		
Line group	E	$C_2(y)$	$C_2(x)$	$C_2^1(z)$	i	$\sigma(xz)$	$\sigma_v(yz)$	$\sigma(xy)$	zero* modes	n†
A_g	+1	+1	+1	+1	+1	+1	+1	+1		3
A_u	+1	+1	+1	+1	−1	−1	−1	−1		1
B_{1g}	+1	−1	−1	+1	+1	−1	−1	+1	R_z	3
B_{1u}	+1	−1	−1	+1	−1	+1	+1	−1	T_z	2
B_{2g}	+1	+1	−1	−1	+1	+1	−1	−1		2
B_{2u}	+1	+1	−1	−1	−1	−1	+1	+1	T_y	3
B_{3g}	+1	−1	+1	−1	+1	−1	+1	−1		1
B_{3u}	+1	−1	+1	−1	−1	+1	−1	+1	T_x	3

* This column gives the species of the zero frequency modes.

† Total number of vibration modes for an isolated, extended, infinite polyethylene chain (including zero modes). Five are infra-red active.

operation of a rotation of $\frac{360^{o}}{p}$ where p = 2, about the z axis, for a molecule with a C_2 (z) symmetry element, would result in E.

$$\text{i.e. } E = C_2(z) \times C_2(z).$$

1.2.2 Point Groups

The maximum combination of symmetry elements for a molecule is known as a point group. Since the presence of certain symmetry elements necessitates the presence of other elements and the presence of other elements precludes others, the maximum number of point groups reduces to 36, each of which is designated by an appropriate point group symbol. For simple molecules, however, the symmetry elements actually form the point groups, all symmetry axes, planes and centres passing through one point. Thus water belongs to the point group designated C_2 v (i.e. C_2 (z)) and methyl chloride to the point group C_3 v (i.e. C_3 (z)).

1.2.3 Classification of Modes of Vibration

When a system is executing a single normal vibration, all the atoms move with the same frequency. If a symmetry operation is performed, then either the sign of all the displacements is changed or none of them. In the first case, the vibration is said to be antisymmetric to the symmetry operation, and in the second case, symmetric to the operation. Table 1 illustrates the symmetry species of the vibrational modes of the point group designated D_2h, containing the following symmetry elements:-

$$E,\ C_2^x, C_2^y, C_2^z, i, \sigma_{xy};\ \sigma_{xz},\ \sigma_{yz}.$$

The following symbols are assigned to the vibrational modes according to their behaviour to the operations which correspond to the various symmetry elements. The characters +1 or -1 indicate vibrations symmetric or

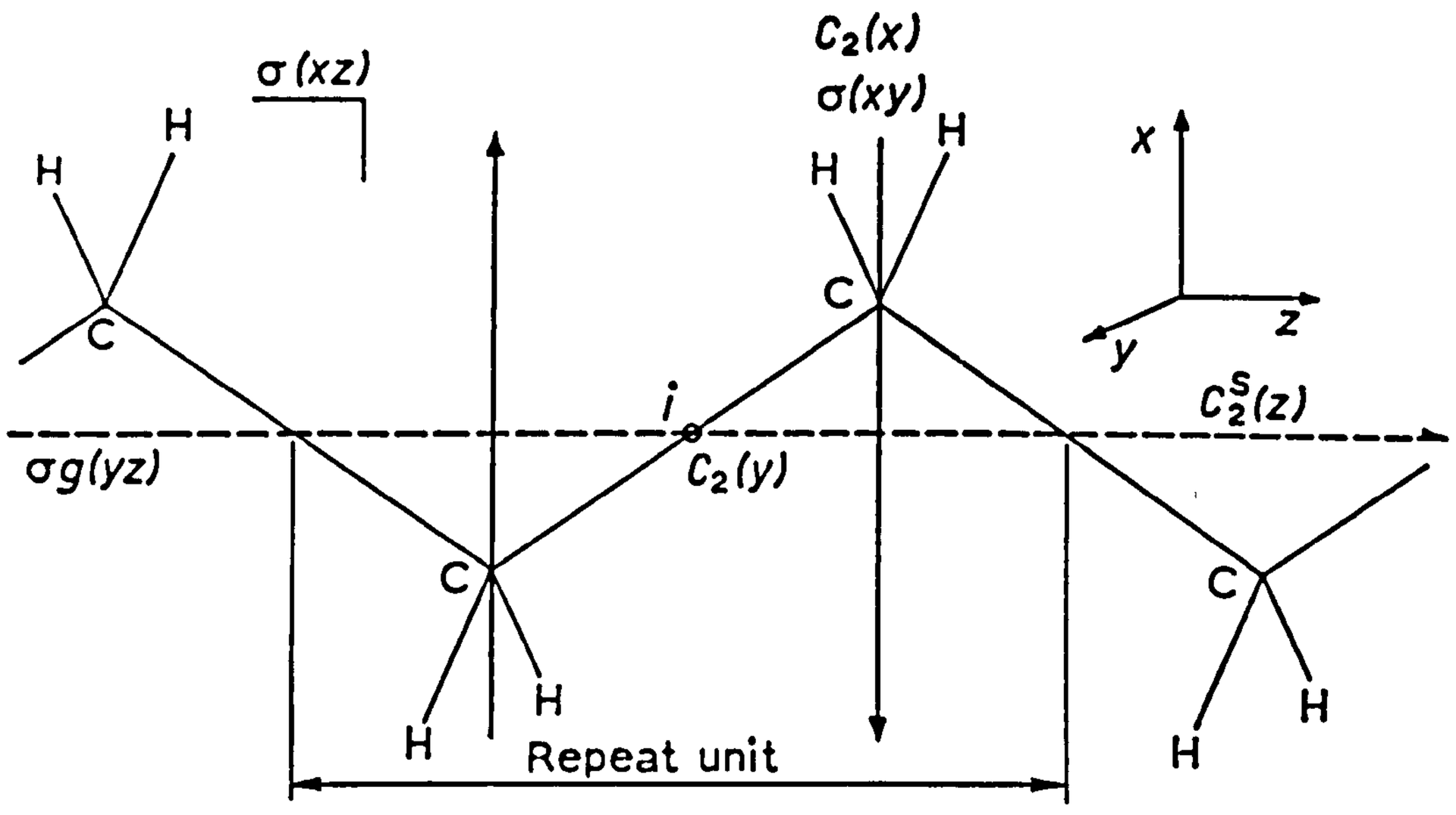

Fig.12 Symmetry elements in an extended polyethylene chain.

antisymmetric respectively to the symmetry operation cited at the top of each column. The letters A and B denote vibrational species which are symmetric and antisymmetric respectively with respect to a rotation axis and the various species of types A and B are distinguished from each other by the subscripts 1, 2 etc A_1 and A_2 etc. Further subscripts g and u indicate that the vibrational species are symmetrical or antisymmetrical to inversion at a centre of symmetry.

1.2.4 Types of Vibration Present in an Isolated Stereo-regular Polymer Molecule of 'Infinite' Length

When considering a stereo-regular polymer molecule of 'infinite' chain length, there are further symmetry elements not present in point groups, namely:-

(i) A p-fold Screw Axis, C_p^s ($C_p^s(x)$, $C_p^s(y)$ or $C_p^s(z)$

The symmetry operation for a p-fold screw axis is a rotation of $\frac{360^o}{p}$ followed by a translation along this axis.

(ii) A Unit Translation

This element is defined as p times the distance of translation associated with the screw axis.

(iii) A Glide Plane σ_g (xy)

The symmetry operation of a glide plane is reflection at the plane followed by translation in a direction parallel to the plane.

These elements all form a line group in which all axes, centres and planes pass through a line, which is the chain axis. The total number of potentially active Raman and infra-red vibrational modes can be predicted from considerations of the symmetry elements of the repeat unit (Fig.12), since this number is dependent only upon the structure of the repeat unit for the isolated stereo-regular polymer molecule of infinite length.

Table II Multiplication table for the point group D_{2h}

	E	$C_2(y)$	$C_2(x)$	$C_2(z)$	i	$\sigma(xz)$	$\sigma(yz)$	$\sigma(xy)$
E	E	$C_2(y)$	$C_2(x)$	$C_2(z)$	i	$\sigma(xz)$	$\sigma(yz)$	$\sigma(xy)$
$C_2(y)$	$C_2(y)$	E	$C_2(z)$	$C_2(x)$	$\sigma(xz)$	i	$\sigma(xy)$	$\sigma(yz)$
$C_2(x)$	$C_2(x)$	$C_2(z)$	E	$C_2(y)$	$\sigma(yz)$	$\sigma(xy)$	i	$\sigma(xz)$
$C_2(z)$	$C_2(z)$	$C_2(x)$	$C_2(y)$	E	$\sigma(xy)$	$\sigma(yz)$	$\sigma(xz)$	i
i	i	$\sigma(xz)$	$\sigma(yz)$	$\sigma(xy)$	E	$C_2(y)$	$C_2(x)$	$C_2(z)$
$\sigma(xz)$	$\sigma(xz)$	i	$\sigma(xy)$	$\sigma(yz)$	$C_2(y)$	E	$C_2(z)$	$C_2(x)$
$\sigma(yz)$	$\sigma(yz)$	$\sigma(xy)$	i	$\sigma(xz)$	$C_2(x)$	$C_2(z)$	E	$C_2(y)$
$\sigma(xy)$	$\sigma(xy)$	$\sigma(yz)$	$\sigma(xz)$	i	$C_2(z)$	$C_2(x)$	$C_2(y)$	E

Table III Multiplication table for the line group of the polyethylene chain (isomorphous with D_{2h})

	E	$C_2(y)$	$C_2(x)$	$C_2^s(z)$	i	$\sigma(xz)$	$\sigma_g(yz)$	$\sigma(xy)$
E	E	$C_2(y)$	$C_2(x)$	$C_2^s(z)$	i	$\sigma(xz)$	$\sigma_g(yz)$	$\sigma(xy)$
$C_2(y)$	$C_2(y)$	E	$C_2^s(z)$	$C_2(x)$	$\sigma(xz)$	i	$\sigma(xy)$	$\sigma_g(yz)$
$C_2(x)$	$C_2(x)$	$C_2^s(z)$	E	$C_2(y)$	$\sigma_g(yz)$	$\sigma(xy)$	i	$\sigma(xz)$
$C_2^s(z)$	$C_2^s(z)$	$C_2(x)$	$C_2(y)$	E	$\sigma(xy)$	$\sigma_g(yz)$	$\sigma(xz)$	i
i	i	$\sigma(xz)$	$\sigma_g(yz)$	$\sigma(xy)$	E	$C_2(y)$	$C_2(x)$	$C_2^s(z)$
$\sigma(xz)$	$\sigma(xz)$	i	$\sigma(xy)$	$\sigma_g(yz)$	$C_2(y)$	E	$C_2^s(z)$	$C_2(x)$
$\sigma_g(yz)$	$\sigma_g(yz)$	$\sigma(xy)$	i	$\sigma(xz)$	$C_2(x)$	$C_2^s(z)$	E	$C_2(y)$
$\sigma(xy)$	$\sigma(xy)$	$\sigma_g(yz)$	$\sigma(xz)$	i	$C_2^s(z)$	$C_2(x)$	$C_2(y)$	E

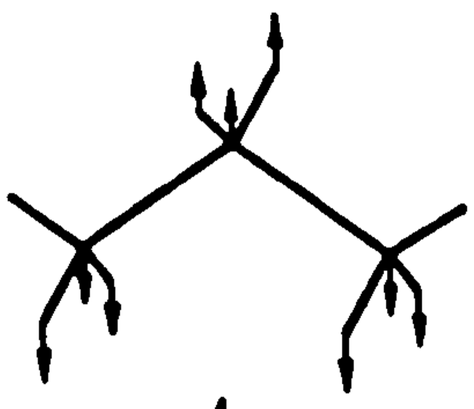

A_g

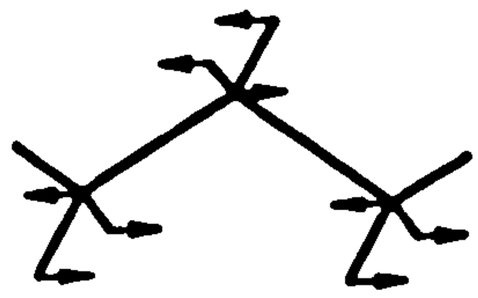

B_{2g}

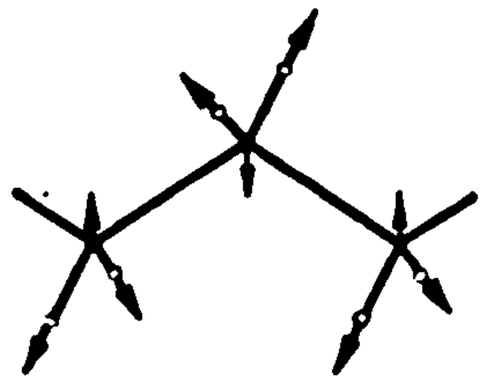

A_g

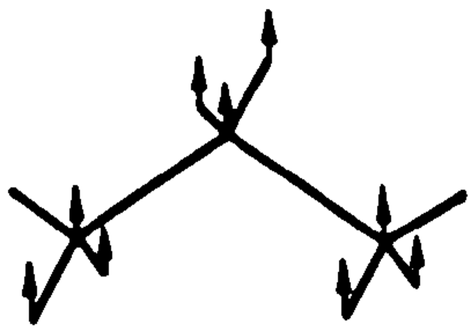

B_{3u}
(T_x)

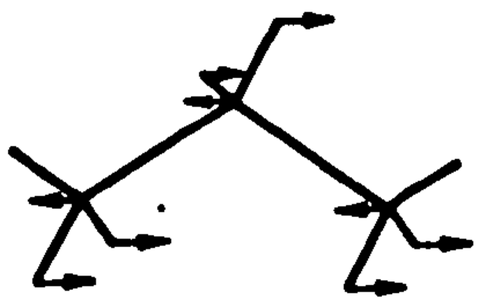

B_{1u}
(1176)

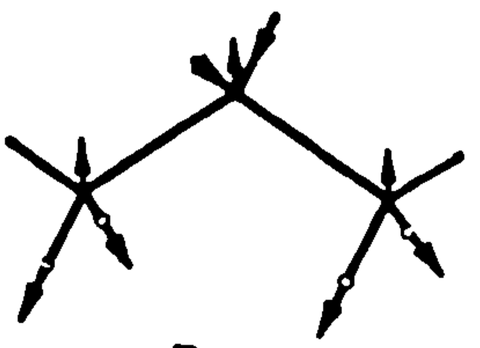

B_{3u}
(2851)

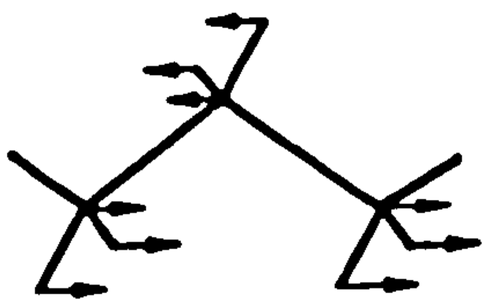

B_{2g}

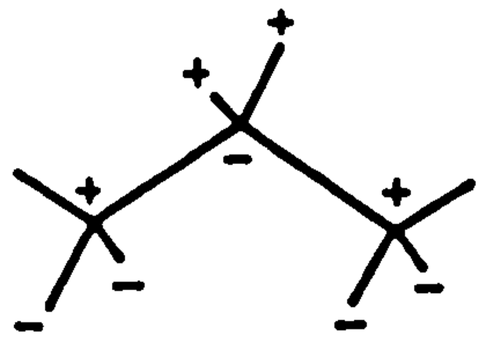

B_{1g}

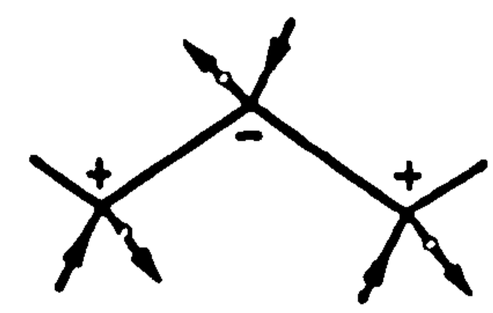

B_{1g}

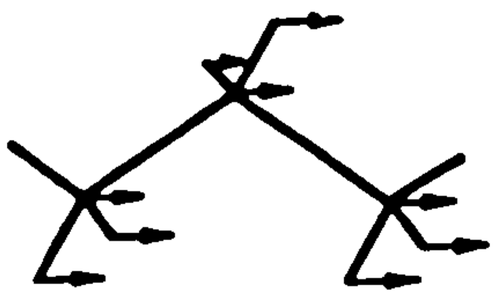

B_{1u}
(T_z)

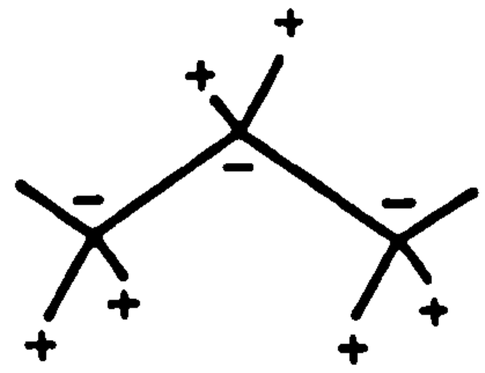

B_{2u}
(720;731)

B_{2u}
(2919)

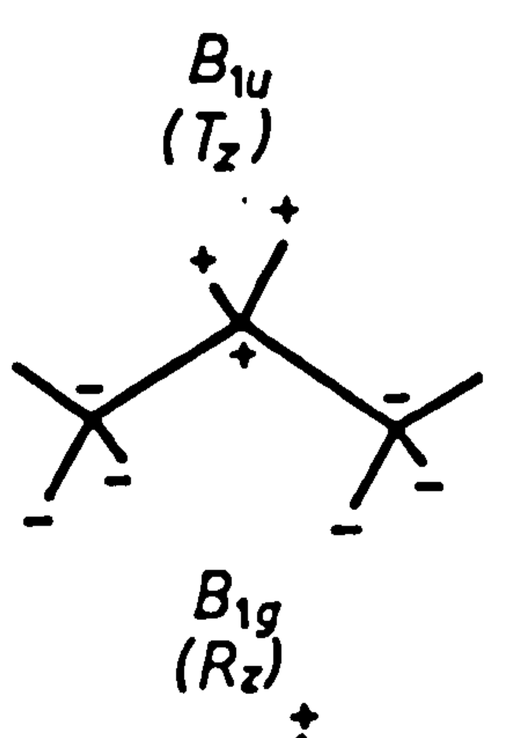

B_{1g}
(R_z)

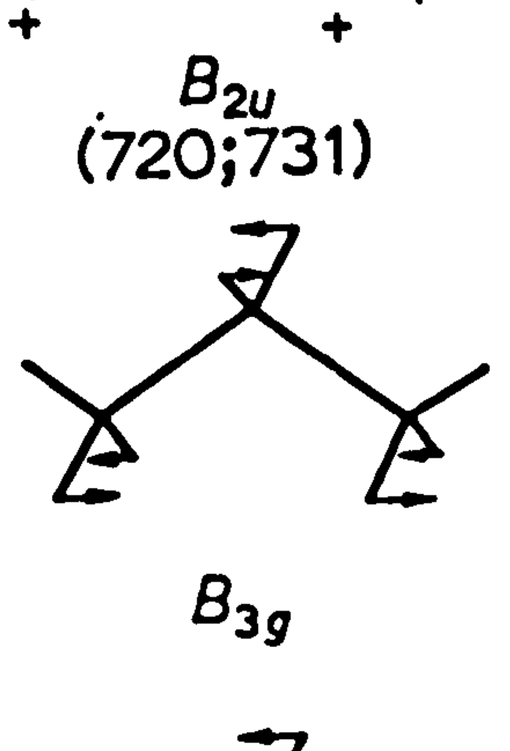

B_{3g}

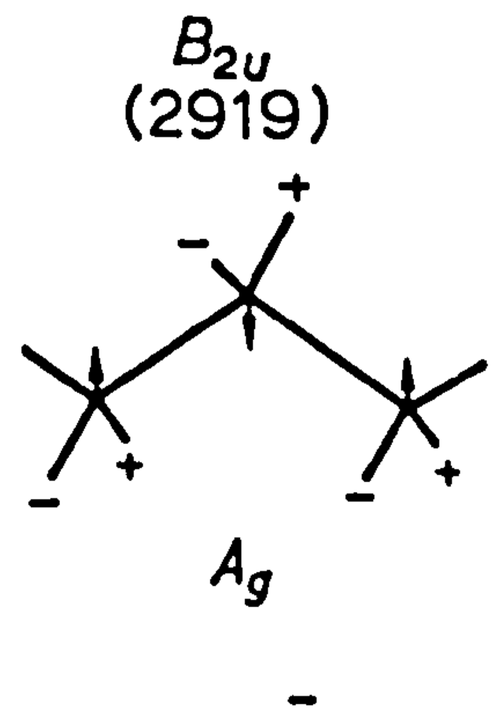

A_g

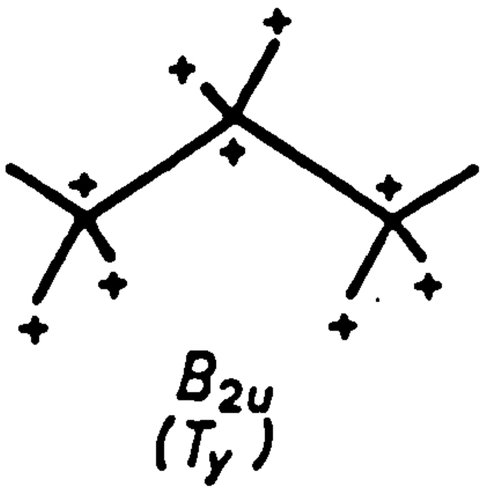

B_{2u}
(T_y)

A_u

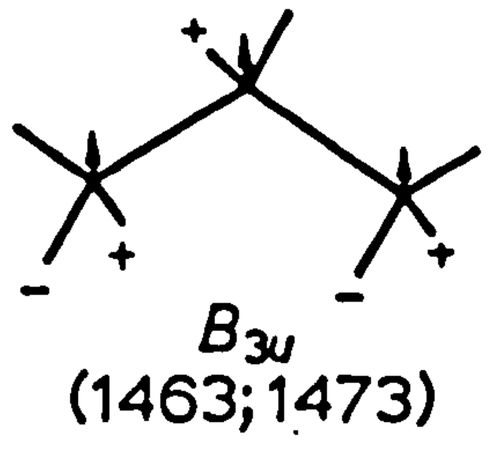

B_{3u}
(1463;1473)

Fig. 13 Symmetry modes of a single polyethylene chain. (Krimm, Liang

The elements of symmetry of the repeat unit together with the unit translation (equivalent to E) form a sub-group of the line group, known as the unit cell group. The unit cell group is not a point group, since it may include screw axes and glide planes.

There is, however, a point group which is isomorphous with the unit cell group, and this is found by writing out a multiplication table for the unit cell group and comparing it with multiplication tables for all the 32 point groups. Tables II and III give the multiplication tables for the point group D_2h and the isomorphous unit cell group for polyethylene. The entry in each space is the symmetry element, which results from an application of the symmetry operation at the head of each column followed by a symmetry operation at the end of the corresponding row. The tables are identical except for the replacement of the symbols $C_2^s(z)$ and $\sigma_g(yz)$ in Table III by the symbols $C_2(z)$ and $\sigma(yz)$ in Table II.

Having established which point group is isomorphous with the unit cell group a particular 'infinite' polymer molecule, the actual types of vibrational mode present (A_1 B_{lu} etc) for the whole molecule follow directly from a consideration of the symmetry elements present in the point group (7, 8).

1.2.6 Determination of the Total Number of Vibrations and the Distribution Between the Various Vibrational Types (A_1 B_{lu} etc.) for the Infinite Stereo-regular Isolated Polymer Chain.

The actual number of vibrations and their distribution may be determined by considering the polymer repeat unit and the number of degrees of freedom which the constituent atoms contribute when they undergo the symmetry operations which correspond to each vibrational species (A_g B_{lu} etc). In polyethylene (Figs. 12 & 13) for example, vibrations of species A_g must be

symmetrical for all operations. The hydrogen atoms are in the σ(xy) plane and must move in this plane during an A_g vibration, contributing two degrees of freedom. The carbon atoms may move symmetrically with respect to the C_2 (x) operation only if they vibrate along the x axis and thus have only one degree of freedom. There are therefore 2 + 1 = 3 vibrations of species A_g corresponding to the three degrees of freedom.

Neither translation Tx, Ty or Tz nor rotation around the z axis is compatible with all symmetry operations, so that the vibrations are real (non-zero) vibrations.

Similar arguments may be applied to all the vibrational species to determine the number of vibrations of each type, but further considerations of dipole moment are required to determine how many of the vibrations are infra-red active. A more mathematical approach to the determination of the total number and distribution of vibrational modes, including degenerate modes, is given by Herzberg (2) and Zbinden (7).

1.2.7 The Effect of Finite Chain Length and Greater Complexity.

(i) The Effect of Finite Chain Length

When the polymer becomes of finite chain length, there are many more potential vibrational modes than in the repeat unit, due partly to the coupling of dipoles within the molecule. This coupling problem has been resolved to some extent by applying the arguments for a linear array of couples of frequency ω_o (7). The vibrational spectra of crystalline paraffins illustrates the effect of increasing chain length, as has been studied by Snyder (11).

(ii) Greater Complexity

In the case of more complex polymers (i.e. those that cannot be regarded as aggregates of isolated polymer chains) further complications arise leading to further spectral bands (in addition to overtone, combination and Fermi resonance bands). A major complication arises from the enormous

number of chemical groups present and the resultant large number of intra and intermolecular interactions, such as hydrogen bonding. Lack of detailed knowledge of the position of every atom and bond in the molecule (i.e. secondary and tertiary structure) often prevents elucidation of all the fine spectral detail.

Differentiation of the polymer into crystalline and less crystalline regions is a further factor which must be considered to give rise to more spectral peaks, although many of these only become observable in derivative spectra (12). Chain folding and the existence of more than one crystalline form are further complications which may also give rise to further spectral peaks.

However, an observed absorption spectrum is not as complex as expected from the above factors. This is due to the fact that many vibrations are so nearly identical that the corresponding absorption bands are not resolved and often the spectrum appears simpler as the molecular weight of the polymer increases. This is not the case in derivative spectroscopy where greater resolution and hence fine spectral detail may be obtained. In practice, a high resolution derivative spectrum of a single absorption peak of 2-3 μm. wavelength spread often contains as many as a hundred minor peaks.

1.2.8 Modifications of basic Group Theory

Modifications of the basic theory have been attempted in order to take some of these factors into account (13, 14). Methods of calculating the normal vibrational modes in helical molecules have been developed (15-17), but their application to simple polymers, such as helical polypeptides, has had only limited success. (18)

1.3 The Effect of Temperature, Hydrogen Bonding, Crystallinity and Crystallisation on Spectra

As the temperature of an absorbing species is increased, the fundamental

vibrational frequency is increased, which results in a corresponding absorption of infra-red radiation at a higher frequency (lower wavelength). However, the broadening of peaks and reduction of peak intensity which occur with increased temperature may obscure this shift. The broadening and reduction in intensity results from the increase in the number and distribution of vibrational energy levels as the temperature is increased. Poor resolution may also account for the apparent absence of anticipated absorption band shifts, although the increased resolution of derivative spectra largely obviates this problem.

In many polymers increasing the temperature beyond 100^{o}C. causes an increase in the total amount of crystalline material present and such crystalline increases often occur at lower temperatures. Such increases affect the infra-red spectra of polymers although many of the details of such effects are only observed in derivative spectra.

The changes in structure which occur on heating samples are complicated by the fact that a polymer cannot be considered as a simple two phase system containing only 'perfectly amorphous' and 'perfectly crystalline' material, but must be considered as possessing a gradation between 'perfectly amorphous' and 'perfectly crystalline' material. Further complications also arise due to the fact that a polymer may contain more than one crystalline phase at the same time.

If heating simply causes an increase in the extent of crystallisation of a polymer, i.e. a transference of 'amorphous' or poorly ordered ('crystallizable') material to 'crystalline' material of a particular crystalline phase already present, then peaks which correspond to that phase will increase in intensity, whilst peaks corresponding to the less ordered 'crystallizable' material will decrease in intensity. In both cases, however, no peak shifts will be observed.

If, however, heating causes an increase in the degree of crystalline

perfection of a particular crystalline phase already present or of the whole system, then an increased restriction of the vibration of certain chemical groups will occur (e.g. OH, C=O C-O-C and to a lesser extent CH and CH_2) due to increased intramolecular and intermolecular interactions, such as hydrogen bonding. Such restrictions will cause a reduction in the fundamental vibrational frequencies of such groups so that infra-red radiation is absorbed at lower frequencies and a shift to lower frequencies (higher wavelengths) of corresponding peak maxima is observed.

Thus at a particular high temperature, an observed peak shift results from opposing 'temperature' and 'increased degree of crystalline perfection' effects.

The observation of spectra at different temperatures is useful for the determination of the temperature range in which increased crystallisation or crystalline transitions occur, so that peaks can be assigned as 'crystalline; 'crystallizable' or 'non-crystallizable' (unaffected). However, permanent changes which occur in the extent of crystallisation in addition to or in place of changes in the degree of crystalline perfection, may be only assessed on comparison of the spectra of untreated samples with the spectra of annealed samples, which were obtained under the same conditions of temperature and humidity. Thus an increase in the degree of crystalline perfection may only be said to have occurred if a spectral peak from an untreated sample occurs at a higher wavelength in the corresponding annealed sample spectrum, when the spectra of both samples are observed under the same conditions of temperature and humidity.

The affect of absorbed water on spectra is important since the presence of water introduces absorption peaks in both the 3 μm. (3333 $cm.^{-1}$) and 6 μm. (1667 $cm.^{-1}$) regions of the spectrum. Water may also bond to OH, C=O and C-O-C groups (and to a small extent to CH and CH_2 groups (12)) reducing vibrational frequencies and thus causing spectral shifts. The effect of

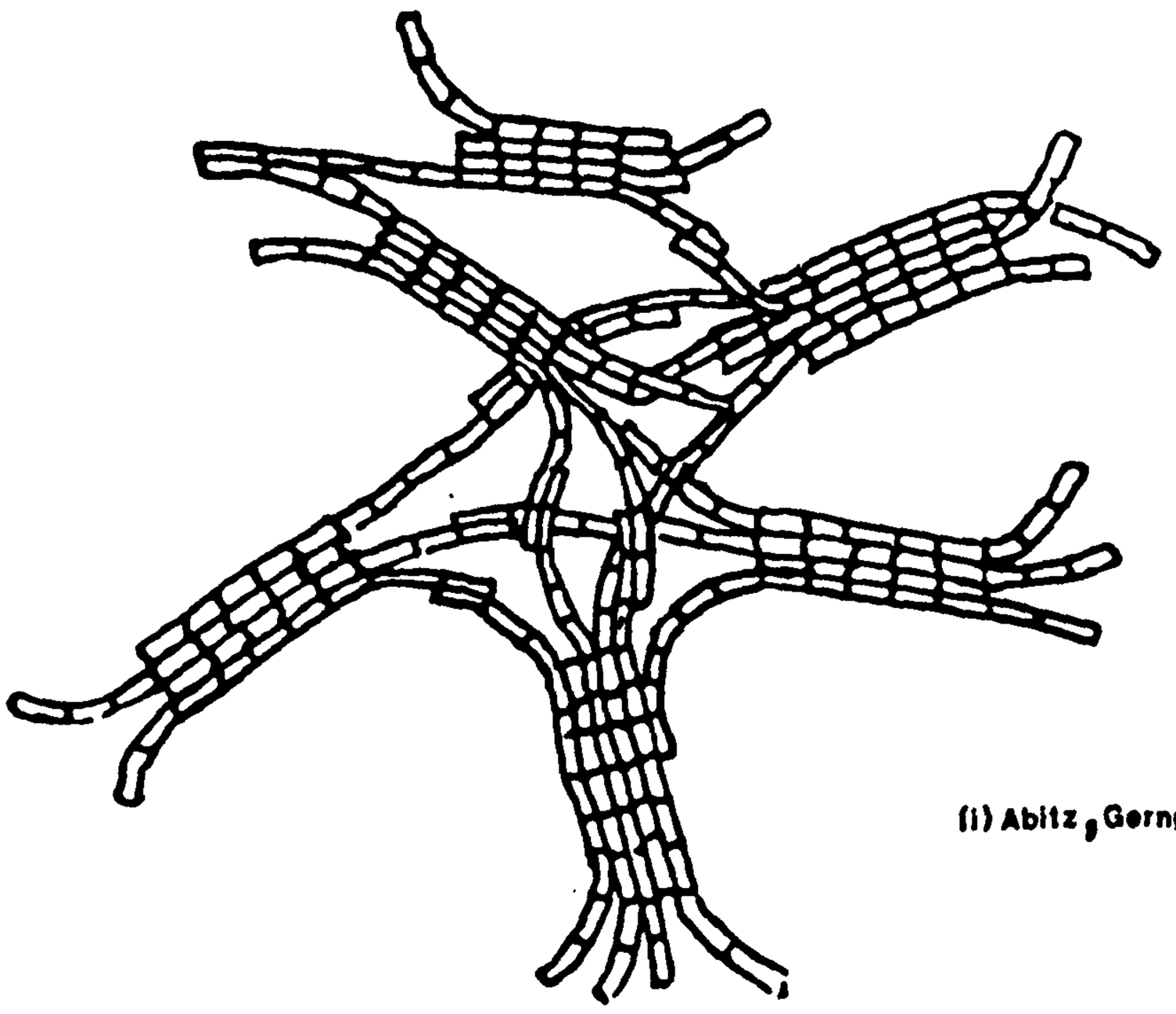

(i) Abitz, Gerngross and Herrmann 1930.

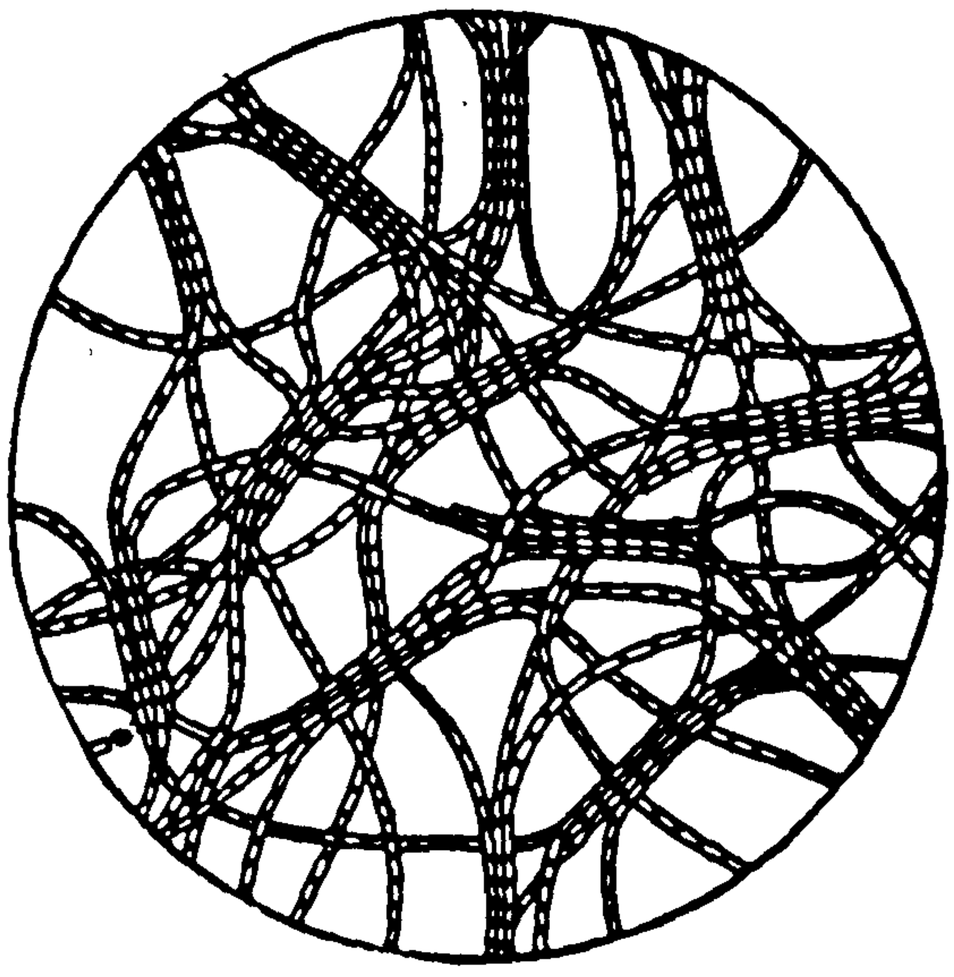

(ii) Gerngross and Herrmann 1932.

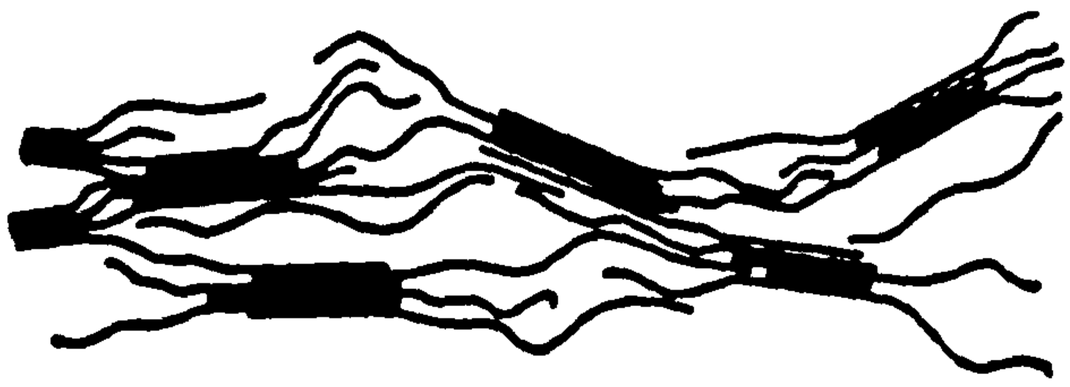

(iii) Kratky and Mark 1937.

FIG. 14 A

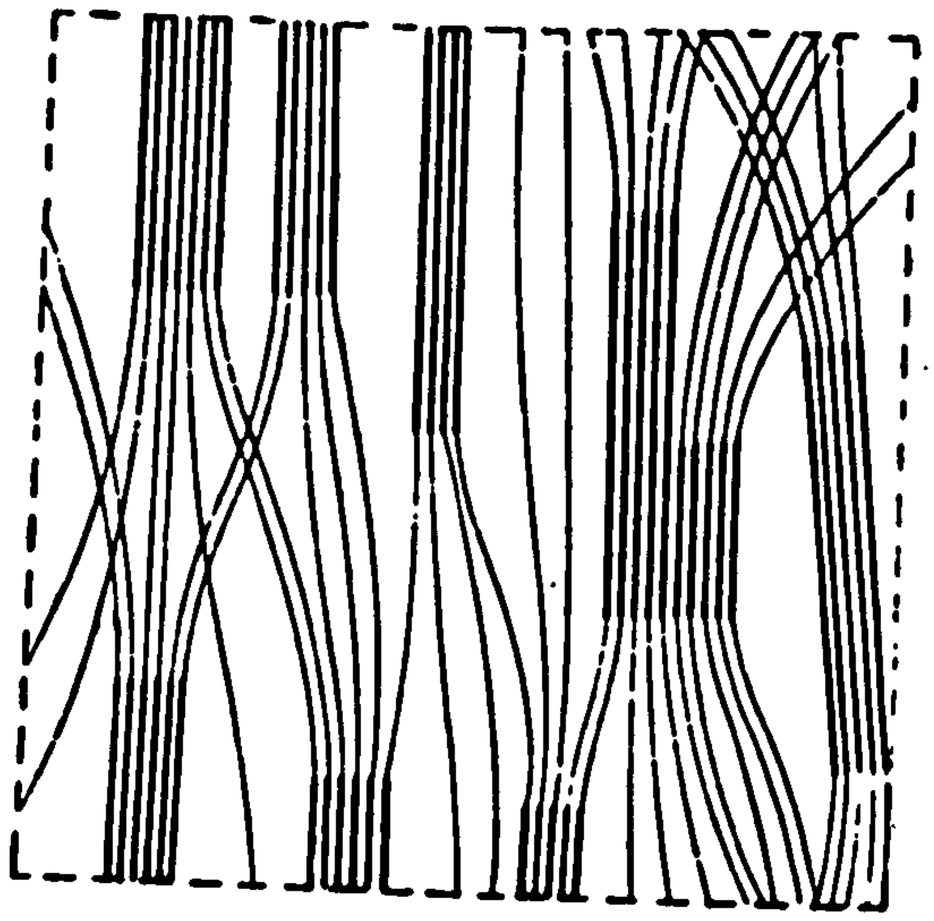

(iv) Frey-Wyssling 1937.

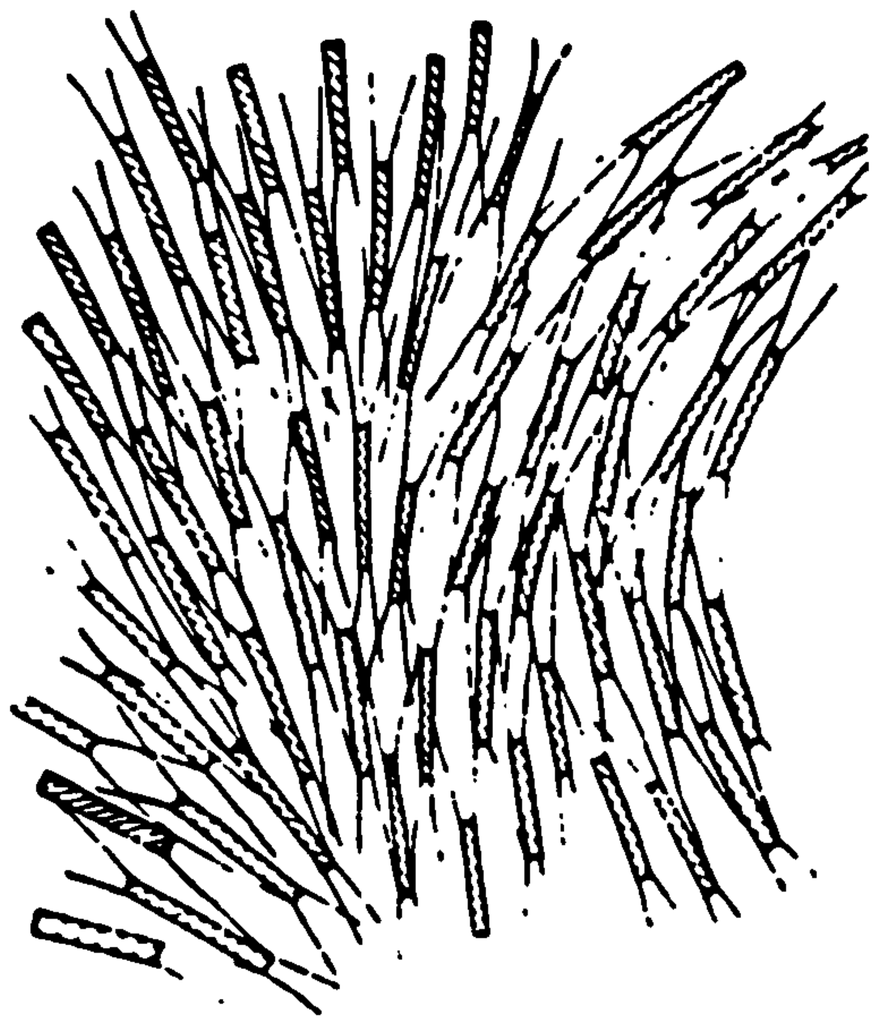

(v) Hermans 1941.

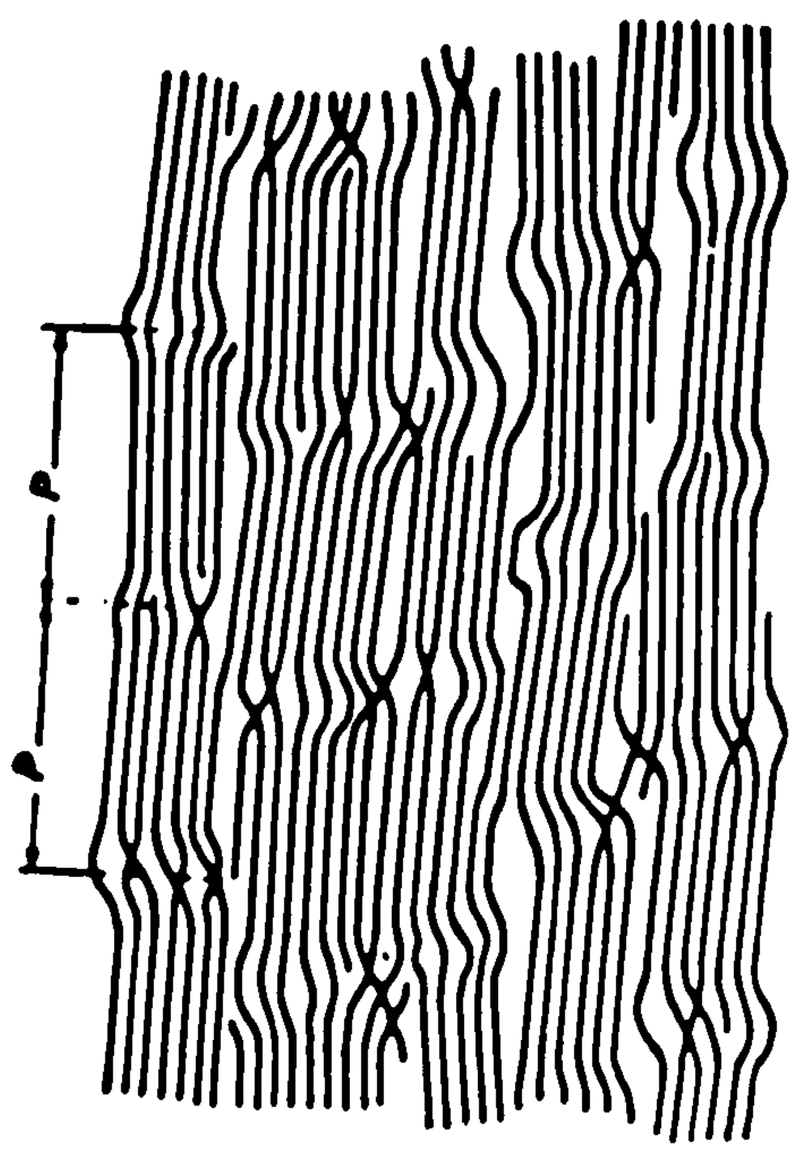

(vi) Hess and Kiessig 1944.

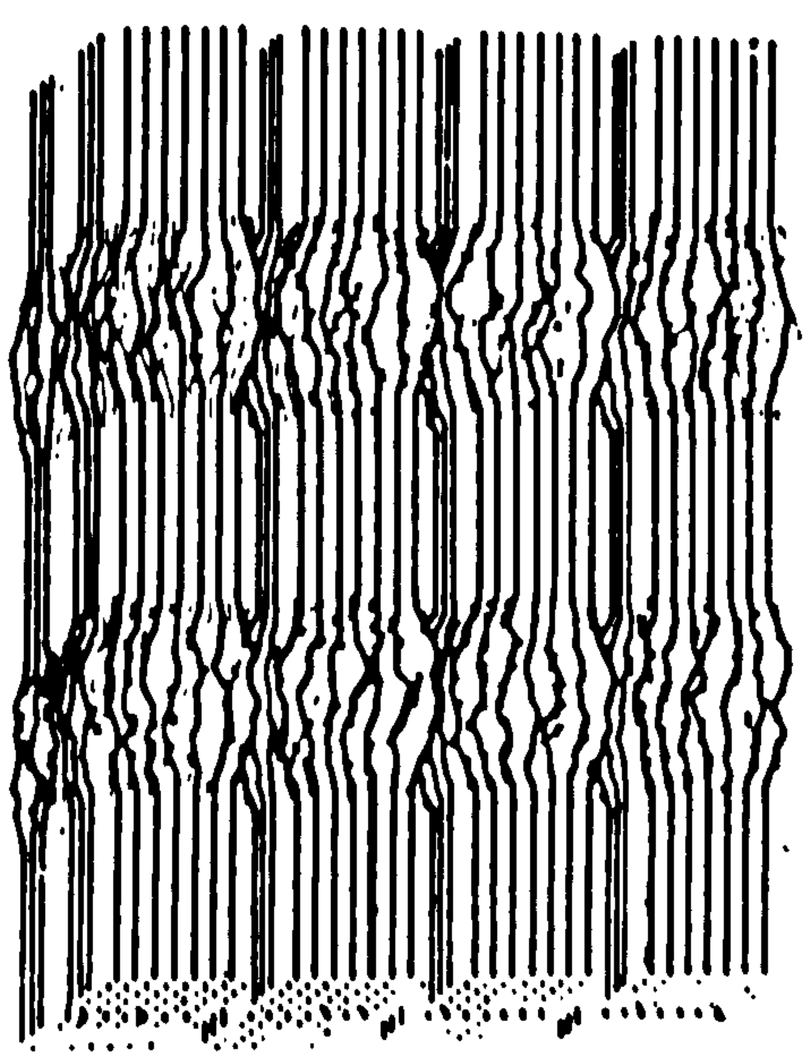

(vii) Hess, Mahl and Gütter 1957.

FIG. 14 A Continued

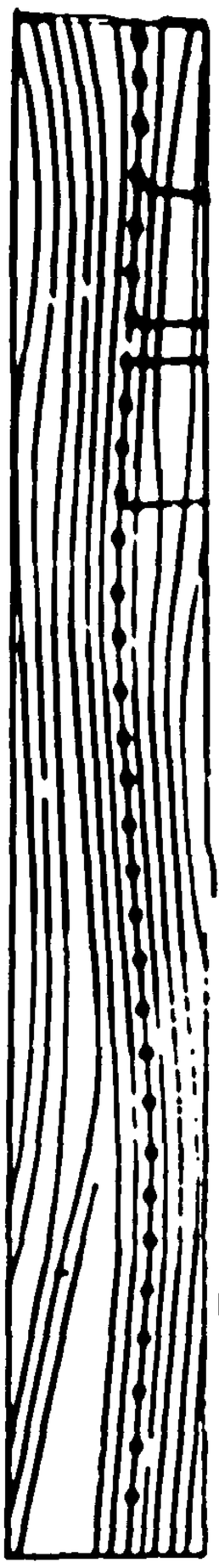

Kratky 1940.

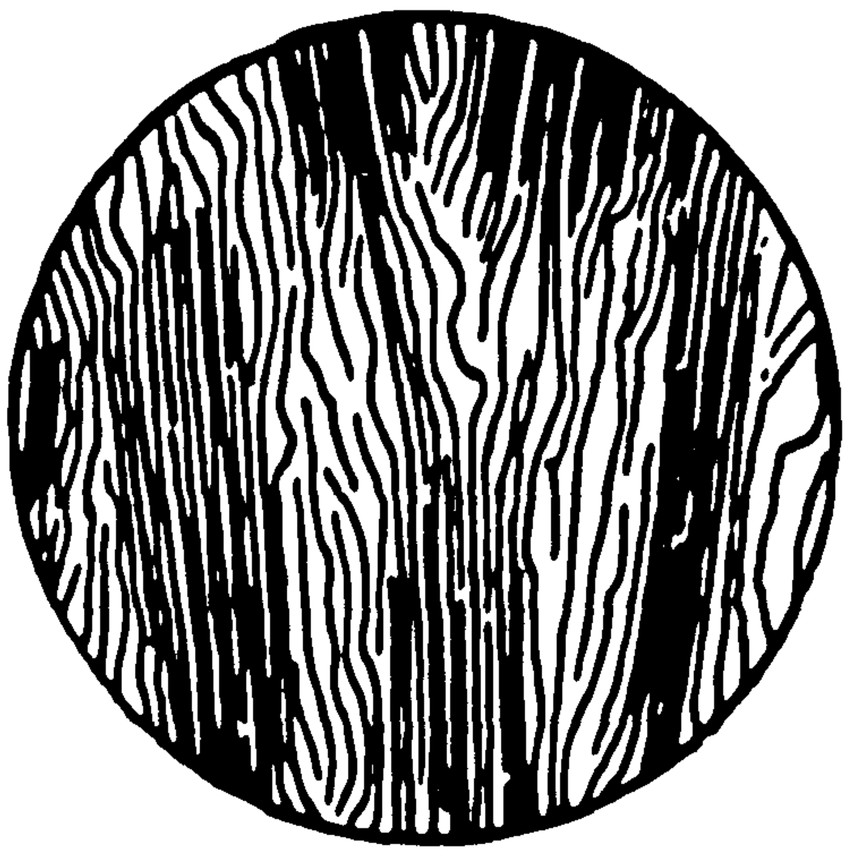

Mark 1940.

Meyer and van der Wyck 1941.

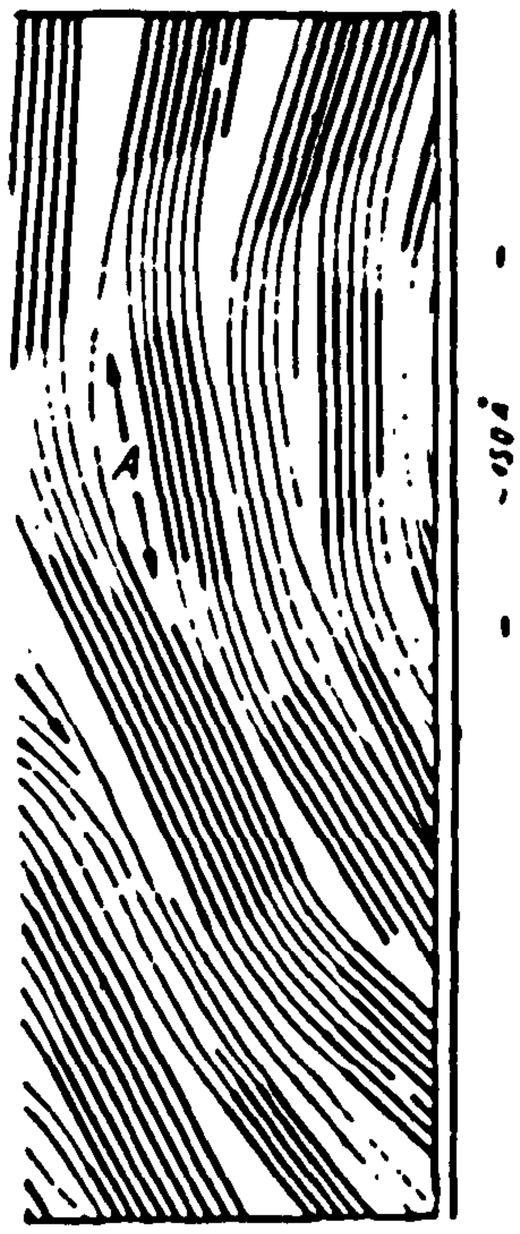

Frey-Wyssling 1951.

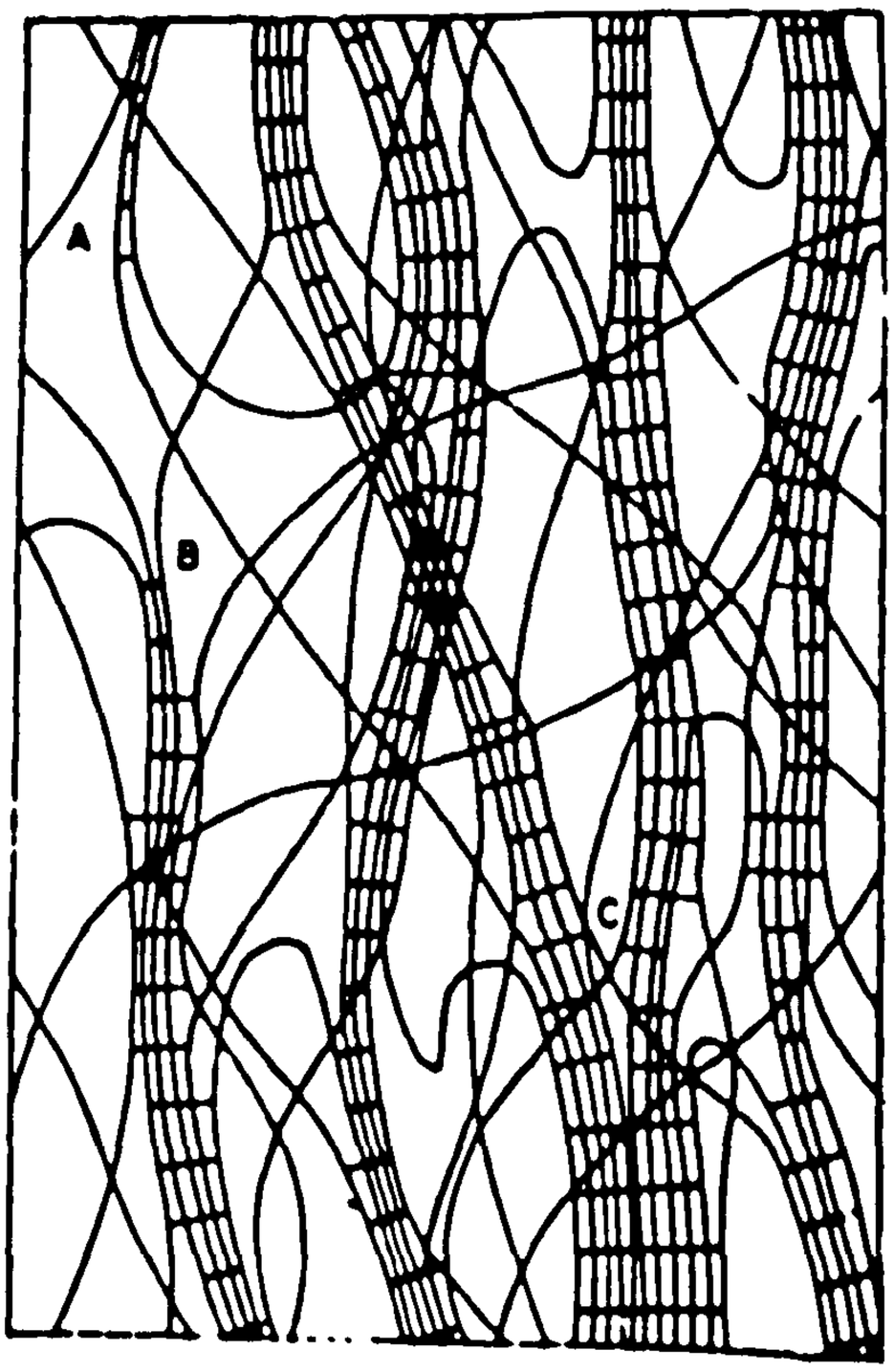

Heerle 1958.

FIG. 14 B

absorbed water is discussed in Chapters 3 and 6.

1.4 The Development of Theories of Crystalline Structure

In 1880 Nägeli proposed a theory to account for the structure of starch grains in terms of crystalline particles called 'micelles', surrounded by an inter-micellar matrix (19). The development and application of X-ray crystallographic techniques to fibres showed conclusively that they contained crystalline regions. These regions were assumed to be composed of small discrete particles, since X-ray photographs were at that time believed to arise from minute discrete, but perfect crystals. Several workers applied modifications of Nägeli's theory to account for fibre structure (20, 21). Micellar dimensions were also calculated from X-ray photographs by Hengstenberg and Mark (22). The dimensions calculated as 60 nm long x 5 nm wide for ramie and 30 nm.long x 4 nm.wide for viscose; were taken as a measure of molecular dimensions until Staudinger, from viscosity measurements, showed that cellulose molecules were approximately ten times longer than previously considered. He thus proposed that high molecular weight crystalline polymers consisted of continuous imperfect crystals, whereas amorphous polymers consisted of a network of irregularly distributed chains.

The micellar theory in its original form was thus rejected, but a modified 'fringed micelle' theory was proposed by Herrmann et al. (24, 25), in which it was assumed that long chain molecules were able to pass through both crystalline micellar regions and amorphous matrix regions. The concept of long chain molecules passing through both crystalline and amorphous regions was generally accepted, but many possible ways in which this could occur were proposed (Figs. 14a and 14b).

The structures shown in Fig.14a indicate a sharp division of material into discrete crystallites and amorphous fringing material and in all these structures, fringing is shown to occur at the ends of crystallites. However, the structures shown in Fig. 14b indicate a system where there is a

FIG.15

Modified fringed-fibril structure

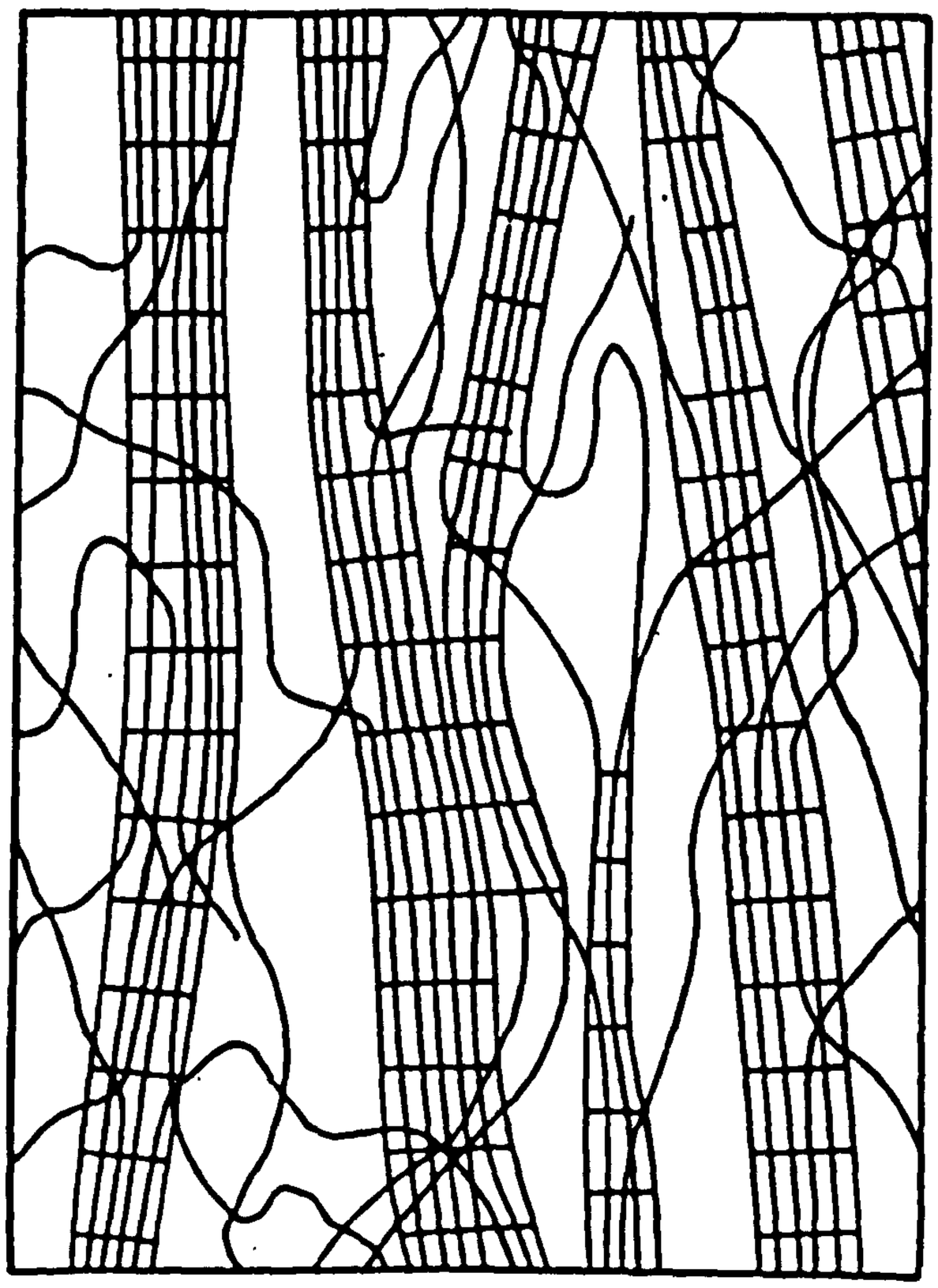

less distinct division between 'crystalline' and 'amorphous' regions. Such a system was thought to be a truer representation of actual structure since in such a system it was not possible to give exact dimensions of crystallites. This system hence gave an explanation for the contradiction between the results of crystallite dimensions obtained from various techniques.

The fringed micelle theory has been very successful in explaining many physical and chemical properties of fibrous polymers, such as water uptake, rate of chemical reaction and variation in dye uptake, based on the assumption that crystalline regions are less penetrated than amorphous regions.

The 'fringed fibril' structure of Hearle (26) shown in Fig.14b(v) differs from the other structures in that it allows molecules to branch off from fibrils (equivalent to crystallites) at any position along fibrils instead of only at the ends of crystallites. This structure also accounts for the possibility that lattice distortion could occur together with fibrillar branching, and is probably the most widely proposed structure. It is also able to account for the existence and mechanism of formation of spherulites observed by Keller (27-29).

Hearle (30) later proposed a 'modified fringed fibril' structure (Fig.15) in which he showed that points where molecules entered or left crystalline fibrils were spread at intervals along fibrils. This was proposed in order to account for X-ray and electron microscope evidence of long period spacings. This modified fringed fibril theory of structure is also able to account for some observed types of crystallisation and for the formation of tablet shaped particles from ultrasonically degraded cotton. Furthermore, the contentions of this theory are compatible with the infra-red observations reported in this thesis concerning crystallinity changes and water absorption. These will be discussed in full in Chapters 3 - 6.

A recent theory by Hosemann (31) attempted to explain certain aspects of crystalline structure in terms of a two dimensional paracrystalline

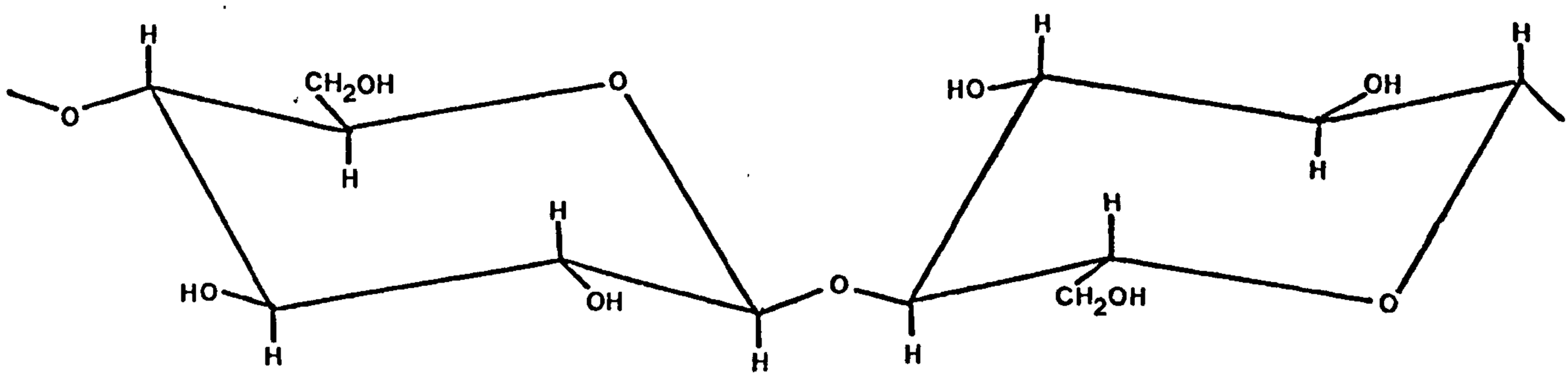

FIG 16

lattice. In such a lattice, it was shown that displacements of atoms from the ideal lattice were able to account for some of the background scatter on X-ray diffraction patterns, not associated with so-called 'amorphous scatter'. Although this theory is widely accepted by crystallographers, it is inadequate in that it does not fully account for the behaviour of long chain molecules in a three dimensional system (32). Also, it does not account for some types of crystallisation and cannot account for the transference of water to crystalline regions (Chapter 3).

1.5 The Structure of Cellulose, Cellulose Diacetate and Cellulose Triacetate.

1.5.1 Structure of Cellulose: (A) Introduction

Cellulose consists of non branched chains of βD glucose units linked through '1-4' glucosidic linkages. The degree of polymerisation is of the order of 3000 in natural celluloses (Cellulose I). In regenerated celluloses e.g. viscose (Cellulose II) there is a distribution of the degree of polymerisation between 0 and approximately 1500, but the most frequently occurring degree of polymerisation (i.e. the degree of polymerisation of the bulk of the material) is usually in the range 300 - 700.

In crystalline regions it is generally accepted that the glucose units are in the 'trans' conformation, (Fig.16). It has also been suggested that a few linkages other than '1-4' β glucosidic linkages may be present to the extent of 1% in both natural and regenerated celluloses, but the evidence for this is still tentative (33 - 35).

1.5.1 (B) X-ray Evidence for the Structure of Cellulose

Early X-ray experiments on natural cellulose by Nishikawa (36) indicated the existence of small crystallites parallel to the fibre axis. Further

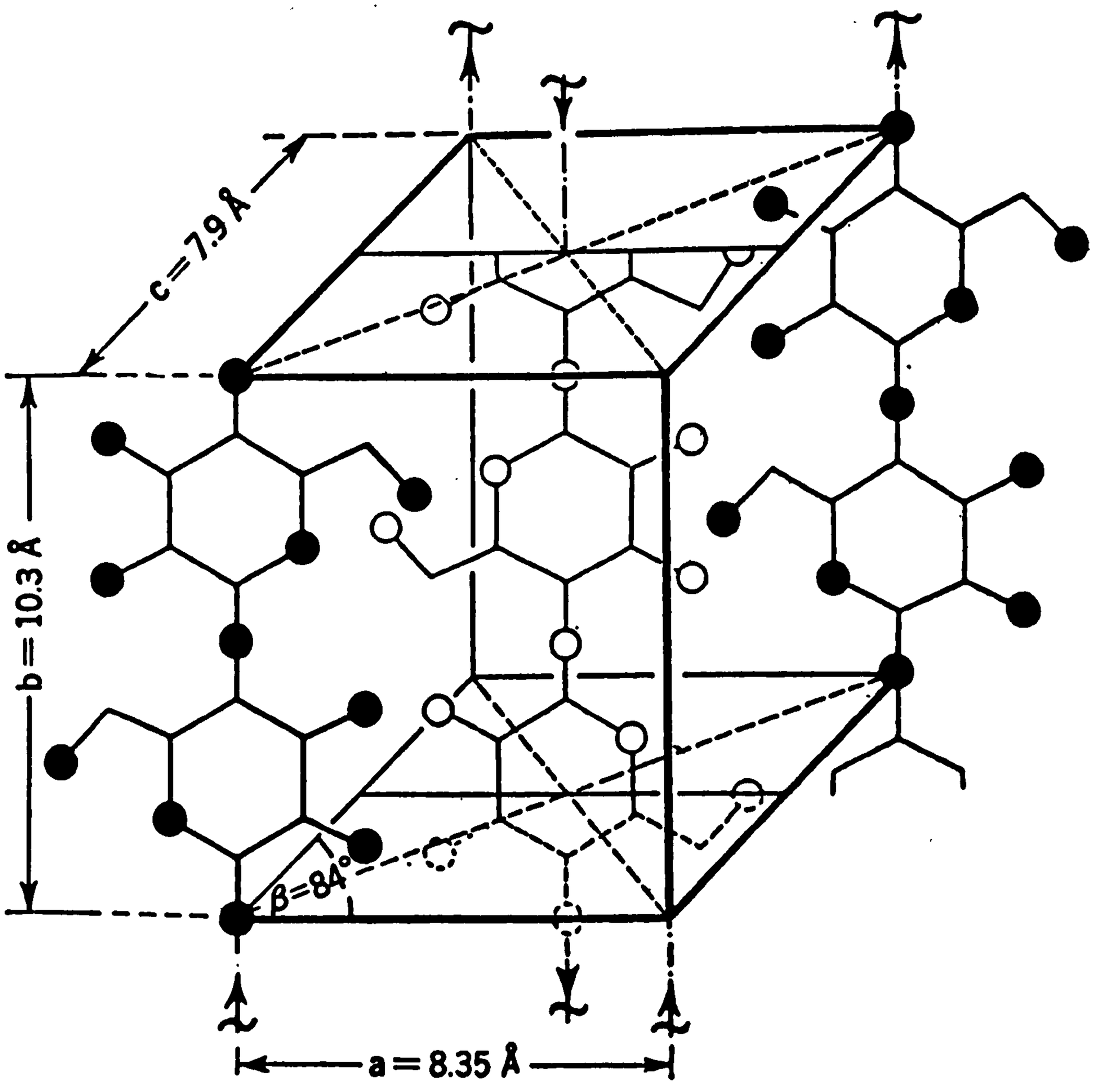

Fig. 17 Diagrammatic representation of the unit cell of native cellulose (Meyer and Misch).

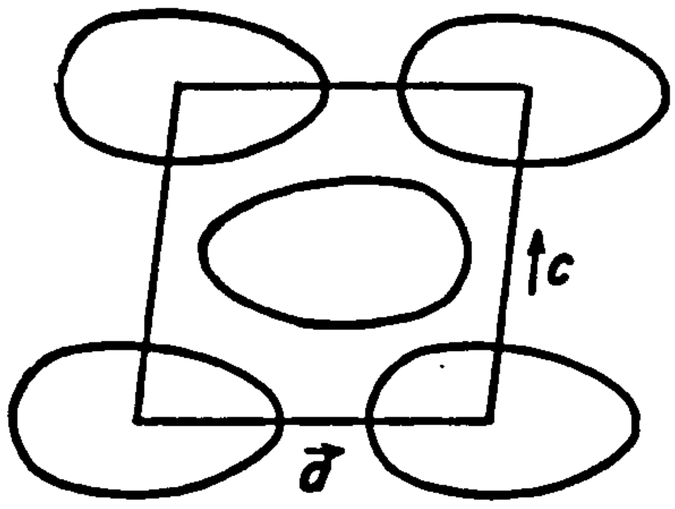

(a) Native cellulose
$a = 8.35$ Å., $c = 7.9$ Å., $\beta = 84°$

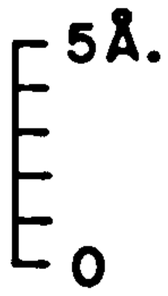

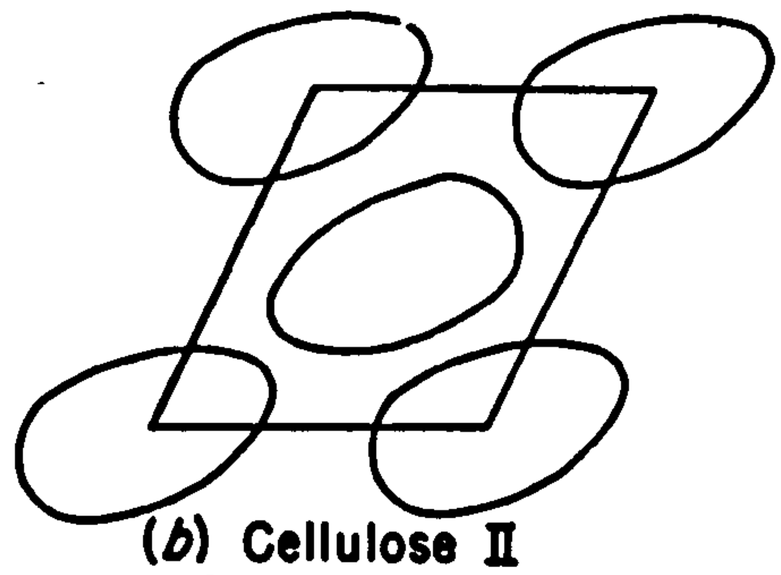

(b) Cellulose II
$a = 8.14$ Å., $c = 9.14$ Å., $\beta = 62°$

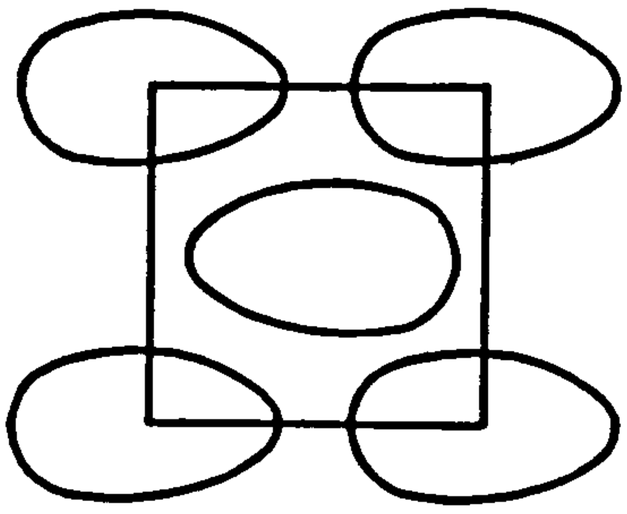

(c) Cellulose T
$a = 8.11$ Å., $c = 7.9$ Å., $\beta = 90°$

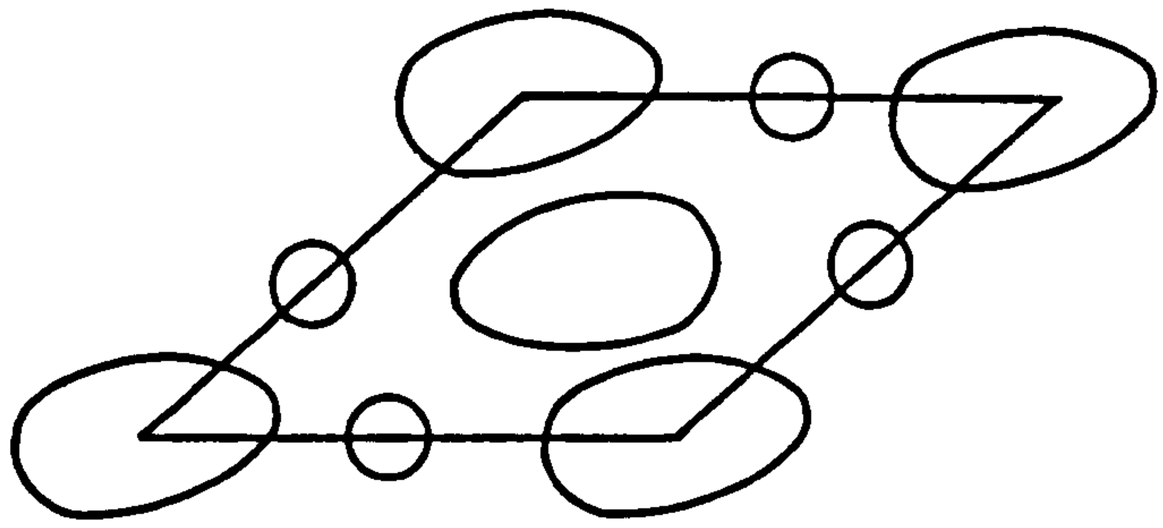

(d) Soda cellulose I
$a = 12.8$ Å., $b = 13.2$ Å., $\beta = 40°$

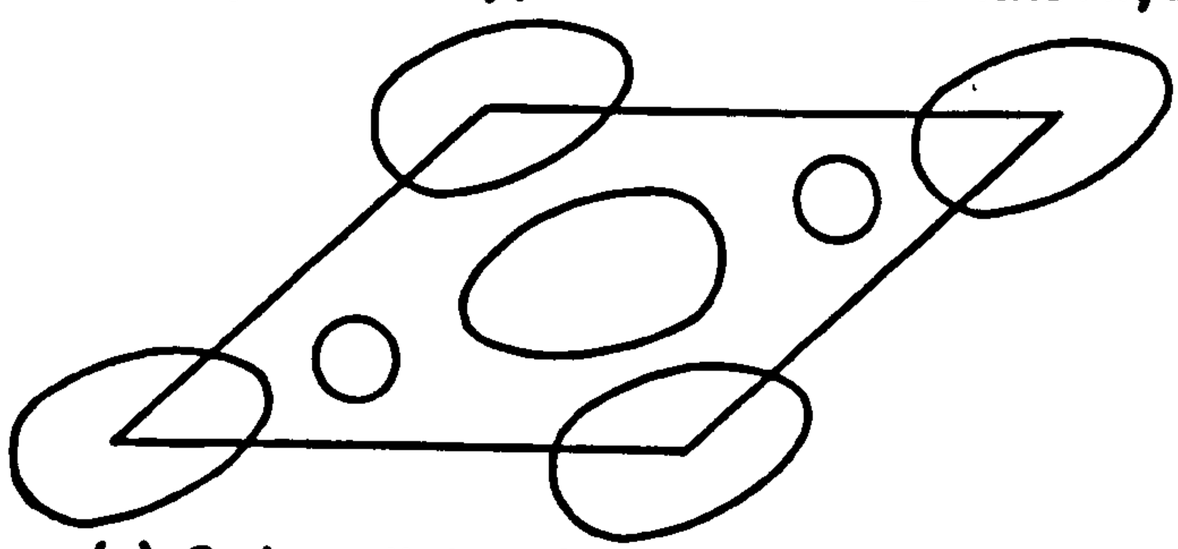

(e) Soda cellulose III
$a = 12$ Å., $c = 14$ Å., $\beta = 40°$

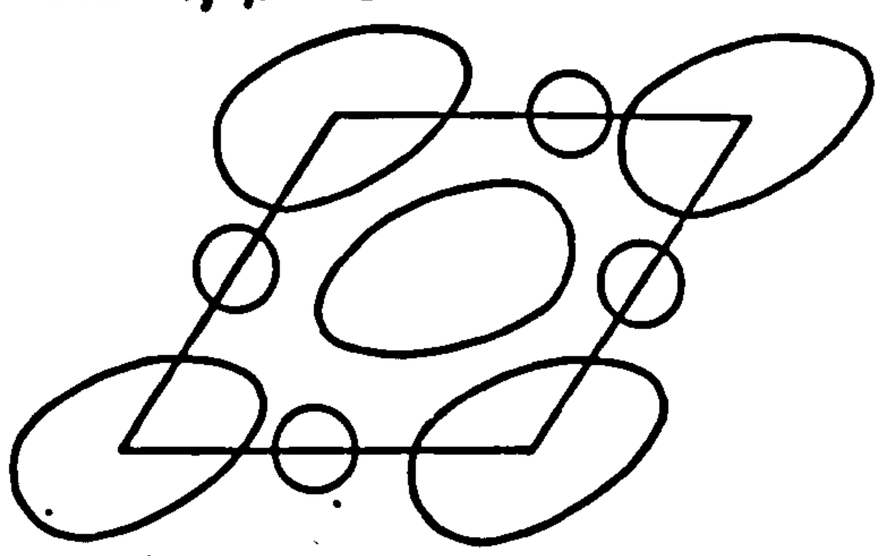

(f) Soda cellulose IV
(water cellulose)
$a = 10.03$ Å., $b = 9.98$ Å., $\beta = 52°$

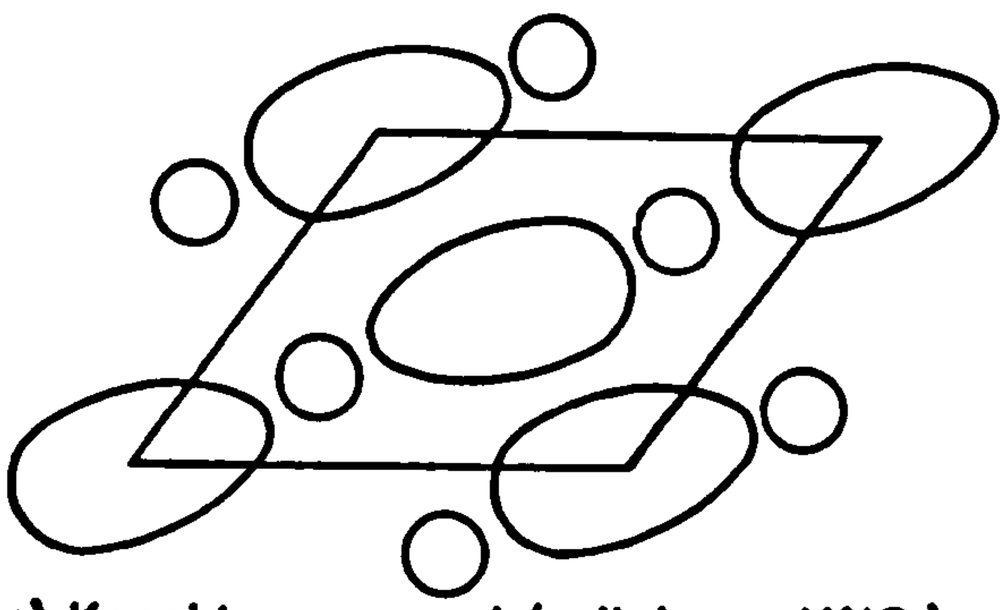

(g) Knecht compound (cellulose–HNO_3)
$a = 12.20$ Å., $b = 10.28$ Å., $\beta = 53°$

Fig. 18 Schematic projections of cellulose chains on the plane $ac \perp b$. The glucose rings are shown as ovals, molecules of reagent as circles.

investigations (37,38) led to the proposal of a rhombic unit cell for the crystallites by Polyani (39). However, more detailed work by Meyer and Mark (40) led them to suggest the presence of a monoclinic unit cell and this was later confirmed by Gross and Clark (41). The orientation of the chains within the unit cell remained unknown for some time, but in 1937 Meyer (42) proposed that the chains were aligned mutually antiparallel. This proposal was upheld by the work of Misch (43), who estimated the intensities of X-ray reflections in various planes from the Meyer unit cell and showed that the high theoretical intensity associated with the 002 plane corresponded with the high measured intensity of the same plane, observed from X-ray photographs. Fig.17 illustrates the generally accepted Meyer-Misch model for natural cellulose (Cellulose I). Measurements of other physical properties also support this model (44).

A different crystalline form from natural cellulose (Cellulose II) was obtained on the treatment of natural cellulose with 18% caustic soda or on the regeneration of cellulose as viscose. Andress (45) proposed a modified monoclinic unit cell for Cellulose II in which

a	=	8.14 Å,	i.e.	0.814 nm.
b	=	10.3 Å	i.e.	1.03 nm.
c	=	9.14 Å	i.e.	0.914 nm.
β	=	62°		

In this unit cell, it was shown that rotation of glucose rings from the ab plane into the diagonal $10\bar{1}$ plane had occurred (Fig.18) and this was confirmed by Kratky (46).

Warwicker et al. (47-49) applied X-ray techniques to cotton (Cellulose I) and cotton swollen in caustic soda (Cellulose II). They attempted to account for the swelling behaviour of cotton in terms of cellulose sheets

TABLE IV

Type	System	a (nm)	b (nm)	c (nm)	β°	Density g/cm^3
I	Monoclinic	0.820	1.030	0.790	83.3	1.625
II	"	0.802	1.030	0.903	62.8	1.620
III	"	0.774	1.030	0.990	58	1.610
IV	Orthor-hombic	0.812	1.030	0.799	99	1.610

in the 101 plane and suggested that the glucose rings within the sheets were oriented normal to the surface of the sheets in Cellulose I, but inclined at an angle in Cellulose II. Lattices constructed from the sheets were also proposed by Warwicker and Jeffries (47).

However, Manjunath (50) pointed out that the packing of 101 planes should be denser in Cellulose II than in Cellulose I on the basis of Warwicker's model; but this was not borne out by X-ray evidence. Manjunath also pointed out that Warwicker's model predicted a greater hydroxyl group reactivity in Cellulose I, whereas a greater reactivity in Cellulose II was observed. He thus suggested that the structures for Cellulose I and Cellulose II proposed by Warwicker should be reversed, thus overcoming these problems.

Manjunath also questioned the existence of Cellulose I sheets, but Warwicker and Jeffries still maintained their existence (51).

Two other basic modifications of cellulose exist, namely Celluloses III and IV. Cellulose III is formed when cellulose is treated with liquid ammonia (52, 53). (Two distinct forms of Cellulose III have been established by Mann and Marrinan and these are discussed later in this chapter). Cellulose IV is formed when cellulose is treated with water under pressure or glycerine, between 100 and 300°C. (54). Unit cell dimensions have been derived for all celluloses by Viswanathan (55) from papers by Ellefsen (56, 57) and these dimensions are shown in Table IV.

1.5.1 (C) Infra-red and other Evidence for the Structure of Cellulose

Mann and Marrinan (58, 59) developed the infra-red deuteration work of Rowen et al (60-62) and produced a method for the determination of the total amount of crystalline material present in samples of cellulose. Spectra in the 3 μm (3333 $cm.^{-1}$) region were observed, before and after

deuteration of samples with D_2O liquid and vapour. The ratio of the new OD peak intensity after vapour deuteration to the remaining crystalline OH peak was taken as the amorphous: crystalline ratio. In measuring such a ratio, they implied a distinct separation between crystalline and amorphous regions, since vapour phase deuteration was assumed to take place only in amorphous regions. Such an implication is not, however, compatible with the X-ray evidence of Hermans et al (63-66), who maintain that water is able to penetrate the crystalline lattice. This implication also accounts for the discrepancy between Mann and Marrinan's results for crystalline : amorphous ratio and accessibility and the results measured by other methods, such as X-ray methods (67, 68), iodine absorption (69) and sorption ratio methods (70, 71).

The work of Mann and Marrinan was, however, very important, since it established the existence of different forms of Celluloses III and IV. Treatment of Cellulose I and Cellulose II with liquid ammonia, followed by evaporation of the liquid ammonia at room temperature, produced Celluloses III_I and III_{II} respectively. In a similar way, Celluloses IV_I and IV_{II} were formed on treatment of Cellulose I and Cellulose II with water under pressure or with glycerine between 100 and 300°C.

Birefringence measurements on Cellulose III made by Manjunath and Peacock (72) showed the birefringence of Cellulose III_I to be greater than that of Cellulose III_{II}. They argued that since these forms had the same lattice structure, i.e. unit cell, there must be some difference in the parent cellulose molecules, namely Celluloses I and II, which was not due to a difference in lattice structure. It was thus contended that this difference was due to the fact that Celluloses I and II possessed different chain conformations and consequently assigned straight and bent chain conformations to Cellulose I and II respectively.

The existence of different forms of Cellulose III and IV, and the reversion of these forms to the parent cellulose on various treatments,

indicate the difficulty of a complete reversion of Cellulose II to Cellulose I, although Manjunath and Peacock (73) do indicate that the recrystallisation of some Cellulose I in Cellulose II occurs under certain conditions (73). Many other workers have made measurements of the relative proportions of crystalline and amorphous material present in cellulose by infra-red deuteration techniques, since important properties, such as tensile strength, water absorption and chemical reactivity are related to this (74-77).

Much important work concerning the observations of absorption spectra of Cellulose I and II and the interpretation of the results in terms of vibrational modes and crystalline structure, was done by Marchessault and Liang (78-80). Their work contributed greatly to the understanding of the structure of cellulose, especially in showing which bonds were intermolecularly and intramolecularly hydrogen bonded and in confirming the orientations of chains in Cellulose I and Cellulose II lattices.

Mann and Marrinan (58) had previously suggested the possibility of intramolecular hydrogen bonding in Cellulose I between C_6 hydroxyl groups and C_3 hydroxyl groups of the next residue in the same chain. However, such bonding was incompatible with Liang and Marchessault's findings that CH_2 symmetric stretching and bending modes showed parallel dichroism. Liang and Marchessault thus suggested that intermolecular hydrogen bonding occurred between C_6 hydroxyl groups and the oxygen bridge atoms of neighbouring chains. In addition it was proposed that such bonding could occur in 101 and $10\bar{1}$ planes, and vibrational modes in these planes were tentatively assigned to spectral bands which occur at 3.026 μm. (3303 $cm.^{-1}$) and 2.937 μm. (3405 $cm.^{-1}$) respectively. It was considered that two such bands could also occur in 002 and $00\bar{2}$ planes, but the intensities of such peaks were expected to be weak and no attempt was made to identify such peaks. They did, however, maintain that intramolecular bonding must occur in order to account for a strong parallel hydroxyl stetching band observed

TABLE V

Infra-red Sepctrum of Cellulose I

Wavelength (μm.)	Frequency cm.$^{-1}$	Polarization	Assignment
15.08	663	$\perp$	OH out-of-plane bending
14.29	700	$\perp$	OH out-of-plane bending
14.20	740	$\perp$?	CH_2 rocking ?
12.50	800	$\perp$?	ring breathing (β)
11.17	895	$\parallel$	antisymmetrical out of phase stretching
10.15	985	$\perp$?	
10.0	1000	$\parallel$?	
9.857	1015	$\parallel$	C-O stretching
9.6618	1035	$\parallel$	
9.4517	1058	$\parallel$	
9.0090	1110	$\parallel$	antisymmetrical in phase ring stretching
8.8888	1125	$\parallel$	
8.6059	1162	$\parallel$	Antisymmetrical bridge oxygen stretching
8.2988	1205	$\perp$	OH in-plane bending ?
8.0971	1235	$\parallel$	
8.0000	1250	$\perp$	
7.8003	1282	$\parallel$	CH bending
7.5930	1317	$\perp$	CH_2 wagging
7.4850	1336	$\perp$	OH in-plane bending
7.3638	1358	$\parallel$	
7.2780	1374	$\parallel$	CH bending
6.9930	1430	$\parallel$	CH_2 bending
6.8729	1455	$\perp$	OH in-plane bending
6.1162	1635		absorbed H_2O
3.505	2853	$\parallel$	CH_2 sym. stretching
3.484	2870	$\perp$	
3.451	2897	$\perp$	CH stretching
3.431	2914	$\perp$	
3.396	2945	$\perp$	CH_2 antisym. stretching
3.367	2970	$\parallel$	CH stretching
3.081	3245	$\parallel$	
3.053	3275	$\parallel$	
3.026	3305	$\perp$	OH stretching (intermolecular hydrogen bonds in 101 plane)
2.985	3350	$\parallel$	OH stretching (intramolecular hydrogen bonds)
2.963	3375	$\parallel$	
2.937	3405	$\perp$	OH stretching (intermolecular hydrogen bonds in $10\bar{1}$ plane)
2.899	3450	$\parallel$	Cellulose II impurity ?

TABLE VI

Infra-red Sepctrum of Cellulose II

Wavelength (μm)	Frequency $cm.^{-1}$	Polarization	Assignment
15.384	650	⊥	OH out-of-plane bending
14.285	700	∥	
13.157	760	⊥	CH_2 rocking ?
12.500	800	⊥	Ring breathing ( )
11.210	892	∥	C_1 group frequency
10.362	965	∥	
10.040	996	∥	
9.950	1005	⊥?	
9.8039	1020	∥	C-O stretching
9.6618	1035	⊥	
9.4340	1060	∥	
9.2764	1078	∥	
9.0334	1107	∥	Antisymmetric in-phase ring stretching (ν_{ai})
8.6580	1155	∥	Antisymmetric bridge oxygen stretching
8.3333	1200	⊥	OH in-plane bending ?
8.1633	1225	⊥	
7.9554	1257	⊥?	
7.8301	1277	∥	CH bending
7.6046	1315	⊥	CH_2 wagging
7.4901	1335	∥	OH in-plane bending
7.3260	1365	∥	
7.2727	1375	∥	CH bending
7.0621	1416	∥	CH_2 bending
6.9444	1440	∥	
6.8027	1470	⊥	OH in-plane bending
6.1162	1635		Absorbed H_2O
3.5088	2850	∥ ?	CH_2 symmetric stretching
3.4795	2874	⊥	CH stretching
3.4590	2891	⊥	
3.4435	2904	⊥	
3.4095	2933	⊥ ?	CH_2 antisymmetric stretching
3.3841	2955	∥	CH stretching
3.3693	2968	∥	
3.3546	2981	⊥ ?	
3.1496	3175	⊥	OH stretching (intermolecular hydrogen bonding)
3.0257	3305	⊥	
2.9851	3350	⊥	OH stretching (intramolecular hydrogen bonding)
2.9011	3447	∥	
2.8670	3488	∥	

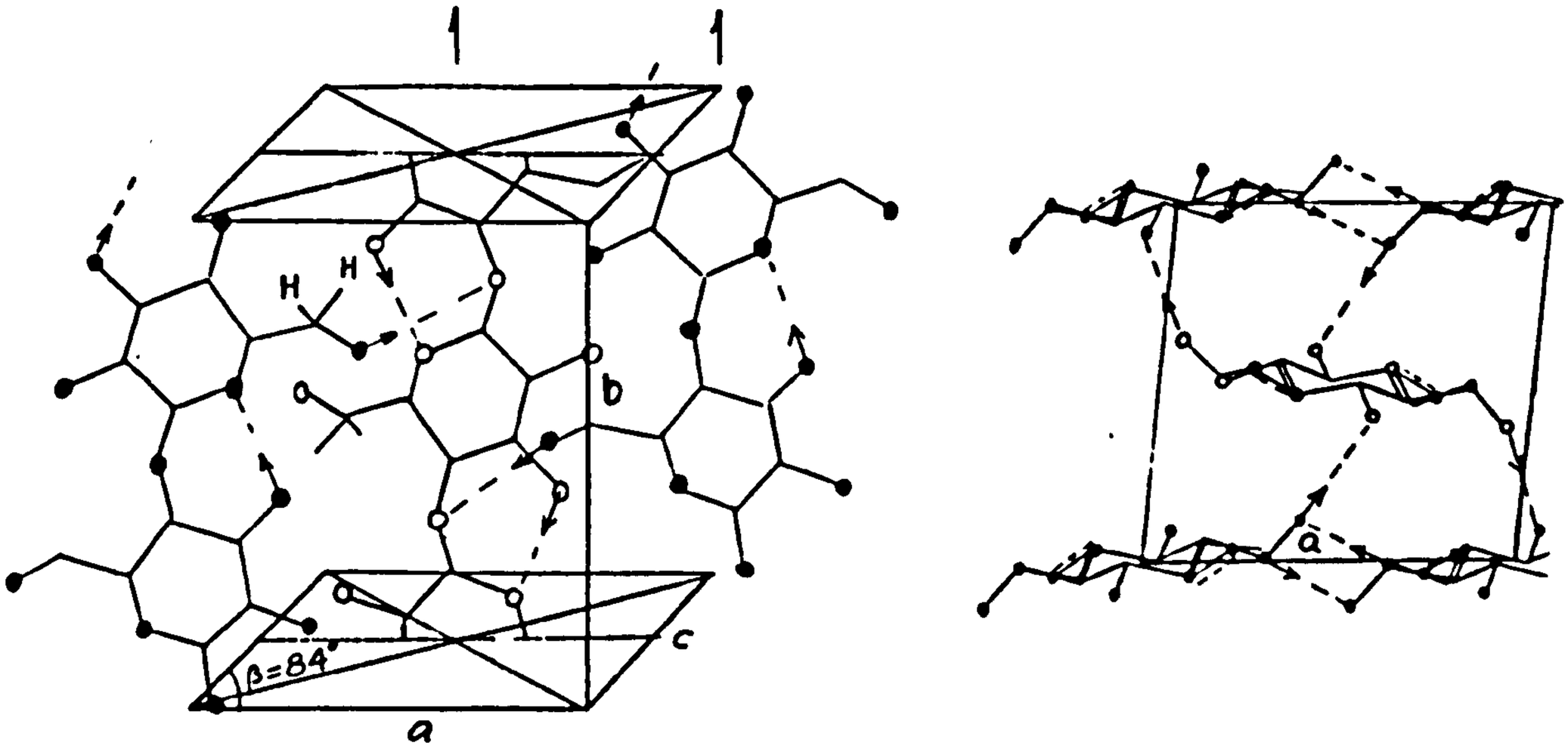

(A) (B)

Fig. 19 (A) Arrangement of CH_2OH groups in cellobiose unit; (B) hydrogen bonds. Cellulose I unit cell.

at 2.985 μm.(3350 cm.$^{-1}$). This peak was assigned to one of the intramolecular hydrogen bonds allowed for by the Herman's model (81), namely a bond between a C_3 hydroxyl group and the ring oxygen atom of the next residue.

The inter- and intramolecular hydrogen bonds proposed by Liang and Marchessault required some bending of chains to occur, but this was not considered to be incompatible with existing unit cell dimensions. The arrangement of chains and hydrogen bonds in the unit cell is shown in Fig.19. Ring stretching frequencies were assigned from the results of work on small analogous ring molecules (82-84).

The observed bands and assignments for Celluloses I and II are shown in Tables V and VI respectively. As can be seen from a comparison of these tables, many of the frequencies of Cellulose I were almost unchanged in Cellulose II. The polarization of CH_2 stretching bands was found to be the same in both structures, thus suggesting similar intermolecular hydrogen bonding involving C_6 hydroxyl groups and intramolecular hydrogen bonding involving C_3 hydroxyl groups. However, in the case of Cellulose II some rotation about $C_1 - O_1$ and $C_4 - O_1'$ linkages was required in order to account for the unit cell structure, in addition to the bent chain conformation also present in Cellulose I. (Atoms labelled with a dash, e.g. O_1' etc are in adjacent residues of the same chain). Thus before intramolecular hydrogen bonding between C_3 hydroxyl groups and O_5' atoms can occur along the length of a molecule, successive glucose residues must have different orientations (Ψ) about the $O_1.....O_1'$ axis (85), with alternate residues similarly inclined. It was thus proposed that successive glucose residues had different environments so that two types of $C_3OH.....O_5'$ intramolecular hydrogen bonds exist. Vibrations for these two types of bond were ascribed to the two parallel bands at 2.901 μm. (3447 cm.$^{-1}$) and 2.867 μm.(3488 cm.$^{-1}$).

The lower dichroism of the CH_2 stretching and bending frequencies of

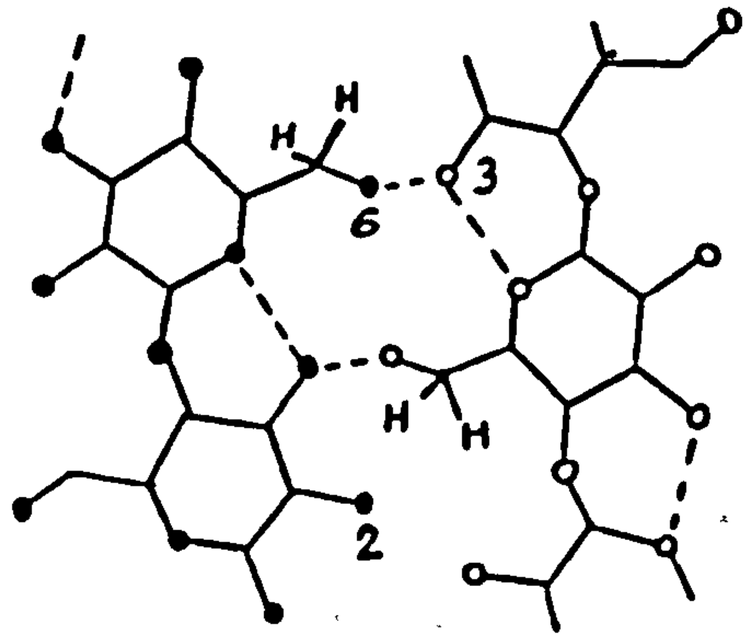

Fig.20A Hydrogen bonding scheme in the $10\bar{1}$ plane: $r \simeq 0.17b$, $\varphi \simeq 30°$.

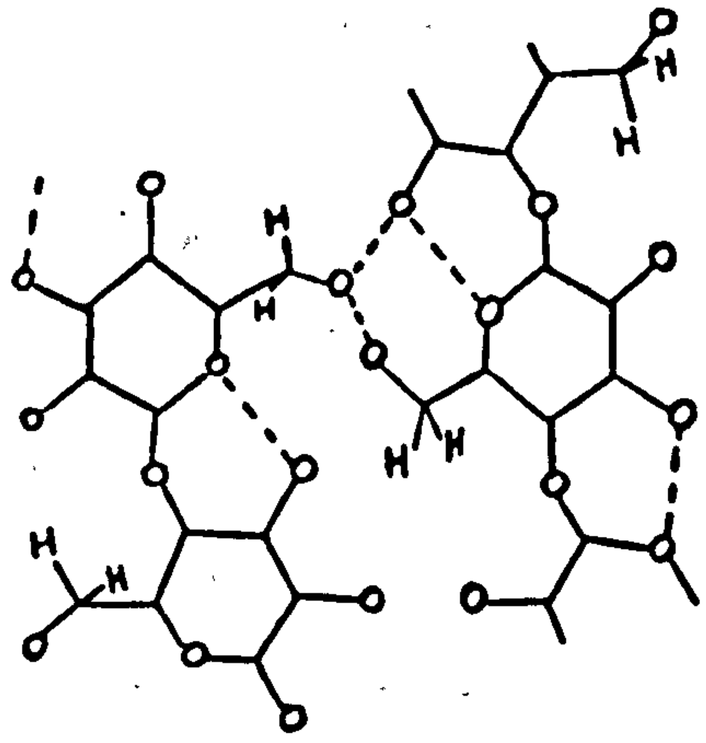

Fig.20B Hydrogen bonding scheme in the $10\bar{1}$ plane: $r \simeq 0.30b$, $\varphi \simeq 30°$.

Cellulose II as compared with Cellulose I was attributed to the skewing of chains and rotation of glucose units. Five other hydroxyl bands were detected in the spectrum of Cellulose II which had counterparts in the Cellulose I spectrum. Changes in the dichroism of some of these bands enabled tentative assignments of the 15.384 μm.(650 $cm.^{-1}$) to the C_6 hydroxyl group and the 6.8027 μm.(1470 $cm.^{-1}$) band to the C_2 or C_3 hydroxyl group.

Marchessault and Liang also constructed schemes of hydrogen bonding (Figs. 20A & 20B) which were compatible with unit cell dimensions. Fig.20B illustrates a scheme involving the reversal of chains. Although they did not find any evidence for reversal or non reversal, the scheme of Fig.20B was preferred, since it could more easily explain the existence of two observed perpendicular bands and was compatible with the Andress unit cell (45). The parameter r , defined by Jones (85) refers to the shift of the central chain in the unit cell relative to one corner of it. Wahba (86) observed the effect of temperature and drying on the infra-red spectrum of Cellulose II films with respect to the second order transition around 25°C., previously reported (87-89). Wahba was also able to demonstrate the existence of two types of hydrogen bond: the first exhibited a rapid response to temperature (i.e. breaking rapidly with increased temperature and reforming rapidly on cooling), while the second type was formed more slowly and at an increasing rate with decrease of temperature below 60°C.

Ramiah and Goring (88) had previously assigned the second order transition near 25°C to the breaking of intramolecular hydrogen bonds between C_3 hydroxyl groups and O_5' atoms, and they assumed that these bonds were weaker than intermolecular hydrogen bonds involving C_6 hydroxyl

groups. Wahba also assigned the bonds which responded slowly to temperature changes to the second order transition at 25°C. and hence to the intramolecular $C_3OH.....O'_5$ hydrogen bonds.

Ramiah and Goring also detected a further transition between 80 and 110°C. from thermal expansion measurements on cellulose and stated that this might be due to the motion of restricted segments of cellulose chains. A further transition between 170 and 240°C., determined from elastic modulus measurements (90), was attributed to a 'glass type' transition.

The application of infra-red spectroscopy to treated celluloses has proved invaluable for the assessment of structural and chemical changes. For example, it has been possible to establish the existence of cross links in resin treated cotton, and in addition, the relative proportions of singularly linked and cross linked reagent (91 & 92).

1.5.2 The Structure of Dicel

Nuclear magnetic resonance (N.M.R.) studies on cellulose diacetate (degree of substitution 2.38) by Goodlet et al (93) showed a multiplicity of peaks for acetyl groups. This multiplicity was caused by a large number of interactions of the acetyl groups with remaining hydroxyl groups. It was hence concluded that dicel molecules do not have a regular structure, i.e. that acetylation has occurred irregularly to produce atactic molecules. This atacticity explains the very low crystallinity of the polymer, i.e. its failure to pack into a regular crystalline lattice. This lack of crystallinity explains why little information may be obtained about the structure of dicel from X-ray diffraction techniques.

Goodlet et al (93) were able to remove the multiplicity caused by hydroxyl peaks by the full acetylation of the diacetate with $CD_3CO.Cl$. The three peaks which corresponded to the original acetyl protons at the C_2, C_3 and C_6 positions of the glucose residues comprising the cellulosic

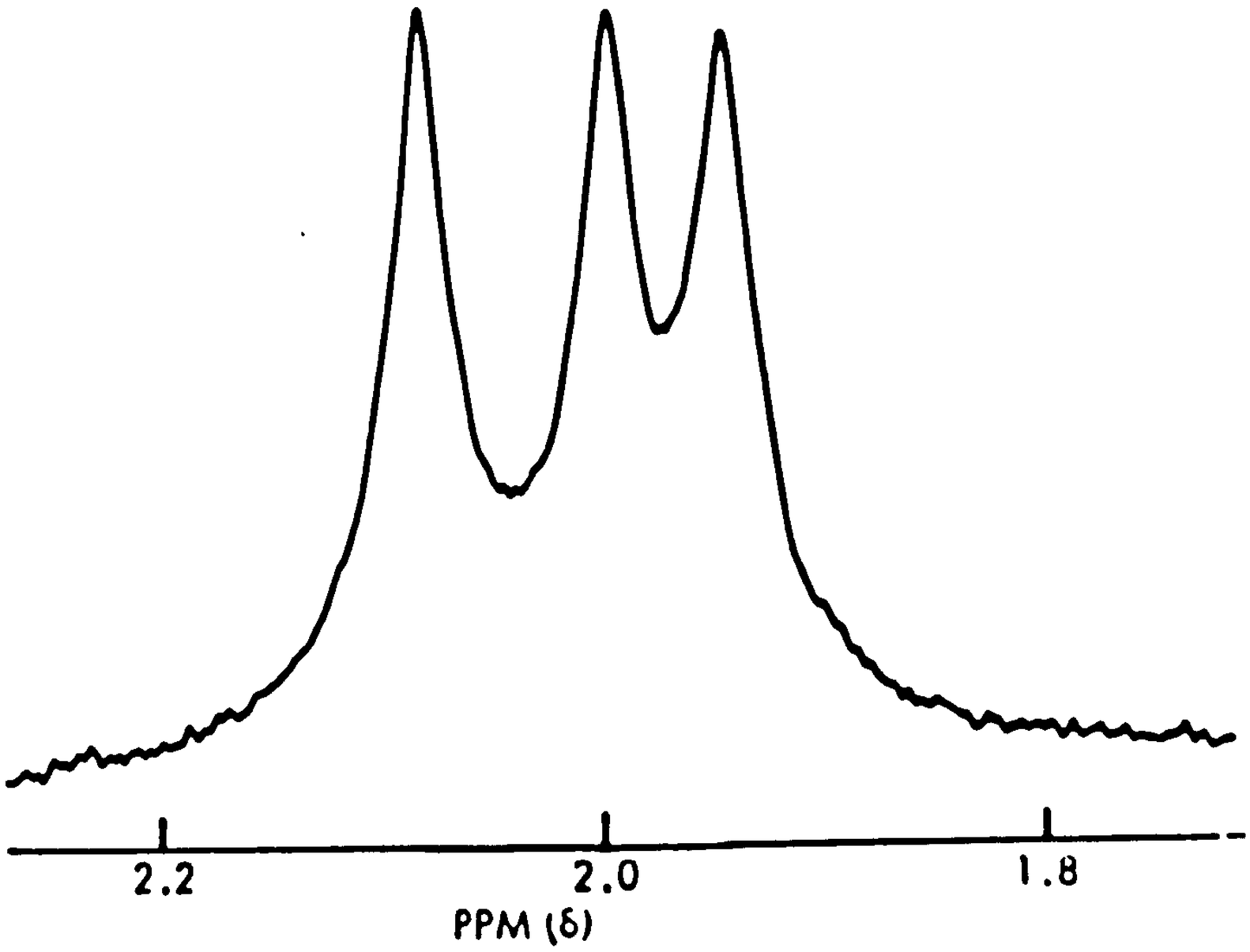

Fig.21A Acetyl peaks of cellulose triacetate.

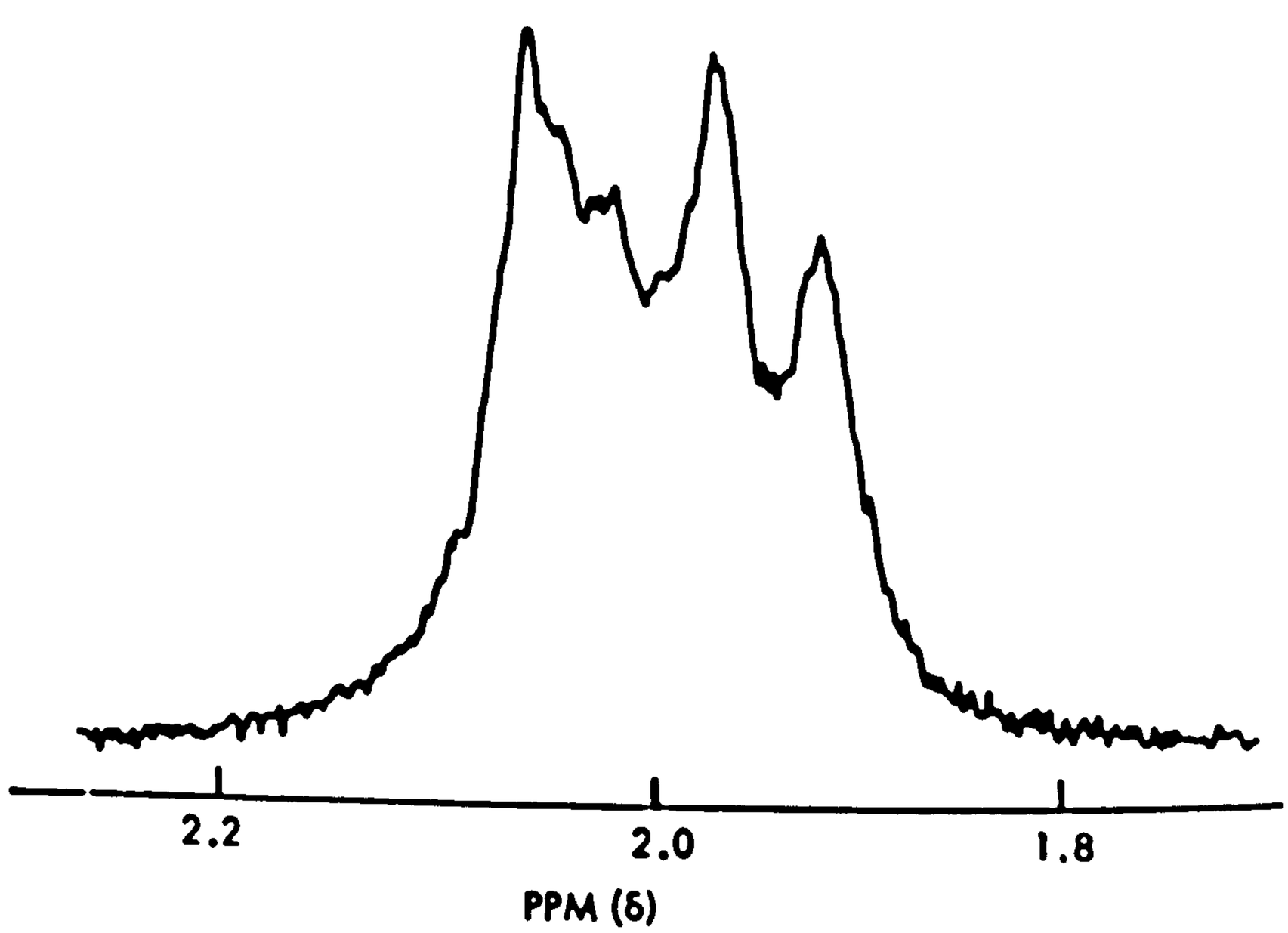

Fig.21A Acetyl peaks of fiber-grade cellulose acetate (D. S. = 2.38).

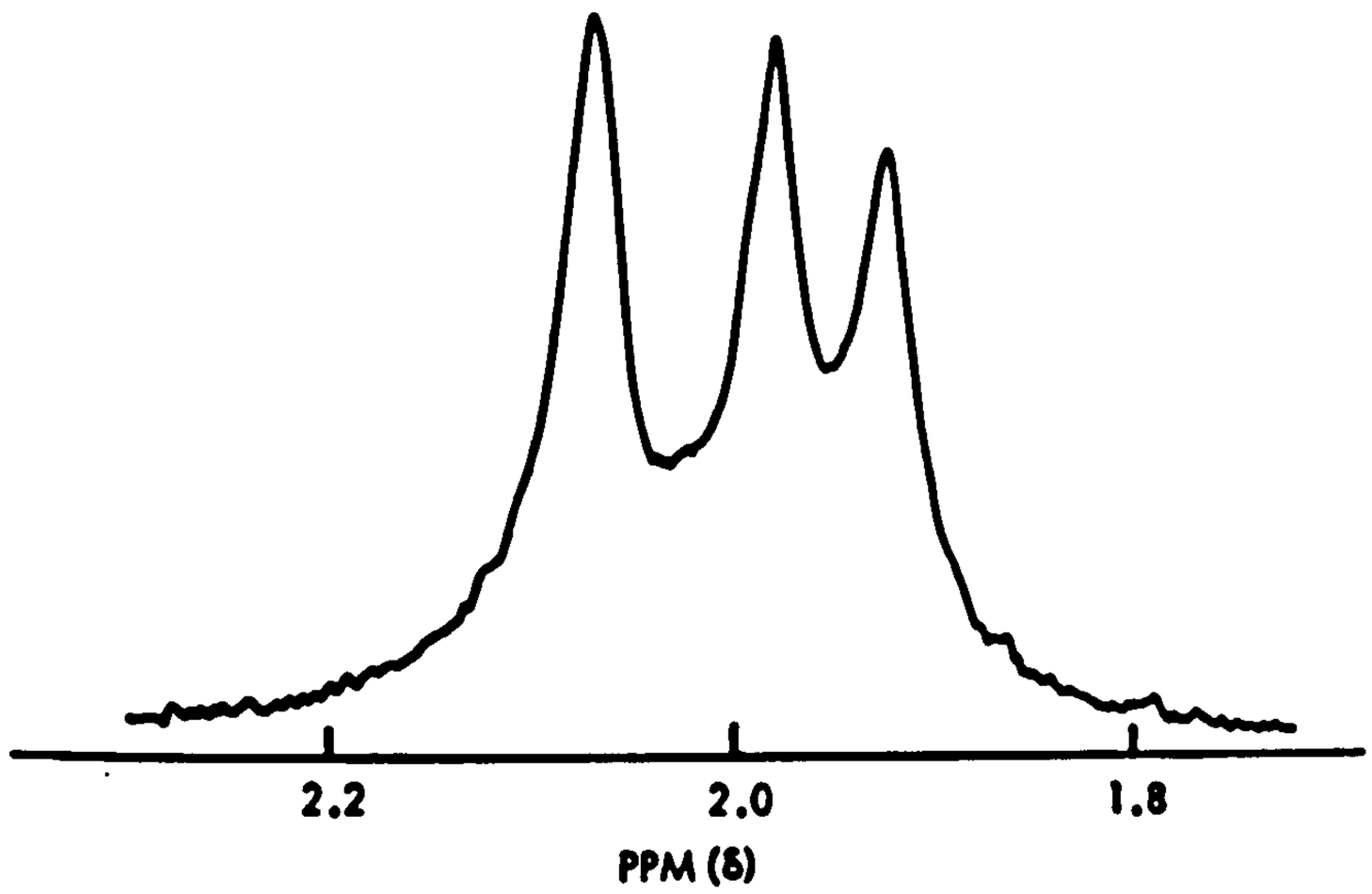

Fig.21B Acetyl peaks of fiber-grade cellulose acetate prepared by hydrolyzing with low water content (treated with CD_3COCl).

backbone of the diacetate molecules, were thus clearly observed. (Figs. 21A & 21B). Peak intensities were compared to evaluate the relative amounts of acetylation at C_2, C_3 and C_6 positions of the glucose residues. The assignments of the three peaks to C_2, C_3 or C_6 positions was made by employing the methods of Malm (94) and Gardner (95). The C_6 position was found to exhibit the lowest extent of actylation and it is possible that this is due to strong intermolecular hydrogen bonding of C_6 hydroxyl groups in the parent cellulose molecules. Similarly, intramolecular hydrogen bonding of C_3 hydroxyl groups in parent cellulose molecules can also account for the low degree of substitution at C_3 positions of glucose residues which comprise the diacetate molecules. However, since the degree of substitution at C_6 positions is slightly lower than at C_3 positions, it is clear that intermolecular hydrogen bonding of C_6 hydroxyl groups is slightly stronger than the intramolecular hydrogen bonding of C_3 hydroxyl groups in the parent cellulose molecules. This is a reasonable deduction, since C_6 hydroxyl groups project from the cellulose chain and may approach the oxygen bridge atoms of neighbouring chains, thus forming very strong hydrogen bonds. However, movement of C_3 hydroxyl groups within a chain is more restricted, so that intramolecular hydrogen bonds will tend to be longer and hence weaker. Such an explanation was upheld by Goring (88) and is also compatible with Marchessault and Liang's scheme of hydrogen bonding.

Acetylation at the C_2 position was found to occur to the highest extent and may be accounted for by assuming that C_2 hydroxyl groups of glucose residues which comprise parent cellulose molecules are the least involved in hydrogen bonding, or are involved in the weakest hydrogen bonding.

1.5.3 The Structure of Tricel

Although a vast amount of work has been done on the structure of cellulose and some cellulose derivatives, comparatively little work has

been carried out on the structure of cellulose triacetate. However, some early X-ray work was done by Herzog (96), Hess and Trogus (97-99) and Naray - Szabado (100). Their results show the presence of two polymorphic forms of cellulose triacetate, namely Triacetate I and Triacetate II, which are formed by acetylation of Cellulose I and Cellulose II respectively. This polymorphism was, however, challenged by Baker (101), Happey (102) and Howsmon (103).

The problem was eventually resolved by Sprague et al (104) who applied Baker and Stoll's technique (105) for sample annealing to increase crystallinity and who were able to produce X-ray photographs which were well enough defined to show, conclusively, the existence of the two different forms of triacetate. Estimates of unit cell dimensions were also made and these are given in Table VII.

TABLE VII

Unit Cell Dimensions of Triacetates I and II

Dimension	Triacetate I	Triacetate II
a	2.26 nm.	2.58 nm.
b (fibre direction)	1.05 nm.	1.05 nm.
c	1.18 nm.	1.145 nm.
	79°	66.4°
No. of cellobiose units	4	4
Calculated density	1.39 g./cc.	1.348 g./cc.

In addition, Dulmage (107) observed the X-ray diffraction patterns of cellulose triacetate films prepared by successive heat treatments and rolling, at temperatures between 160 and 215°C.. He suggested that the

TABLE VIII Summary of Dependence of Triacetate Structure on Cellulose Structure and Process History

Cellulose I	Acetylate heterog. (Low swelling)	Triacetate I	Saponify	Cellulose I
			Dissolve, Reppt.	Triacetate II → Saponify → Cellulose II
	Acetylate heterog. (High swelling)	Triacetate II or mixture of triacetates I and II		
	Acetylate Homog.	Triacetate II	Saponify	Cellulose II
Cellulose II	Acetylate (All conditions)	Triacetate II	Saponify	Cellulose II
Cellulose IV(a)	Acetylate Heterog.	Triacetate II	Saponify	Cellulose II

TABLE IX

Summary of Dependency of Triacetate Structure on Cellulose Structure and Process History[a] (Present Investigation)

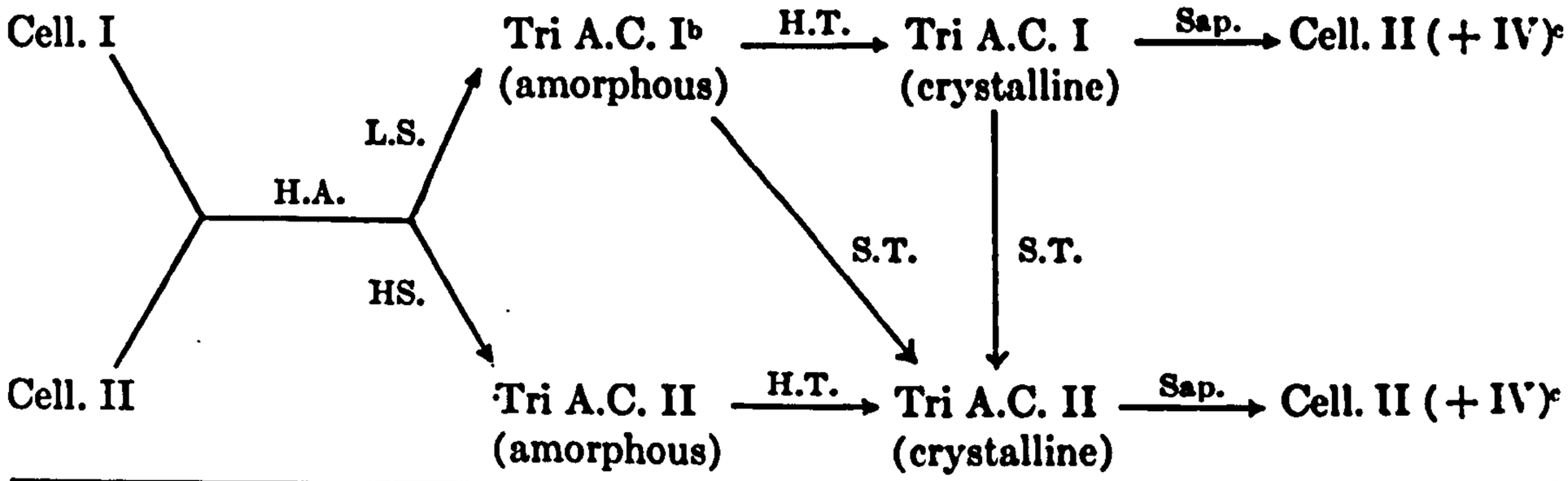

[a] Notation: Cell. = cellulose, Tri A.C. = cellulose triacetate, H.A. = heterogeneous acetylation, L.S. = low swelling, H.S. = high swelling, H.T. = heat treatment, Sap. = saponification, S.T. = steam treatment.

[b] Amorphous triacetate I is converted to a initial cellulose I.

[c] The saponification products approach cellulose II as the crystallinity of triacetates increases.

unit cell of cellulose triacetate contained four cellobiose acetate units in a pseudo-orthorhombic unit cell, with dimensions:-

a = 0.245 nm.

b = 1.156 nm.

c = 1.043 nm. (fibre axis)

Sprague also investigated some of the factors which influence the formation of each type of triacetate (Table VIII) and showed that Triacetate II was the most stable.

Further investigations by Watanabe (108) also showed that some Triacetate I could be formed from the heterogeneous acetylation of Cellulose II, which had been pretreated in a swelling medium; thus contradicting Sprague's earlier contention that Triacetate I could only be formed from Cellulose I. Watanabe also showed Triacetate I could be converted to Triacetate II on heating with superheated steam and that highly ordered Triacetates I and II were converted largely to Cellulose II upon saponification (Table IX).

Several other techniques, such as gas chromatography (109-112), differential scanning calorimetry (113) and dilatometry (114-118) have also been applied to studies of triacetates in order to assess structural modifications which arise. The dilatometry measurements of Sharples (117) showed that tricel possessed three second order transitions at 46, 112 and 157°C.. Sharples and Sperling (117) concluded that the transition at 46°C. was due to a 'boat to chair' conformational change in the acetylated glucose residues which constitute the cellulose triacetate molecules. They attributed the transition at 112°C. to a side chain transition, since the transition became much less marked with increased side chain length in related polymers. The third transition at 157°C. was known to correspond to the glass transition temperature.

Nakamura (113) also found another transition in tricel, from gas chromatography measurements on tricel film, when samples cast on modified Kieselghur gave a transition at 83°C.. Dilatometry measurements on tricel

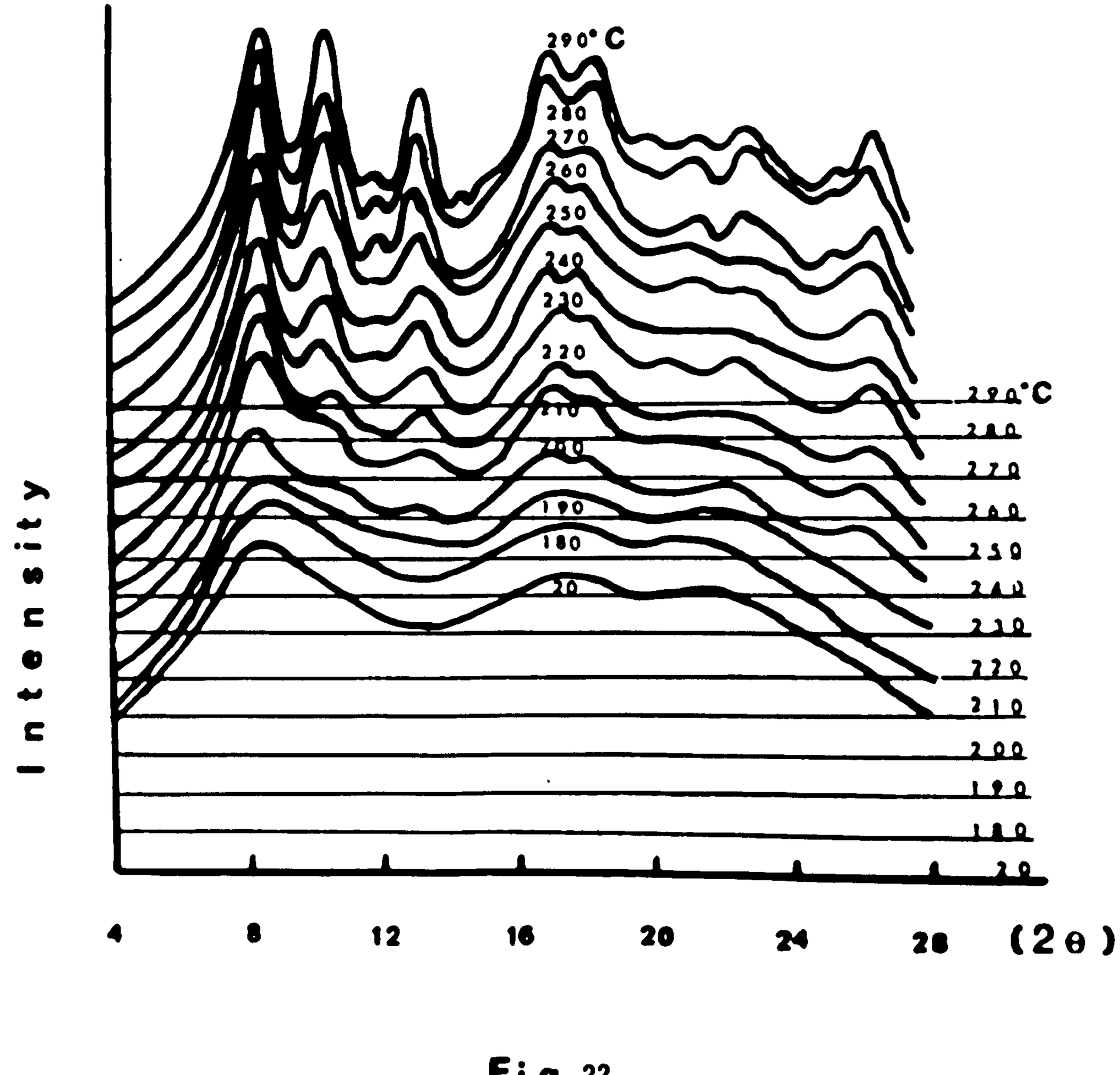
290° C
280
270
260
250
240
230
220
210
200
190
180
170
160
150
140
130
120
110
100
90
Intensity
4
8
12
16
20
24
28
(2θ)

Fig.22

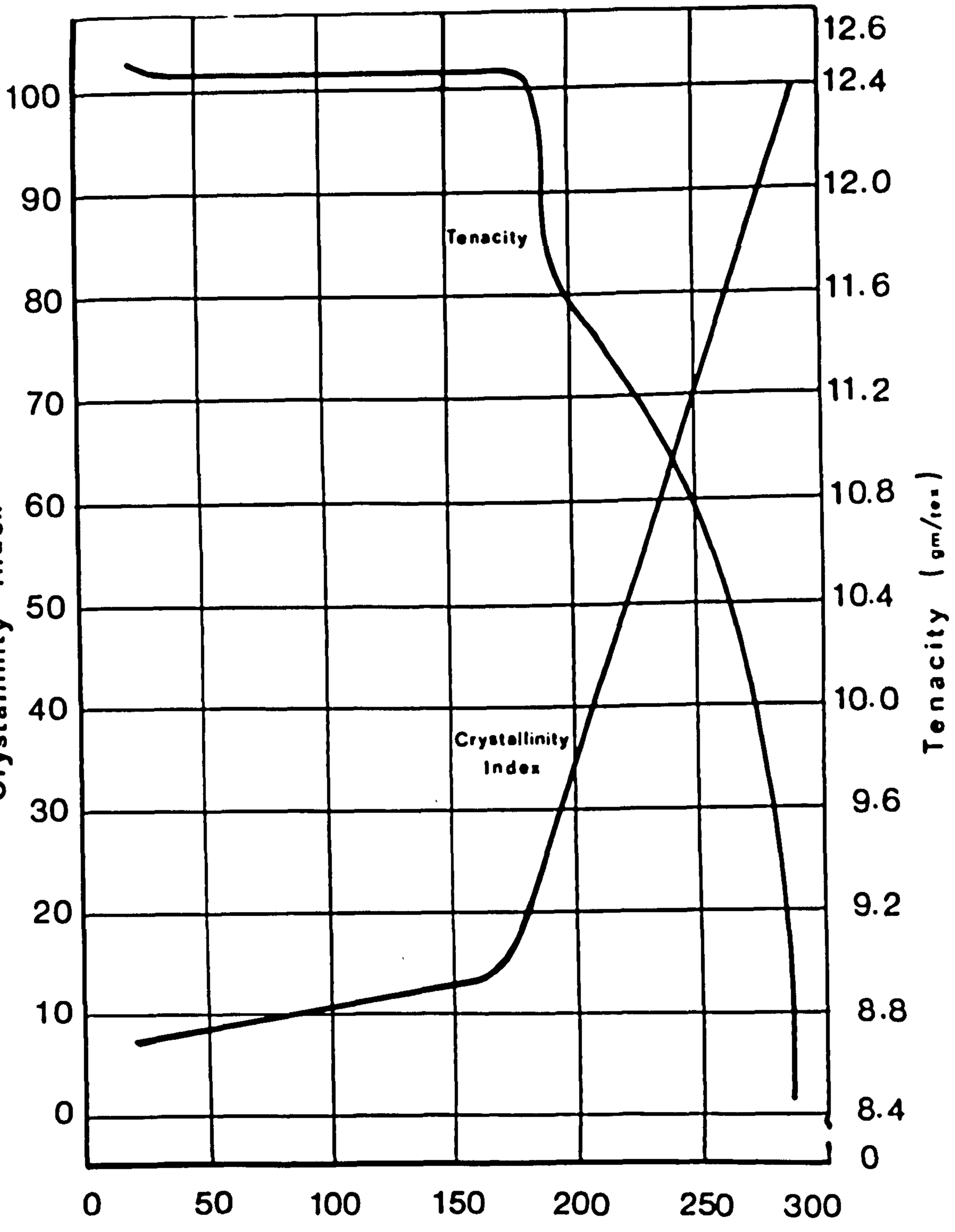

Fig.23 Crystallinity Index and Tenacity

film also gave a transition at 91°C. and Nakamura suggested that these transitions could be related to side chains.

Hindeleh (119) observed the X-ray diffractograms of various samples of cellulose triacetate and noted that large changes took place above 180°C.. Diffractograms of triacetate yarn annealed at various temperatures for 10 minutes were then taken. (Fig.22). An analysis of the results in terms of crystallinity index and temperature (Fig.23) showed that a sharp rise in crystallinity index (i.e. rapid crystallization) had occurred near 180°C..

1.6 The Structure of Water and Ice

1.6.1 Introduction

As will be seen in Chapters 3 and 4, much of the work carried out has been concerned with the absorption of water by cellulosic materials. It is relevant therefore to examine, at this point, the current theories of water structure, since these are necessary to an understanding of the results obtained. A brief discussion of the main theories of the structure of ice is also included, since some of the theories of the structure of liquid water propose that some ice structures are present within the liquid water system.

1.6.2 Structure of Water

Despite the immense amount of research devoted to studies of water, the structure of this material is not yet fully understood. This is due largely to the ability of water to hydrogen bond in many different ways. However, much important work on its structure has been done from observations of the infra-red and Raman spectra of water over a wide wavelength range (120-125). A computer analysis of infra-red spectra in the 3 μm.(3333 $cm.^{-1}$) region indicated that four Gaussian components were required to fit the spectrum with wavelengths (frequencies) at:-

3.086 μm. (3240 $cm.^{-1}$)

2.911 μm.	(3435 $cm.^{-1}$)
2.825 μm.	(3540 $cm.^{-1}$)
2.762 μm.	(3620 $cm.^{-1}$)

Similar peaks were also found for Raman spectra. Studies of the temperature dependence of these spectra led Walrafen (120-125) to assign the components at 2.825 μm, (3540 $cm.^{-1}$) and 2.762 μm, (3620 $cm.^{-1}$) to vibrations of non hydrogen bonded, i.e. 'free' water, and the vibrations at 2.911 μm. (3435 $cm.^{-1}$) and 3.086 μm. (3240 $cm.^{-1}$) to hydrogen bonded lattice water.

X-ray studies (126, 127) have also indicated the presence of a tetrahedral lattice structure in water and a hydrogen bonded model for such a structure was proposed by Walrafen (121), which corresponded to the basic structure of ice. Walrafen also studied the temperature dependence of intermolecular hydrogen bonded OH stretching and librational intensities throughout the range from 2.5 - 20 μm. (4000 - 500 $cm.^{-1}$) and found that his results could not be explained in terms of a previous continuum model. He thus suggested the presence of a structure which involved an equilibrium between 'free' and 'lattice bound' water.

A more sophisticated model was presented more recently by Frank (128), in which he proposed that cold water consisted of 'hydrogen bonded four co-ordinated framework regions with interstitial monomers occupying some of the cavities enclosed by the framework'. The precise geometry of the framework was not specified, but thought to be more regular at lower temperatures.

Such models do not, however, adequately explain all the properties of water (129).

Del Bene and Pople (130) undertook molecular orbital calculations to determine the energies of small groups of water molecules and suggested the presence in liquid water of cyclic trimers, tetramers, pentamers and hexamers, thus accounting for the radial distribution function in liquid water (129).

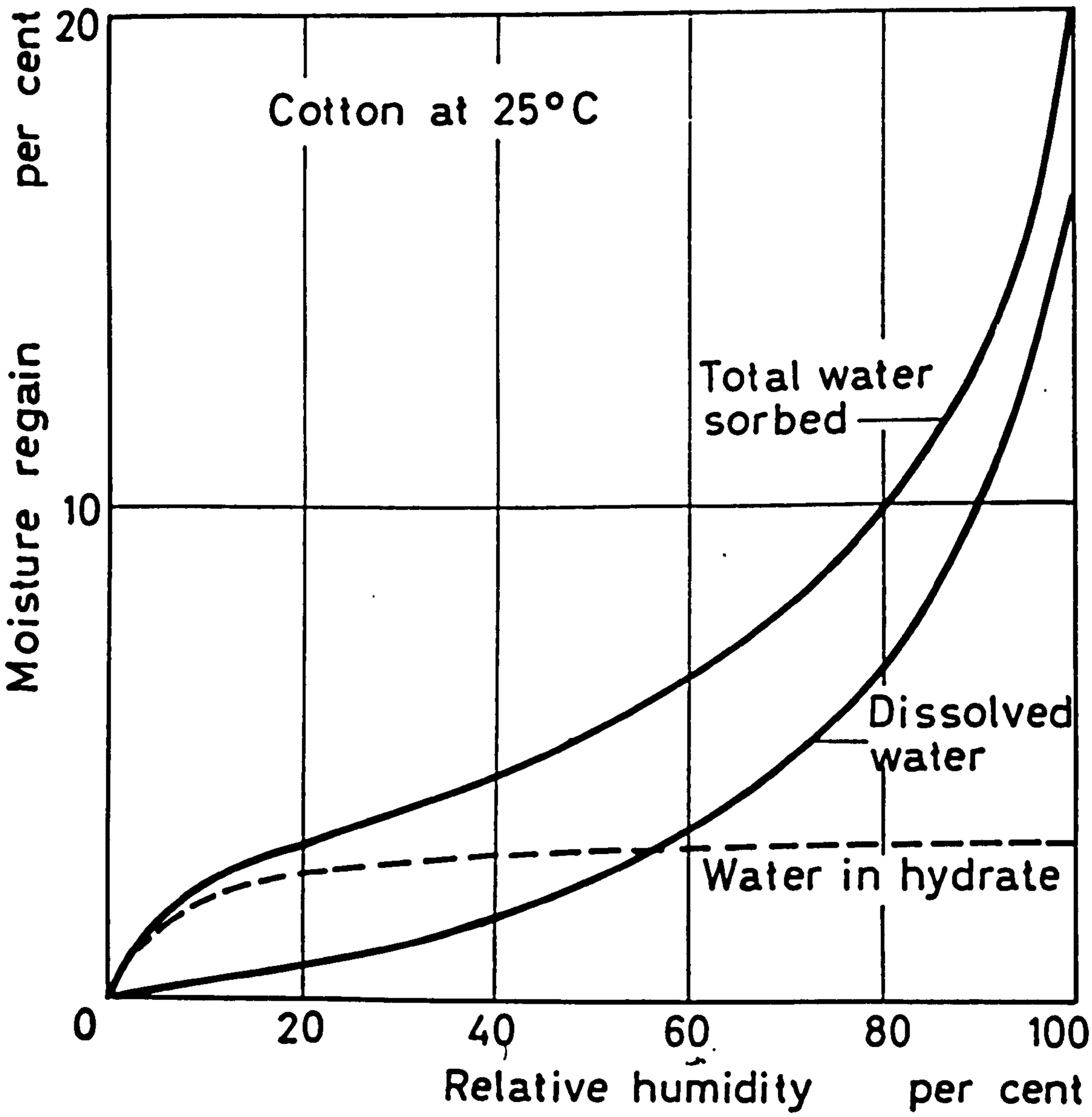

Figure 24. Composite sigmoid absorption curves

1.6.3 Structure of Ice

Ice has been shown to exist in at least ten different structures over a range of pressures and temperatures. (131,132). X-ray studies have shown that at atmospheric pressure, three forms of ice may be formed (133, 134), namely vitreous ice (I_v), cubic ice (I_c) and hexagonal ice (I_h). Vitreous ice is formed by rapidly condensing water vapour at temperatures lower than -163°C. Between -163°C. and -123°C., vitreous ice has been shown to transform to cubic ice (135-138). A further transformation from cubic to hexagonal ice has been shown to occur between -113 and -53°C. However, Beaumont (139) showed that whereas the vitreous to cubic ice transformation occurred at an increasing rate between -163 and -123°C. and at -123°C. was virtually complete within a few minutes, the cubic to hexagonal transformation took place at a much slower rate, i.e. over several hours, between -63 and -23°C. Such findings explain the inconsistency between X-ray, infra-red and calorimetric results, since the type of ice formed is dependent upon the technique and conditions of sample preparation (140 - 143).

Baptiste and Whalley (144) were able to show that the infra-red spectra of crystalline cubic and hexagonal ices were equivalent, at least for mull samples. Such a finding is consistent with the very similar structure of the two crystalline ice forms. The cubic and hexagonal lattices merely reflect different packing of units of four hydrogen bonded water molecules, co-ordinated tetrahedrally, (as in the lattice structure for water, given by Walrafen (121)).

1.7 The Absorption of Water by Cellulosic Materials

The sorption isotherm characteristic of most fibrous polymers and shown for cotton in Fig.24, was attributed by Brunauer (145) to multimolecular absorption. This view was not taken by Peirce (146) and Hailwood (147), who attributed the isotherm to the resultant of two simultaneous processes,

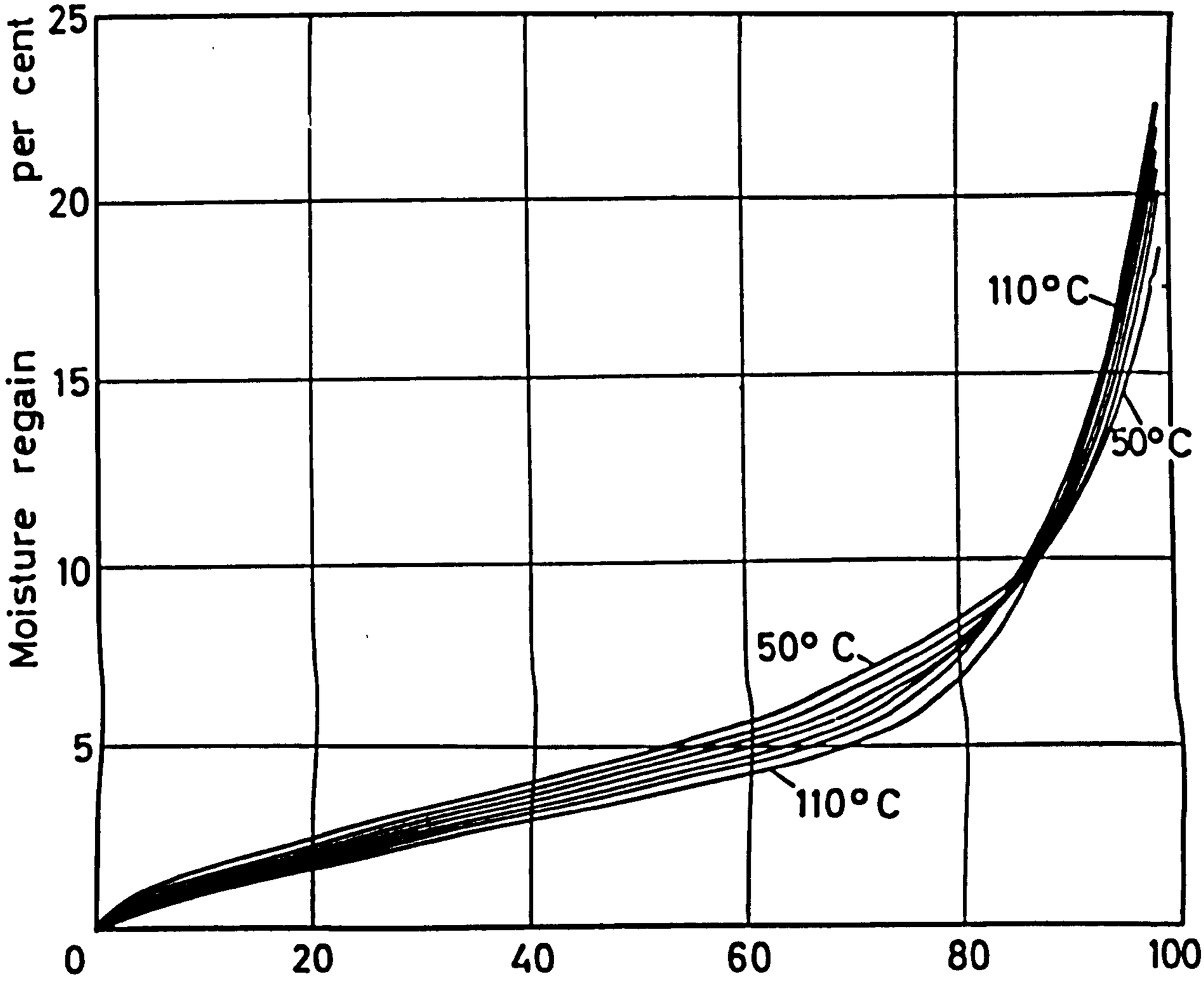

Figure 25 Effect of temperature (50–110°C) on sorption isotherms for cotton

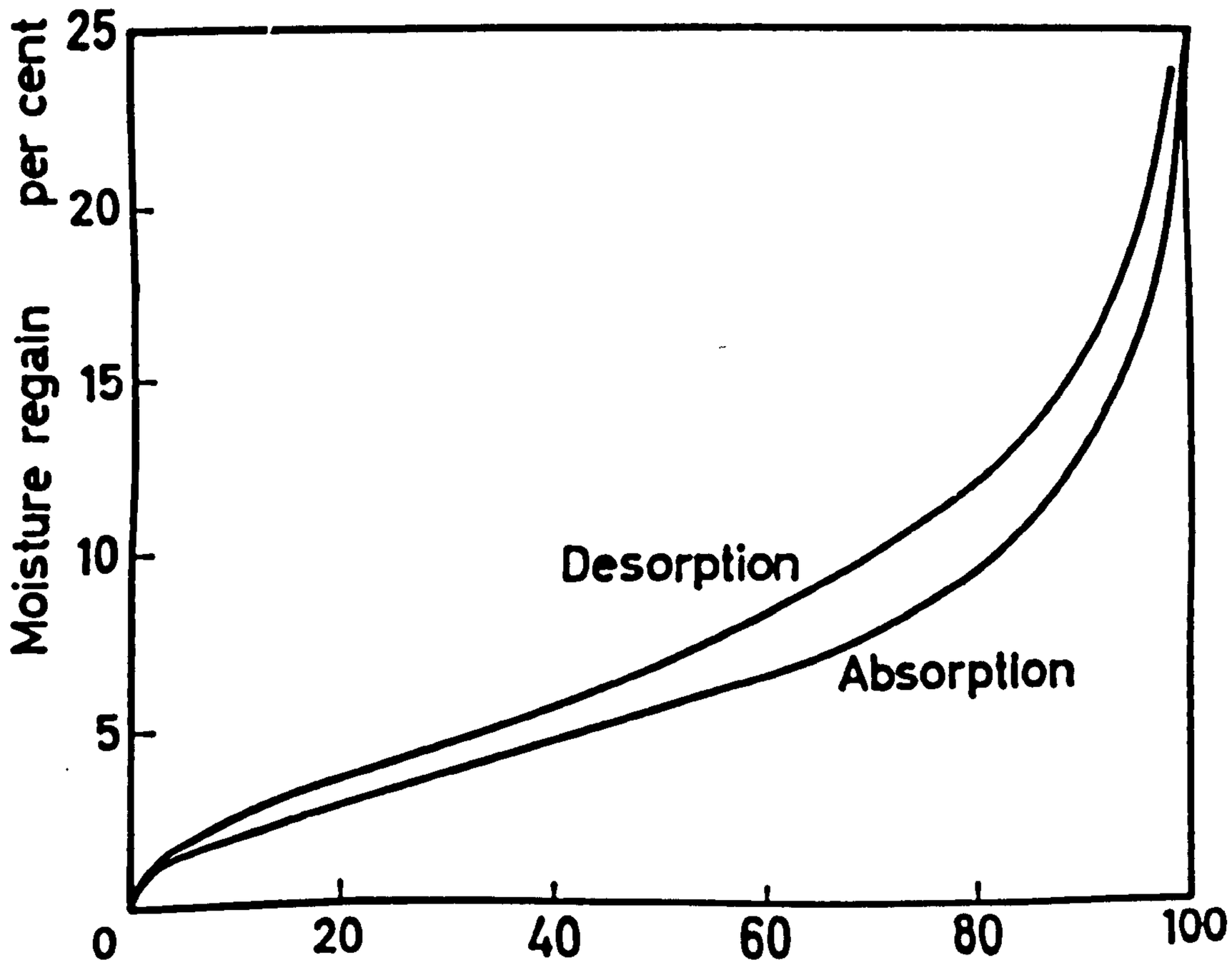

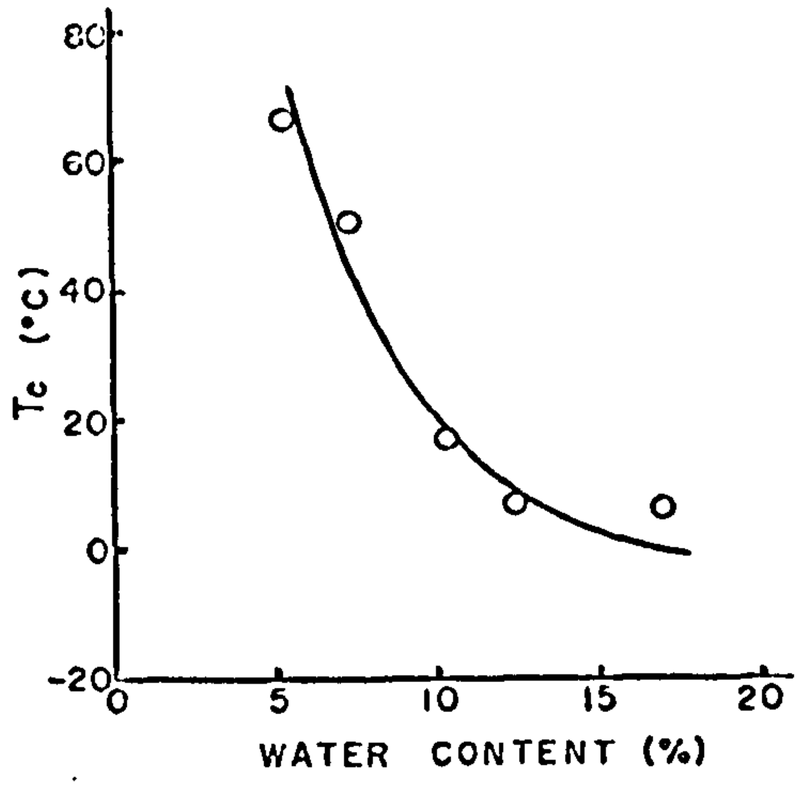

Fig.26A Relationship between T_c and water content in cotton samples.

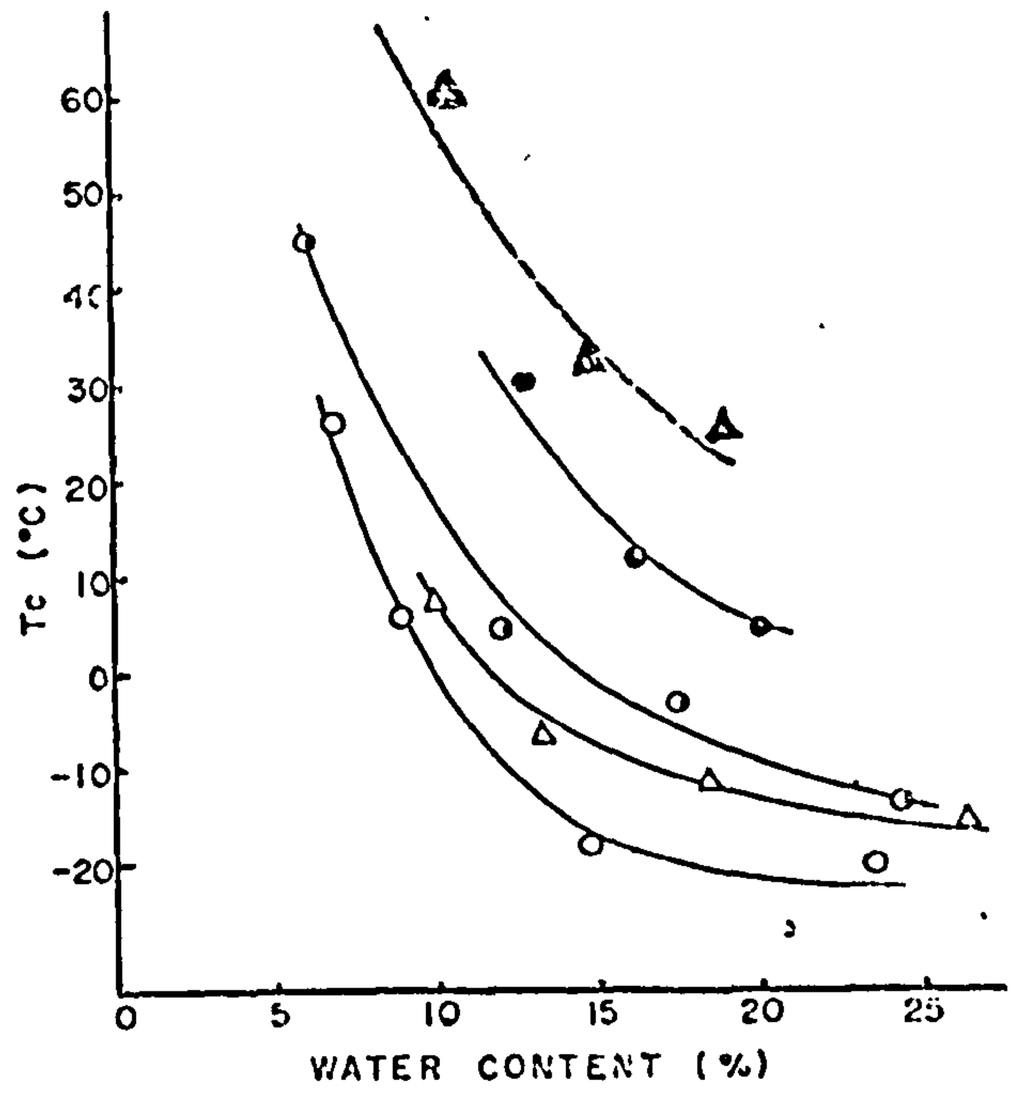

Fig.26B Relationship between T_c and water content: (○) unbeaten DP; (●) beaten DP (41°SR); (◆) beaten DP (61°SR); (△) unbeaten SCP; (▲) beaten SCP (80°SR).

(DP = Softwood Pulp ; SCP = Hardwood Semichemical Pulp ;)

namely direct combination of water molecules to fibre molecules and looser binding due to Van der Waal forces. Sorption isotherms at increasing temperatures indicated a cross over point for cotton (Fig.25), which was attributed by Urquhart (148) to water penetrating the crystalline regions of the cotton in such a way that breakage of cross links produced an increase in the total number of hydroxyl groups. Such a process is unlikely, however, since there is little spectroscopic evidence to suggest the existence of covalent crosslinks or for an increase in the total number of cellulosic hydroxyl groups at higher temperatures.

The absorption of water by cellulose has also been studied by N.M.R. spectroscopy (149-152). Ogiwara (149) measured the spectra of water in cellulose at various humidities and suggested that as the water content increased, the strength of the bonding involved in binding such water decreased. (cf Feughelman's findings for wool (153)). Ogiwara also showed that it was possible to determine the boundary temperature, T_c at which water molecules became bound to cellulose. It was shown that T_c corresponded to the glass transition temperature of a water containing sample and was dependent upon the type of cellulose and its water content (Fig.26).

The infra-red spectra of cellulose, water and the cellulose/water system have not previously been well enough resolved to reveal details of the state of water in cellulose, and a similar situation also exists for cellulose derivatives. However, Ant-Wuorinen and Visapää (154) did show that the 5.8 μm. (1724 $cm.^{-1}$) C=O peak of Cellulose I almost disappeared at humidites greater than 30% R.H., and they attributed this to the hydrogen bonding of water to C=O groups.

1.8. Scope of the Present Work

Although much work has been carried out on the structure and properties

of Cellulose II, little rigorous comparative work has been done on the cellulose derivatives dicel and Tricel II. The three substances viscose, dicel and tricel represent various degrees of acetylation from 0 to 2.95 and thus provide a means of determining how progressive acetylation affects structural and other properties such as water absorption. The application of derivative spectroscopy to these three substances now provides a means of determining much more fine structural detail and how such structure varies with water absorption.

CHAPTER 2

TABLE X

Film	Thickness (μm)	Degree of Substitution	Additives, etc.
Viscose	44	0%	Glycerol (Percentage not Quoted)
Dicel (Code: 123Y075)	75	88.3% (Representing an average of 2.65 of every 3 hydroxyl groups substituted, per glucose residue)	Residual Solvent 0.5% Triphenyl Phosphate 2 Alkyl Phthalates } 20%
Tricel (Code: 200Z090	90	98.3% (Representing an average of 2.95 out of every 3 hydroxyl groups substituted, per glucose residue)	Residual Solvent 0.5% Triphenyl Phosphate 2 Alkyl Phthalates (not specified) } Approx. 20%

CHAPTER 2

MATERIALS, METHODS AND EARLY EXPERIMENTS

2.1 Materials

2.1.1 Commercial Films

In order to compare the properties of laboratory prepared films with those produced industrially, commercial samples of 'cellophane' (Cellulose II) were obtained from British Cellophane Limited (155) and films of dicel and tricel from Bexford Limited (156). The films obtained were the thinnest commercially available, for which thickness, degree of substitution and the nature and amount of additives were known. Such parameters are shown in table X. The films were examined for spectroscopic suitability and in all cases were found to be too thick for examination in the 3 μm. (3333 $cm.^{-1}$) region.

In order to reduce the film thickness, experiments were carried out which involved compression between rollers (20 tons pressure) at 100°C., but no changes in thickness were observed. Attempts to reduce thickness by stretching the films were also unsuccessful, since the films ruptured under this treatment. However, thin films were eventually produced by carefully rubbing the commercial films on fine emery paper. Unfortunately, such films were highly opaque and produced very poor spectra due to their high scatter of the infra-red light. The opacity and scatter of dicel and tricel films were reduced considerably, however, when the surfaces of the films were wiped with cotton wool moistened in acetone. The acetone partly dissolved the surface of the film and hence decreased its opacity and scatter. However, great care was necessary to avoid swamping the films with acetone since the films then dissolved completely. In the case of viscose films, scatter was reduced and better spectra obtained by immersing the films in carbon tetrachloride in a fixed plate liquid cell,

prior to spectral examination.

In all cases the spectra obtained contained large interfering peaks, due to the presence of plasticizing additives. Furthermore, it was not possible to remove these additives from the dicel and tricel films, and in the case of the viscose films it was not possible to ascertain when all the glycerol additive had been removed by washing. All the commercial films were thus assessed as being totally unsuitable for our research purposes and ways of producing pure additive - free films were thus developed.

2.1.2 (A) Production of Pure Viscose Films

Samples of pure additive - free viscose film were produced by regeneration from a solution of cellulose xanthate in 6% caustic soda. The cellulose xanthate solution was produced by treating cellulose with 31% by weight of carbon disulphide and dissolving the resultant cellulose xanthate in 6% caustic soda. The actual cellulose content of the final solution was 7% by weight. The acid bath regenerating solution supplied had the following composition:-

Sulphuric Acid	:	10.5%
Sodium Sulphate	:	20.0%
Zinc Sulphate	:	1.5%

The cellulose xanthate solution was divided into 100 ml. aliquots and stored for long periods at -20°C. Such storage was found to be necessary, since the solution tended to 'gel' and become unusable when left at room temperature for more than a few days. Very thin films were produced on ground glass plates, which induced small surface irregularities without increasing the opacity. Such induced irregularities were found to be necessary for very thin films of viscose in order to eliminate interference fringes.

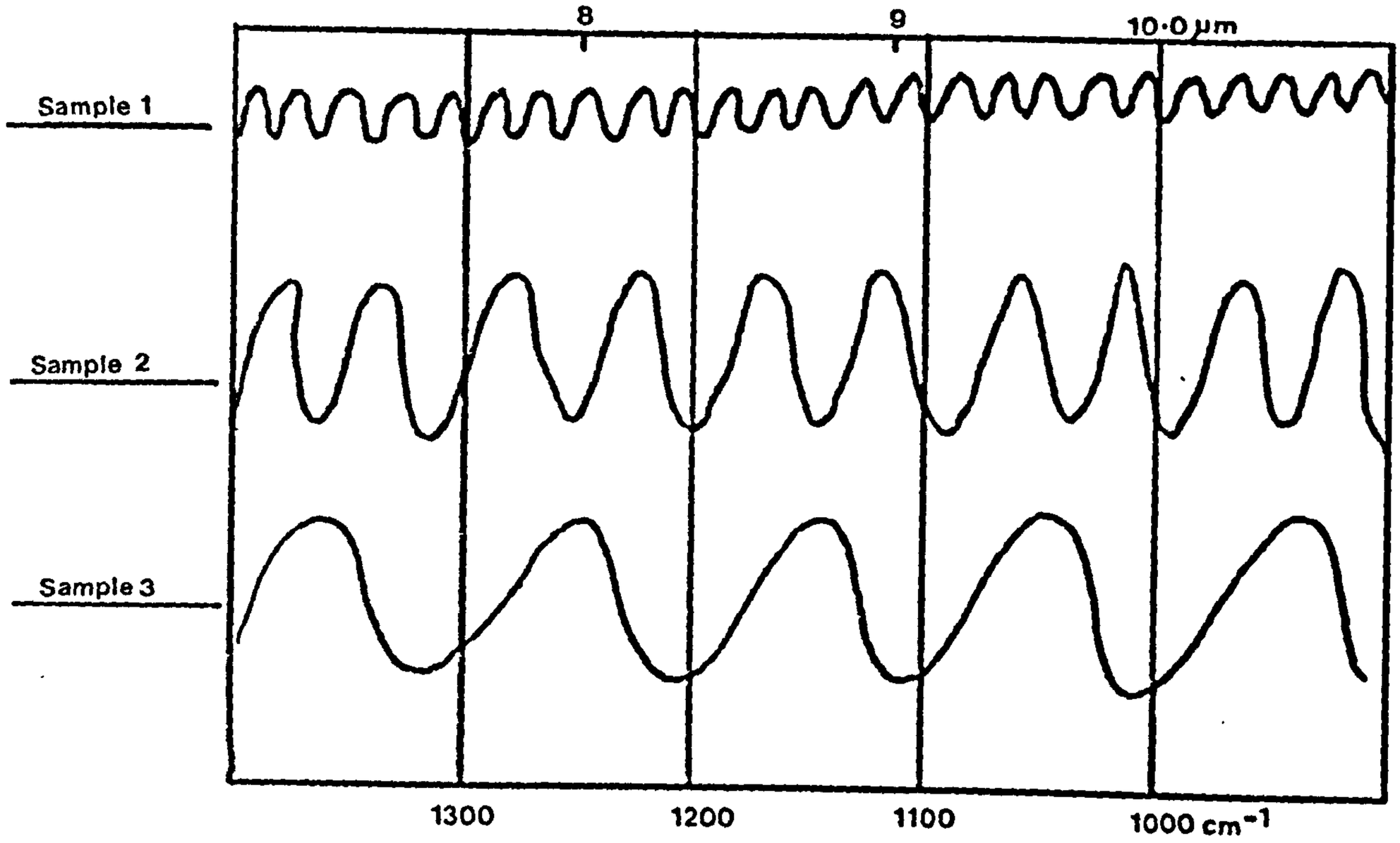

FIG. 27

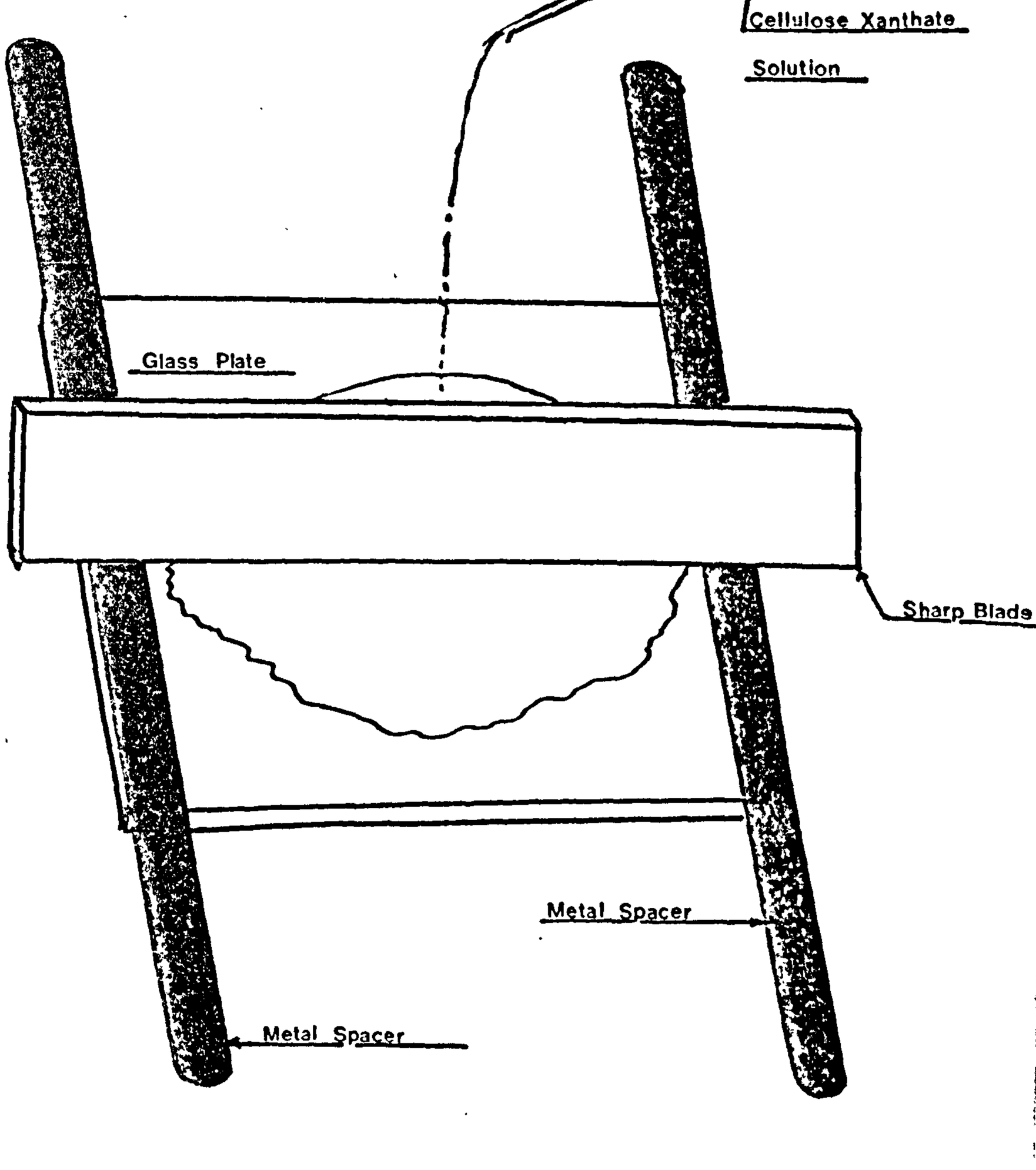
Cellulose Xanthate
Solution
Glass Plate
Sharp Blade
Metal Spacer
Metal Spacer

FIG 28

TABLE XI

Dilution of Acid: Solution: Water Ratio	Appearance of Film
1 : 0	Very Opaque
1 : 1	Very Opaque
1 : 2	Opaque
1 : 4	Slightly Opaque
1 : 6	Slightly Opaque
1 : 8	Very Slightly Opaque
1 : 10	Clear
1 : 12	Clear, but not evenly formed
1 : 16	No Film Produced

TABLE XII

Regenerated Films
Wash in Water for 1 hr.
Desulphurize in 10% Na_2S at 50°C. for 5 mins.
Wash in Water for 5 mins.
Bleach in 1% H_2O_2 at R° for 15 mins.
Wash in Water for 12 hrs.

Interference fringes are often produced when sample thickness is of the same order as the impinging infra-red radiation and the film dimensions are of a high order of regularity. Internal reflection of some radiation occurs at the sample/air or at the sample/cell plate interface. The combination of doubly, quadruply etc. reflected rays, with rays passing straight through the sample cell, occurs to produce interence fringes, as is well known. The form of such fringes is shown in Fig.27 for an optically flat sample. Interference fringes may be used to calculate the sample thickness d according to the equation:-

$$d = (n/2). \quad \lambda_1 . \lambda_2 \; / \; (\lambda_1 - \lambda_2)$$

where λ_1 = One arbitrary wavelength, expressed in μm.

λ_2 = A second arbitrary wavelength, expressed in μm.

n = The number of fringes between λ_1 and λ_2

The actual method of film preparation involved spreading small amounts of the cellulose xanthate solution on ground glass plates (for thin films) or plane glass plates (for thicker films) with a sharp blade. The thickness of the film produced was determined by using sellotape or standard metal spacers of different thicknesses at the edges of the plate (Fig.28). The plates spread with cellulose xanthate solution of different thicknesses were then immersed in the regenerating acid solution in a small tray for 2-4 mins. to produce regenerated cellulose films.

With the standard regenerating solution supplied, thick films of viscose were found to be opaque, even after purification treatments. However, it was found that dilution of the acid bath produced films of greater clarity, which induced a smaller scattering of the incident infra-red radiation. Optimum regeneration conditions were found to occur at a dilution of 1 part of the standard regenerating solution to 10 parts of water (table XI). Films were purified by desulphurizing and bleaching

TABLE XIII

Type of Glass Plate	Type of Spacer	Thickness of Spacer (μm. $\pm$ 5 μm)	Thickness of Viscose film produced (μm. $\pm$ 5 μm)	Spectral Region (μm)
Ground	1 Thickness of Sellotape	56	8 - 10.5	2.5 - 5
Ground	No Spacer	-	5 - 8	9 - 12
Plane	Steel Spacers	270	22 - 23	5 - 9

according to the scheme given in table XII.

The samples of film were then arranged on flat polypropylene or teflon plates and excess water removed by blotting with absorbent paper. The samples were then sellotaped at their edges onto the plates and allowed to dry for several hours in the atmosphere. The use of polypropylene or teflon plates was found to reduce the adhesion between the dry films and plates, thus enabling the films to be removed from the plates by carefully cutting round the edges with a razor blade.

Many different spacers were used initially to produce a range of film thicknesses. All these films were tested for suitability in different spectral regions and films with the most suitable thicknesses for each particular range were then produced on a large scale (Table XIII).

2.1.2 (B) Production of Pure Dicel and Pure Tricel Films

Samples of pure dicel (degree of substitution 2.3) and pure Tricel II (degree of substitution 2.95) flake were obtained from Eexford Ltd. (156). The manufacturers recommended the use of a mixture of methylene chloride and methanol as a solvent for these materials, but methanol was shown to be unsuitable, since films produced by using such a solvent gave large spurious OH peaks in the 3 μm. (3333 $cm.^{-1}$) region of derivative spectra, due to the presence of residual amounts of methanol, which could not be removed, even when samples were heated to a temperature of 150^{o}C. for several hours. It was thus decided to use a mixture of methylene chloride and acetone as a solvent for dicel and pure methylene chloride as a solvent for tricel.

Difficulties were experienced in obtaining homogeneous solutions of the polymers and samples often had to be subjected to continuous mechanical agitation for several days to effect complete dissolution. Films were prepared initially by spreading a thin layer of the polymer solution over

TABLE XIV

Material	Solution	Type (and Thickness of Spacer μm ±5 μm)	Thickness of Film (μm ±5 μm)	Spectral Region (μm)
Pure Dicel	5gms/120 mls. of Solvent*	Steel, (13,750)	45 - 50	0 - 5, 10.5 - 19
Pure Dicel	"	Steel (270)	10 - 5	5 - 7.5
Pure Dicel	"	Sellotape (56)	3 - 5	7.5 - 10.5
Pure Tricel	5gms/80 mls. of Methylene Chloride	Steel (810)	35-45	0 - 5 10.5 - 19
Pure Tricel	"	Sellotape (112)	6.5	5 - 7.5
Pure Tricel	"	No Spacer	3.0	7.5 - 11.5

* The Solvent is 3 Parts Analar Methylene Chloride: 1 part Analar Acetone.

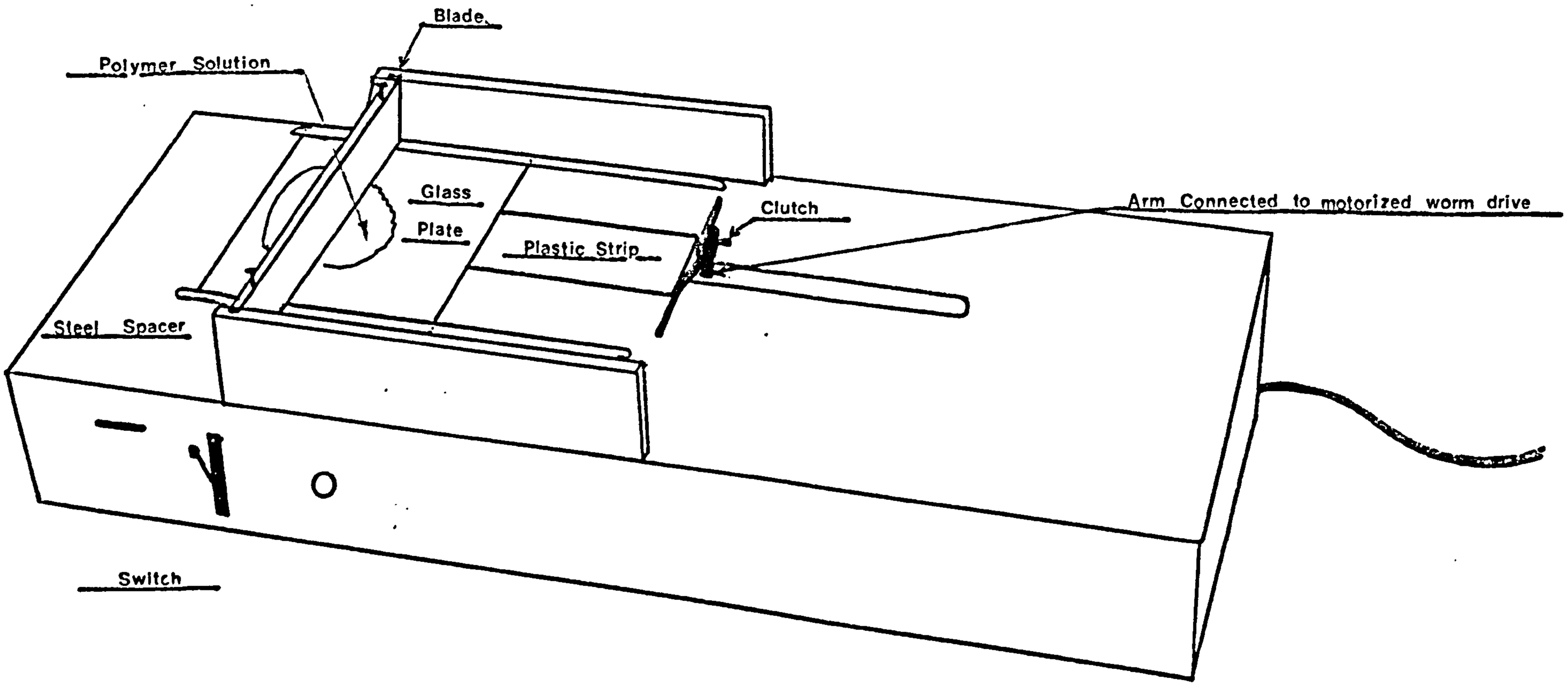
Blade
Polymer Solution
Glass
Plate
Plastic Strip
Clutch
Arm Connected to motorized worm drive
Steel Spacer
Switch

FIG. 29

a plane glass plate (with spacers at the edges) with a blade and allowing the solvent to slowly evaporate from the layer by placing the plate in a cabinet with a small dish of the solvent to reduce the rate of evaporation of solvent from the layer of polymer solution. If such a precaution was not taken and the layer of polymer solution was allowed to dry in the atmosphere, the rapid evaporation at the edges of the layer tended to cause more solution to flow to the edges from the centre, especially with thick layers of polymer solution, and produce a film which was thicker at the edges than at the centre.

It was also necessary to produce a dry atmosphere within the cabinet by including a small dish of P_2O_5, since otherwise the condensation of atmospheric water vapour onto the layer of drying polymer solution (due to the cooling effect of the evaporation of solvent) tended to produce films which were cloudy.

Many trial experiments were conducted to ascertain the correct concentrations and spacer thicknesses required in order to produce films suitable for the different spectral regions. Dilute solutions of polymers were found to be unsuitable, since layers of such polymer solutions cast on glass plates were found to break up into droplets of liquid before a film could be formed by the solvent evaporating. However, the solution conditions shown in Table XIV were found to produce suitable films. Spacer and film thicknesses are also indicated in this table.

Greater speed of preparation, film regularity and reproducibility were obtained by using an automatic plate spreader (Fig.29) which was developed for the preparation of even layers of Kieselghur suspensions in thin layer chromatography. (157). This consists of an aluminium bed along which plates are traversed at a constant rate by an arm connected to a motorized worm drive. For our purposes, plates were traversed one at a time and

the drive from the arm was connected to the glass plate by a plastic strip, as shown in Fig.29. In the starting position shown, the edge of the plate passes under a blade whose height above the glass plate is determined by the positioning of adjustment screws, located on either side of the blade. However, in practice greater reproducibility was obtained from the alternative use of sellotape or steel spacers at either side of the blade.

To produce a film, a thin ribbon of polymer solution was poured onto the plate immediately behind the blade, the motor switched on and the plate traversed. At the end of the traverse, a microswitch switched the motor off and the plate was then transferred rapidly to the drying cabinet containing small dishes of the solvent and P_2O_5. The instrument was then switched off and the arm returned to its original position by disengaging a clutch connecting it to the worm drive. The blade was then removed, cleaned with acetone, returned to its original position on another glass plate and the whole procedure repeated.

When the films were completely dry, the glass plates on which they were cast were removed from the drying cabinet. Considerable difficulty was experienced in removing the films from the glass plates, but this was overcome by condensing a thin layer of moisture on the films and carefully removing the films with a razor blade. When thin films were removed from the plates, they tended to wrinkle and fold up as the layer of moisture evaporated, making them impossible to fold without tearing. This folding phenomenon was attributed to an accumulation of static charge due to the very low regain of dicel and tricel. This folding phenomenon was not, however, observed with thicker films, where their rigidity was large enough to withstand any forces due to the accumulated static charge. The problem with thinner films was overcome by supporting them with damp tissue paper as they were removed from the glass plates. These films were then stored between two sheets of tissue paper prior to use. When small samples of such film were required for spectroscopic purposes, they were cut from the

film whilst it was sandwiched between the sheets of tissue. In this way, folding up of the sample and the remaining film was prevented.

2.1.3 Preparation of Samples for the KBr Disc Technique

Samples of viscose, dicel and tricel film were chopped finely and placed in agate ball mills with 0.5 g. aliquots of spectroscopic grade KBr. The samples were then milled for 24 hours, but surprisingly no grinding had occurred and the film samples were found to be distributed around the edges of the mills, leaving the KBr at the bottom. Samples of dicel and tricel flake treated similarly also produced the same results. It was clear that the failure of the samples of film and flake to disintegrate was due in part to an accumulation of static charge causing the film or flake particles to separate from the KBr matrix and from each other. Such samples could thus not be used to produce KBr discs since they would not disperse finely in the KBr matrix. A fine dispersion in the KBr is essential, since poor dispersion results in poor sample transmission, high scatter and hence poor spectra. It was thus decided to produce viscose, dicel and tricel in the form of particular precipitates, which could be dried and then finely dispersed in KBr.

2.1.3 (A) Preparation of Viscose, Regenerated as a Fine Precipitate

Several attempts to produce a precipitate of viscose by regeneration from cellulose xanthate solution were made, but without much success. In all these cases, the regeneration process took place at too rapid a rate and large pieces of film were produced. However, the following method of slow regeneration was found to produce a precipitate with the necessary characteristics:-

50 mls. of cellulose xanthate solution were dissolved in 500 mls. of distilled water at room temperature. The mixture was then stirred vigorously as 0.1N. sulphuric acid was added dropwise until a neutral pH

was obtained. The mixture was then allowed to stand for several minutes, whereupon a flocculent pale yellow precipitate of regenerated viscose was produced. The precipitate was centrifuged off and purified according to the scheme shown in Table XII. The purified precipitate was finally placed in a sample bottle and dried in a vacuum desiccator at 40°C.

2.1.3 (B) Preparation of a Dicel Precipitate

A solution of dicel in acetone was found to produce a suitable precipitate on the addition of water. 2 gms. of pure dicel flake were dissolved in 200 mls. of acetone and distilled water gradually added to the mixture with constant stirring. After the addition of approximately 100 mls. of water, a flocculent white precipitate of dicel was formed. This was centrifuged off, washed several times with distilled water and dried in a vacuum desiccator at 40°C.

2.1.3 (C) Preparation of a Tricel Precipitate

Tricel flake was dissolved in methylene chloride and attempts were made to precipitate the tricel by the addition of various solvents and aqueous solutions of solvents. None of the solvents which mixed with methylene chloride caused precipitation of tricel to occur, even on the addition of large excesses of these solvents. The aqueous solutions of solvents did not mix with the methylene chloride and were thus unable to effect precipitation. Solutions of tricel in acetone did not produce precipitates on addition of water, but merely produced large particles of film.

The following method was, however, found to produce a suitable precipitate. 2 gms. of pure tricel flake were dissolved in 100 mls. of methylene chloride and 100 mls. of pure acetone slowly added to the solution, with constant stirring. Pure methanol was then slowly added to the mixture, again with constant stirring. After the addition of approximately 500 mls.

TABIE XV

Precipitale	Mgms. Precipitate/150 mgm. KBr	Spectral Region of Disc (μm.)
Viscose	3	7 - 12
	6	2.5-5, 5-15
	(12)	(2.5-5) (5-8)
Dicel	1	5 - 10
	6	2.5-5, 10-20
Tricel	3	5 - 12
	6	2.5-5
	12	10-20

of methanol, a flocculent white precipitate of tricel was produced. This was centrifuged off and washed several times with pure methanol. The precipitate was finally washed several times with distilled water, centrifuged and dried in a vacuum desiccator at 40°C.

2.1.3 (D). Preparation of KBr Discs

Samples (1-12 mgm.) of the precipitates of viscose, dicel and tricel were ground by hand in an agate mortar with an agate pestle and were then mixed with 150 mgm aliquots of spectroscopic grade KBr. The samples were then transferred to agate ball mills and milled for 0.5 hr, before being compressed into discs in a die, under evacuation and 2 tons pressure. The die was warmed to 50°C. prior to use to minimise the risk of atmospheric moisture contaminating the samples and producing cloudy discs. Samples and discs were also stored in desiccators over P_2O_5 to minimise the risk of clouding in the discs due to the presence of absorbed moisture. Trial experiments were conducted with different concentrations of the precipitates in the KBr to determine the optimum conditions required to give suitable spectra in each spectral region (Table XV).

2.2 Methods

2.2.1 The Grubb Parsons Spectromaster, Mark II

The experimental work was carried out on a Grubb Parsons 'Spectromaster', (Mark II) infra-red spectrometer. This instrument may be used in either a single or a double beam mode, but all experiments carried out in this work were conducted with the instrument operating in the double beam condition. In such a mode, interfering absorptions from atmospheric carbon dioxide and water vapour are eliminated. The use of identical ('matched') cell plates in both the sample and reference beams also eliminated any absorptions produced by the plates. Care had to be taken when using such plate matching

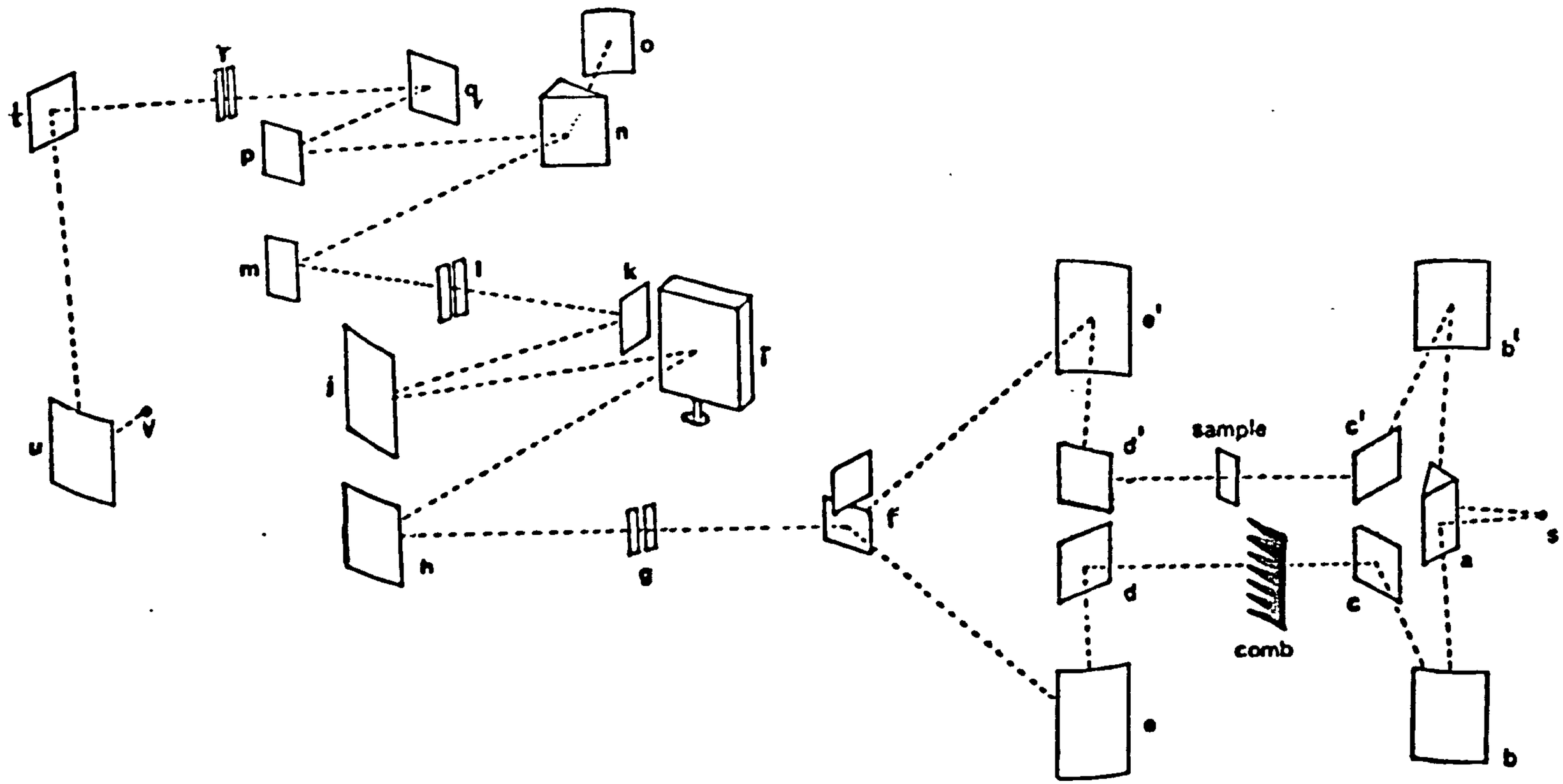

FIG. 30A

KEY TO FIG. 30A.

s :- Source of Infra-red Radiation (Nernst Filament),

a :- Double Mirror, dividing Radiation into two equal Beams,

b,b':- Focussing Spherical Mirrors,

c,c':- Plane Mirrors,

d,d':- " " ,

e,e':- Spherical Mirrors,

f :- Reciprocating Mirrors,

g :- Entrance Slit,

h :- Focussing Spherical Mirror,

i Diffraction Grating,

j :- Condensing Spherical Mirror,

k :- Collimating Mirror,

l :- Exit Slit,

(g to l comprise the Monochromator)

m :- Collimating Mirror,

n :- KBr. Prism,

o :- Littrow Mirror,

p :- Collimating Mirror,

q :- Plane Mirror,

r :- Slits,

s :- Plane Mirror,

u :- Ellipsoidal Mirror,

v :- Detector.

techniques, however, since when the absorptions of the plate were significant, the sensitivity and resolution of the instrument were proportionally reduced, with consequential effects on the spectrum produced.

Facilities exist for varying chart speed, wavelength scan speed, scale expansion and time constant. Suitable combinations were used to ensure optimum sensitivity, spectral resolution and spectral reproducibility.

The optical system of the spectrometer is shown in figure 30A. The principles of operation of the instrument are now well known and will not be covered here. However, in view of the use of derivative techniques, the cam operated by the servo motor, which is used to attenuate the reference beam, was replaced by one which gave an output directly in terms of optical density in the range 0 to 1.0. Wavelength calibration was also effected using polystyrene film as a standard reference material.

2.2.2 Derivative Spectroscopy

2.2.2 (A) Introduction

The theory of differentiation and development of a differentiator capable of producing second derivative spectra have been discussed in detail elsewhere (12), but in view of the wide use of this technique in this work, a brief account is given here. In a normal absorption spectrum, if two bands are not well separated, mutual overlapping occurs, so that the resolution of these peaks is either inadequate or incomplete. For example, a band of low intensity which is overlapped by one of a higher intensity may be observed as a 'shoulder' or 'inflection' or 'dissymmetry' in the band of higher intensity and in some cases may not be observed at all. The analysis of overlapping bands pioneered by Henrich (158), Giesse and French (159) led Pemsler (160) to develop an optical technique for producing derivative spectra, but the form of such spectra was not very useful, since it made interpretation very difficult.

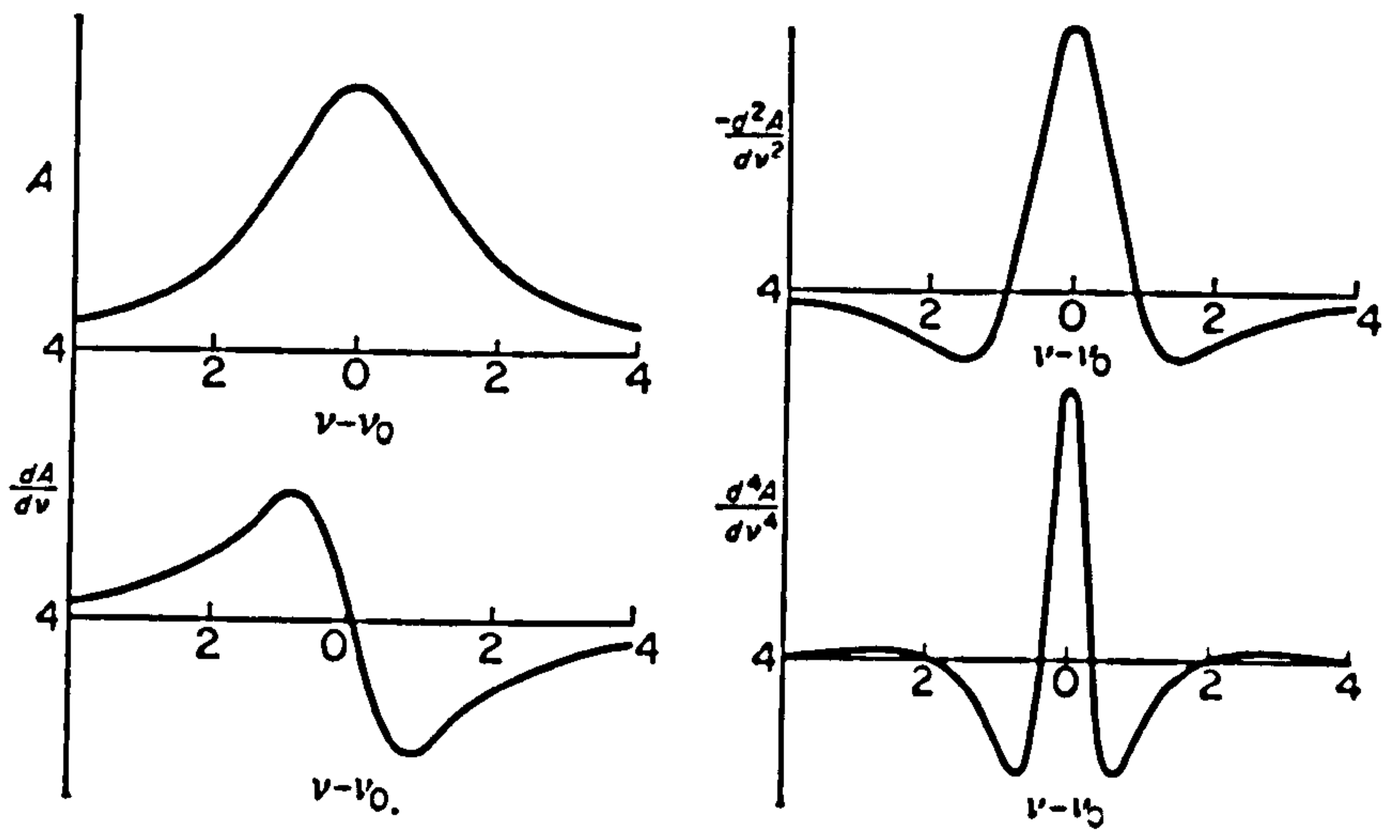

FIG.30B. Successive differentiation of a curve drawn according to the Lorentz equation, which is a suitable model for infrared absorption peaks. The second and fourth derivatives show the sharpening effect

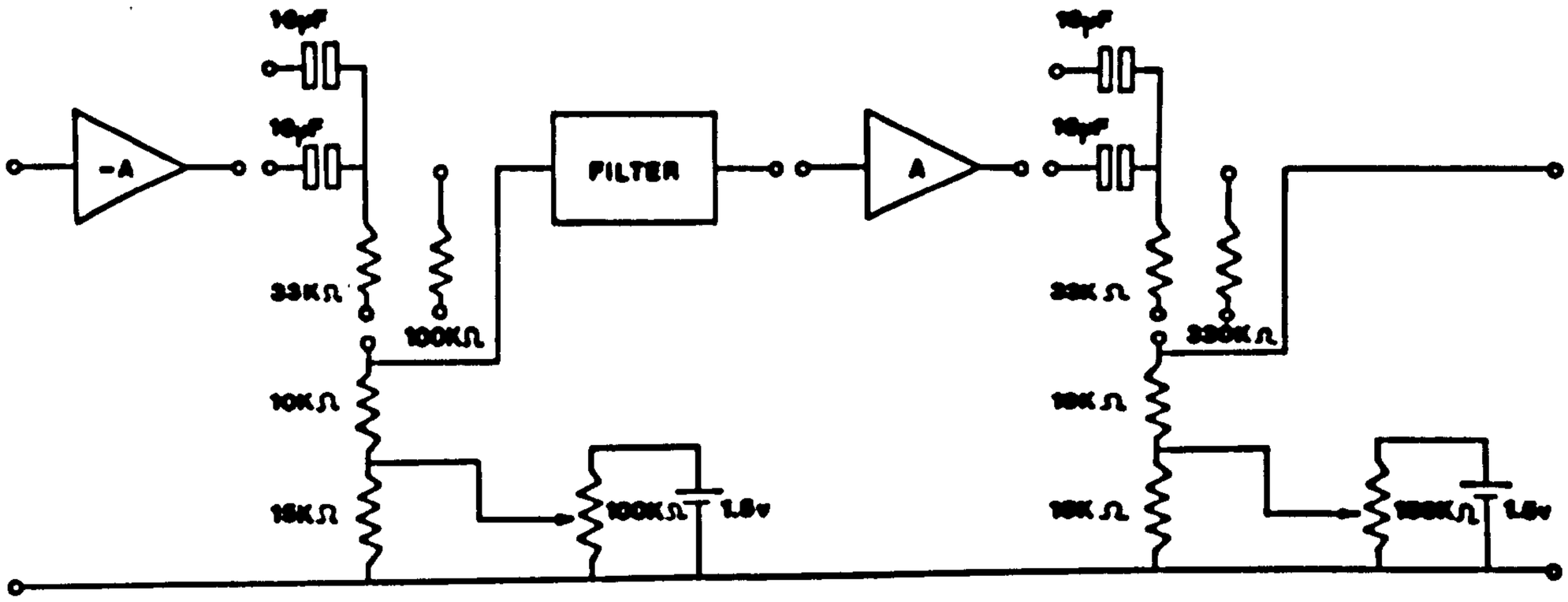

Complete Circuit

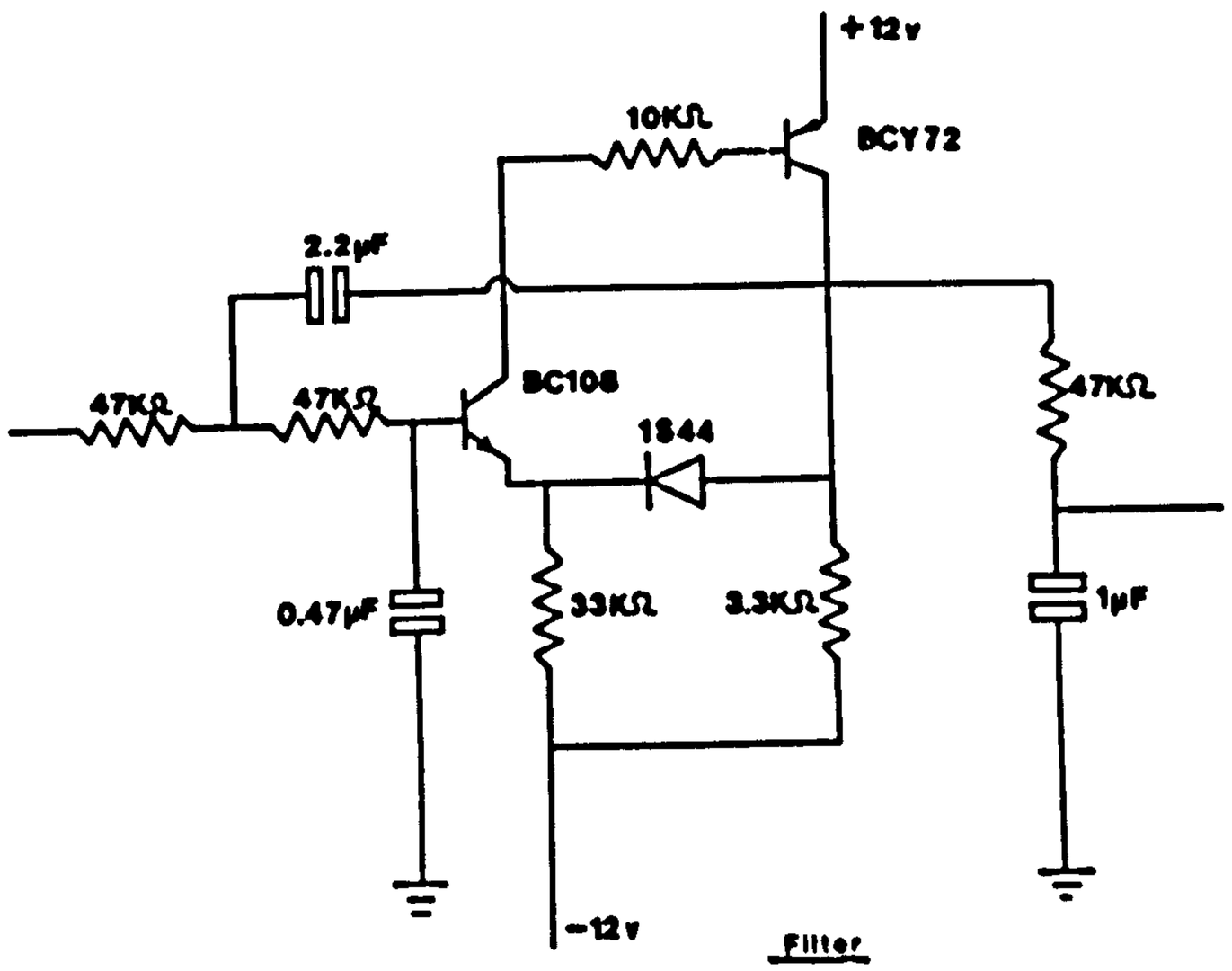

Filter

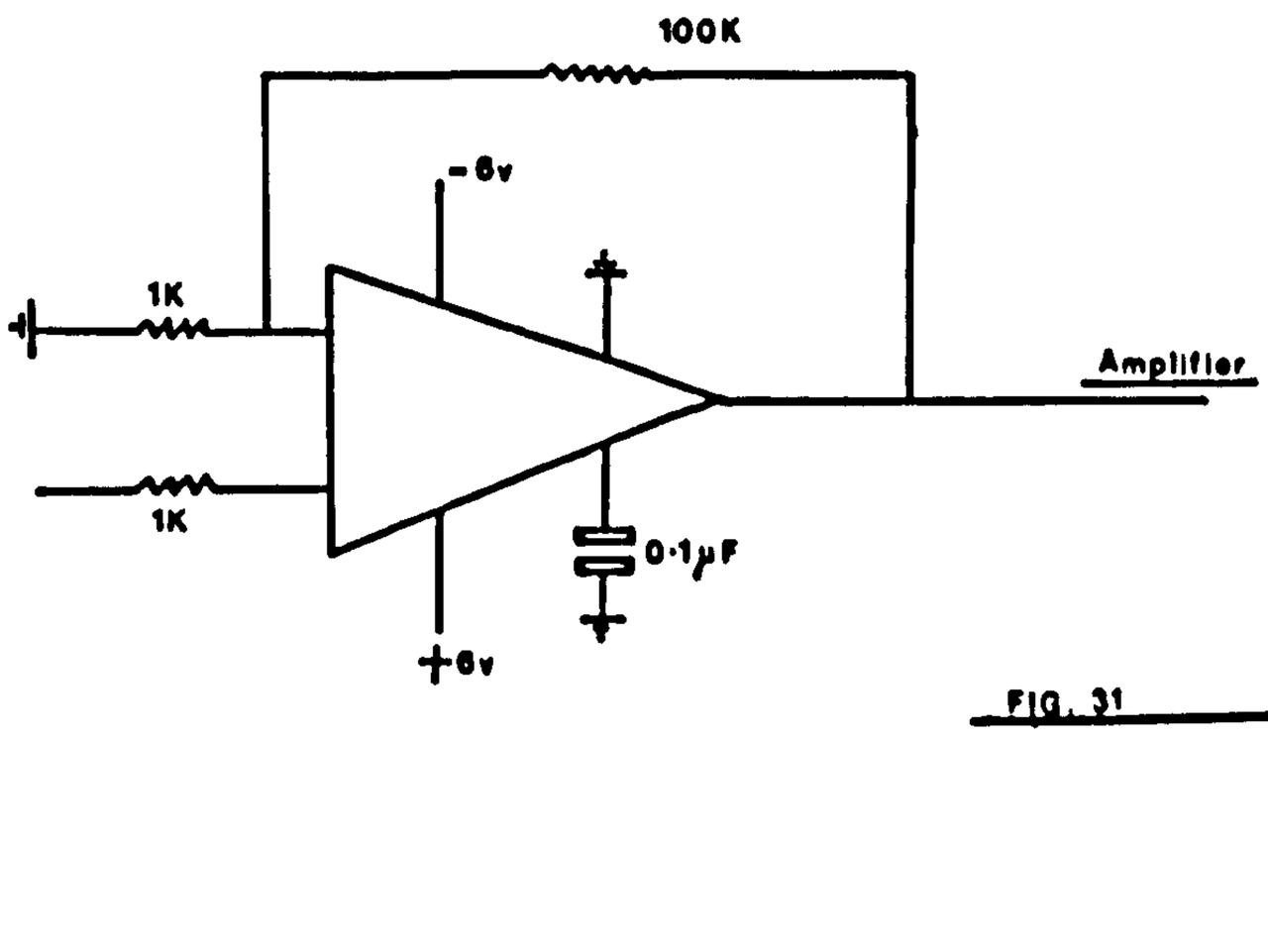

FIG. 31

Fig. 30B shows the derivative peaks produced by successive differentiation of a typical absorption band. The second and fourth derivatives are similar in appearance to the parent band, but are considerably sharper, since the width at half height is approximately 1/3 that of the parent absorption band for the second derivative and 1/5 for the fourth derivative. Such a sharpening of peaks in the second and fourth derivatives enables greater resolution to be attained. It can be seen from Fig.30B that "even" derivatives are more useful than "odd" derivatives since the former have a central peak which corresponds to the parent absorption peak. However, satellite peaks also occur in "even" derivatives and these are likely to induce anomalies into the spectra so that in practice the second derivative is accepted as being the most suitable. The acceptance of the theory of derivative techniques has been shown to be based on the similar behaviour of Lorenzian and Gaussian distribution peaks to the absorption peak when such are plotted as second derivatives.

2.2.2 (B) Development of a Differentiator

The technique of derivative spectroscopy was developed in this laboratory (12) to assist in the detection of overlapping peaks which form part of broad unresolved bands characteristic of polymers. The electronic circuitry used for this work is shown in Fig.31. The development of the time-derivative computer ('differentiator') was only allowed after the advent of operational amplifiers which allow high amplifications to be achieved at low noise levels. Electronic valves were thus unsuitable for this work.

The 'differentiator' was suitably connected with the spectrometer electronics so that the amplifier output was passed into the differentiator and the consequential output was fed directly to the chart recorder.

2.2.2 (C) Characteristics of Derivative Spectroscopy

(i) Spectrometer and Sample Requirements

The technique of examining samples by derivative spectroscopy to obtain good derivative spectra from which valid interpretations could be made was more complicated than the technique required to produce good absorption spectra. However, the validity of a good derivative spectrum is dependent upon the accuracy with which the parent absorption spectrum is produced. Thus in order to obtain optimum performance during differentiation, the spectrometer had to be set up to optimum conditions, since any slight distortion in the absorption spectrum produced magnified changes in the derivative spectrum.

In order to obtain highly resolved derivative spectra, sample concentration had to be adjusted so that the absorption ranged between 10 and 80% transmission, and in order to simplify this the optical density cam was used in all cases. In many circumstances, however, several samples were necessary in order to obtain sensitivity in a particular wavelength range.

(ii) The Effect of Scan Speed

Changes in the scan speed have been shown to change the relative heights of derivative peaks due to differences in band width. This effect was most useful for our purposes, since a careful choice of scan speed enabled certain peaks to be enhanced, which had previously been obscured when recorded at a different scan speed.

(iii) Band Shift

When a second derivative spectrum of a single absorption was obtained, the derivative peak was found to have moved to a higher wavelength than the parent absorption. This was due to a time lag induced by the time constant

of the differentiator circuit and was found to vary with changes in R and C of the whole 'differentiator'/spectrometer circuit. Thus changes in the time constant of the spectrometer as well as the differentiator caused changes in the shift. Changes in scan speed also induced changes in peak shift, a reduction of scan speed causing a reduction of peak shift.

The magnitude of the total peak shift was determined as for absorption spectra using a polystyrene standard. A derivative spectrum of the polystyrene standard was obtained using the same conditions of chart speed, scan speed, time constant etc. as was used for the sample.

It has been shown (12) that in some derivative spectra, relative peak positions varied slightly with different experimental conditions, especially when the parent absorption spectrum was constituted from broad overlapping peaks. It has been shown mathematically (12) that this particular type of band shift arises as a consequence of overlapping peaks and that it does not occur when peaks are well separated. Hence when a number of peaks overlap, it is very difficult to measure the true absorption wavelengths, but the use of derivative techniques has shown that greater accuracy can be obtained than when measured in the absorption mode due to the much greater resolution produced by derivative techniques. However care must still be taken during the analysis of derivative spectra containing many peaks, since changes in the wavelength of a particular vibrational peak may induce changes in the parameters of one or more peaks in its vicinity.

(iv) <u>The Effect of Time Constant and Slit Width</u>

The four values of time constant available on the spectrometer electronics gave increasingly suppressed noise levels, but with loss of sensitivity and hence lower instrumental resolution. The time constant selected in each case for derivative spectra was dependent in part on the sample and/or scan speed conditions, as is the case for normal absorption spectra. The time

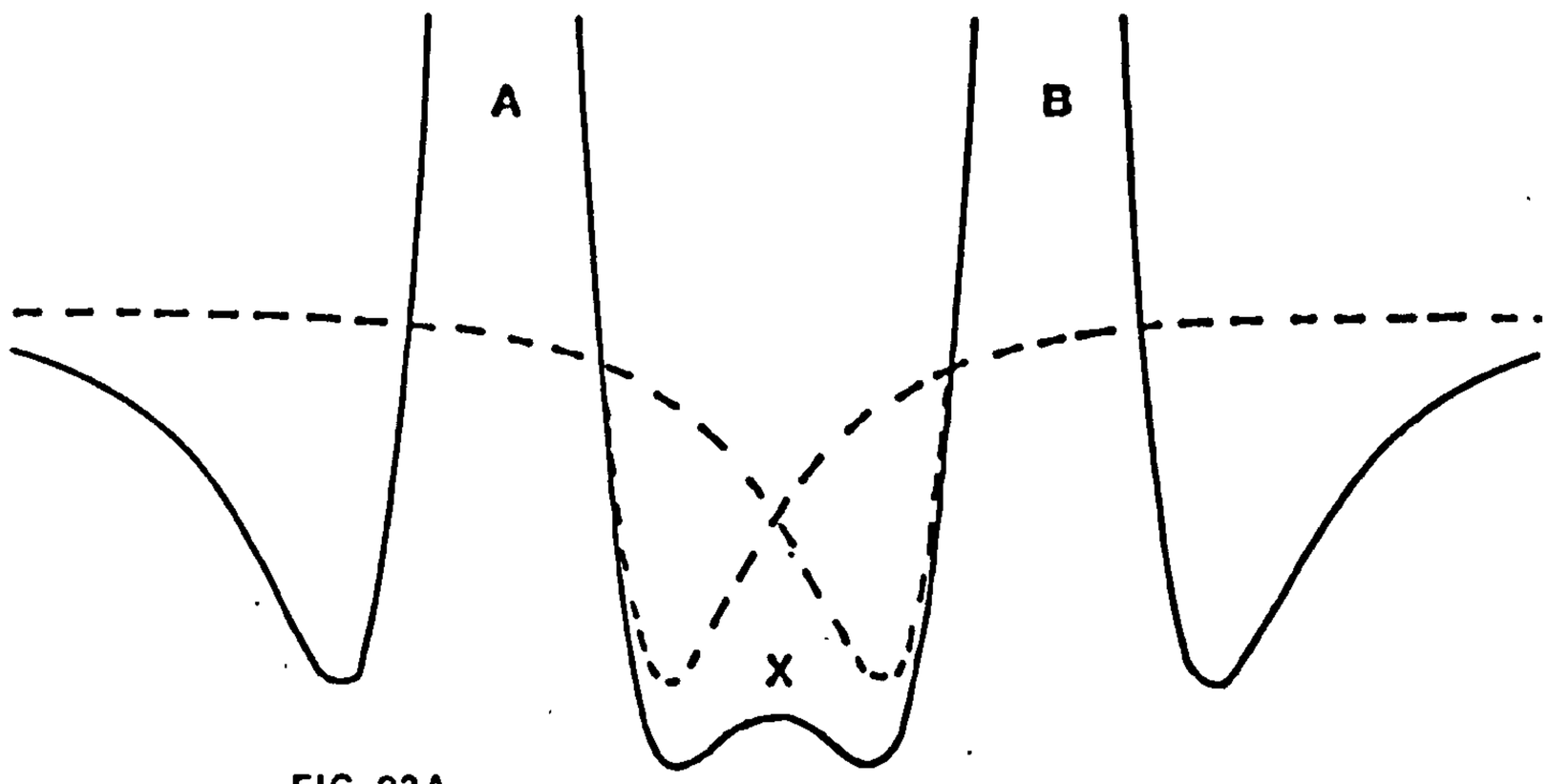

FIG.32A

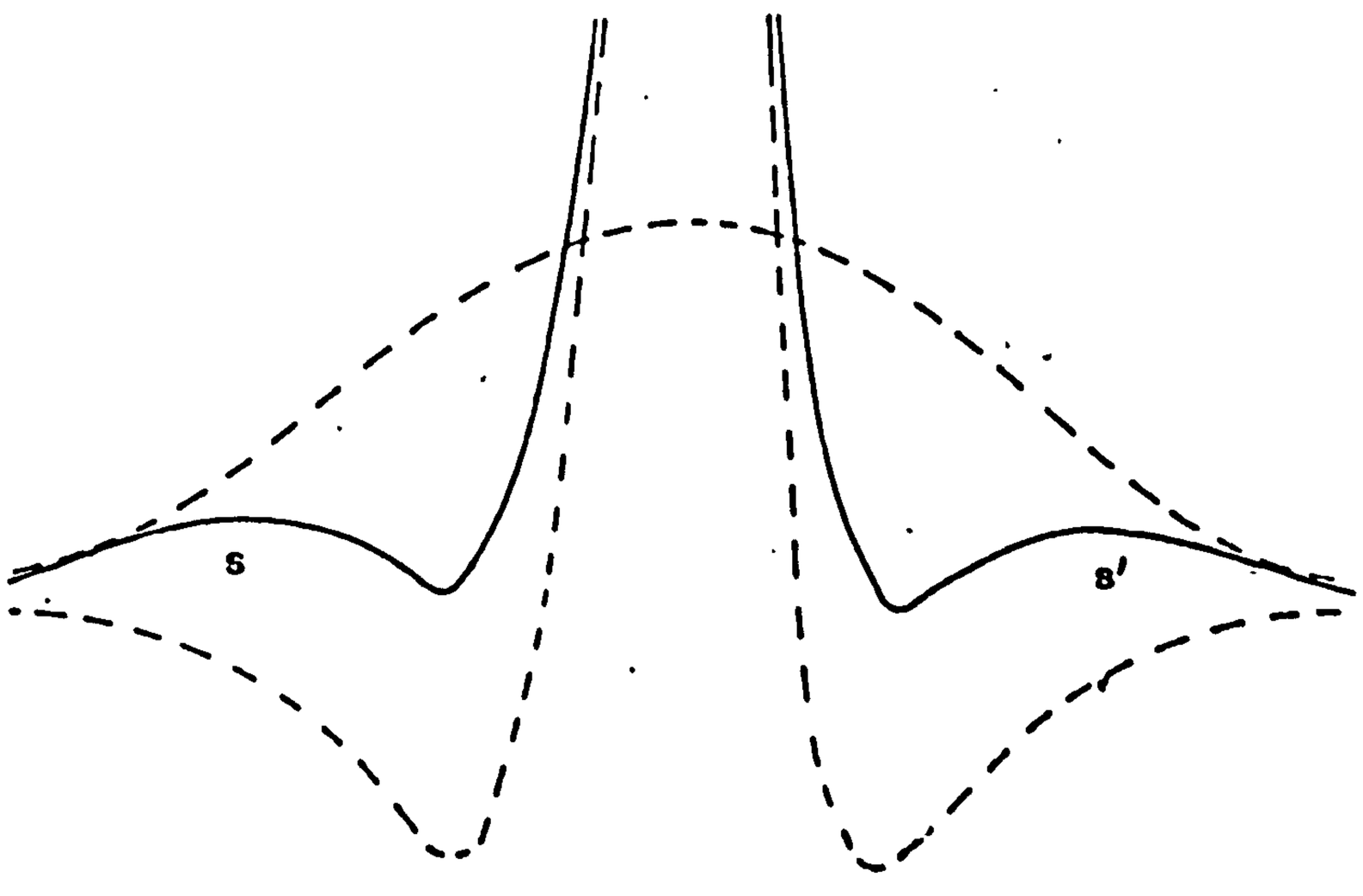

FIG.32B

constant was selected so as to give minimum noise coupled with adequate resolution.

The effect of decreasing the slit width was to improve the resolution obtained, but this necessitated increasing the spectrometer gain to maintain a satisfactory response. Unfortunately, such an increase often caused an unacceptable increase in the inherent noise of the derivative spectrum and the slit width was thus not usually decreased below the broad '10' setting.

(v) Possible Consequences of Overlapping Second Derivative Peaks

The possibility of the presence of spurious peaks which arise as a consequence of peaks overlapping has been examined and two cases which may occur are shown in Fig.32. Fig. 32A shows that when 2 singlet second derivative peaks just overlap, a third spurious peak X occurs as a consequence of the summation of the two negative satellites of the derivatives. However, such spurious peaks will only occur between the two peaks on the negative side of the second derivative curve. Fig.32B shows a second anomaly in which a narrow derivative peak has its maximum superimposed near or on the maximum of a broad peak. In this case, two shoulders S and S' on either side of the broad peak will be observed as a consequence of the summation of the satellites of the narrow peak upon the major portion of the broader peak.

The presence of such spurious peaks in an actual second derivative spectrum cannot be ruled out, but peak separation is often sufficient for these peaks not to be observed. In practice, if such cases arise, the situation can be clarified from the results of alteration of the variable parameters of the system.

TABLE XVI

		Normal Spectrum: Band Shift (μm) In 0-5 μm. Region	Normal Spectrum: Band Shift (μm) In 5-20 μm. Region	2nd Derivative Band Shift (μm) In 0-5 μm. Region	2nd Derivative Band Shift (μm) In 5-20 μm. Region
Conditions I	Chart Speed 4 Scan Speed 1 Scale Expansion 1 or 2 Time Constant 3	0.006	0.020	0.023	0.085
Conditions II	Chart Speed 2 Scan Speed 0.5 Scale Expansion 1 or 2 Time Constant 3	0.002	0.001	0.0158	0.050

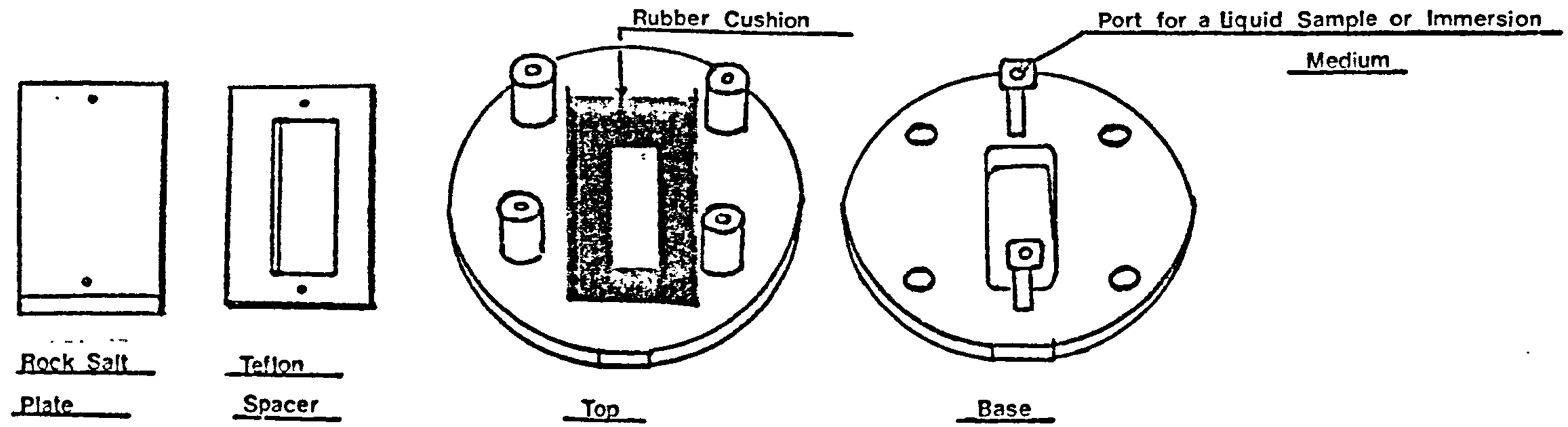

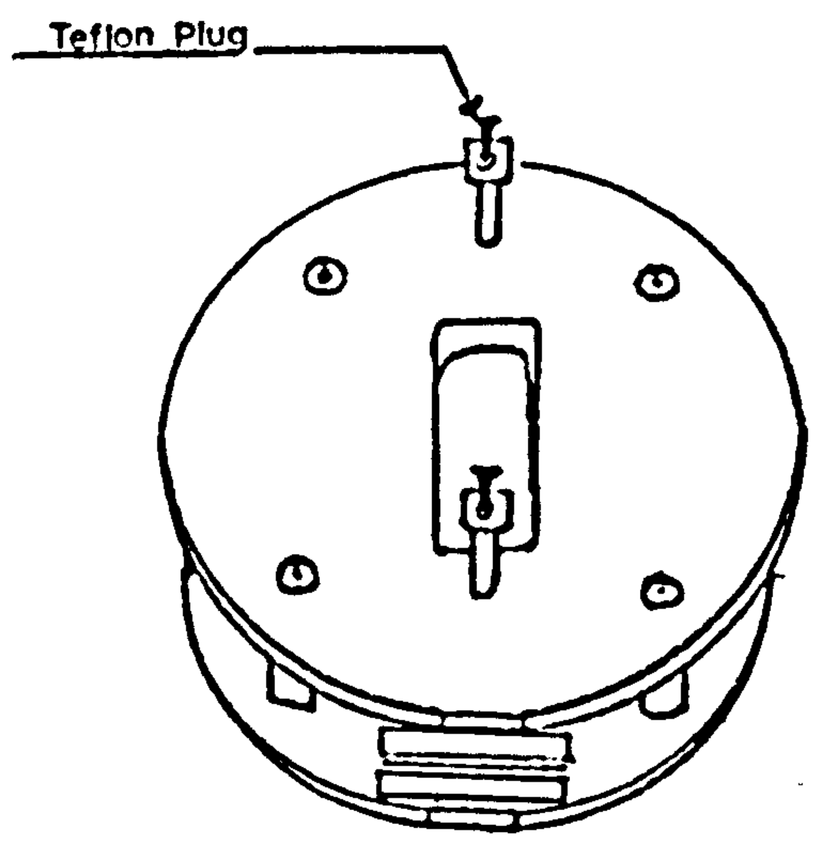

FIG. 33

DIAGRAM OF A FIXED PLATE CELL

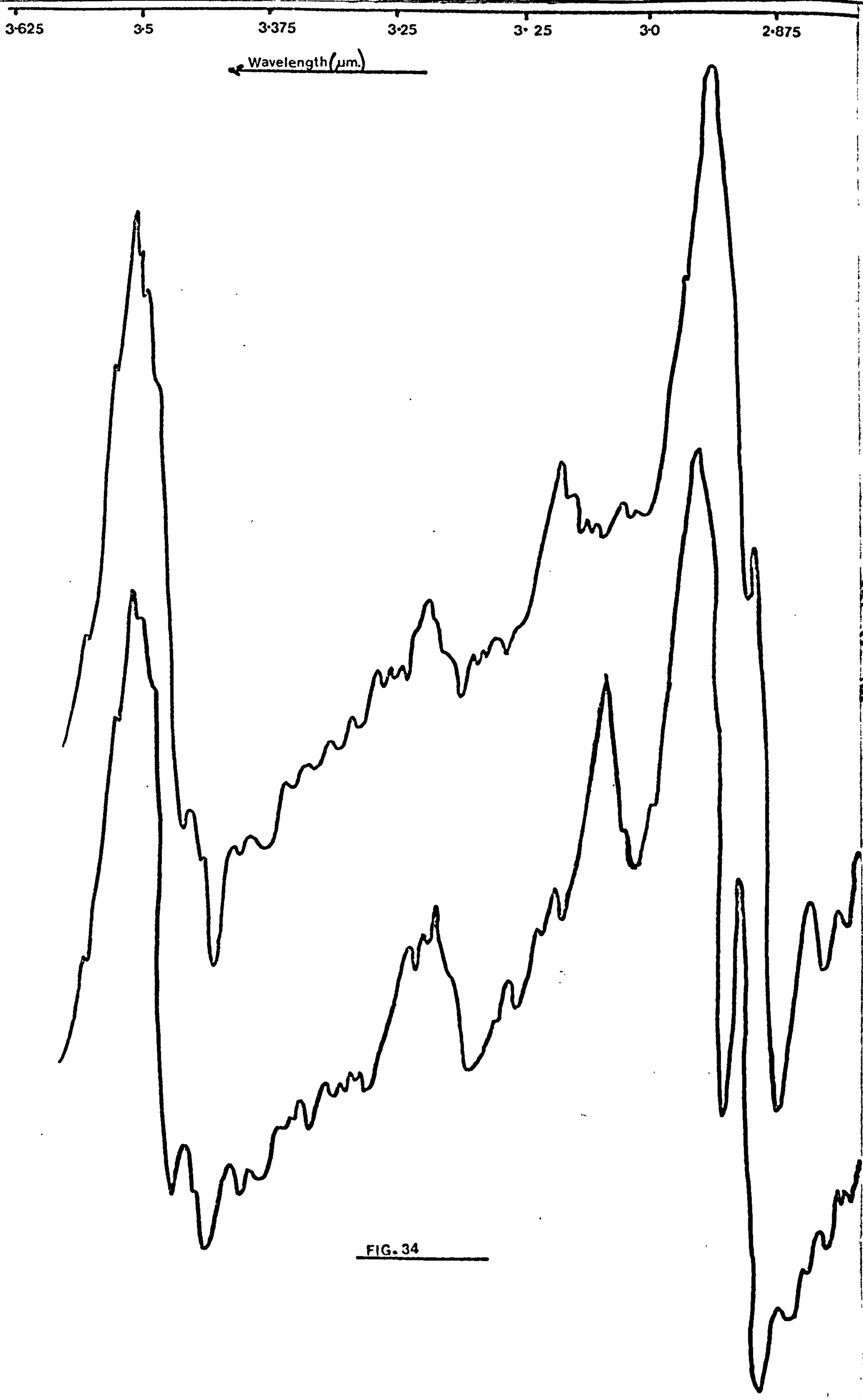

FIG. 34

(vi) Conditions Used for Obtaining Good Derivative Spectra

Many trial experiments with viscose, dicel and tricel were conducted in order to determine the spectrometer settings required to give the most ideal derivative spectra. Two sets of conditions in each region of the spectrum were found to give such spectra and these conditions together with their associated band shifts are quoted in Table XVI.

2.3 Early Experiments

Early experiments were conducted on samples of viscose, dicel and tricel film mounted in fixed plate cells in the atmosphere (Fig.33). Samples were mounted in the cells, sandwiched between two rock salt windows and placed in the sample beam. A cell fitted with identical rock salt windows was placed in the reference beam to balance out any small absorptions due to the rock salt windows. Absorption and second derivative spectra were obtained initially in the 2.5 - 5 μm. (4000 - 2000 $cm.^{-1}$) and 5 - 10.5 μm. (2000 - 952 $cm.^{-1}$) regions. Although the spectra of all the films were reproducible in the absorption mode, the second derivative spectra which showed much fine detail were irreproducible in the 3 and 6 μm. (3333 and 1667 $cm.^{-1}$) regions where vibrations due to cellulosic OH groups and absorbed water occurred. The irreproducibility was most marked for samples of viscose, which contains the greatest proportion of cellulosic OH groups and absorbed water.

Fig.34 illustrates the magnitude of this irreproducibility for two consecutive derivative spectra recorded in the 3 μm. (3333 $cm.^{-1}$) region under the same spectrometer conditions. Such a variation clearly makes any interpretation invalid. Derivative spectra of dry samples of viscose, dicel and tricel film were also recorded to eliminate any interference from large amounts of absorbed water, and when consecutive spectra were compared, they were also shown to be irreproducible; although the magnitude of this variation was less than for samples conditioned at room humidity.

It is well known that hydroxyl groups, including those of absorbed water, are able to form strong hydrogen bonds. In addition, water is capable of forming hydrogen bonds with other water molecules and also with cellulosic OH groups (161). Hydrogen bond strengths are highly sensitive to changes in temperature, so that a small temperature change is likely to induce a large change in vibrational frequencies. The irreproducibility of spectra in the 3 and 6 μm. (3333 and 1667 cm.$^{-1}$) regions of the derivative spectra of viscose, dicel and tricel was hence attributed to variations in hydrogen bond strength which arise as a consequence of variations in sample temperature.

2.3.1 Causes of Variation of Sample Temperature

A considerable variation in sample temperature was suspected, due to the absorption of infra-red radiation by the sample, since it is well known that the absorption of infra-red radiation may cause an increase in temperature. The following experiment was devised to ascertain if sample temperature was in fact increasing significantly as the sample was placed in the infra-red beam:-

Two identical samples of viscose film, 500 μm. thick, were soaked in water overnight. The spectrometer was preset to a maximum of a suitable water OH peak at 1.94 μm. (5159 cm.$^{-1}$) and both beams of the instrument blanked off at the specimen chamber entrance with a piece of card. Both samples were then removed from the water at the same instant, blotted with absorbent paper to remove excess water and mounted in sample holders. Both samples were then placed in the same horizontal plane above the spectrometer bed in the sample cavity, so as to be exposed to the same atmospheric conditions (draughts etc)., but one sample, designated as sample 1, was mounted in the beam absorption position of the spectrometer. The chart recorder was then switched on at the same instant as the card was removed from both beams. The percentage absorption (in terms of optical density) of the trace at a particular point thus represented the total amount of

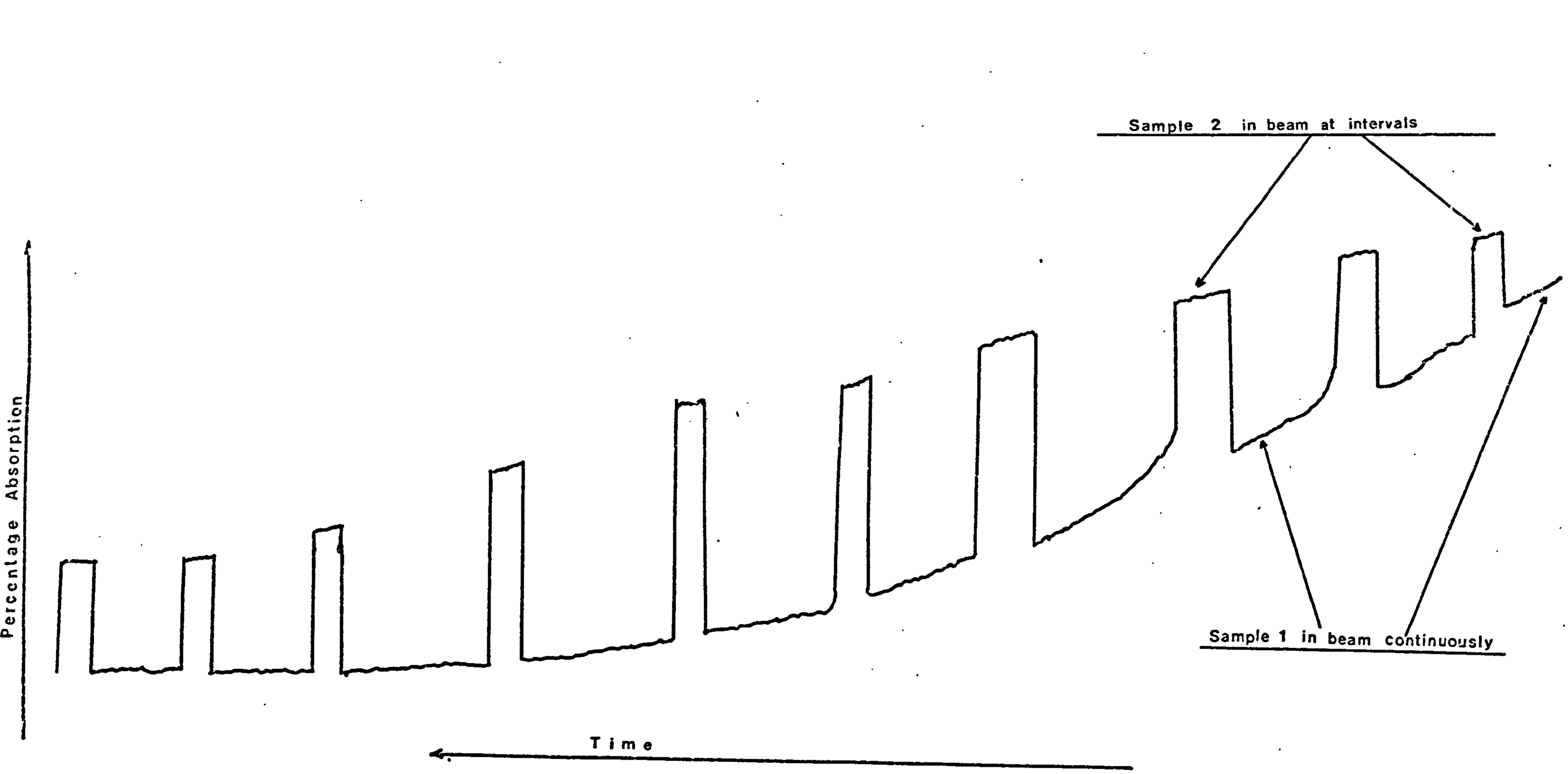
Sample 2 in beam at intervals
Sample 1 in beam continuously
Percentage Absorption
Time

FIG 35 A

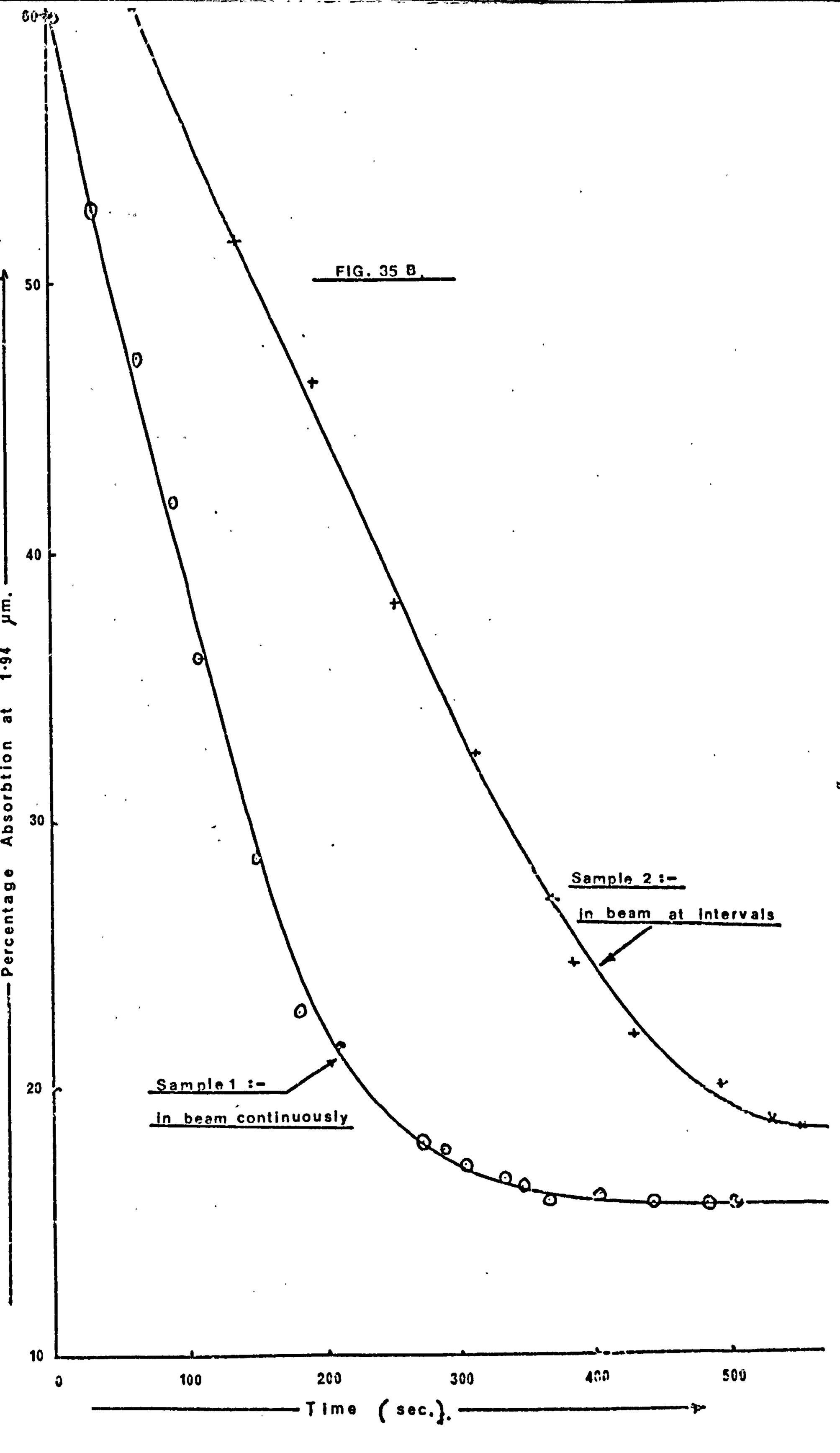
60
50
40
30
20
10
Percentage Absorbtion at 1·94 μm.
0
100
200
300
400
500
Time (sec.).
Sample 1 :-
in beam continuously
Sample 2 :-
in beam at intervals

FIG. 35 B.

water present in the sample at the time corresponding to that point. After two minutes, the samples were rapidly exchanged for just sufficient time to record a maximum for the second sample. The samples were then rapidly exchanged again and the absorption of the first sample again recorded for another two minutes. The whole procedure of swapping the samples at intervals of two minutes to bring the second sample into the beam for just sufficient time to record its maximum absorption was repeated several times until a constant percentage absorption was obtained for both samples, indicating that the water content of both samples had reached a constant level.

Water loss from the samples occurred primarily by evaporation as the samples were exposed to the atmosphere, but the results obtained and illustrated in Figs. 35A and 35B clearly show that sample 1 took a much shorter time to lose its water than sample 2 and that the rate of water loss from sample 1 was much greater than from sample 2. Since sample 1 was in the spectrometer beam for much longer periods of time than sample 2, it is clear that additional water loss from sample 1 has occurred due to the heating effect of absorbed infra-red radiation.

It is thus clear that samples placed in the infra-red beam will often be at a higher temperature than the surrounding atmosphere. Any small changes in atmospheric conditions such as draughts will cause heat to be conducted away from the sample at different rates, thus causing a continual variation in sample temperature and a consequential continual variation in temperature sensitive hydrogen bonded OH peaks.

Smaller variations in sample temperature were also thought to occur due to variations in the spectrometer bed temperature (due to an insensitive thermostat) and variations in room temperature.

2.3.2 The Use of Organic Solvents to Cool Samples in the Spectrometer Beam and Act as a Buffer against Temperature Changes

The use of various organic solvents as immersion media was investigated, in an attempt to produce more reproducible spectra. Samples were mounted in fixed plate cells between spacers and surrounded by various suitable organic solvents prior to the recording of spectra. Solvents were selected on the basis of absorption characteristics in the regions under investigation. Spectroscopic grade carbon tetrachloride or hexachlorobutadiene were found to be suitable for the 2.5 - 5 μm.(4000 - 2000 cm.$^{-1}$) region, since they did not absorb significantly in this region. The second derivative spectra of viscose, dicel and tricel films immersed in carbon tetrachloride or hexachlorobutadiene showed an increased reproducibility, indicating that these solvents do in fact act as a buffer against temperature changes. An increase in spectral resolution was also observed when these solvents were used as immersion media. These results indicate the suitability of carbon tetrachloride or hexachlorobutadiene as immersion media, but there are in fact several problems which arise when they are used, especially with samples containing water.

The first problem arises due to the fact that samples conditioned at humidities greater than room humidity lose water when immersed in carbon tetrachloride or hexachlorobutadiene, conditioned at room humidity. Samples of viscose, dicel and tricel film, conditioned at a humidity greater than room humidity, were shaken with 5 ml. samples of spectroscopic grade carbon tetrachloride or hexachlorobutadiene which had been previously exposed to the atmosphere. The absorption spectra of carbon tetrachloride and hexachlorobutadiene after shaking with conditioned film samples were compared in the 3 μm.(3333 cm.$^{-1}$) region with the absorption spectra of carbon tetrachloride or hexachlorobutadiene conditioned at room humidity. In all cases, an increase in the water peak near 3 μm.(3333 cm.$^{-1}$) of 5-10% was observed for spectra of solvents shaken with conditioned film samples, when compared with spectra of solvents conditioned in the atmosphere, clearly showing that the solvents had extracted water from the film samples.

This problem was initially overcome by using immersion media of carbon tetrachloride or hexachlorobutadiene conditioned at the same humidity as the film sample. Any absorptions due to water in the carbon tetrachloride were 'balanced out' by using an equal thickness of the solvent similarly conditioned in the reference beam, although achieving such a thickness was in practice very difficult and tedious since it necessitated many 'trials' with a variable path length cell. The use of this technique also reduces the sensitivity in the 3 μm.(3333 $cm.^{-1}$) region where peaks due to absorbed water and cellulosic OH groups occur.

A further problem arises due to the fact that carbon tetrachloride (164) or hexachlorobutadiene interact with water by affecting the hydrogen bonding in the water system and thus producing changes of peak frequencies in the infra-red spectra of water. This effect has been studied in greater detail by Whitaker (162), who observed the second derivative spectra of a series of 'water-in-solvent' systems.

In view of these unfavourable factors, it was decided to abandon the use of carbon tetrachloride or hexachlorobutadiene as immersion media and construct a sealed cell system capable of accurately controlling sample temperature (and humidity).

2.4 Development of a Dual Beam Controlled Temperature and Humidity Cell

2.4.1 Introduction

Several other systems have been developed for controlling the temperature (166-168) or humidity (169) of samples whilst spectra are being recorded, but these involve single beam cells. A dual beam cell constructed by Neu (170) was found capable of taking spectra of samples at temperatures up to 500°C. but the temperature control of such a system was not accurate enough for the purposes required in this work near room temperature.

A dual beam system was thus designed, which was capable of producing

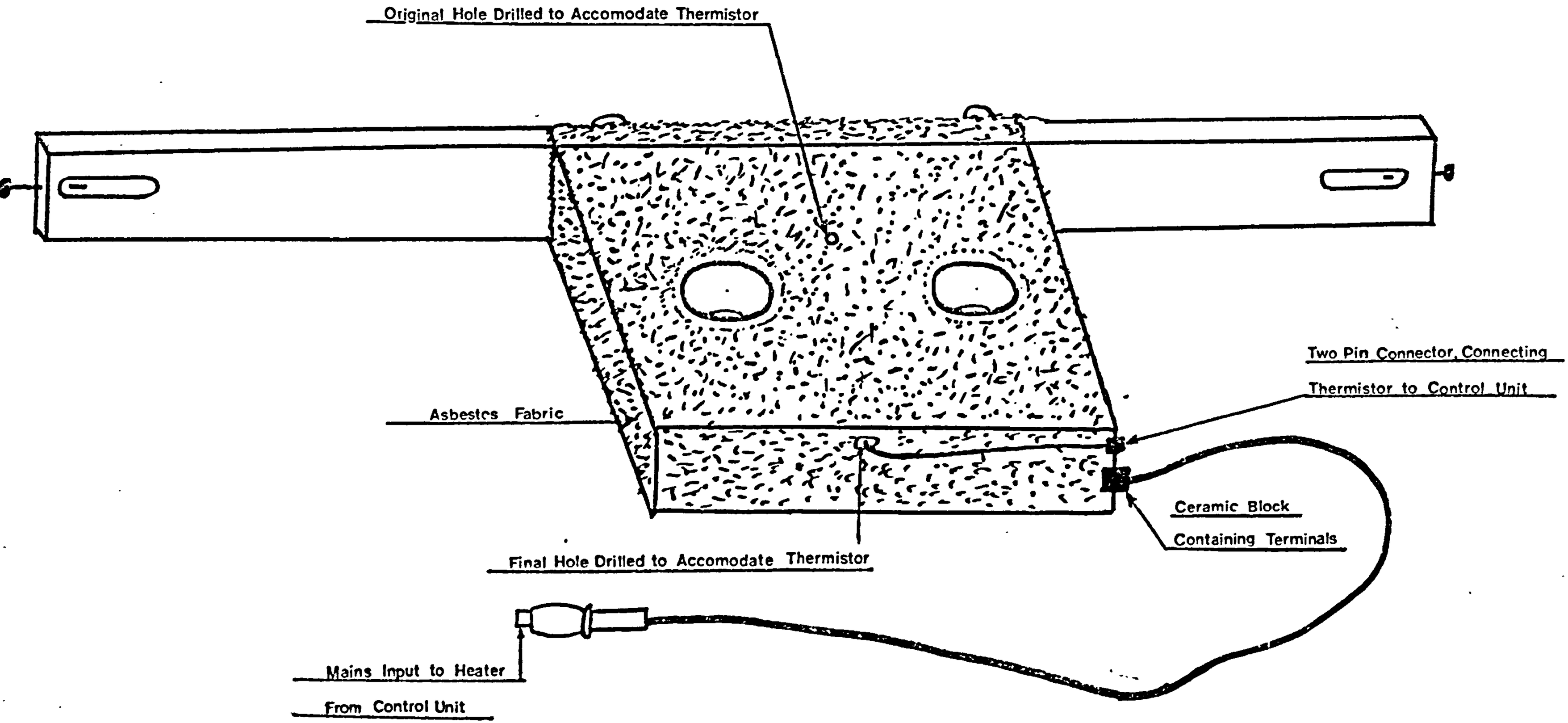
Original Hole Drilled to Accomodate Thermistor
Two Pin Connector, Connecting
Thermistor to Control Unit
Asbestos Fabric
Ceramic Block
Containing Terminals
Final Hole Drilled to Accomodate Thermistor
Mains Input to Heater
From Control Unit

FIG.36

accurate control of temperature near room temperature and which also enabled selected sample humidities to be accurately controlled. The system also allowed sample temperature to be varied up to 300°C. to investigate changes in structure which occur with rise in temperature. The mounting of the sample within the cells was also designed so as to rapidly conduct heat to or from the samples and thus minimise any variation due to sample heating by absorption of infra-red radiation. In practice, samples were allowed to come to 'steady state' temperatures within the cells over a period of 10-15 min. prior to the recording of spectra. A minimum working temperature of 44°C. was chosen to eliminate any variation in sample temperature due to variations in external spectrometer or room temperatures.

In considering the design and performance of such a system, the requirements of several workers were taken into account and the following system constructed.

2.4.2 Components of the Dual Beam Controlled Temperature and Humidity Cell System

The system constructed consists of the following basic components:-

(i) A Heated Block

(ii) Sealed Sample and Reference Cells

(iii) A Temperature Control Unit

(iv) A Spectrometer Mounting System

(v) A Temperature Measuring Thermocouple System

(i) The Heated Block

.The heated block constructed of aluminium is shown in Fig.36. The holes for the sample cells were spaced so that sample and reference beams passed through their centres when the block was mounted in the spectrometer. The diameter of the holes was $2\frac{1}{16}$" so that standard fixed plate cells and

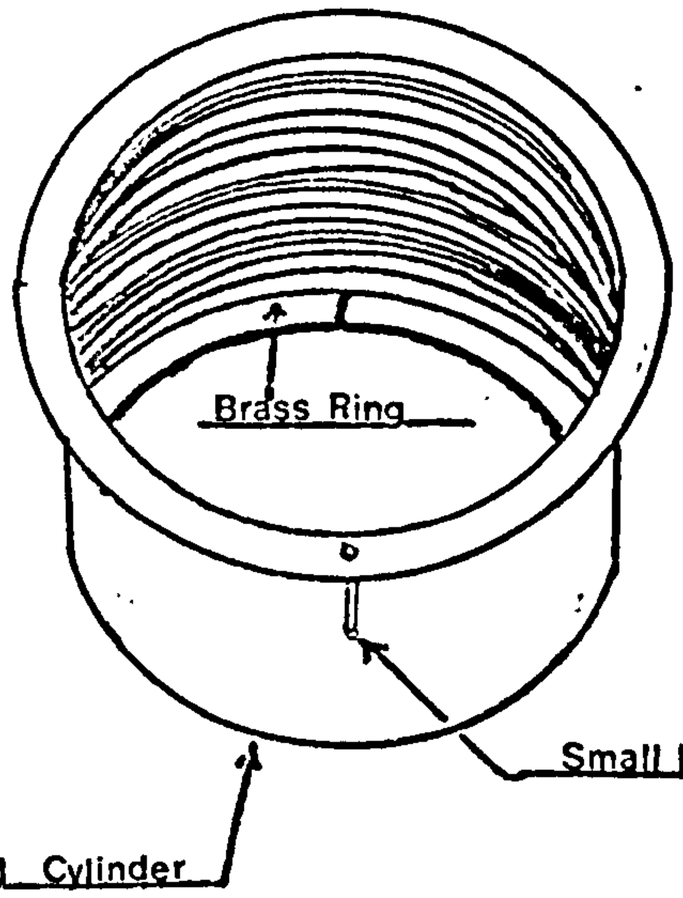

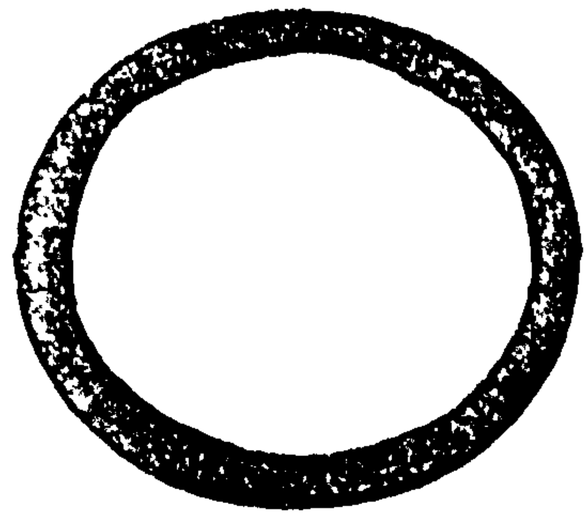

Plate Finish Neoprene Washer

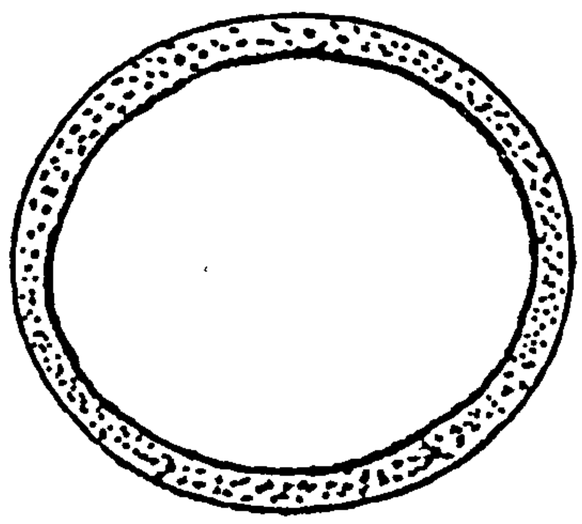

Paper Washer

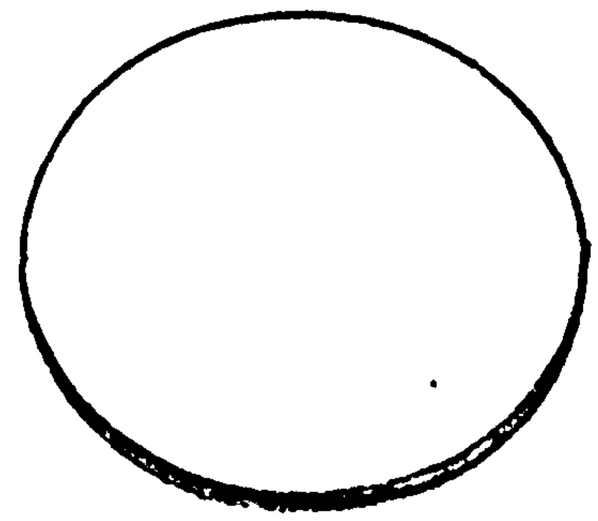

Rock Salt Window

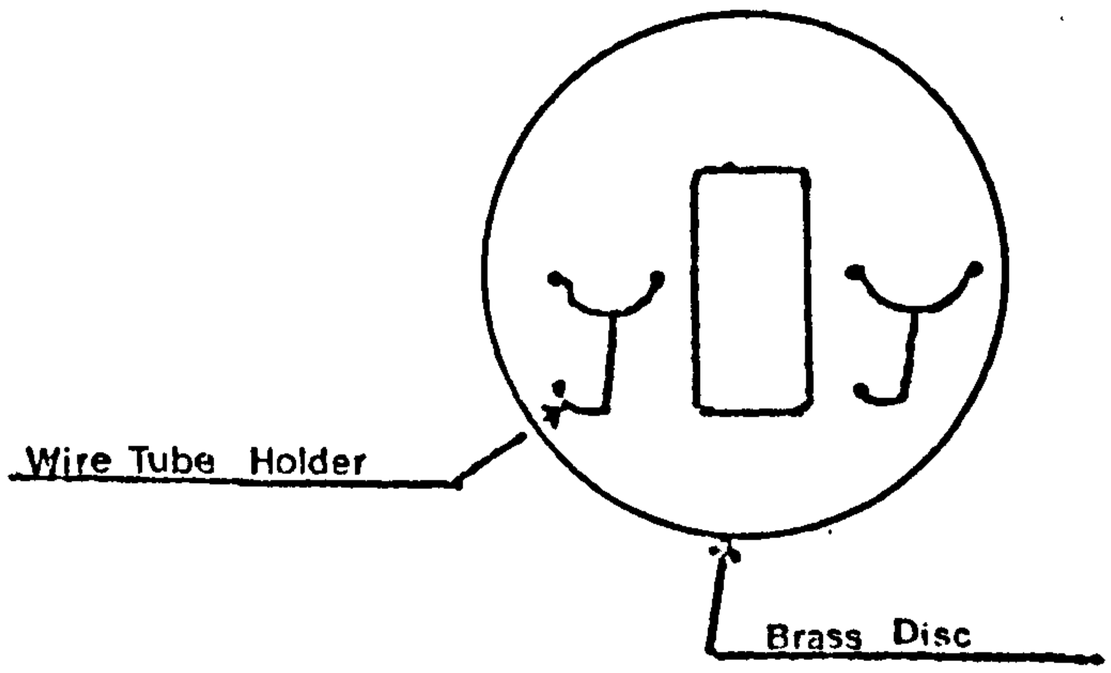

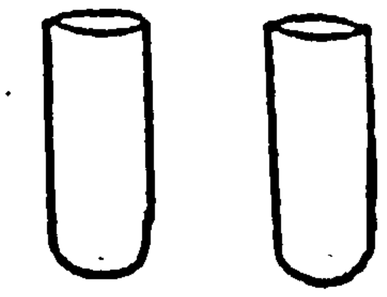

Small Glass Tubes

FIG 37

other samples cells could be accommodated. A smaller hole approximately $\frac{1}{2}$" in diameter was drilled at an angle between these two holes and accommodated a thermometer or thermistor.

The heating coil was mounted in a groove cut round the edge of the block. The dual requirements of the coil being electrically insulated and in good thermal contact with the block were satisfied with the use of a cement made up from 1 part of Seagar cement and two parts of calcined alumina. A small amount of this mixture was made into a thick paste by adding water, and the bottom and sides of one section of the groove lined with it. Each lined section was allowed to dry slowly overnight with a damp cloth covering it to reduce the rate of evaporation and thus prevent cracking. The lining process was repeated with each of the four sections of the groove until completion.

The heating element was constructed from nicrome wire with a resistance of 6.32 ohms metre^{-1} and it was calculated that 8 metres were required to give an acceptable mains heater of 400 watts rating. The wire was then wound into a coil over a glass rod and carefully placed in the groove. The two ends of the wire were then connected to heat resistant terminals embedded in a small ceramic block at one corner of the aluminium block. A large quantity of the cement paste was then made up and the groove filled section by section with it so as to completely encapsulate the heating coil. The cement was then allowed to dry as before.

(ii) <u>Sealed Sample and Reference Cells</u>

The sealed cells constructed are shown in Fig.37. Aluminium was used as a suitable material and a small hole drilled through the flange of each cell leading to a groove running half way along the cylinder to accommodate a thermocouple lead. The cylinders were continuously threaded and fitted with brass rings to retain the cell windows and sample holder.

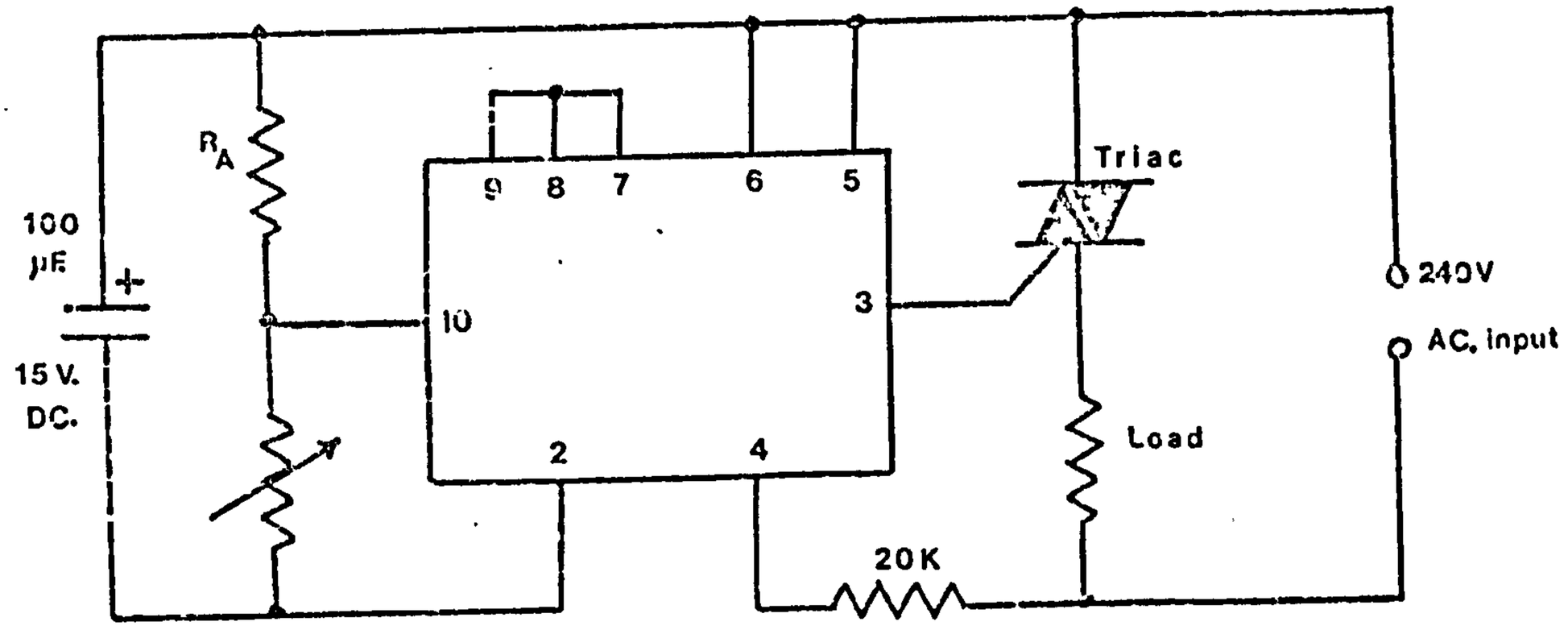

R_A negative temp. coefficient thermister.

FIG. 38 A

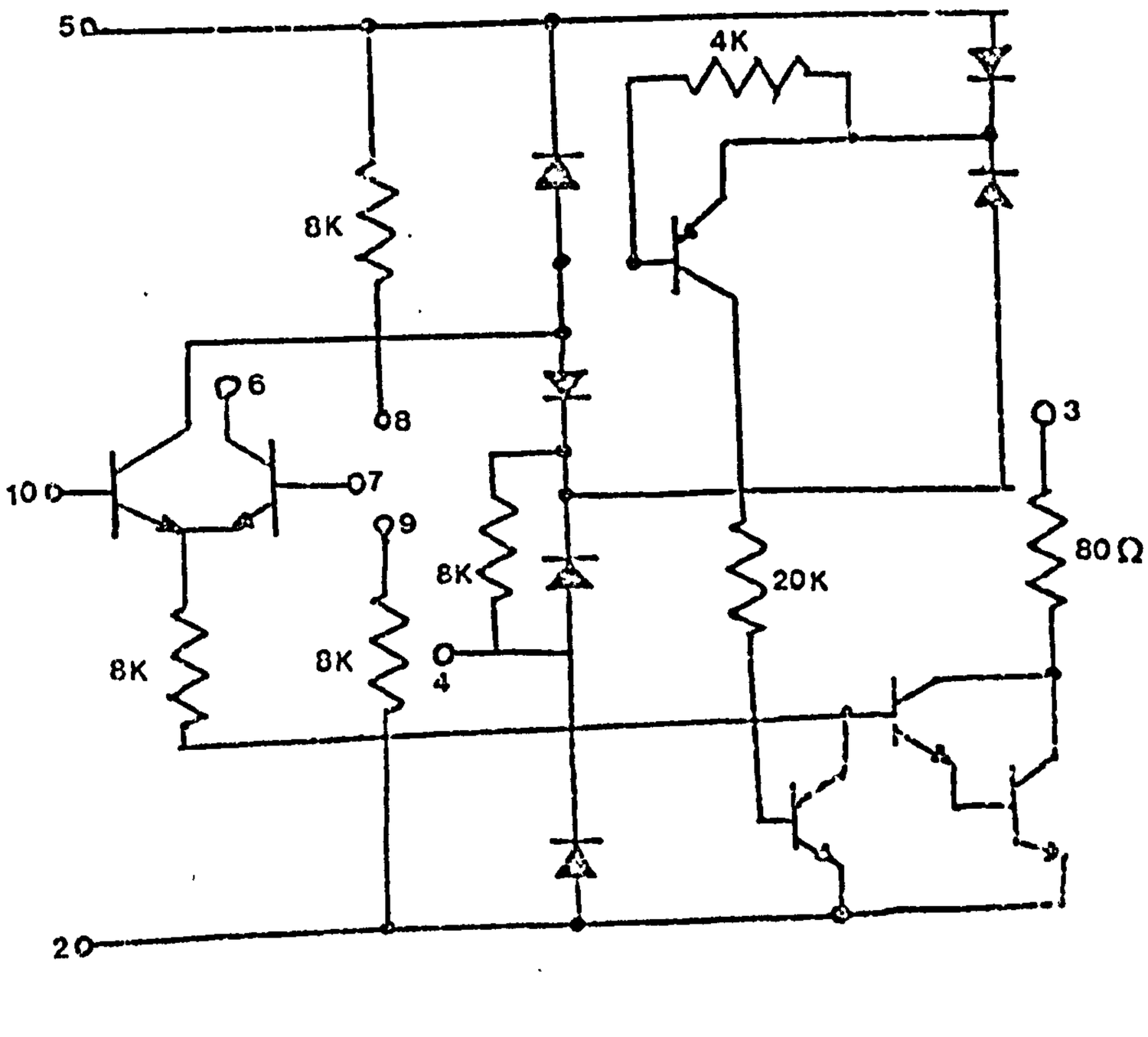

FIG. 38 B

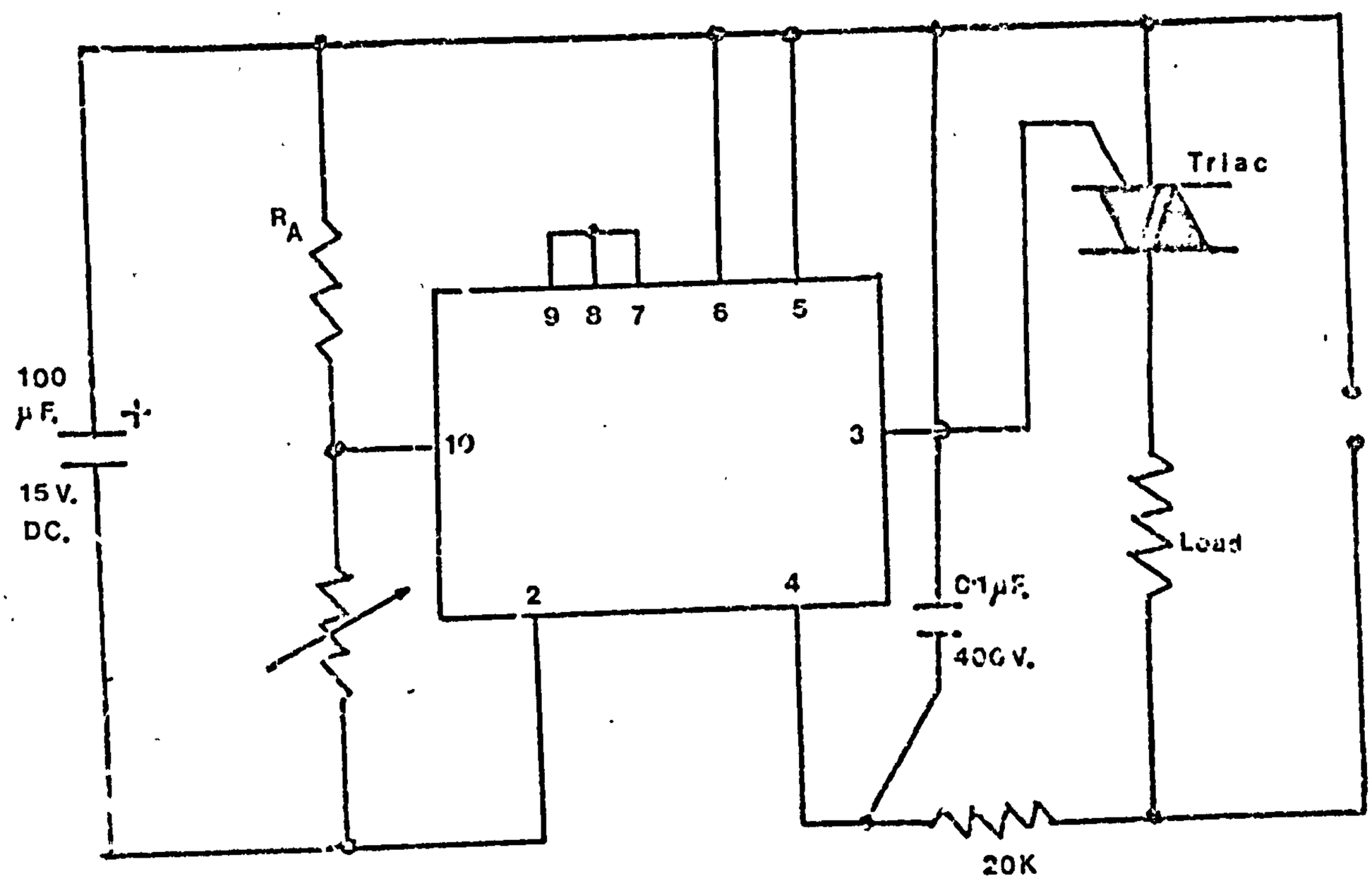

FIG. 38 C

The rock salt or vitreosil windows retained by the brass rings were cushioned on the inside by thick paper spacers and sealed on the outside by plate-finish 1/32" thick neoprene washers. Neoprene washers could not be used inside the cells at high temperatures because of their tendency to degrade and contaminate the samples.

Samples were mounted inside the cells on brass discs in which a rectangular hole $1\frac{1}{2}$ x 1 cm. had been cut and across which samples were attached with sellotape (Fig.37). Each brass disc was fitted with two wire tube holders on either side of the hole. Small tubes were supported by the holders and these tubes were used to contain either P_2O_5 to produce a dry atmosphere and dry samples, or the saturated solutions of various salt solutions in contact with undissolved solid, to produce given humidities. The humidity of the atmosphere in the cells could thus be varied over the whole R.H. range. Since the temperature was also accurately controlled, the exact conditions in the cell could be established. In some cases two sample discs with four tubes were used, with the sample retained between them. When four tubes were used, a more rapid drying or conditioning of the atmosphere in the cell was achieved.

By the use of a blank reference cell set up with the same path length, cell windows and internal atmosphere, any small absorptions due to the windows or water vapour were eliminated without a consequential large loss of sensitivity in the spectral regions where these small absorptions occur.

(iii) (a) The Temperature Control Unit

A commercial circuit (Fig. 38A) incorporating a G.E.C. TO100 integrated circuit (Fig. 38B) and a 1 Meg ohm thermistor was used as a basis for the temperature control unit. This circuit differs from the one actually used (Fig.38C) in that two of the connections to the triac were reversed and a 0.1 μF 400 volt capacitor was included between pins 4 & 5 of the integrated

circuit. The capacitor was included to produce a smoother output to the heated block. The circuit operates in such a way as to balance out the resistance of the thermistor against the resistance of a variable potentiometer. When the resistance of the thermistor is higher than that of the potentiometer, the triac allows an output to flow to the heating element of the block, but when the two are 'equal', the current supply is interrupted. The variation in the resistance of the thermistor is thus used to control the temperature of the cell body. In practice the balance is not a true 1:1 ratio of potentiometer resistance to thermistor resistance and the ratio varies with potentiometer setting. However, the ratio is constant for any particular potentiometer setting and hence temperature.

(iii) (b) Difficulties and Refinements of the Temperature Control Unit

With the system described above, the temperature of the block, measured with thermometers reading accurate to 0·1°C., was found to vary by 0.5°C. at temperatures near 30°C. and by 5°C. at temperatures near 200°C.. Such a large variation was considered unsatisfactory and was attributed to the thermistor being too far away from the heating element, so that the time taken for the thermistor to respond to heat from the heating element was too great. However, a more rapid thermistor response was obtained by mounting the thermistor in a small hole in the top of the block near the element. The thermistor was fixed in this hole with cement and the thermistor leads electrically and thermally insulated with asbestos sleeving. The leads were then connected to a miniature two pin socket located in a small metal plate at one edge of the aluminium block. A miniature two pin plug fitting the socket connected the thermistor to the control unit.

To reduce heat losses from the block and hence further decrease temperature variation, an asbestos jacket was made for the block from fabric $\frac{1}{8}$" thick. By means of such refinements, much smaller block temperature variations were obtained, i.e. $\pm$ 0.1°C. at temperatures near 30°C. and

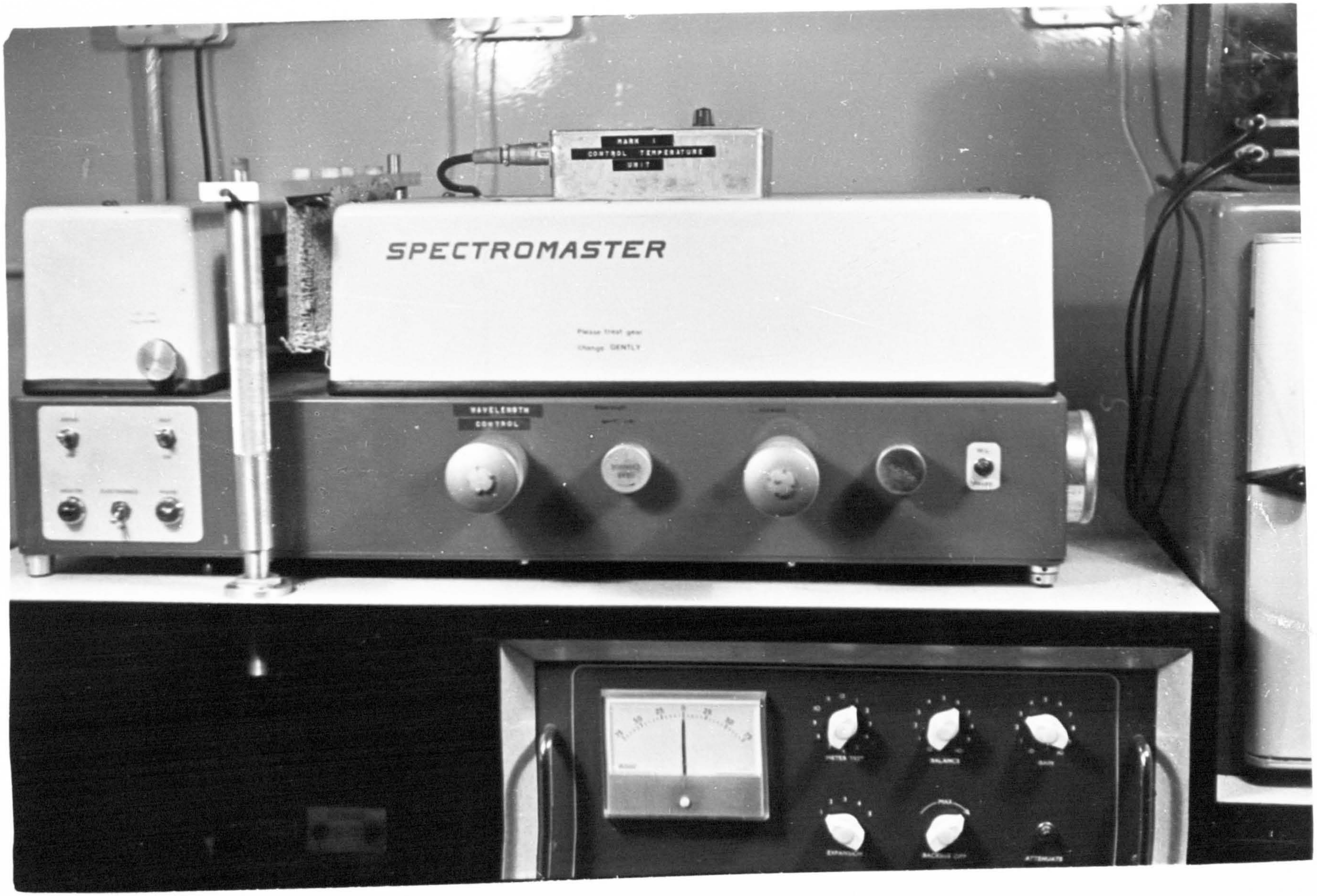
MARK I
CONTROL TEMPERATURE
UNIT
SPECTROMASTER
Please treat gear
change GENTLY
WAVELENGTH
CONTROL

FIG. 39

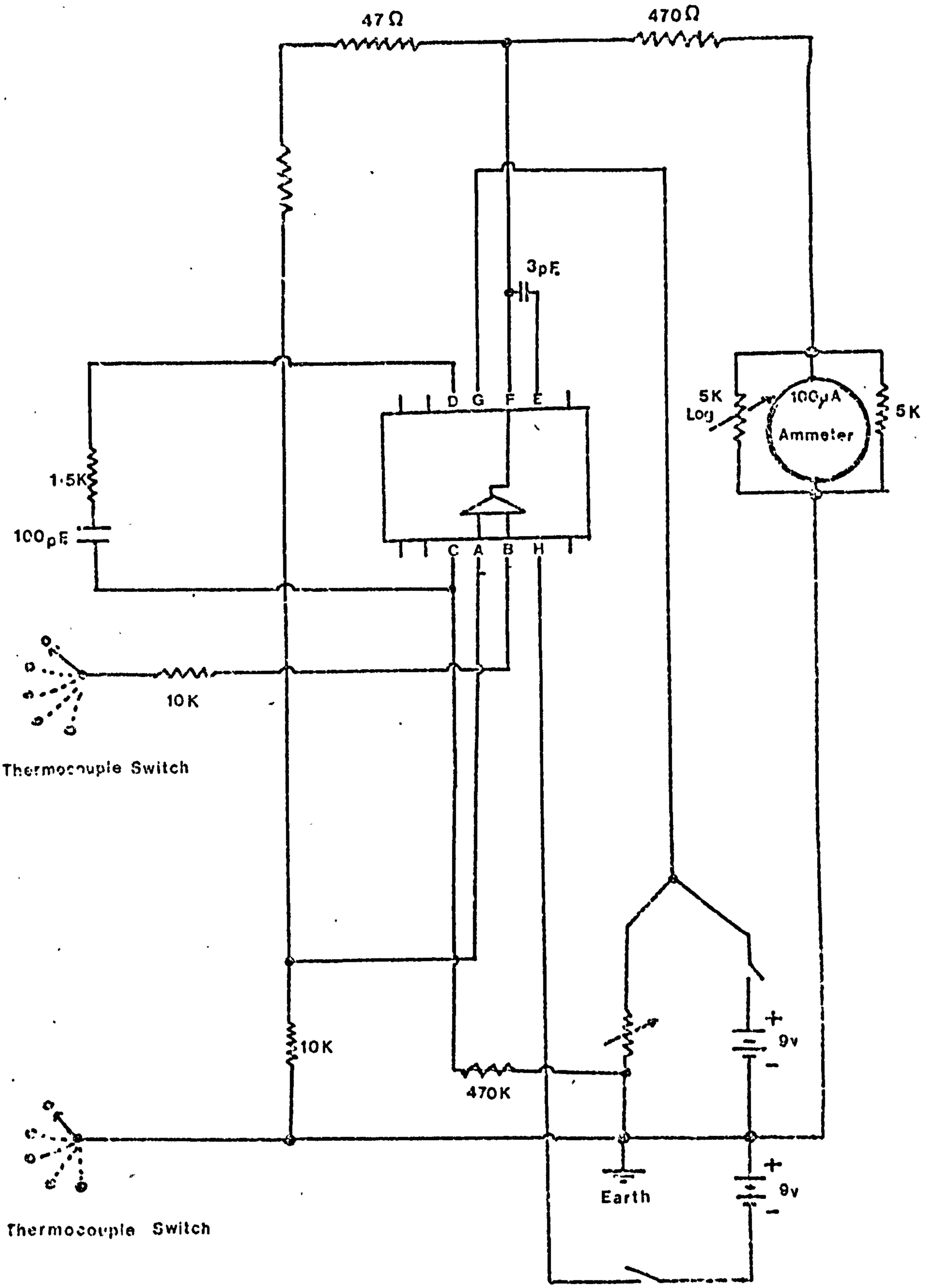
47 Ω
470 Ω
3pF.
D G F E
1·5K
100pF.
C A B H
5K
Log
100μA
Ammeter
5K
10K
Thermocouple Switch
10K
470K
9v
9v
Earth
Thermocouple Switch

FIG. 40 A

$\pm$ 1°C. at temperatures near 200°C..

The potentiometer was fitted with a pointer and scale and calibrated against temperature. However, the best calibration in terms of temperature range was found using a thermistor with a resistance of 120 K. ohm at 20°C. and 1K ohm at 300°C. and, using the circuitry described, adequate calibration was obtained between 30 and 300°C..

(iv) The Spectrometer Mounting

A spectrometer mounting for the block was designed so that the block containing the cells could be suspended above the spectrometer bed and thus prevent transfer of heat to the spectrometer base. To assist the reduction of radiative transfer, asbestos fabric was placed on the spectrometer base and along the walls of the sample cavity to provide further shielding.

The heated block and its mounting above the spectrometer bed are shown in Fig.39. Adjustments in lateral and vertical position could be allowed for by means of screw adjustments. The lateral movement was incorporated into the system to enable the spectra of wedge shaped samples to be observed and thus cover a much wider spectral range. A similar widening of spectral range was obtained by making a composite sample from two strips of material, one thick and one thin, side by side on the sample holder. The composite sample was then traversed to find the correct 'thickness' for the region of the spectrum under investigation. Such a technique was found to be time saving, since samples had to be left to condition for at least 12 hr. prior to spectral recording.

(v) Temperature Measuring Unit

In order to accurately measure sample temperature, (spectrometer base, heated block and lamp housing temperatures), a unit capable of accurately measuring temperatures by thermocouples was constructed. This unit was based upon the circuit shown in Fig. 40A and incorporates a G.E.C. 709-OPA

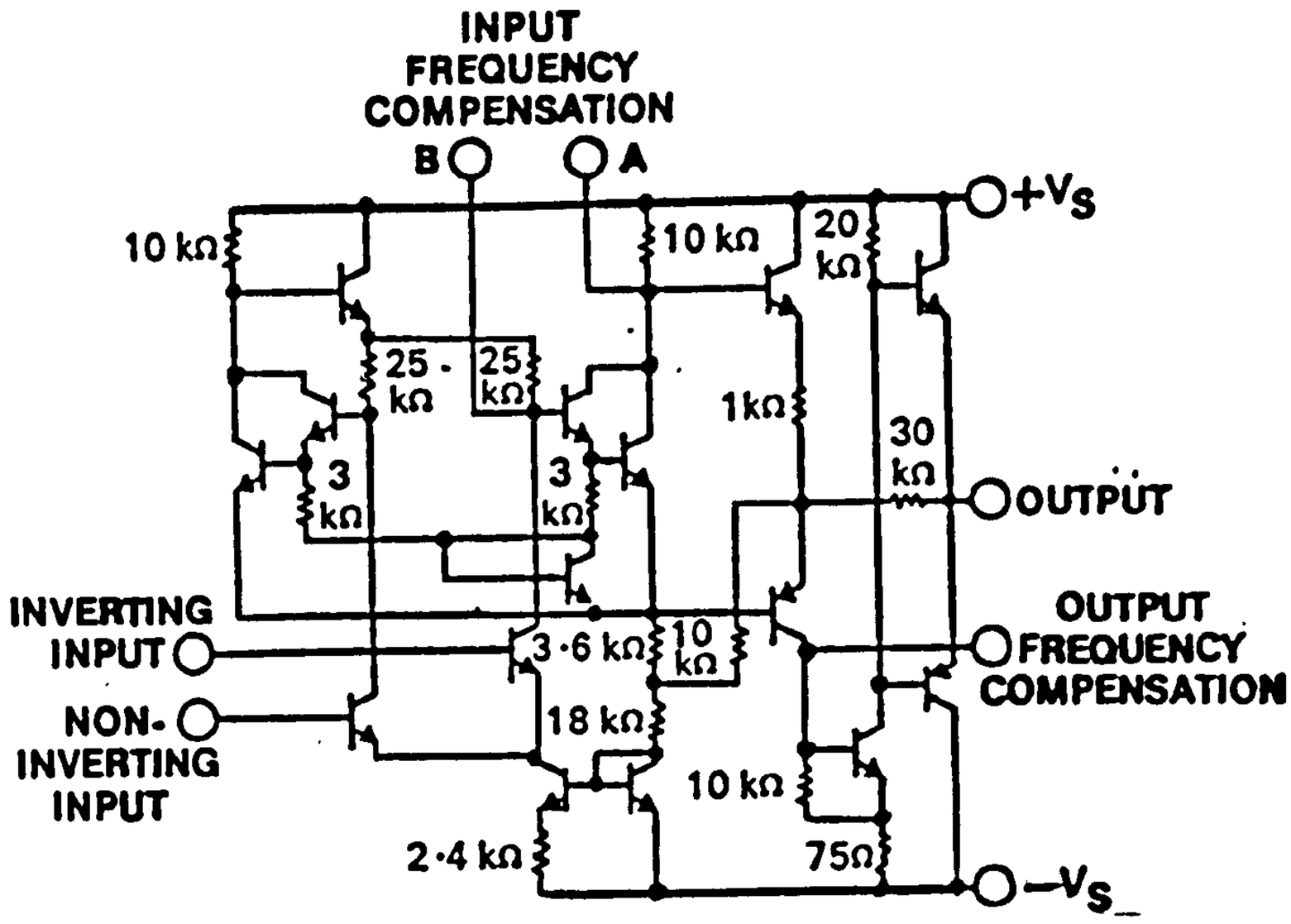
INPUT
FREQUENCY
COMPENSATION
B
A
+Vs
10 kΩ
10 kΩ
20
kΩ
25
kΩ
25
kΩ
1kΩ
30
kΩ
3
kΩ
3
kΩ
OUTPUT
INVERTING
INPUT
3·6 kΩ
10
kΩ
OUTPUT
FREQUENCY
COMPENSATION
NON-
INVERTING
INPUT
18 kΩ
10 kΩ
2·4 kΩ
75Ω
-Vs

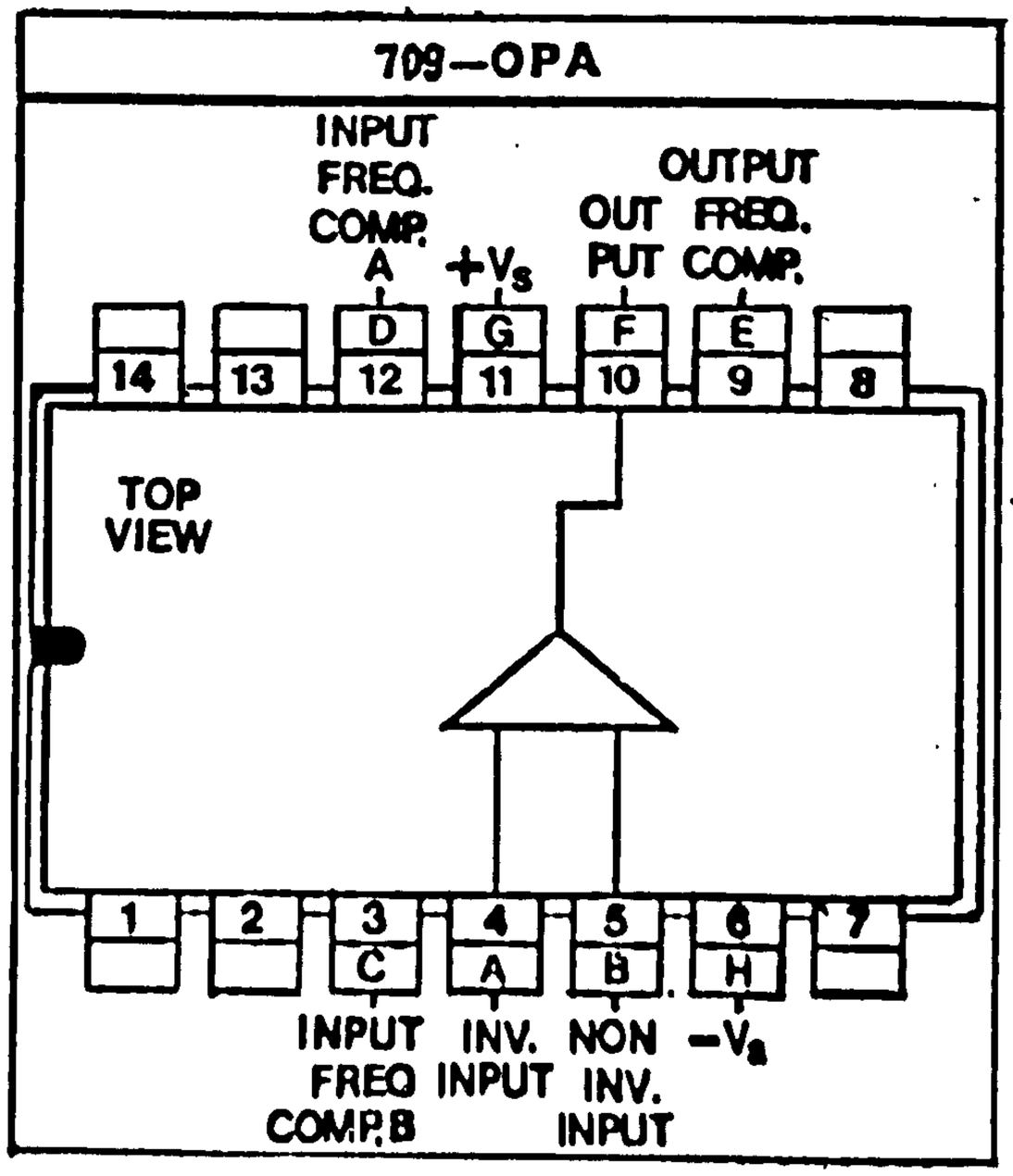
709—OPA
INPUT
FREQ.
COMP.
A
+Vs
OUT
PUT
OUTPUT
FREQ.
COMP.
D
G
F
E
14
13
12
11
10
9
8
TOP
VIEW
1
2
3
C
4
A
5
B
6
H
7
INPUT
FREQ
COMP.B
INV.
INPUT
NON
INV.
INPUT
-Va

FIG. 40 B

$\pm$ 1°C. at temperatures near 200°C..

The potentiometer was fitted with a pointer and scale and calibrated against temperature. However, the best calibration in terms of temperature range was found using a thermistor with a resistance of 120 K. ohm at 20°C. and 1K ohm at 300°C. and, using the circuitry described, adequate calibration was obtained between 30 and 300°C..

(iv) The Spectrometer Mounting

A spectrometer mounting for the block was designed so that the block containing the cells could be suspended above the spectrometer bed and thus prevent transfer of heat to the spectrometer base. To assist the reduction of radiative transfer, asbestos fabric was placed on the spectrometer base and along the walls of the sample cavity to provide further shielding.

The heated block and its mounting above the spectrometer bed are shown in Fig.39. Adjustments in lateral and vertical position could be allowed for by means of screw adjustments. The lateral movement was incorporated into the system to enable the spectra of wedge shaped samples to be observed and thus cover a much wider spectral range. A similar widening of spectral range was obtained by making a composite sample from two strips of material, one thick and one thin, side by side on the sample holder. The composite sample was then traversed to find the correct 'thickness' for the region of the spectrum under investigation. Such a technique was found to be time saving, since samples had to be left to condition for at least 12 hr. prior to spectral recording.

(v) Temperature Measuring Unit

In order to accurately measure sample temperature, (spectrometer base, heated block and lamp housing temperatures), a unit capable of accurately measuring temperatures by thermocouples was constructed. This unit was based upon the circuit shown in Fig. 40A and incorporates a G.E.C. 709-OPA

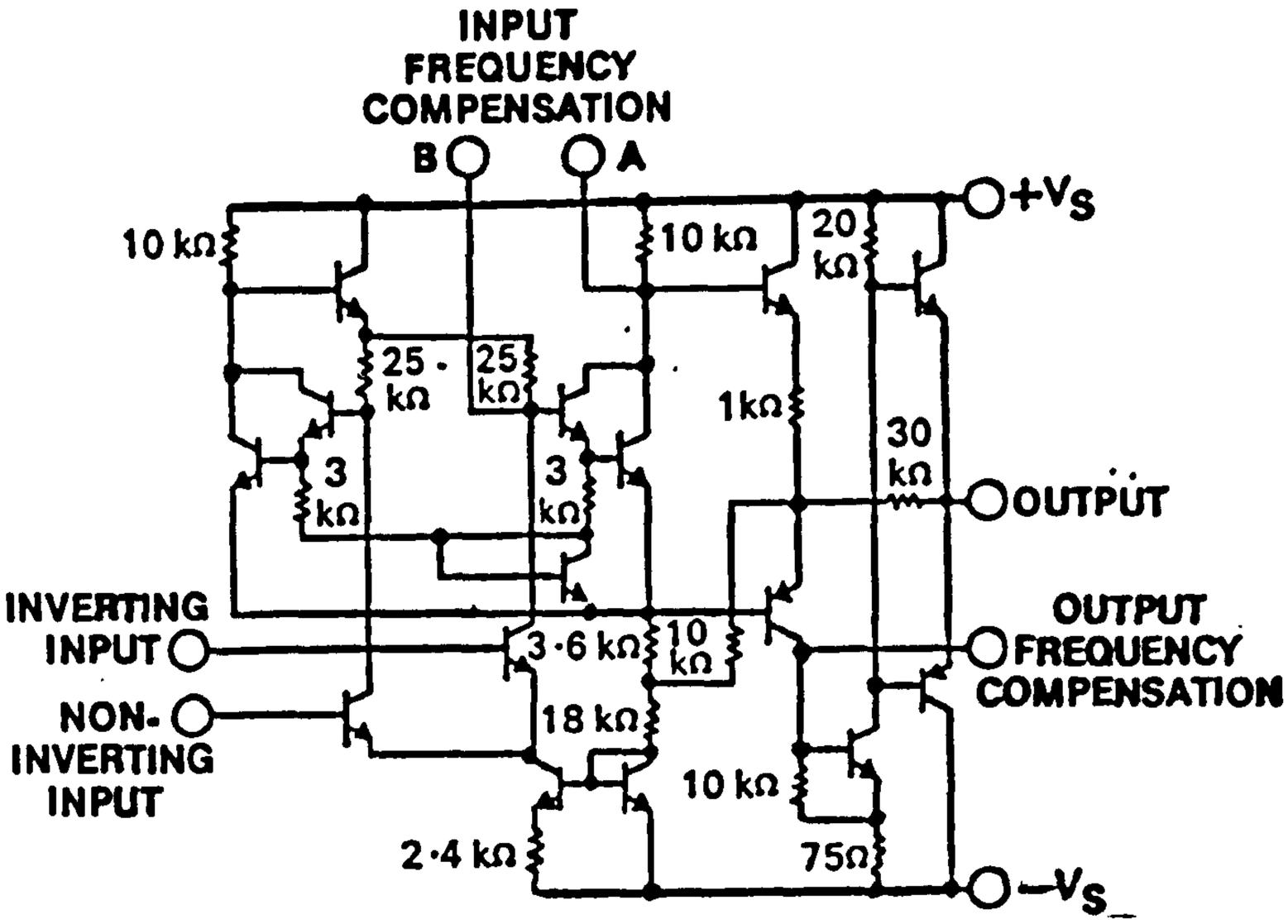
INPUT
FREQUENCY
COMPENSATION
B
A
+Vs
10 kΩ
10 kΩ
20
kΩ
25
kΩ
25
kΩ
1kΩ
3
kΩ
3
kΩ
30
kΩ
OUTPUT
INVERTING
INPUT
3·6 kΩ
10
kΩ
OUTPUT
FREQUENCY
COMPENSATION
NON-
INVERTING
INPUT
18 kΩ
10 kΩ
2·4 kΩ
75Ω
-Vs

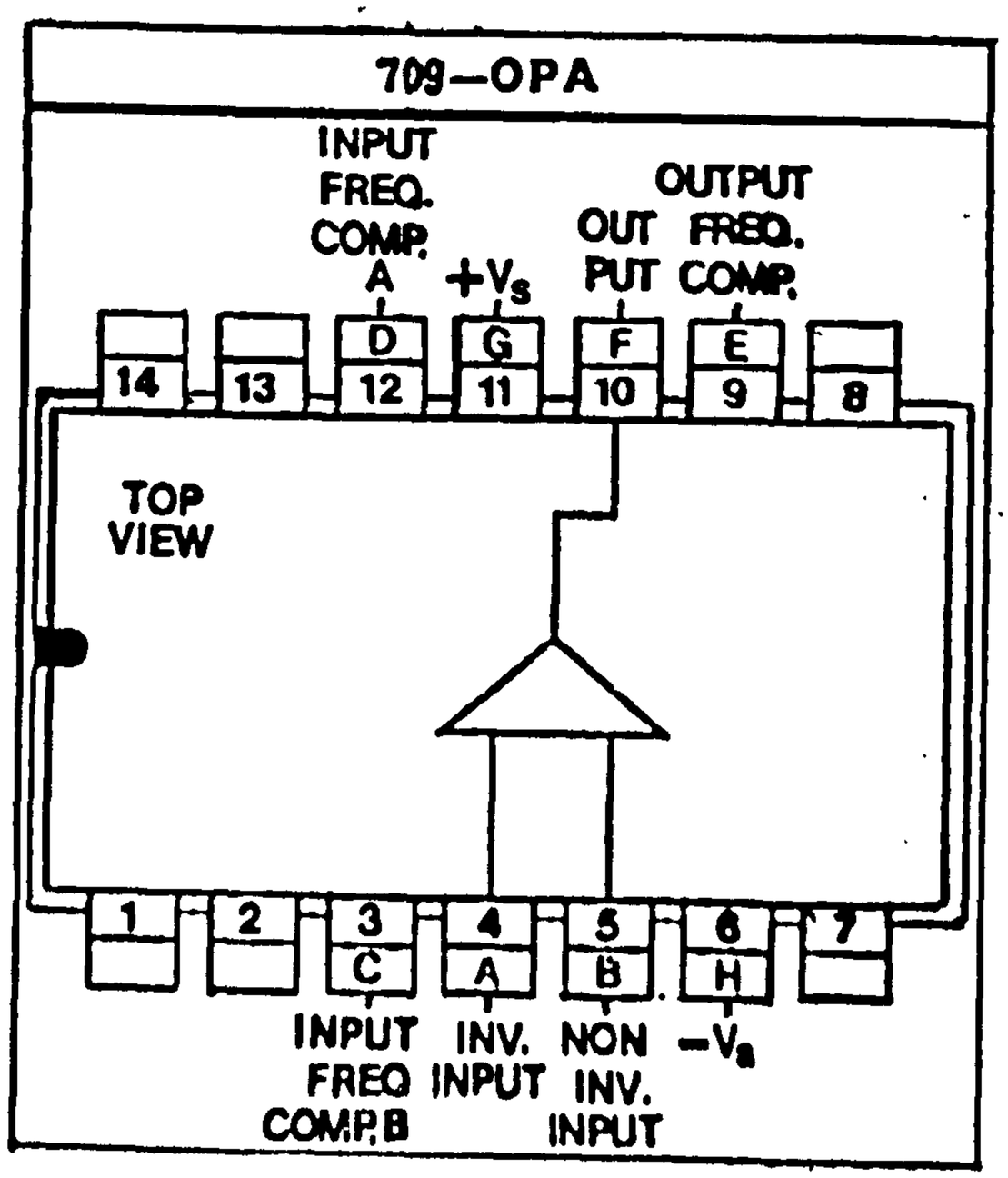
709—OPA
INPUT
FREQ.
COMP.
A
+Vs
OUT
PUT
OUTPUT
FREQ.
COMP.
14
13
D
12
G
11
F
10
E
9
8
TOP
VIEW
1
2
3
C
4
A
5
B
6
H
7
INPUT
FREQ
COMP.B
INV.
INPUT
NON
INV.
INPUT
-Vs

FIG. 40 B

integrated circuit operational amplifier (Fig.40B) and copper/constantan thermocouples. A 5 K.ohm logarithmic potentiometer enables the sensitivity of the instrument to be adjusted so as to accept narrow or wide temperature ranges on the meter. A 100 K.ohm linear potentiometer enables the bias of the circuit to be varied to obtain a meter zero reading. The thermocouples are connected to the unit via a junction box mounted on the spectrometer and a multi-way switch.

The unit works by comparing the e.m.f. developed by a measuring thermocouple switched into the circuit (thermocouples 3 - 6) with the e.m.f. of a reference thermocouple (thermocouple 1) kept at a standard temperature of $0^{o}C.$ in an ice/water mixture. E.m.f. differences are amplified by the unit and shown as meter readings. A further reference thermocouple (thermocouple 2) was also kept in the ice/water mixture at $0^{o}C.$ to produce a zero e.m.f. difference with thermocouple 1 and allow the meter reading to be zeroed.

Trial experiments were conducted to find the sensitivity settings required to produce suitable temperature ranges on the meter scale. A sensitivity of 2.3 was found to be suitable in the range 0 - $120^{o}C$, giving an accuracy of temperature measurement of $\pm$ $0.25^{o}C$, although the actual temperature of the heated block and sample varied by $\pm$ $0.1^{o}C.$ at temperatures near room temperature for a particular control unit setting. A sensitivity of 0.9 was found to be suitable in the 0 - $260^{o}C$., giving an accuracy of temperature measurement of $\pm$ $0.6^{o}C$., although the temperature of the heated block and sample in this range varied by $\pm$ $1^{o}C.$ at temperatures near $200^{o}C.$ for a particular control unit setting.

Thermocouples were calibrated by noting the meter readings produced at different temperatures by either water (in the 0 - $120^{o}C.$ range) or methyl salicylate (in the 0 - $260^{o}C.$ range), cooling from their boiling points. Thermometers reading accurate to $0.1^{o}C.$ were used to measure the temperatures of the liquids. Calibration graph for each of the four measuring thermocouples (thermocouples 3-6) were then drawn for each temperature range

Fig. 41 A, Thermocouple Calibrations, Sensitivity 2·3.

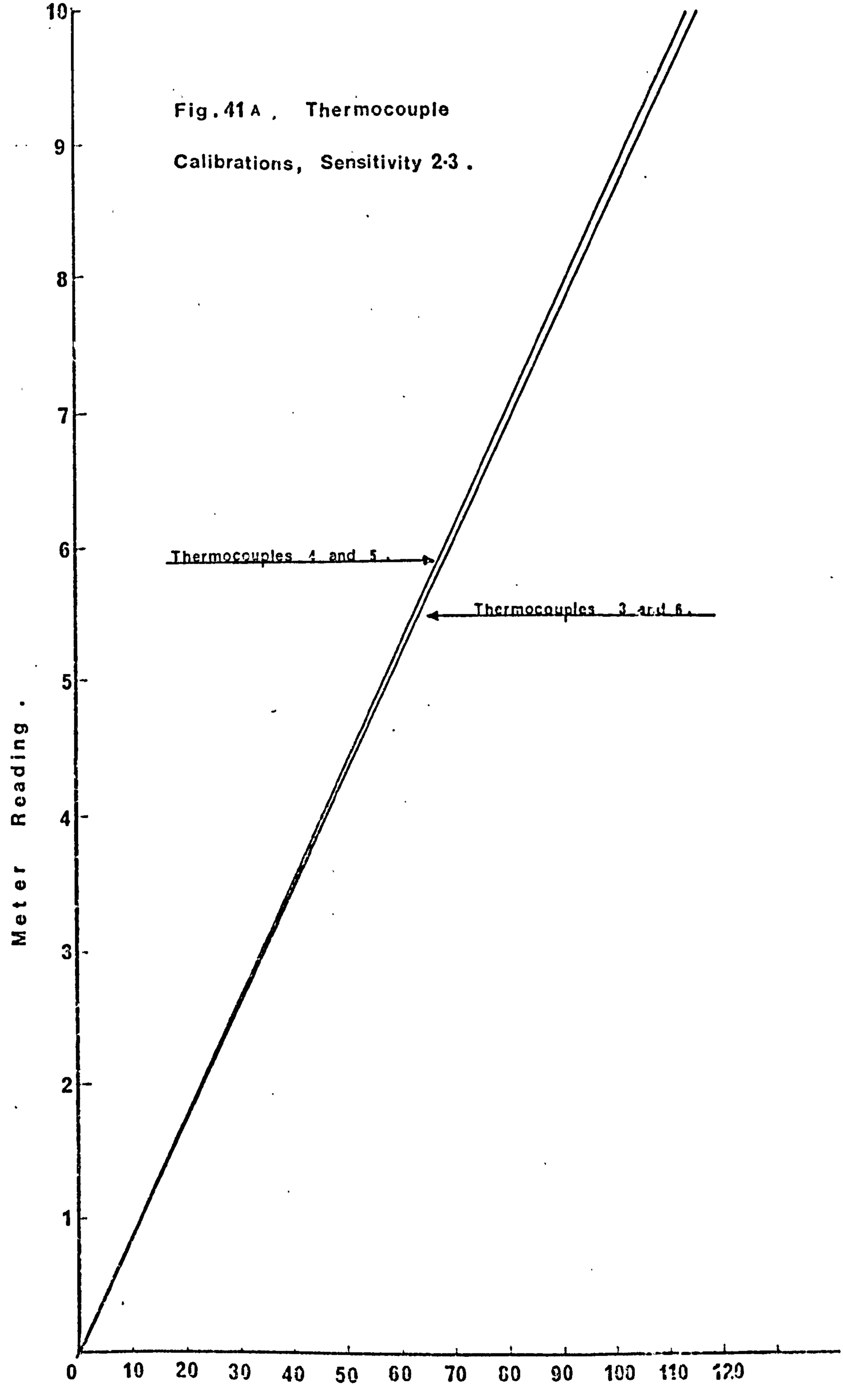

Fig. 41 B Thermocouple

Calibrations, Sensitivity 0·9.

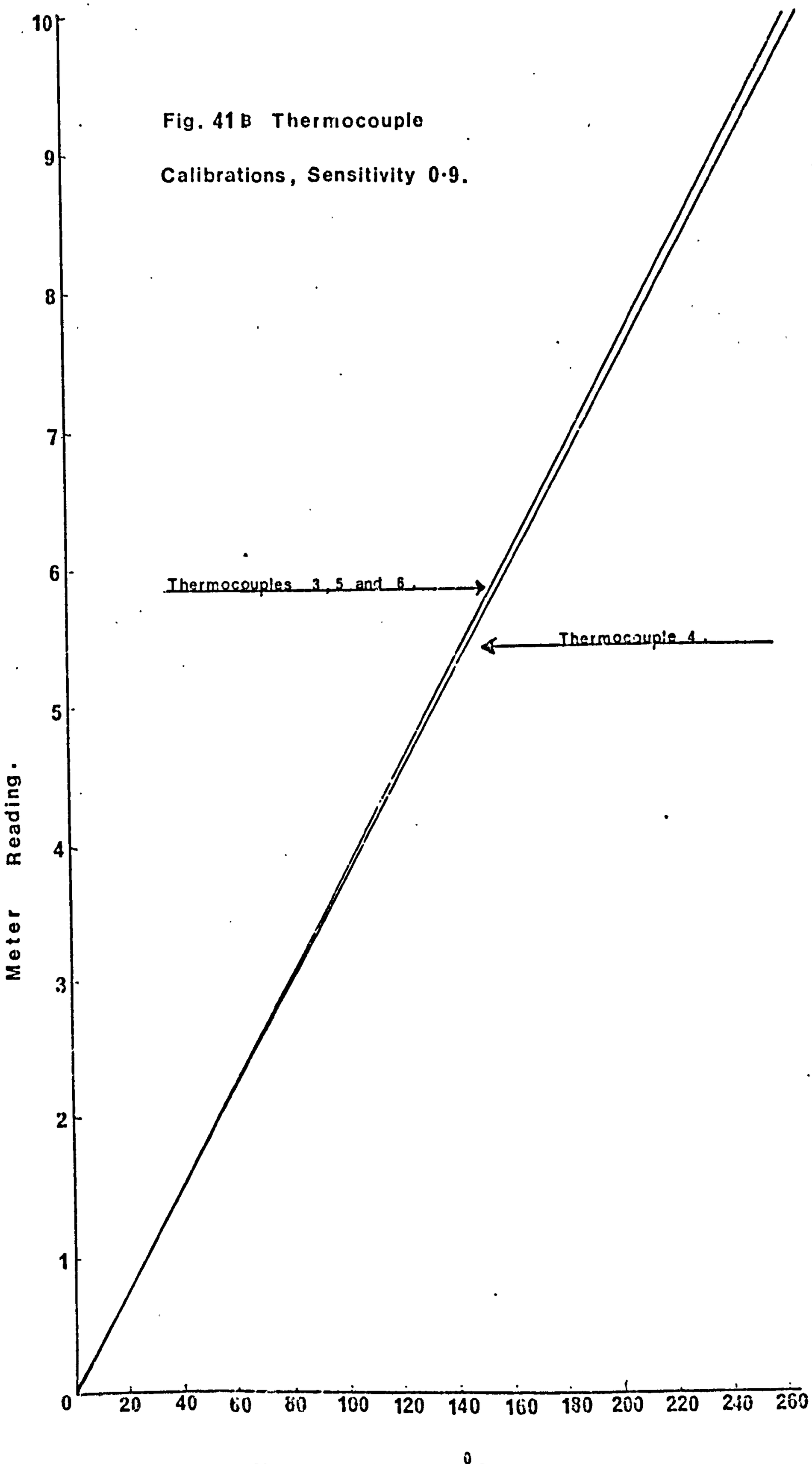

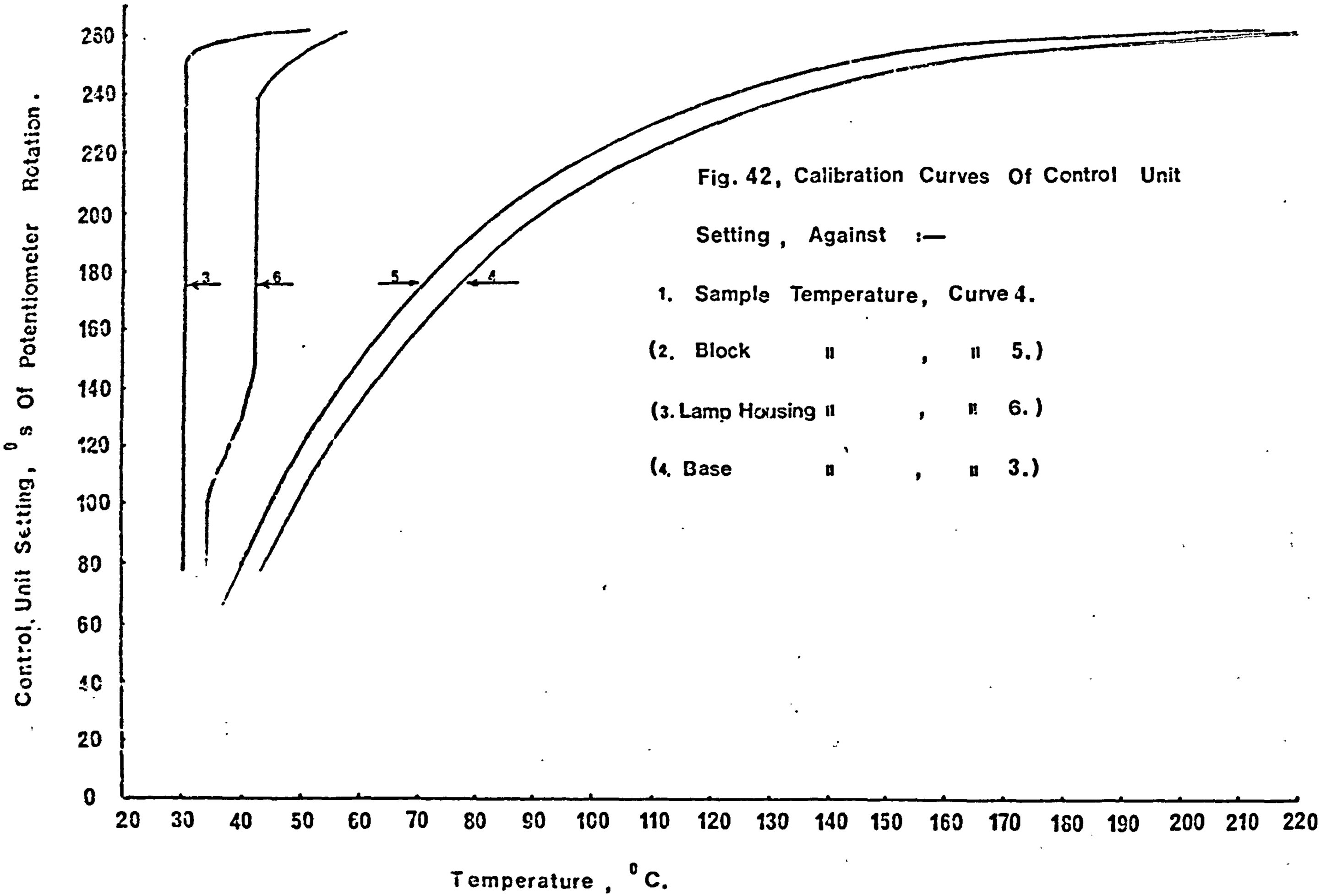

Fig. 42, Calibration Curves Of Control Unit Setting, Against :—

1. Sample Temperature, Curve 4.
(2. Block " , " 5.)
(3. Lamp Housing " , " 6.)
(4. Base " , " 3.)

(Figs. 41A and 41B).

2.4.3 Calibration of the Temperature Control Unit

Using the temperature measuring unit and the measuring thermocouple 4, the temperature of a sample mounted inside a sample cell in the heated block (and a blank reference cell also in the block) was measured for a series of control unit settings over the range 0 - 240°C. The heated block (thermocouple 5), lamp housing (thermocouple 6) and spectrometer base (thermocouple 3) temperatures were also monitored for this series of control unit settings. The monitoring of the lamp housing and spectrometer base temperatures was necessary in order to ensure that no damage was caused to the spectrometer due to excessive radiation from the heated block at high temperatures.

Calibration curves of control unit setting against sample, block, lamp housing and spectrometer temperature were then drawn and these are shown in Fig. 42.

CHAPTER 3

CHAPTER 3

THE EFFECTS OF HEATING AND ANNEALING AND COOLING ON THE SPECTRA OF VISCOSE (CELLULOSE II), CELLULOSE I, DICEL AND TRICEL

Introduction

The work in this chapter deals with the fundamental second derivative spectra of viscose (Cellulose II), dicel and tricel films recorded at 44°C., within the spectral range 2.5 - 15 μm. (4000 - 667 $cm.^{-1}$), and is concerned with the assigmment of spectral peaks to vibrations of various chemical groups (CH, CH_2, OH. etc.). Corresponding absorption spectra recorded at 44°C., are also shown for comparison.

Spectra of film samples recorded at higher temperatures (100°C., 159°C. and 220°C.), are also considered, together with the spectra of annealed samples recorded at 44°C.. The spectra of KBr disc samples, including those of Cellulose I, are also considered in this section.

Method

Samples of viscose, dicel and tricel film were mounted on pieces of supporting photographic film suitably cut to fit the cells of the heated block. Composite samples were produced of thick and thin material, as previously described, so that the whole of the spectral range 2.5 to 15 μm. (4000 - 667 $cm.^{-1}$) could be analysed from a single composite sample. Samples were allowed to dry over P_2O_5 for 24 hrs. prior to mounting in the cells and were then allowed to dry for a further 24 hrs. inside the cells, with P_2O_5 in the small glass tubes. During this final period, sample cells were kept inside a desiccator to prevent clouding of the rock salt windows.

KBr disc samples of viscose, dicel and tricel were prepared by the method previously described and in the concentrations previously determined for each spectral range (Table XV). KBr disc samples of Cellulose I were also prepared from ultrasonically degraded Egyptian cotton (170). Such a

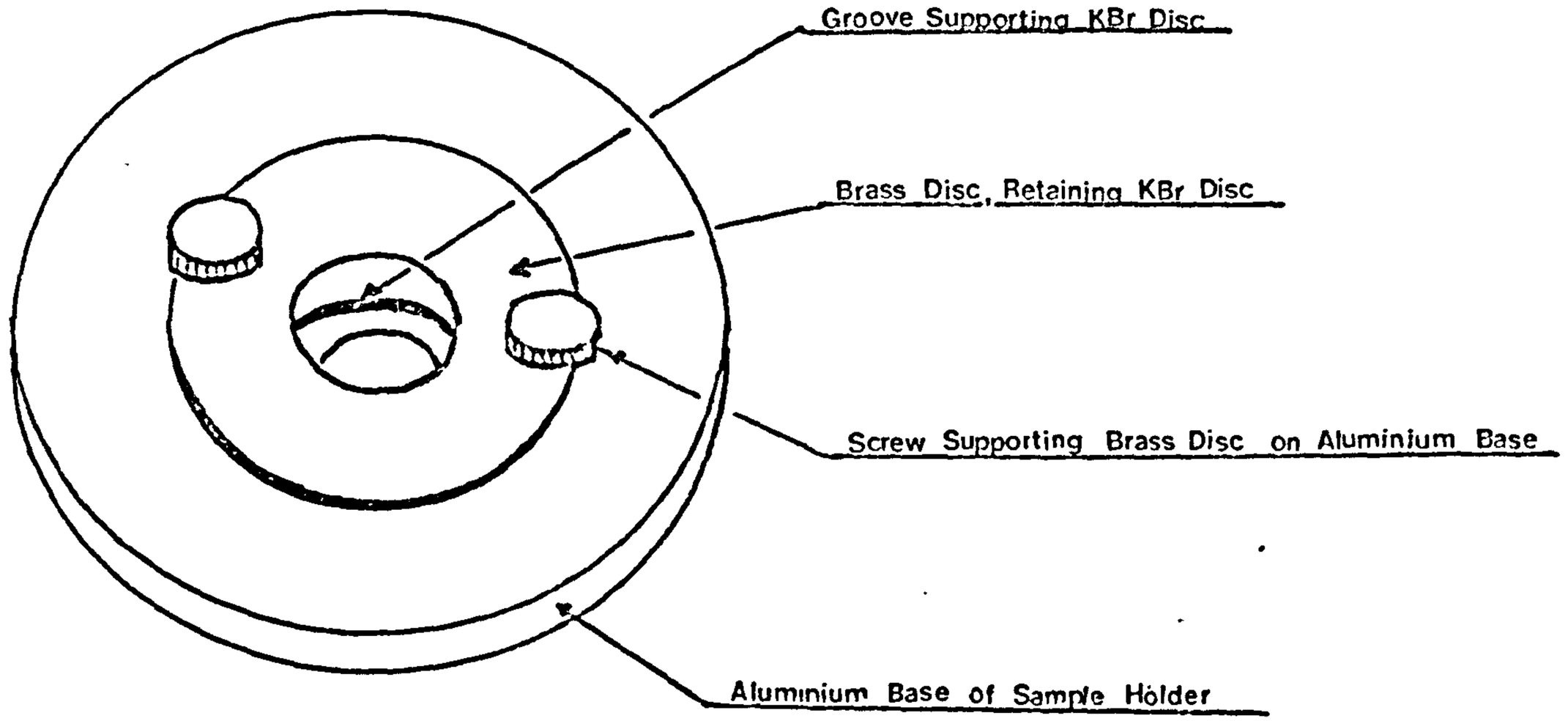
Groove Supporting KBr Disc
Brass Disc, Retaining KBr Disc
Screw Supporting Brass Disc on Aluminium Base
Aluminium Base of Sample Holder

FIG. 43

preparative method was found to be necessary for Cellulose I, since all other methods (56, 75) produced irreproducible and unresolved derivative spectra.

KBr disc samples were mounted in sample holders (Fig.43) specifically designed to fit in the sample cells, together with ordinary brass sample discs containing tubes of P_2O_5, in order to keep KBr discs dry prior to and during the recording of spectra.

Absorption and second derivative spectra of viscose, dicel and tricel films were recorded over the range 2.5 - 15 μm.(4000 - 667 $cm.^{-1}$) at 44°C., 100°C., 159°C. and 220°C., together with the spectra of annealed samples, recorded at 44°C.. The spectra of KBr disc powder samples and annealed powder samples, including Cellulose I, were also recorded at 44°C.. In all cases, the annealing of films or powder was carried out under a nitrogen atmosphere, for $\frac{1}{2}$ hour periods, in a small furnace designed for the purpose (119). An annealing temperature of 220°C. was chosen, since higher temperatures caused samples to degrade, especially in the case of tricel. Such degradation resulted in higher spectral scatter and hence poorly resolved and irreproducible spectra.

Since the spectrometer divides the spectral range coverable into two regions, namely 0.5 - 5 μm. and 5 - 25 μm, the spectra are displayed and results discussed in two sections:-

i.e.	Section	Spectral Range Covered
	A	2.5 - 5 μm. (4000 - 2000 $cm.^{-1}$)
	B	5 - 15 μm.(2000 - 667 $cm.^{-1}$)

SECTION A

3A 1.1 Results For Viscose

The results obtained from viscose (Cellulose II) film are discussed first, since viscose is the fundamental cellulosic material on which our studies were based. Powder samples, including Cellulose I, were used only

to confirm assignments and crystalline behaviour, since such powder samples exhibit an inherent factor of high scatter which results in spectra not as clearly resolved as those of film samples. Large spurious peaks are also observed in the derivative spectra of such samples due to interactions between the sample and the KBr matrix (12) and to the existence of absorbed water in the KBr, which cannot be removed by normal drying procedures.

An analysis of the derivative spectra of viscose, dicel and tricel films enabled peaks to be assigned to vibrations of various cellulosic chemical groups (OH, CH, C-O etc), or to absorbed water, by comparing peak wavelengths (frequencies) with those previously quoted in papers (78 - 80, 181), structural assignment charts (3 - 5) and with the wavelengths (frequencies) of the derivative spectral peaks of water and ice (see Chapter 6, figures 72 and 73).

Derivative spectra of films, recorded at higher temperatures (100°C., 159°C. and 220°C.) and the derivative spectra of annealed samples recorded at 44°C., also enabled peak assignments to be confirmed as well allowing 'crystalline' 'crystallizable' or 'non crystallizable' regions of the film structure to be determined in terms of assigned peaks. These spectra also enabled deductions to be drawn concerning the crystalline structure of films and changes which occur on heating.

However, as was pointed out previously, permanent changes which occurred in the proportion of crystalline material present or changes which occurred in the degree of crystalline perfection within a film sample, could only be assessed from observations of differences in peak intensities and wavelengths (frequencies) between the spectra of annealed film samples and untreated samples for the same conditions of temperature (44°C.) and humidity (both samples dried over P_2O_5).

There is some confusion over the use of the terms 'crystalline' and 'crystallizable' in the literature. These terms are thus defined in the context of this work and are based upon Hearle's modified fringed fibril

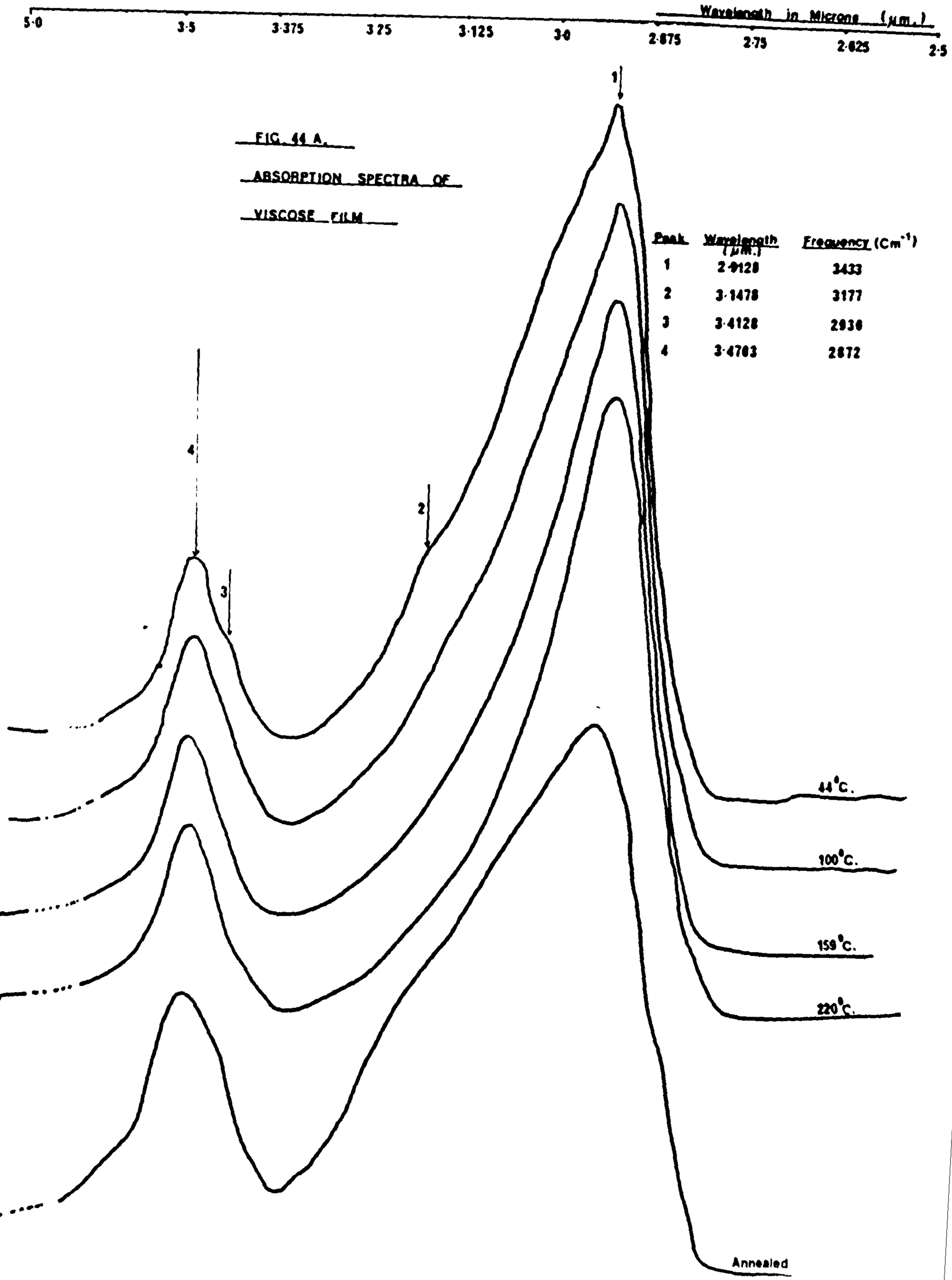

FIG. 44 A.

ABSORPTION SPECTRA OF

VISCOSE FILM

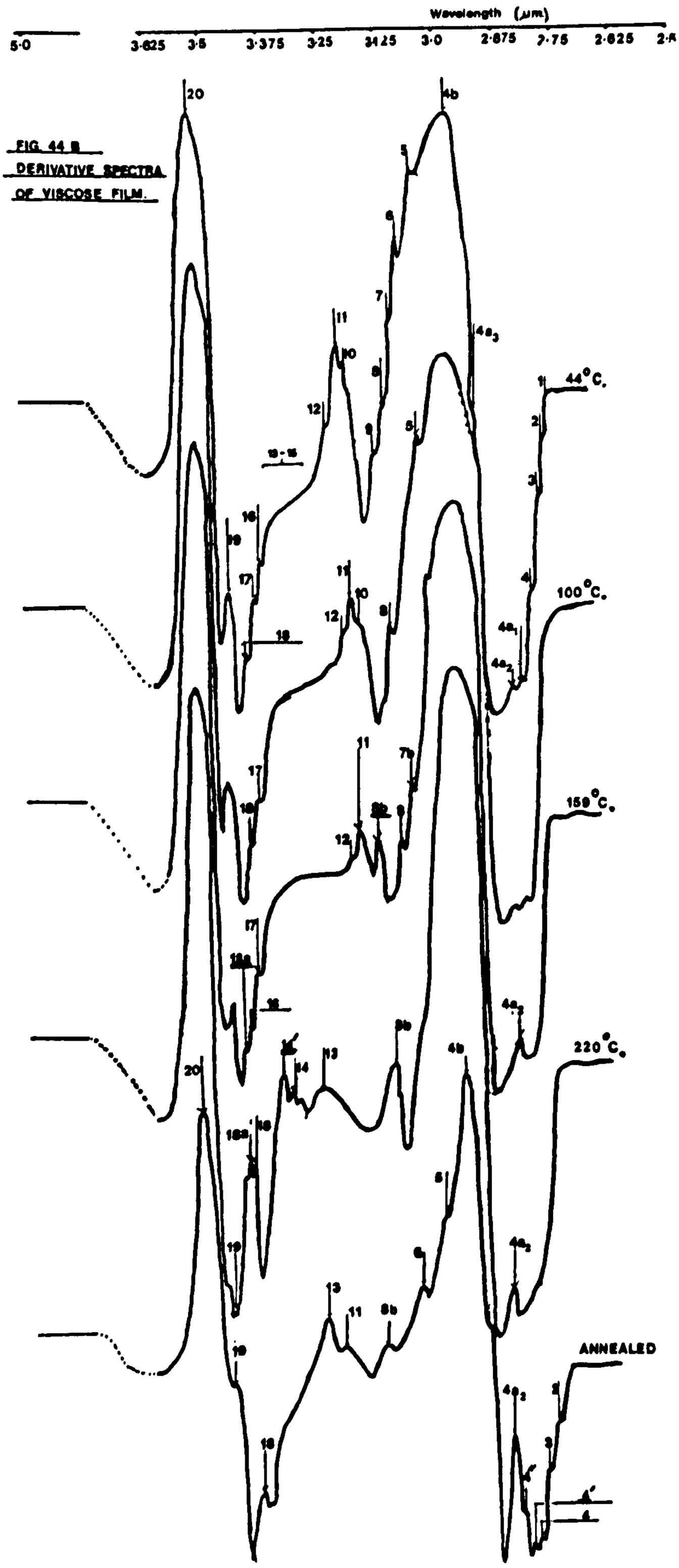

FIG. 44 B
DERIVATIVE SPECTRA
OF VISCOSE FILM.

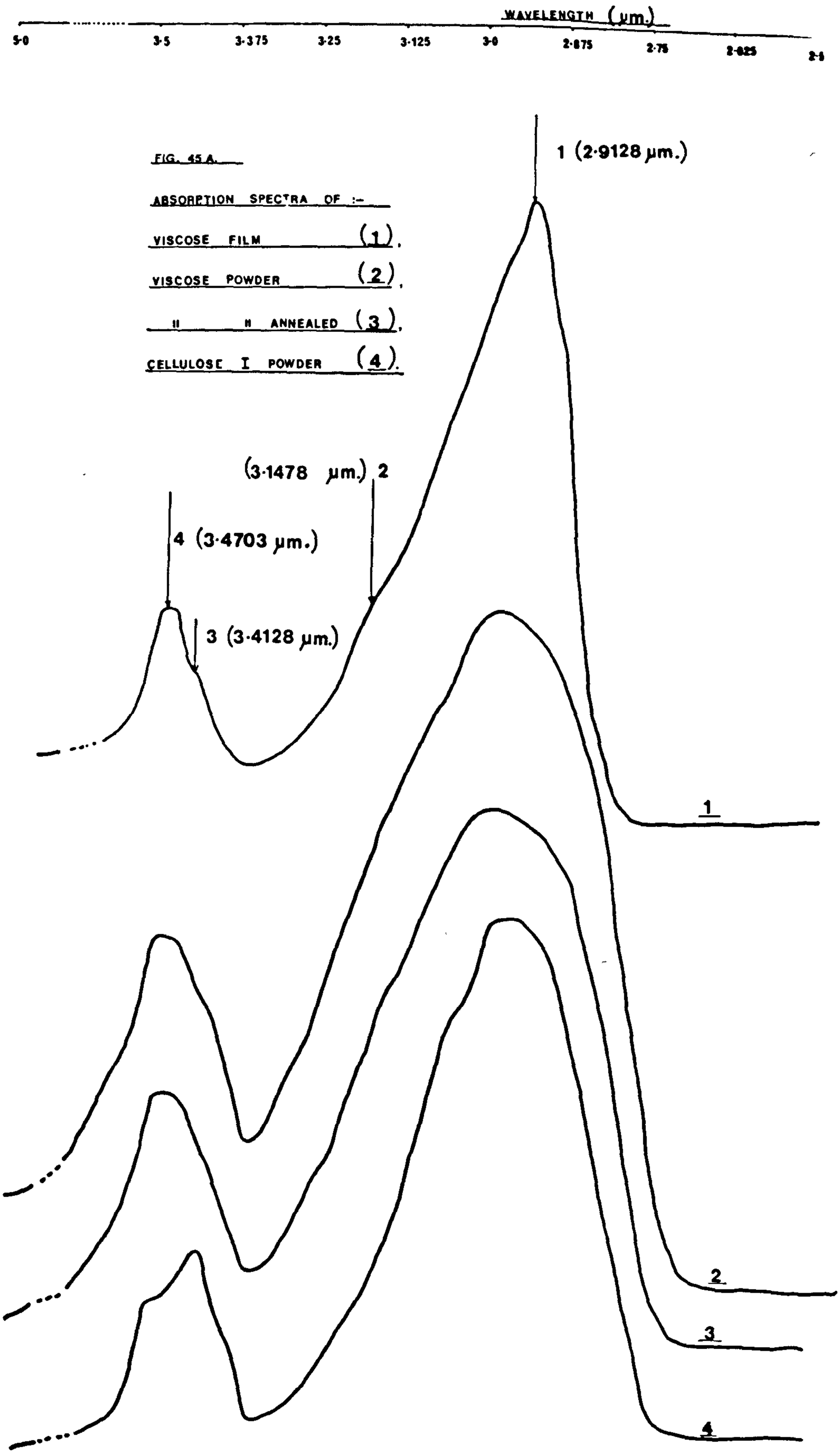
WAVELENGTH (μm.)
5·0
3·5
3·375
3·25
3·125
3·0
2·875
2·75
2·625
2·5
FIG. 45 A.
ABSORPTION SPECTRA OF :-
VISCOSE FILM (1).
VISCOSE POWDER (2).
" " ANNEALED (3).
CELLULOSE I POWDER (4).
1 (2·9128 μm.)
(3·1478 μm.) 2
4 (3·4703 μm.)
3 (3·4128 μm.)
1
2
3
4

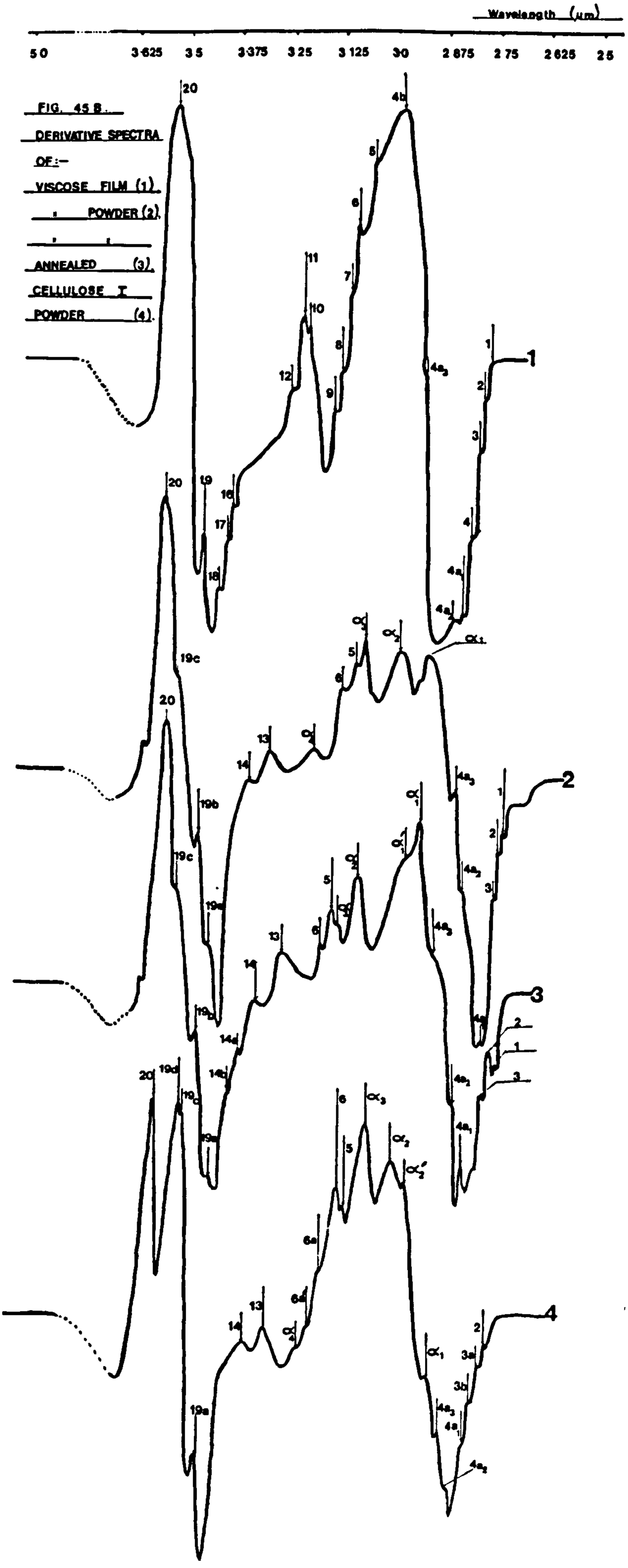
Wavelength (μm)
5·0
3·625
3·5
3·375
3·25
3·125
3·0
2·875
2·75
2·625
2·5
FIG. 45 B.
DERIVATIVE SPECTRA
OF:—
VISCOSE FILM (1).
" POWDER (2).
" "
ANNEALED (3).
CELLULOSE I
POWDER (4).

theory of structure:-

'Crystalline' Material is material which is packed into an extended crystalline lattice structure. This lattice may be distorted, however, to allow for fibrillar branching etc.

'Crystallizable' Material is material which has no extended lattice structure. Chain molecules do not pack into any extended ordered system.

As is seen from Hearle's fringed fibril model (Fig.15) there is no sharp dividing point between 'crystalline' and 'crystallizable' regions. Chain molecules may diverge from 'crystalline' regions at any point into 'crystallizable regions'.

In terms of behaviour some 'crystallizable' material may be converted to 'crystalline' material by annealing etc.

'Non Crystallizable' Material

This term is used simply to describe material which is unaffected by annealing treatments etc., i.e. material which cannot be converted to 'crystalline' material by annealing etc.

Derivative peaks were thus designated as 'crystalline' or 'crystallizable' if a large increase or decrease in peak intensity occurred in the derivative spectrum of an annealed film sample, recorded at 44°C., compared with the derivative spectrum of the untreated sample, also recorded at 44°C. Peaks were thus designated as 'non crystallizable' (largely unaffected) if little or no change occurred in peak intensities in the derivative spectra of annealed samples.

The absorption and second derivative spectra of viscose film are shown in Fig. 44A and 44B respectively, whereas absorption and second derivative spectra of viscose powder (and also Cellulose I powder.) are shown in Figs. 45A and 45B respectively.

Figs. 44A and 45A show that the absorption spectra of viscose and of Cellulose I consists of 2 major peaks, which in viscose film occur at 2.913 μm. (3433 $cm.^{-1}$) and 3.4703 μm. (2872 $cm.^{-1}$), and which are assigned to OH and CH stretching modes respectively (3-5, 78), with associated minor

LIST I

Peak or Peak Response	Designation
1. 'Crystalline' Peaks	I
'Crystallizable' ('Amorphous') Peaks	II
'Non Crystallizable' (Largely unaffected) Peaks	III
2. Effect of Temperature on Derivative Spectra of Film Samples Heated Above 44°C	
Peak which show intensity increases in one or more spectra,	1
Peak which show intensity decreases in one or more spectra,	2
Peak which increase in intensity initially and then decrease,	3
Peak which decreases in intensity initially and then increase,	4
Peak which show completely varied intensity changes.	5
Peak whose intensity is largely unaffected	6
Peak which disappear above 44°C	Mh
Peak which show wavelength increases in one or more spectra	(i)
Peak which show wavelength decreases in one or more spectra	(ii)
Peak which increase in wavelength initially and then decrease	(iii)
Peak which decrease in wavelength initially and then increase	(iv)
Peaks which give completely varied wavelength changes	(v)
Peaks whose wavelength is largely unaffected	(vi)
3. Affect of Annealing, Comparing Derivative Spectrum at 44°C of Annealed Film Sample, with Derivative Spectrum of Film at 44°C.	
Peaks which increase in intensity in annealed sample	A
Peaks which decrease in intensity in annealed sample	B

LIST I (continued)

Peak or Peak Response	Designation
Peaks whose intensity is unaffected in annealed sample	C
Peaks missing in annealed sample	Ma
Peaks which increase in wavelength in annealed sample	a
Peaks which decrease in wavelength in annealed sample	b
Peaks which wavelength is unaffected in annealed sample	c
5. Peaks Assigned to Absorbed Water	w
6. Peaks Whose Assignment as 'Crystaline' 'Crystallizable' or 'Non-crystallizable' is Upheld by Powder and Annealed Powder Samples	x

TABLE XVII (Viscose) From Figs. 44B and 45B

Peak	Wavelength (μm)	Wavenumber ($cm.^{-1}$)	New Peak at (in)	Previous Interpretation	Present Interpretation	Code.
1	2.7320	3660	-	-	Loosely Bound Water	w *
2	2.7406	3649	-	-	" " "	w *
3	2.7520	3634	-	-	" " "	w
4	2.7720	3620	-	Free (Non Hydrogen Bonded) Water at 2.76 μm. (120-125)	Same as previous Interpretation, or Loosely Bound Water	w
4′	2.7795	3597	Annealed Sample	-	Loosely Bound Water	w
$4a_1$	2.7870	3588	-	Possibly Cellulosic OH Stretching Vibration (177)	Water with an 'Ice Type' structure	w
4″	2.7995	3572	Annealed Sample	-	" " "	w
$4a_2$	2.8158	3551	-	-	Water with an 'Ice Type' structure	w
$4a_3$	2.8820	3470	-	OH Stretching Vibration (Intramolecular Hydrogen Bonding $C_3OH\cdots O_5'$) (80)	Same as previous Interpretation	III,Mh,Cc.
4b	2.9120	3434	-	" "	Same as previous Interpretation. Also possibly Water with an 'Ice Type' structure.	w and III 6 vi Cc
5	3.0120	3320	-	OH Stretching Vibration (Intermolecular Hydrogen Bonding $C_6OH\cdots$Bridge oxygen atoms of neighbouring chains) (78).	Same as previous Interpretation	III Mh Cb

TABLE XVII (Continued)

Peak	Wavelength (μm)	Wavenumber ($cm.^{-1}$)	New Peak at (in)	Previous Interpretation	Present Interpretation	Code.
6	3.0470	3282	-	-	More Strongly Bound Water	w
7	3.0658	3262	-	-	More Strongly Bound Water	w
7b						
8	3.0858	3240		Hydrogen Bonded Lattice Water with a Tetrahedral Structure (120-125)	Water with an 'Ice Type' Structure	w
8b	3.0920	3234	159°C.	-	Water with an 'Ice Type' Structure	w
9	3.1020	3224	-	-	Bound Water	w
10	3.1633	3162	-	-	" "	w
11	3.1758	3149	-	OH Stretching Vibration (Intermolecular Hydrogen Bonding C_6OH---Bridge Oxygen of Neighbouring chains) (78)	Same as Previous Interpretation.	II 2ii Bb
12	3.2008	3124	-	-	Strongly Bound Water	w
13	3.2170	3108	220°C.	-	OH Stretching Vibration peak, probably of OH groups which are Intramolecularly hydrogen bonded	I, A,a.
14	3.2720	3056	220°C.	-	CH Stretching Vibration	III, Ma

TABLE XVII (Continued)

Peak	Wavelength (μm)	Wavenumber ($cm.^{-1}$)	New Peak at (in)	Previous Interpretation	Present Interpretation	Code
14'	3.2945	3035	220°C.	-	CH Stretching Vibration	III,Ma
16	3.3445	2990		-	CH Stretching Vibration	II,Mh, Ma
17	3.3620	2974	-	CH Stretching Vibration (80,177)	Same as Previous Interpretation	II,Mh, Ma.
18	3.3795	2959		-	CH or CH_2 Vibration	I 1(ii) A,b.
18a	3.3808	2952		-	CH Vibration	-
19	3.4120	2931		CH Stretching Vibration (80)	Same as Previous Interpretation, but probably due to CH Vibrations of Cellulose I Present in the Viscose (Cellulose II).	II2vBc
20	3.4775	2875		CH Stretching Vibration (80)	Same as Previous Interpretation	III 6vi Cc

peaks at 3.1478 μm. (3177 $cm.^{-1}$) and 3.4128 μm. (2930 $cm.^{-1}$). Few changes are observed in the absorption spectra of viscose at higher temperatures or in the annealed viscose spectrum, except that the two minor peaks are less well resolved. However, the greater resolution afforded by second derivative spectroscopy results in a second derivative spectrum of viscose, which at 44°C. contains a total of 20 peaks, 17 of which are reproducible and are shown (Fig.44B). Peaks 13 - 15 are of a low level intensity and are irreproducible at 44°C., so they are not shown. However, at 220°C. peaks 13 and 14 increase in intensity and become reproducible, and they are thus shown in the spectrum at 220°C..

An analysis of the derivative spectra of viscose film (Fig.44B) also enables information to be obtained concerning structural changes and changes in absorbed water which occur upon heating and annealing. New peaks which appeared in heated or annealed sample spectra were denoted by underlined labels, e.g. Peak 18a in the derivative spectrum of viscose film at 159°C, and were also referred to as new peaks in the assignment tables (Table XVII).

The behaviour of each derivative peak on heating and in annealed sample spectra was classified according to the scheme in List I.

Table XVII shows the assignment and designation of all the derivative peaks in viscose film from Fig. 44B, confirmed by powder spectra peaks from Fig. 45B.

3A.1.2 Discussion of Results for Viscose

(a) Water Peaks (due to OH stretching in water)

Fig. 44B shows that there are a large number of peaks associated with absorbed water. The binding of such water to the viscose is obviously fairly strong, since such water has not been removed from the sample by drying over P_2O_5. Of such water peaks, peaks 1 - 4 represent the more loosely bound water, since they occur at lower wavelengths and disappear on heating, indicating that such water is easily lost on heating. Peak

$4a_2$ could be interpreted as being due to cellulosic OH groups, since it increases in intensity in heated and annealed samples. It is probable, however, that it is associated with highly ordered groups of water molecules since it it present in the second derivative spectra of both water and ice (see Figs. 72 and 73 Chapter 6). In the present discussion, and in any future discussion, any derivative peaks which correspond to such groups of water molecules and have corresponding derivative peaks in the spectra of water and ice are said to correspond to water with an 'ice type' structure. The increase in intensity of this peak in heated and annealed sample spectra appears to be anomalous, but it is consistent with either or both of the following explanations: Explanation 1 or Explanation 2.

Explanation 1: As temperature rises, thermal vibrations in both 'crystalline' and 'crystallizable' regions of the viscose film increase in amplitude, causing a proportion of the hydrogen bonds to be broken. This will affect the ordered regions since lateral movement of chains occurs and allows penetration of water into the crystalline regions of the structure to occur.

In this context, Hearle's modified fringed fibril theory of structure is very useful, since it already provides for the existence of weak points along the boundaries of 'crystalline' regions (crystallites) where it is possible for water molecules to penetrate at high temperatures.

Once inside 'crystalline' regions, water molecules may become located singly or may aggregate into groups of water molecules with an 'ice type' structure, adding to the groups of such water molecules already present. Such aggregates of water molecules cannot easily pass out of the crystalline regions and are trapped, thus accounting for the increase in intensity of peak $4a_2$ in heated and annealed sample spectra.

The fact that heating samples to high temperatures fails to break up such groups of water molecules may be attributed in part to the very strong hydrogen bonding present in such groups, and also to the possibility of hydrogen bonding between such groups and cellulosic hydroxyl groups

(intermolecular hydrogen bonding).

Water molecules in 'crystallizable' regions become available for transfer to 'crystalline' regions when hydrogen bonds binding such water to cellulosic OH, C-O etc. groups are broken at higher temperatures, as exemplified by the disappearance of the more loosely bound water peaks, (peaks 1 - 4). Undoubtedly, some of this water is lost from the viscose film altogether, and is picked up by the P_2O_5 in the small tubes of the sample cells, when samples are heated, but some may become available for transfer to crystalline regions.

The transference of water to crystalline regions is in accord with the X-ray results of Hermans et al (63 - 66), who maintain that water is able to penetrate the crystalline lattice of Cellulose.

Explanation 2 An alternative and simpler explanation not involving transfer of water to crystalline regions, is that water molecules which have dissociated from the cellulose at high temperatures then aggregate into groups of molecules with an 'ice type' structure in both 'crystalline' and 'crystallizable' regions. This explanation cannot, however, account for the retention of such groups of water at high temperatures by 'crystallizable' regions, except by assuming very strong hydrogen bonding between such groups of water molecules and cellulosic hydroxyl groups in the 'crystallizable' regions. This explanation is thus the less acceptable of the two.

Peaks $4a_1$, 8 and 8b have also been assigned to groups of water molecules with 'ice type' structures. Peak 8b shows a similar behaviour to peak $4a_2$ except that it decreases slightly in intensity in the annealed sample spectrum, and its behaviour is thus similarly explained. However, peaks $4a_1$ and 8 show a different behaviour in that they are not present in the spectrum recorded at 159°C. or in the annealed sample spectrum. The different behaviour of peaks $4a_1$ and 8 may be due to them representing a different 'ice type'

structure of water to that represented by peaks $4a_2$ and 8b.

(b) <u>OH Stretching Vibration Peaks</u>

The main OH peak 4b at 2.912 μm. (3434 $cm.^{-1}$) has been assigned to the OH stretching mode quoted by Marchessault (78) who measured its absorption at 2.90 μm. (3488 $cm.^{-1}$). This peak was considered to represent OH groups involved in intramolecular hydrogen bonding between C_3 OH groups and O_5' atoms of adjacent glucose residues. The discrepancy between our observed wavelength for such a peak and that reported by Marchessault may be accounted for in terms of better resolution induced by derivative techniques, since band shifts associated with overlapping peaks have been reduced.

As peak 4b is largely unaffected in wavelength and intensity in heated and annealed sample spectra, the intramolecular hydrogen bonding involved in the corresponding C_3 OH group must be very strong. It is possible that such bonding can be maintained at high temperatures by the occurrence of conformational changes within the viscose (Cellulose II) molecules.

Marchessault also suggested the existence of a second C_3 OH ---O_5' intramolecular hydrogen bond due to alternate residues in the Cellulose II chain having different orientations to the chain axis, as previously described (Jones (85)). This hydrogen bonded hydroxyl species was attributed to a peak at 2.8670 μm (3488 $cm.^{-1}$) and has been assigned to peak $4a_3$ (2.8820 μm, 3470 $cm.^{-1}$) in our case.

The hydrogen bonding of this species is, however, weaker than in the OH species corresponding to peak 4b, since peak $4a_3$ occurs at a lower wavelength than peak 4b and also disappears above 44°C., only reappearing in the annealed sample spectrum.

Thus the alternate orientations of glucose residues in Cellulose II proposed by Marchessault give rise to alternate C_3 OH ---O_5' intramolecular hydrogen bonds of different strengths. Hence the distance between hydrogen atoms of C_3 OH groups and O_5' atoms in the stronger intramolecular hydrogen bond (Peak 4b) must be shorter than in the weaker intramolecular hydrogen

bond (Peak $4a_3$). Since peak 4b also corresponds to peaks in the derivative spectra of water and ice, it is possible also to assign this peak to water with an 'ice type' structure, but this is discussed further in Chapter 6.

Peaks 5 and 11 which occur at 3.0120 μm.(3320 $cm.^{-1}$) and 3.1758 μm. (3149 $cm.^{-1}$) have been assigned to the OH stretching modes quoted by Marchessault at 3.0257 μm.(3305 $cm.^{-1}$) and 3.1496 μm.(3175 $cm.^{-1}$). These peaks were considered to represent OH groups involved in intermolecular hydrogen bonding between C_6 OH groups and bridge oxygen atoms of neighbouring chains. These two peaks illustrate that intermolecular hydrogen bonds are temperature sensitive, since they disappear when the sample is heated to 159°C.but re-appear in the annealed sample spectrum.

Thus although intermolecular hydrogen bonds ascribed to peaks 5 and 11 occur at higher wavelengths than the intramolecular hydrogen bond ascribed to peak 4b, and are in theory stronger bonds, they are more easily broken on heating than the intramolecular hydrogen bond which corresponds to peak 4b. This may be due to intermolecular movement between chains, occurring more easily than intramolecular movement inside chains (due to steric hindrance etc), when samples are heated.

Peak 5 is largely unchanged in the annealed sample spectrum, but peak 11 exhibits a 'crystallizable' behaviour, since it appears in the annealed sample spectrum with a lower intensity. However, a new hydrogen bonded OH peak, peak 13 (3.2017 μm, 3108 $cm.^{-1}$), not previously reported, appears at 220°C. and is 'crystalline', since its intensity increases in the annealed sample spectrum. This peak has not yet been assigned to either an inter or intramolecular hydrogen bonded OH group, but it is more probable that it is associated with an intermolecular hydrogen bonded OH group, since it occurs in the higher wavelength range with the other intermolecular hydrogen bonded OH group peaks (5 and 11).

The fact that peak 11 shows a 'crystallizable' behaviour illustrates that the differentiation of material within the film into 'crystalline'

and 'crystallizable' regions is valid. Such differentiation can be adequately explained by Hearle's modified fringed fibril theory of structure.

Since the material in the 'crystallizable' regions is more disordered, the strength of intermolecular hydrogen bonding should be lower than in the 'crystalline' regions and this is borne out by the fact that peak 11 ('crystallizable') occurs at a lower wavelength than peak 13 ('crystalline'). The increase in intensity of peak 13 in the annealed sample spectrum and decrease in intensity or no change in intensity of other hydrogen bonded OH group peaks (peaks $4a_3$, 4b, 5 and 11), illustrates that annealing does cause an increase in the total proportion of 'crystalline' material present in the viscose film. The shift of peak 13 to a higher wavelength in the annealed sample is also very important, since it illustrates that there is an increase in the degree of perfection of at least one crystalline phase present within the viscose film.

(c) <u>CH Stretching Vibration Peaks</u>

Peaks 14 - 20 have been attributed to CH stretching vibrations, but of these peaks, only peaks 17 - 20 have been previously reported and assigned. As with OH peaks, there are wavelength differences between these derivative peaks and those previously reported from normal absorption spectra.

The increase in intensity of some of these peaks and decrease in intensity of others also confirms that annealing causes an increase in the total proportion of crystalline material. It also indicates for the first time that the environment of CH groups differs in 'crystalline' and 'crystallizable' regions and indicates the possibility of CH groups of cellulose being involved in hydrogen bonding. Support for the involvement of CH or CH_2 groups in such hydrogen bonding has also been obtained by Rhodes (12) working on keratin. Peak 18, although assigned as a 'crystalline' peak, shows a decrease in wavelength in heated and annealed sample spectra. This

indicates that a decrease in the degree of perfection of at least one crystalline phase within the viscose film has occurred on heating.

(d) The Whole Spectrum

When we consider the whole spectrum, the fact that certain peaks shift to higher wavelengths in heated and annealed sample spectra, whereas other peaks shift to lower wavelengths, indicates that both increases and decreases in the degrees of perfection of crystalline states are occurring concurrently within the viscose film; thus the presence of more than one crystalline state within the viscose structure is indicated. It has been suggested previously (73) that mercerized cotton and viscose rayons (mainly Cellulose II) contain residual amounts of Cellulose I due to the incomplete disruption of the parent Cellulose I lattice during the mercerization process or in the alkali treatment of Cellulose I with caustic soda (prior to the formation of cellulose xanthate and the subsequent dissolution of the xanthate in caustic soda, and regeneration of the cellulose as viscose in an acid bath). This residual Cellulose I in viscose rayon may thus account for the existence of more than one crystalline state within viscose film, i.e. small amounts of Cellulose I and large amounts of Cellulose II existing together in the viscose film.

(e) Results From Powder Spectra

Fig.45B illustrates the large differences between the derivative spectra of viscose film and viscose powder, or Cellulose I powder, although many of the differences were not observable in the absorption spectra of Fig. 46A. Peaks α_2 and α_3 observed in the derivative spectra of KBr disc samples of viscose powder are probably due to absorbed water in the KBr which cannot be removed by drying over P_2O_5. The presence of such spurious peaks and other spurious 'KBr interaction peaks' (12) makes accurate interpretations in this region difficult.

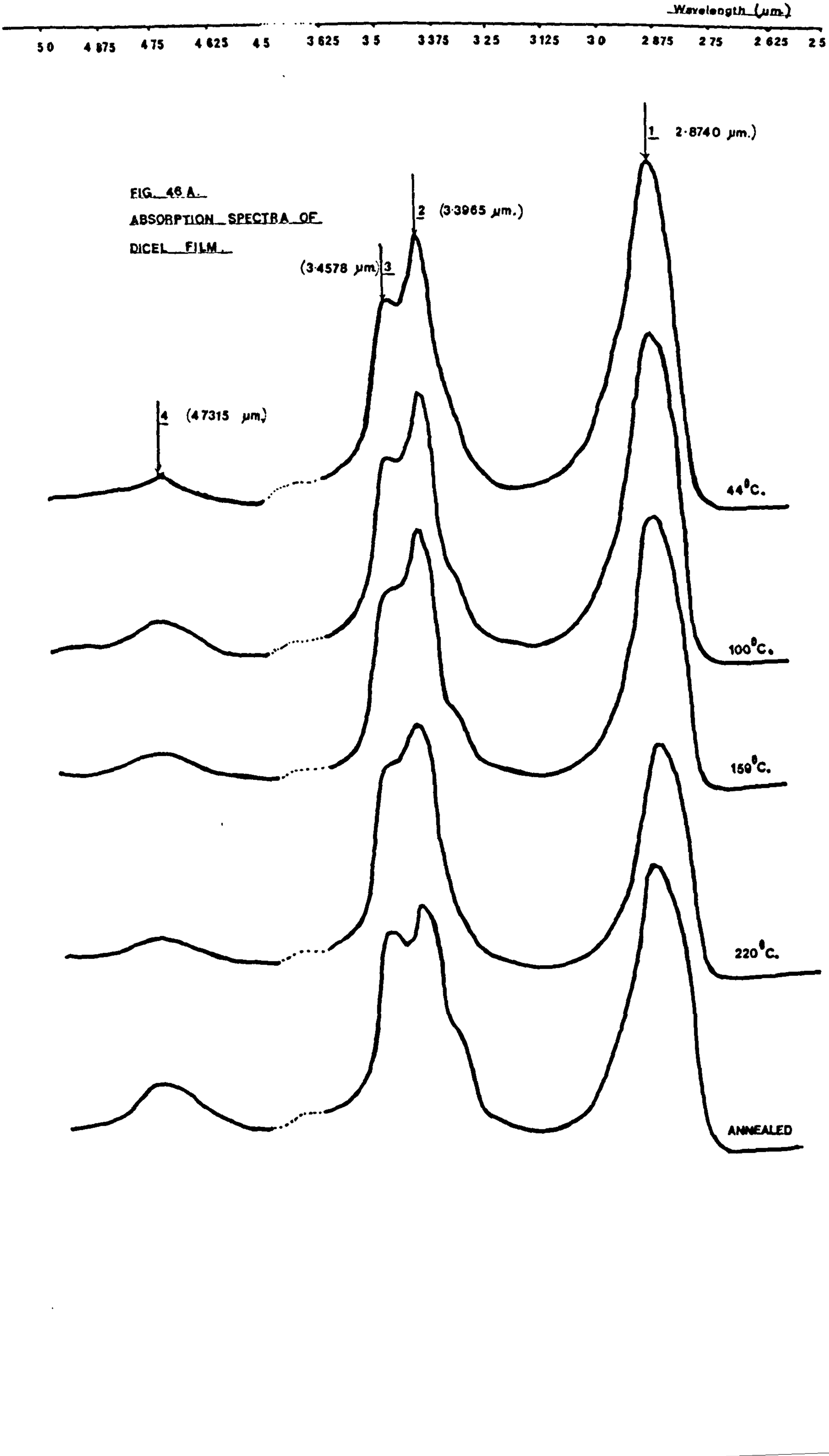

FIG. 46 A.

ABSORPTION SPECTRA OF DICEL FILM.

FIG. 46 B.

DERIVATIVE SPECTRA OF

DICEL FILM

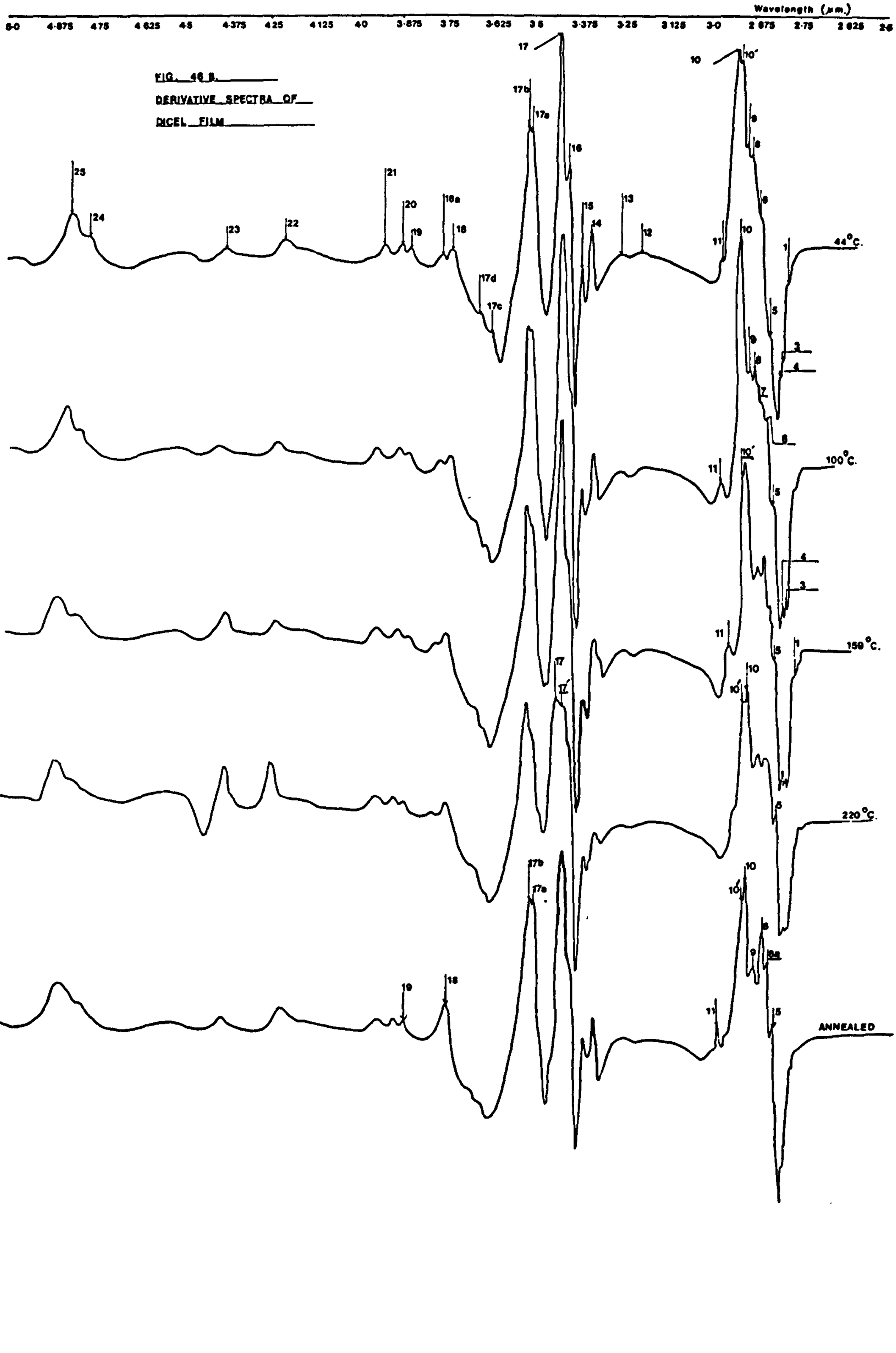

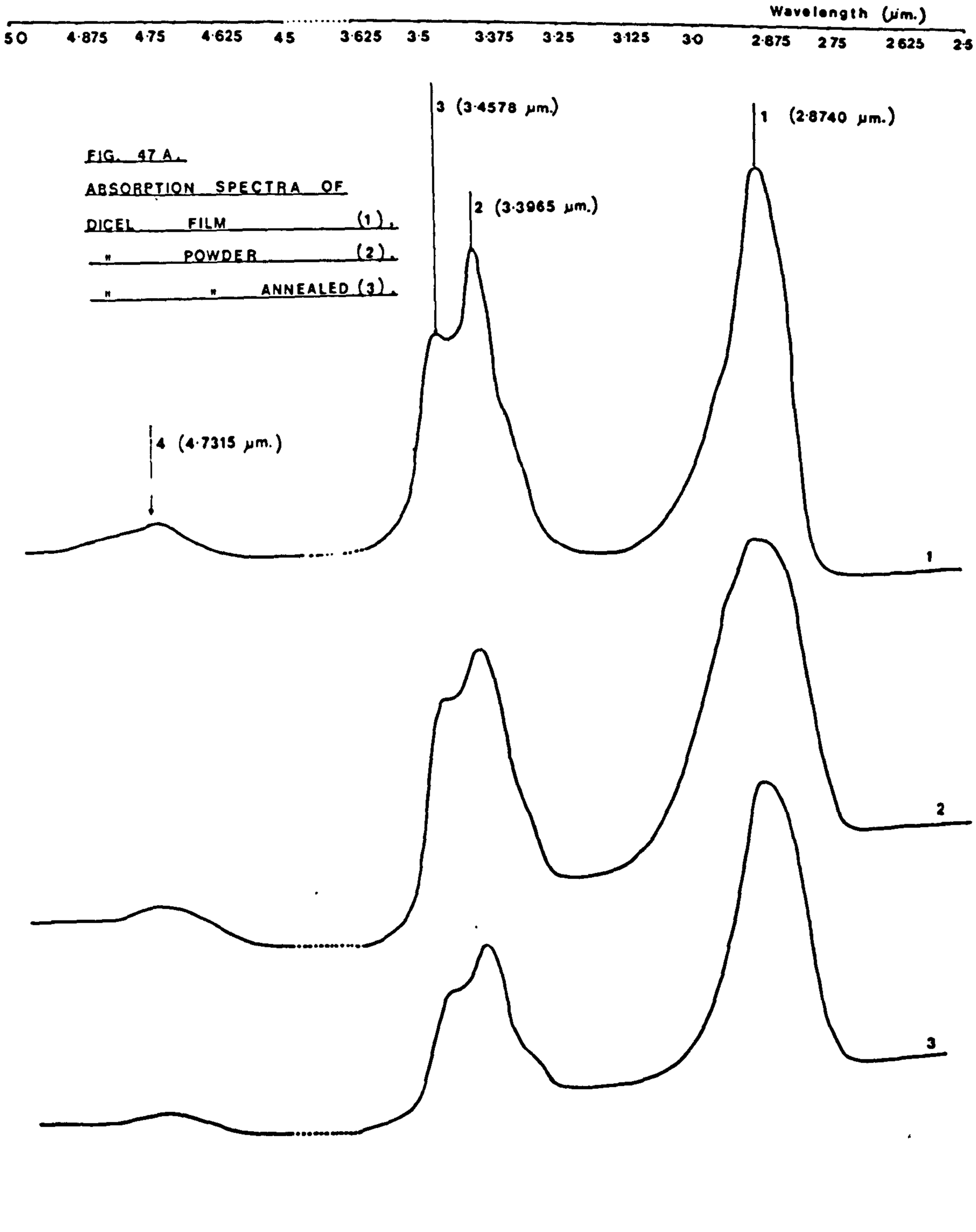

FIG. 47 A.

ABSORPTION SPECTRA OF

DICEL FILM (1).

" POWDER (2).

" " ANNEALED (3).

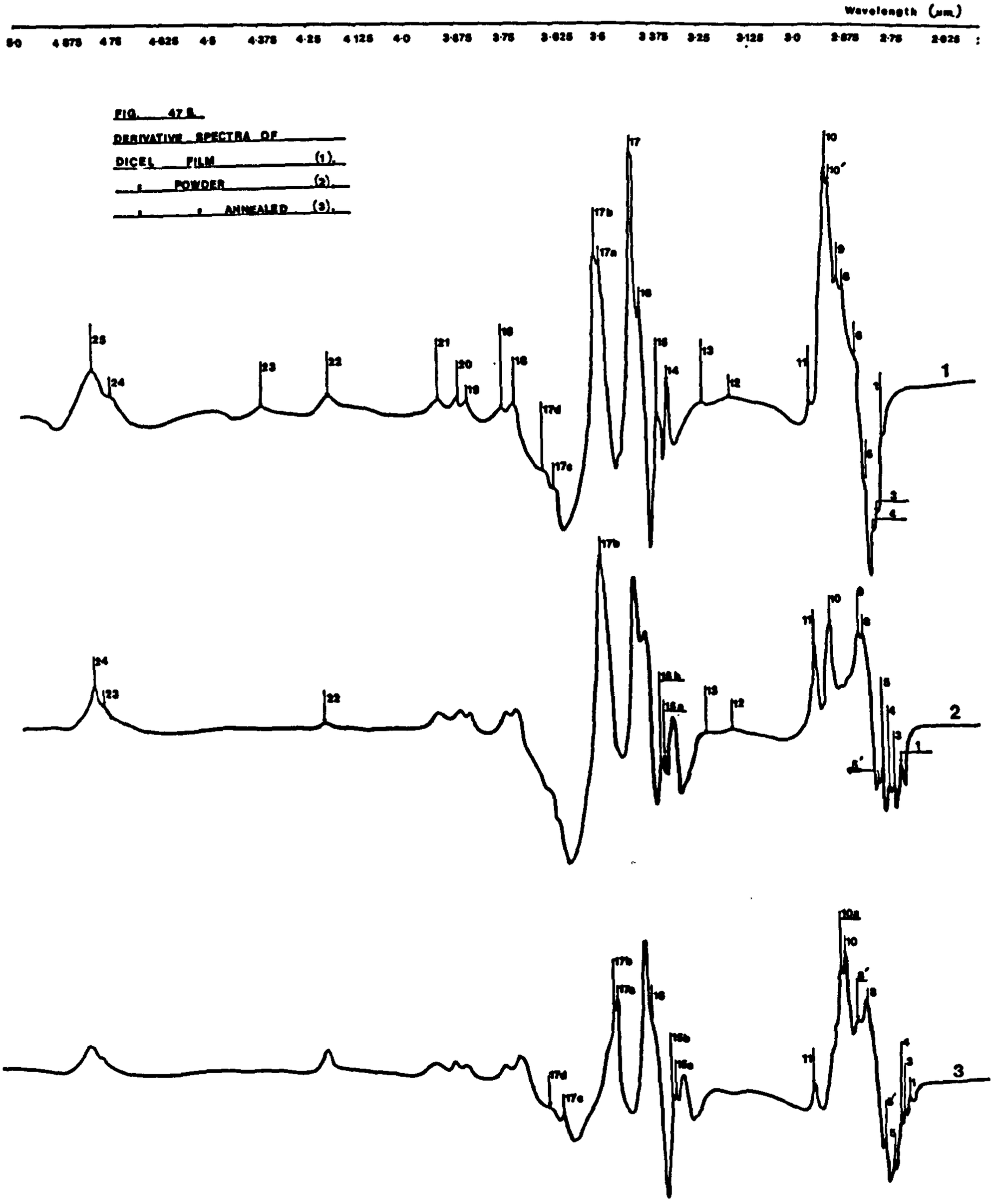
Wavelength (μm.)
5·0 4·875 4·75 4·625 4·5 4·375 4·25 4·125 4·0 3·875 3·75 3·625 3·5 3·375 3·25 3·125 3·0 2·875 2·75 2·625
FIG. 47 B.
DERIVATIVE SPECTRA OF
DICEL FILM (1).
" POWDER (2).
" " ANNEALED (3).

FIG 48 A

ABSORPTION SPECTRA OF TRICEL FILM

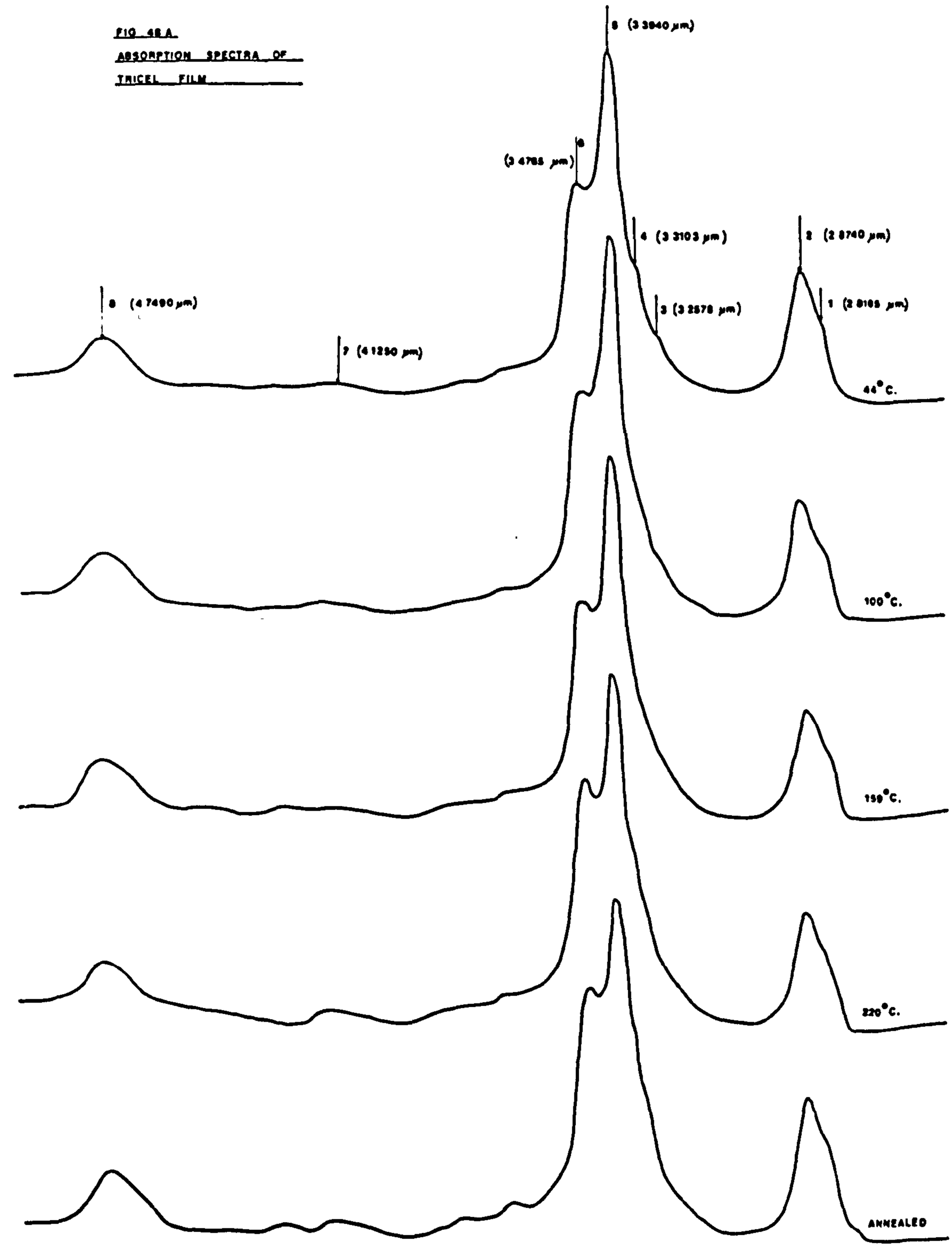

FIG. 48 B.

DERIVATIVE SPECTRA OF · TRICEL FILM.

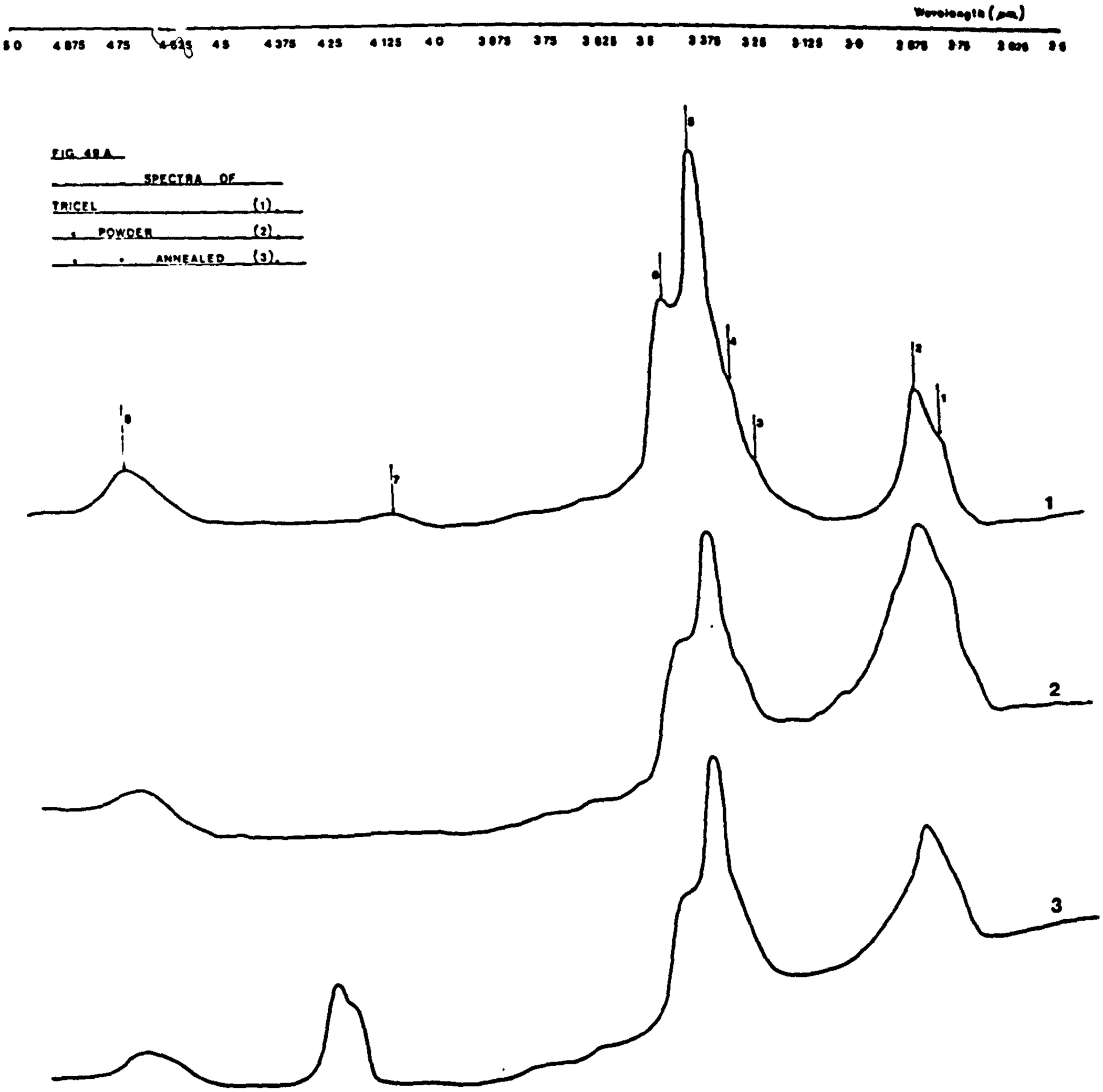

FIG. 48 A

SPECTRA OF

TRICEL (1).

" POWDER (2).

" " ANNEALED (3).

Wavelength (μm

3·0 4·875 4·75 4·625 4·5 4·375 4·25 4·125 4·0 3·875 3·75 3·625 3·5 3·375 3·25 3·125 3·0 2·875 2·75 2·625

FIG 42 B.

DERIVATIVE SPECTRA OF

TRICEL FILM (1).

" POWDER (2).

" " ANNEALED (3).

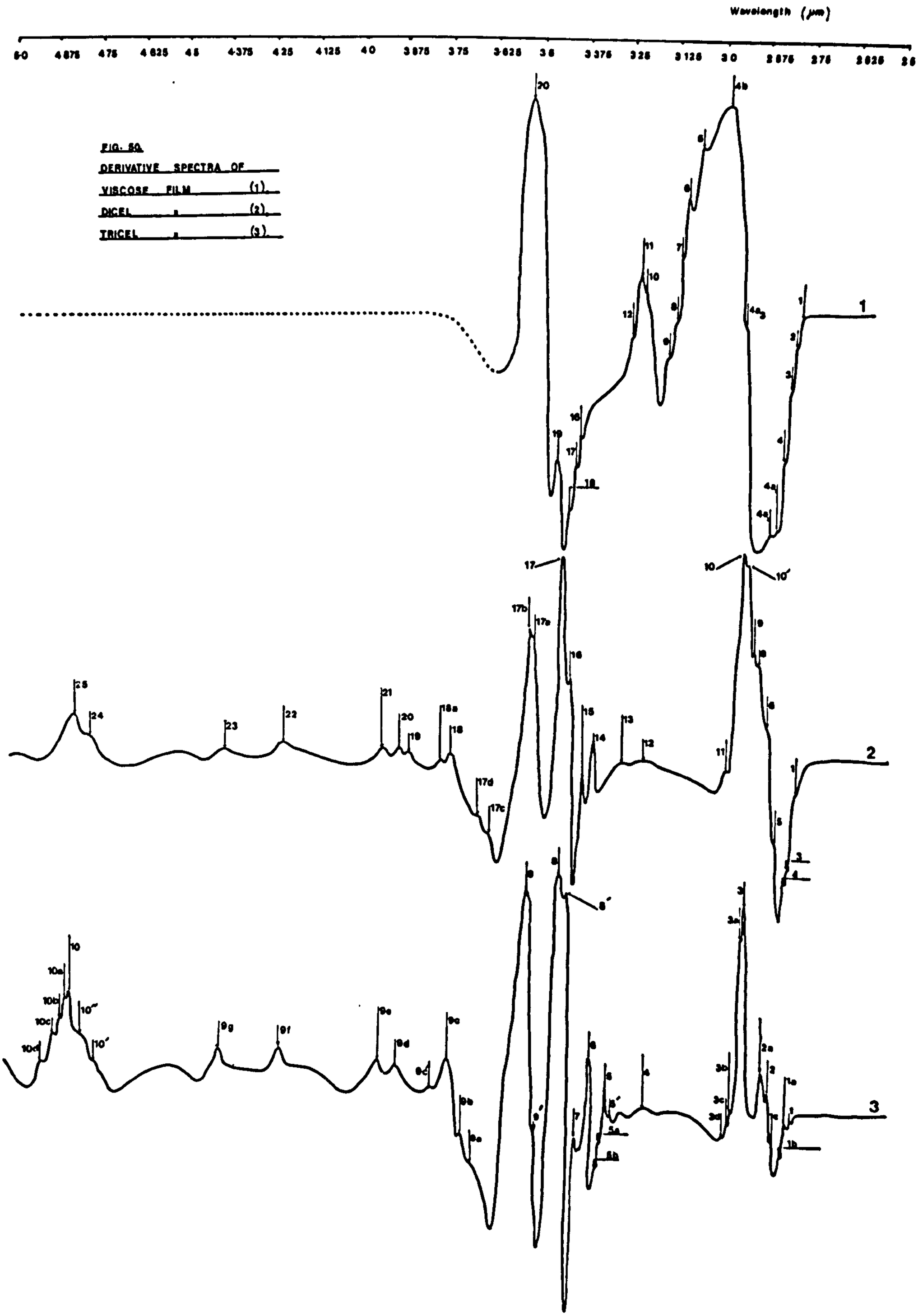

FIG. 50

DERIVATIVE SPECTRA OF

VISCOSE FILM (1)

DICEL " (2)

TRICEL " (3)

TABLE XVIII From Figs. 46B (& 47B) (Dicel)

Peak	Wavelength (μm)	Wavenumber ($cm.^{-1}$)	New Peak at (in)	Corresponding Peak in Viscose (μm)	Corresponding Peak in Tricel (μm)	Interpretation	Code
1	2.7455	3669		2 (2.7406)	1 (2.7392)	Loosely Bound Water	w
3	2.7680	3613		3 (2.7520)	1a(2.7517)	Loosely Bound Water	w
4	2.7717	3608		4 (2.7720)	1b(2.7642)	Loosely Bound Water (120-125)	w
5	2.7905	3583		-	-	Possibly OH Intramolecular Hydrogen Bonding	I6viCc
6	2.8142	3554		-	2 (2.8042)	Cellulosic OH, (Intermolecular Hydrogen Bonding)	II Mh M
8a	2.8042	3566		4"(2.7995)	-	Possibly Water with an 'Ice-Type' Structure	w
8	2.8442	3516		$4a_2$(2.8158)	2a(2.8217)	Water with an 'Ice-Type' Structure	w
9	2.8542	3504		$4a_3$(2.8820)	2a(2.8217)	Cf.Viscose, OH Stretching Intramolecular Hydrogen Bonding	II2ii Bb *
10'	2.8830	3469		4b(2.9120)	3 (2.8767)	Cf.Viscose, OH Stretching Intramolecular Hydrogen Bonding	III6vi Cc
10	2.8892	3461			3a(2.8830)	" " Also Probably Water with an 'Ice-Type'	III3viCc and w

TABLE XVIII (Continued)

Peak	Wavelength (μm)	Wavenumber ($cm.^{-1}$)	New Peak at (in)	Corresponding Peak in Viscose (μm)	Corresponding Peak in Tricel (μm)	Interpretation	Code
11	2.9292	3414	100°C.	8 (3.0858)	3c(2.9155)	Strongly Bound Water with 'Ice-Type' Structure Cf.Viscose	w
12	3.1467	3178		10(3.1633)	4 (3.1492)	Bound Water	w
13	3.2242	3102		-	-		III6vi Co
14	3.3055	3025		16(3.445)	6 (3.3067)	Cf.Viscose. CH Stretching Vibration but also of CH_3 of Acetyl Group	III2vi Cc *
15	3.3355	2998		17(3.3620)	7 (3.3392)	" "	III2ii Cc *
16	3.3755	2962		19(3.4120)	8'(3.3792)	Cf. Viscose CH Stretching Vibration	II2viBc
17	3.3967	2944			8 (3.3992)	" "	II2viBc
17'	3.3930	2947	220°C.	-	-	Transitory CH Species Stretching Vibration	III Ma
17a	3.4779	2875		20(3.4775)	9"(3.4779)	Cf.Viscose. CH Stretching Vibration	I2viAc
17b	3.4880	2867			9 (3.4855)	" "	III 1vi Cc
17c	3.5683	2803			9a(3.5895)	Possibly CH_3 Vibration of Acetyl Group.	III 6vi Cc

TABLE XVIII (Continued)

Peak	Wavelength (μm.)	Wavenumber ($cm.^{-1}$)	New Peak at (in)	Corresponding Peak in Viscose (μm.)	Corresponding Peak in Tricel (μm.)	Interpretation	Code
17d	3.6033	2775		-	9b (3.6420)	Possibly $6H_2$ Vibration of Acetyl Group	III 6vi Cc
18	3.6845	2714		-	9c (3.6883)	CH, CH_2 or CH_3 Vibrations of Acetyl Group	III 6vi Cc
18a	3.7362	2677			9c' (3.7245)		III 6vi Cc
19	3.8020	2630		-	-		II Mh Ma
20	3.8258	2614		-	9d (3.8208)	Probably CH, CH_2 (or CH_3) Vibrations of Acetyl Group	III 6vi Cc
21	3.8783	2579			9e (3.8795)		III 6vi Cc
22	4.1645	2401		-	9f (4.1608)		I li Ac
23	4.3295	2309		-	9g (4.3320)		III liv Cc
24	4.7245	2116		-	10" (4.7295)	Probably Acetyl Group C-O (or C=O) Stretching Vibrations	III 6vi Cc
25	4.7670	2098		-	10 (4.7670)		III 6vi Cc

TABLE XIX From Figs. 48B (& 49B) (Tricel)

Peak	Wavelength (μm)	Wavenumber ($cm.^{-1}$)	New Peak at (in)	Corresponding Peak in Viscose (μm)	Corresponding Peak in Dicel (μm)	Interpretation	Code
1	2.7392	3651		2 (2.7406)	1 (2.7455)	Cf. Viscose & Dicel Loosely Bound Water	w
1a	2.7517	3634		3 (2.7506)	3 (2.7680)	" "	w
1b	2.7642	3618		4 (2.7720)	4 (2.7717)	" "	w
1c	2.7842	3592		-	-	" "	w
2′	2.7967	3575			-	Possibly OH Species Vibration	III Mh Ma
2	2.8042	3566			6 (2.8145)	Cellulosic OH Vibration (Intermolecular Hydrogen Bonding)	II 3ii Bc
2a	2.8217	3544		$4a_2$(2.8158)	8 (2.8442)	Water with an 'Ice Type' Structure	w
2a	2.8217	3544		$4a_3$(2.8820)	9 (2.8542)	Cf. Viscose & Dicel OH Stretching Vibration (Intramolecular Hydrogen Bonding)	II 2iv Bb
3	2.8767	3476		4b (2.9120)	10′(2.8830)	Cf.Viscose and Dicel. OH Stretching Vibration (Intramolecular Hydrogen Bonding)	III 2vi Cc
3a	2.8830	3469			10 (2.8892)	" " Also Water with an 'Ice Type' Structure	III Mh Cc and w

TABLE XIX (Continued)

Peak	Wavelength (μm.)	Wavenumber ($cm.^{-1}$)	New Peak at (in)	Corresponding Peak in Viscose (μm.)	Corresponding Peak in Dicel (μm.)	Interpretation	Code
3b	2.9092	3438		-	-	Water with an 'Ice Type' Structure	w
3c	2.9155	3430		8 (3.0858)	11 (2.9292)	" "	w
3d	2.9242	3420		-	-	" "	w
4	3.1492	3176		10(3.1363)	12 (3.1467)	Water	w
5′	3.2430	3084		-	-	CH, CH_2 (or possibly CH_3)	II Mh Ma
5	3.2542	3073		-	-	Vibrations of Acetyl Group.	II 2ii Bb
5a	3.2742	3054		-	-		II 6vi Ma
5b	3.2805	3048		-	-		II 6vi Ma
6	3.3067	3024		16(3.3445)	14 (3.3055)	Cf. Dicel, CH_3 Vibration of Acetyl Group	III 2vi Ma
7	3.3392	2995		17(3.3620)	15 (3.3355)	" "	I 2v Ac
8′	3.3792	2959		19(3.4120)	16 (3.3755)	CH Stretching (177)	II 2ii Bc
8	3.3992	2942		19(3.4120)	17 (3.3967)	" "	II 2ii Bc
9′	3.4630	2888		-	-	" "	III 6vi C
9″	3.4779	2875	Annealed	20(3.4775)	17a(3.4779)	" "	I
9	3.4855	2869			17b(3.4880)	" "	III 3ii C

TABLE XIX (Continued)

Peak	Wavelength (μm)	Wavenumber ($cm.^{-1}$)	New Peak at (in)	Corresponding Peak in Viscose (μm)	Corresponding Peak in Dicel (μm)	Interpretation	Code
9a	3.5895	2786		-	17c (3.5683)	Cf.Dicel, Possibly CH_3 Vibration of Acetyl Group	II 5i Bc
9b	3.6420	2746		-	17d (3.6033)	Cf.Dicel, Possibly CH_2 Vibration of Acetyl Group	III 5v Cb
9c	3.6883	2711		-	18 (3.6845)		III 5ii Cc
9c′	3.7245	2685		-	18a(3.7362)		II 5ii Bc
9c″	3.8145	2621	220°C.	-	-		Ma
9d	3.8208	2617		-	20(3.8208)	Cf.Dicel, CH, CH_2 or CH_3 Vibration of Acetyl Group	I 5i Ac
9e	3.8795	2577		-	21(3.8783)		III 2ii Ac
9f	4.1608	2403		-	22(4.1645)		I 5v Aa
9f″	4.2408	2358	220°C.	-	-	CH or CH_2 Peak, due to degradation	-
9g	4.3320	2308		-	23(4.3295)	CH, CH_2 or (CH_3) Vibration of Acetyl Group	I 4i Ab
9h	4.3970	2274	220°C.	-	-	CH or CH_2 Peak, due to degradation	-

TABLE XIX (Continued)

Peak	Wavelength (μm.)	Wavenumber ($cm.^{-1}$)	New Peak at (in)	Corresponding Peak in Viscose (μm.)	Corresponding Peak in Dicel (μm.)	Interpretation	Code
9h′	4.4270	2259	220°C.	-	-	CH or CH_2 Peak, due to degradation	-
10′	4.7063	2135		-	-	C-O Vibration of Acetyl Group	I 6vi Cc
10″	4.7295	2114		-	24 (4.7245)	Cf. Dicel Probably C-O (or C=O) Stretching Vibrations.	I 6vi Cc
10	4.7670	2198		-	25 (4.7670)		I 5v Ac
10a	4.7758	2094		-	-	Probably C-O or C=O Vibrations of Acetyl Group	III Mh Cb
10b	4.7883	2089		-	-		III Mh Cb
10c	4.8070	2080		-	-		II Mh Ma
10d	4.8358	2068		-	-		II Mh Ma
10α	4.8708	2050	100°C.	-	-		I 3iii Ac

However, the spectrum of Cellulose I contains two large peaks, 19c and 19d, which may correspond to the much smaller peak, peak 19 in the viscose film spectrum. Peak 19 in the viscose film spectrum may thus be due to the presence of small amounts of Cellulose I, within the viscose film.

3A.2.1 Results For Dicel and Tricel

Absorption and second derivative spectra of dicel film and dicel powder samples are shown in Figs. 46A - 47B and for tricel film and powder in Figs. 48A - 49B. Derivative spectra of dicel and tricel films recorded at 44°C. were compared with the derivative spectrum of viscose film, also recorded at 44°C. in Fig. 50.

Peaks in the derivative spectra of film samples were designated as 'crystalline', 'crystallizable' or 'non crystallizable' in the same way as for the spectra of viscose film. Changes in the intensities and frequencies (wavelengths) of such peaks were also designated as previously by the scheme shown in List I. The designation and assignment of all the derivative peaks of dicel and tricel film spectra are shown in Tables XVIII and XIX respectively.

Powder sample spectra were again only used to confirm previous designations and assignments.

3A.2.2 Discussion of Results for Dicel and Tricel

(a) Water Peaks (due to OH stretching in water)

Fig. 50 shows that loosely bound water is present in dicel (peaks 1, 3 and 4) and tricel films (peaks 1, 1a, 1b and 1c) in addition to being present in viscose film. However, since two of these peaks in dicel (peaks 1 and 3) occur at higher wavelengths than corresponding peaks in viscose or tricel, the strength of binding of such water by hydrogen bonding involving

cellulosic OH groups (and/or other cellulosic groups) is stronger in dicel than in viscose or tricel. This is also upheld by the fact that the peaks in dicel (1 and 3) do not disappear on heating until a temperature of 220°C, is reached, whereas corresponding peaks in viscose and tricel disappear at lower temperatures.

The fact that the strength of binding of such water by hydrogen bonding is stronger in dicel than in viscose or tricel may be accounted for by comparing the structures of viscose dicel and tricel molecules. Viscose (Cellulose II) molecules contain a regular pattern of OH groups along their length which is a major factor enabling some of them to pack into a regular hydrogen bonded crystalline lattice in 'crystalline' regions and into a less crystalline lattice (or no lattice at all) in 'crystallizable' regions. There are thus relatively few 'free' (non hydrogen bonded) cellulosic OH groups available to form very strong hydrogen bonds with absorbed water. It is possible, however, that at high humidities strong hydrogen bonding of water may take place with cellulosic hydroxyl groups by partial disruption of existing cellulosic hydrogen bonds.

In dicel however, chain molecules cannot pack into a regular crystalline lattice due to their irregular structure. This irregular structure results from the random way in which acetylation of cellulosic OH groups has occurred over the whole length of parent Cellulose II molecules. There is thus no evidence to suggest any regular pattern of acetylation of the glucose residues which constitute the Cellulose II chain at any of the three OH positions (C_2, C_3 and C_6) of the glucose residues. Relative degrees of acetylation at each of these positions do differ, however, and have been shown (90) to be in the order $C_2 > C_3$, slightly $> C_6$ for acetylation at C_2, C_3 and C_6 hydroxyl positions.

The lack of regular crystalline structure in dicel indicates that there are more 'free' (non hydrogen bonded) OH groups in dicel (than in viscose),

which are able to form strong hydrogen bonds with absorbed water. In tricel, however, the almost complete acetylation of parent cellulose molecules produces molecules which have a much more regular structure than those of dicel. Some tricel molecules are thus able to pack into a regular crystalline lattice (107) so that the classification of material into 'crystalline' and 'crystallizable' regions of structure is similar to the case of viscose. As in the case of viscose, the regularity in both 'crystalline' and 'crystallizable' regions of tricel compared to dicel, means that of the few remaining hydroxyl groups in tricel, there are very few 'free' (non hydrogen bonded OH groups available to form strong hydrogen bonds with absorbed water. This is also upheld by the fact that tricel is a hydrophobic polymer which absorbs little water.

Water with an 'ice type' structure also occurs in dicel (peaks 8, 8a and 11) and tricel (peaks 2a, 3b, 3c and 3d), since there are water peaks which correspond to these peaks in the derivative spectra of both water and ice (Figs. 72 and 73). Such water peaks in dicel increase in intensity in heated and annealed sample spectra, as does peak 4b in the spectrum of viscose. As in the case of viscose, it is possible that water in dicel may or may not be transferred to crystalline regions. However, the transference of water from 'crystallizable' to 'crystalline' regions in dicel is less probable than in viscose since dicel is not a very crystalline polymer so that the difference in structure between 'crystalline' and 'crystallizable' regions in terms of energy difference and stability is much smaller in dicel than in viscose.

However, aggregation of water molecules into 'ice type' structures which correspond to peaks 8, 8a and 11 of the spectrum of viscose must occur in dicel at high temperatures, (whether in 'crystalline' or 'crystallizable' regions) in order to account for the increased intensity of these peaks in heated and annealed sample spectra.

The fact that such groups of molecules are not broken up and lost from the relatively amorphous dicel structure indicates that such groups are

strongly bound by hydrogen bonding to cellulosic OH (and other) groups. This strong binding is confirmed by the fact that peaks which correspond to such groups occur at a higher wavelength in dicel than in viscose.

In tricel, peaks assigned to water with an 'ice type' structure and recorded at 44°C. (peaks 2a, 3b, 3c, 3d, Fig. 48B), disappear in heated and annealed sample spectra. This shows that the binding of groups of water molecules which have an 'ice type' structure and correspond to these peaks, is very weak in tricel. The fact that such 'ice type' water is lost from tricel on heating, but not from dicel or viscose, may be explained on the basis of strong hydrogen bonding occurring between cellulosic OH groups and such water in viscose and dicel, whereas in tricel there are few cellulosic OH groups present to form strong hydrogen bonds with such groups of water molecules.

(b) <u>OH Stretching Vibration Peaks</u>

Peaks assigned to stretching vibrations of intramolecularly hydrogen bonded OH groups in viscose ($4a_3$, 4b) have counterparts in the spectra of dicel (9, 10′ and 10) and tricel (2a, 3 and 3a). These peaks occur at decreasing wavelengths in dicel and tricel, showing that the strength of such hydrogen bonding is in the order viscose > dicel > tricel. The weaker hydrogen bonding in dicel may be accounted for in part by the atactic structure of dicel molecules which results in their failure to pack into a regular crystalline lattice. The even weaker hydrogen bonding in tricel may be accounted for in part by the high degree of substitution of C_3 OH groups (of glucose residues in the parent cellulose molecules) by bulky acetyl groups, which tend to sterically hinder the formation of C_3 OH --- O'_5 intramolecular hydrogen bonds by any remaining C_3 OH groups in tricel. Acetyl groups in tricel may also hinder the formation of C_3 OH --- O'_5 hydrogen bonds by providing for alternative hydrogen bonding of C_3 OH groups with acetyl C=O or C-O groups. Such an explanation may also partially apply

to dicel.

Dicel and tricel do not possess any peaks which correspond to the two intermolecular hydrogen bonded OH peaks in viscose (peaks 5 and 11) which involve hydrogen bonding between C_6 OH groups and bridge oxygen atoms of neighbouring chains. However, one peak in the spectrum of dicel (peak 6) and tricel (peak 2) has been attributed to such bonding, from structural assignment charts (3-5). Since these peaks in dicel and tricel occur at lower wavelengths than any peaks assigned to OH bonding involving C_6 OH groups in viscose, it is proposed that the strength of hydrogen bonding for C_6 OH groups is in the order viscose $>$ dicel $>$ tricel, in accordance with the explanation for intramolecularly hydrogen bonded OH peaks. Since peaks 10 in dicel and 3a in tricel correspond to peaks in the derivative spectra of water and ice, it is also possible to assign these peaks to water with an 'ice type' structure, but this is discussed further in chapter 6.

(c) <u>CH Stretching Vibration Peaks</u>

Peaks 16 and 17 in viscose, which correspond to CH vibrations, have corresponding peaks in dicel (14 and 15) and tricel (6 and 7), which are largely unaffected in heated and annealed sample spectra. However, since the intensity of these peaks increases from viscose $\longrightarrow$ dicel $\longrightarrow$ tricel, CH stretching vibrations of acetyl groups must also contribute to such peaks. The fact that these peaks occur at lower wavelengths in dicel and tricel also indicates that the CH groups which correspond to these peaks may be involved in some intra or intermolecular interactions (or both), such as hydrogen bonding (e.g. with cellulosic OH or C-O groups), the strength of which decreases in dicel and tricel. The strength of any such bonding is thus in the order viscose $>$ dicel $\simeq$ tricel and further evidence for the existence of such hydrogen bonding is given by Rhodes (12).

An analogous situation is seen for the CH stretching vibrations which correspond to peak 19 in viscose and which correspond to peaks 16 and 17

in dicel and 8′ and 8 in tricel and which occur at lower wavelengths and with increasing intensities in dicel and tricel.

The region from 3.625 to 5 μm.(2759 - 2000 $cm.^{-1}$) has no resolvable peaks in the derivative spectra of viscose, but the spectra of dicel and tricel contain peaks which must thus be due to the vibrations of substituted acetyl groups. Peaks 17c - 23 in dicel, which correspond to peaks 9a - 9g in tricel, were thus assigned to CH, CH_2 or CH_3 group vibrations of acetyl groups, from structural assignment charts (3 - 5). Most of these peaks in dicel are largely unchanged in heated or in annealed sample spectra, but approximately half of the peaks in tricel show a 'crystalline' or 'crystallizable' behaviour. This behaviour confirms that the differentiation of tricel into 'crystalline' and 'crystallizable' material is greater than in dicel, and that CH, CH_2 or CH_3 groups may be involved in hydrogen bonding.

In tricel, several new peaks occur at 220°C., (9f′, 9h, 9h′) and other peaks (9f and 9g) increase in intensity. This may be attributed to the onset of degradation in tricel between 159 and 220°C. Such degradation does not, however, occur in the annealed sample, since annealing was carried out under a nitrogen atmosphere.

(d) <u>C-O Peaks</u>

Several peaks occur in the derivative spectra of dicel and tricel, which we have attributed to C-O vibrations of acetyl groups from structural assignment charts (3 - 5). Peaks 24 and 25 in dicel are largely unaffected in heated and annealed sample spectra, but corresponding peaks in tricel (peaks 10″ and 10) show a slightly 'crystalline' behaviour. In addition there are several other peaks (10′, 10a, 10b, 10c, 10d and 10∝) present in tricel but not present in dicel, which show a mixture of 'crystalline', 'crystallizable' and 'non crystallizable' behaviour. The fact that the peaks

in dicel are fewer in number than in tricel and are largely unaffected, substantiates the view that dicel is a very poorly ordered polymer, i.e. it is not well defined into 'crystalline' and 'crystallizable' regions.

(e) The Whole Spectrum

The fact that there are more 'crystalline' or 'crystallizable' peaks in tricel and viscose than in dicel, over the whole spectrum from 2.5 - 5 μm. (4000 - 2000 $cm.^{-1}$), also confirms that tricel and viscose are more well defined into 'crystalline' and 'crystallizable' regions than dicel, i.e. the difference in structure between 'crystalline' and 'crystallizable' regions in terms of energy difference and stability is greater in viscose and tricel than in dicel.

The presence in tricel of a large number of 'mixed response' peaks (eg. peaks 2a, 2, 7, 9a, 9b, 9c, 9c", 9d and 9e) which change in intensity and wavelength or both on heating initially, and which then similarly change on further heating and for which no similar response is determined for corresponding peaks in dicel and viscose, indicates that a larger number of crystalline phases and/or crystalline phase changes occur in tricel than in dicel or viscose.

FIG. 51 A.

ABSORPTION SPECTRA OF VISCOSE FILM

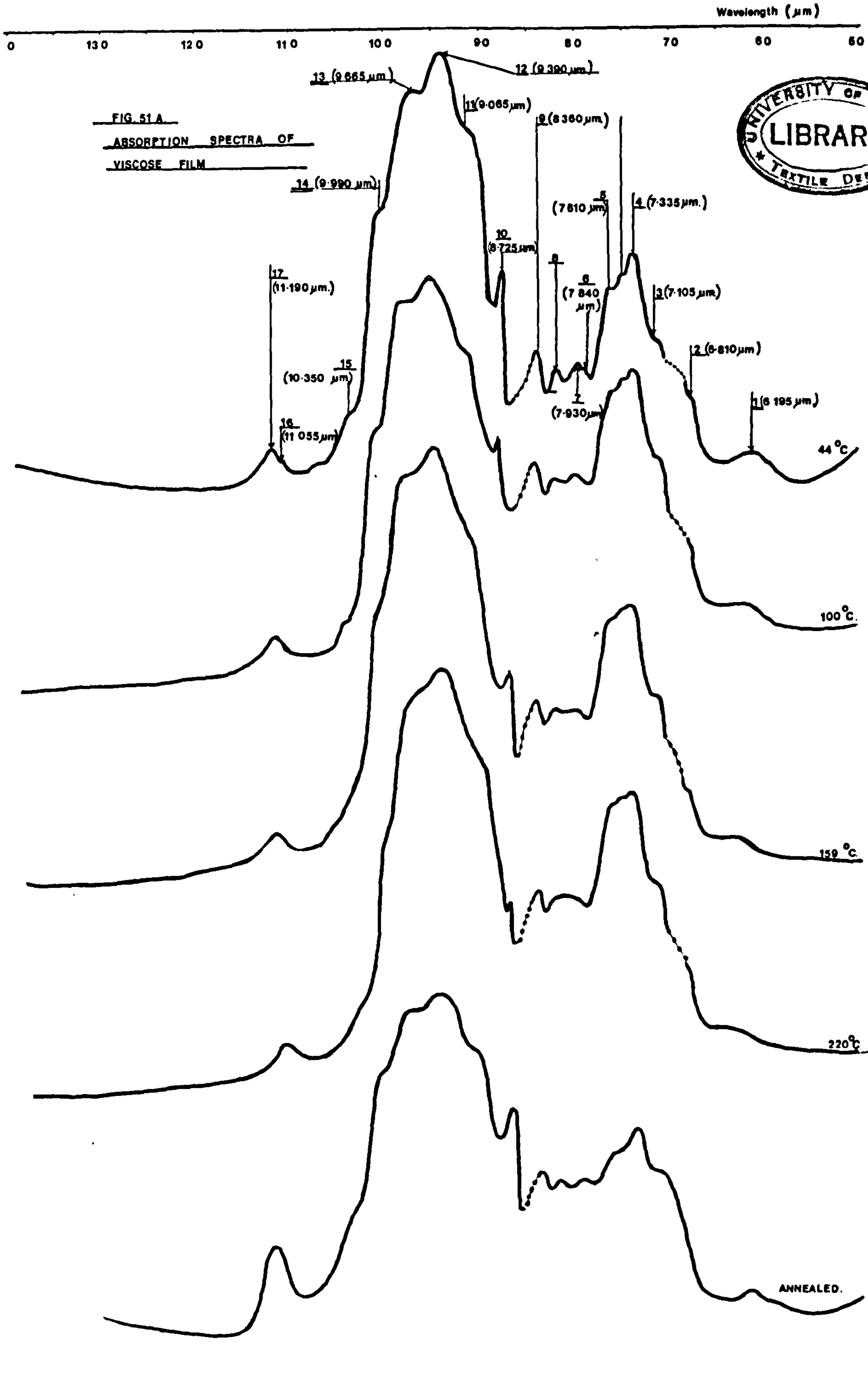

FIG. 81B.

DERIVATIVE SPECTRA OF VISCOSE FILM

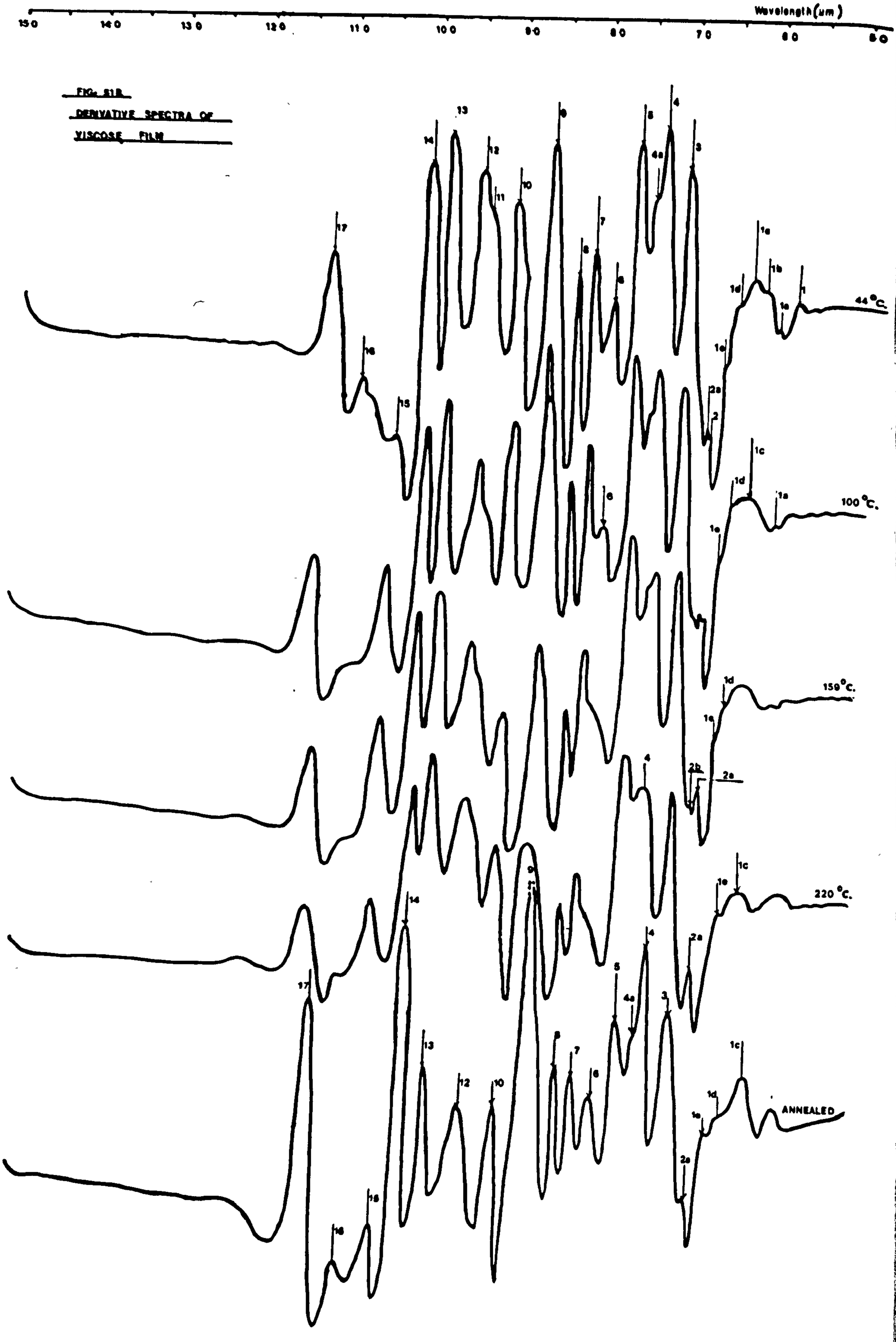

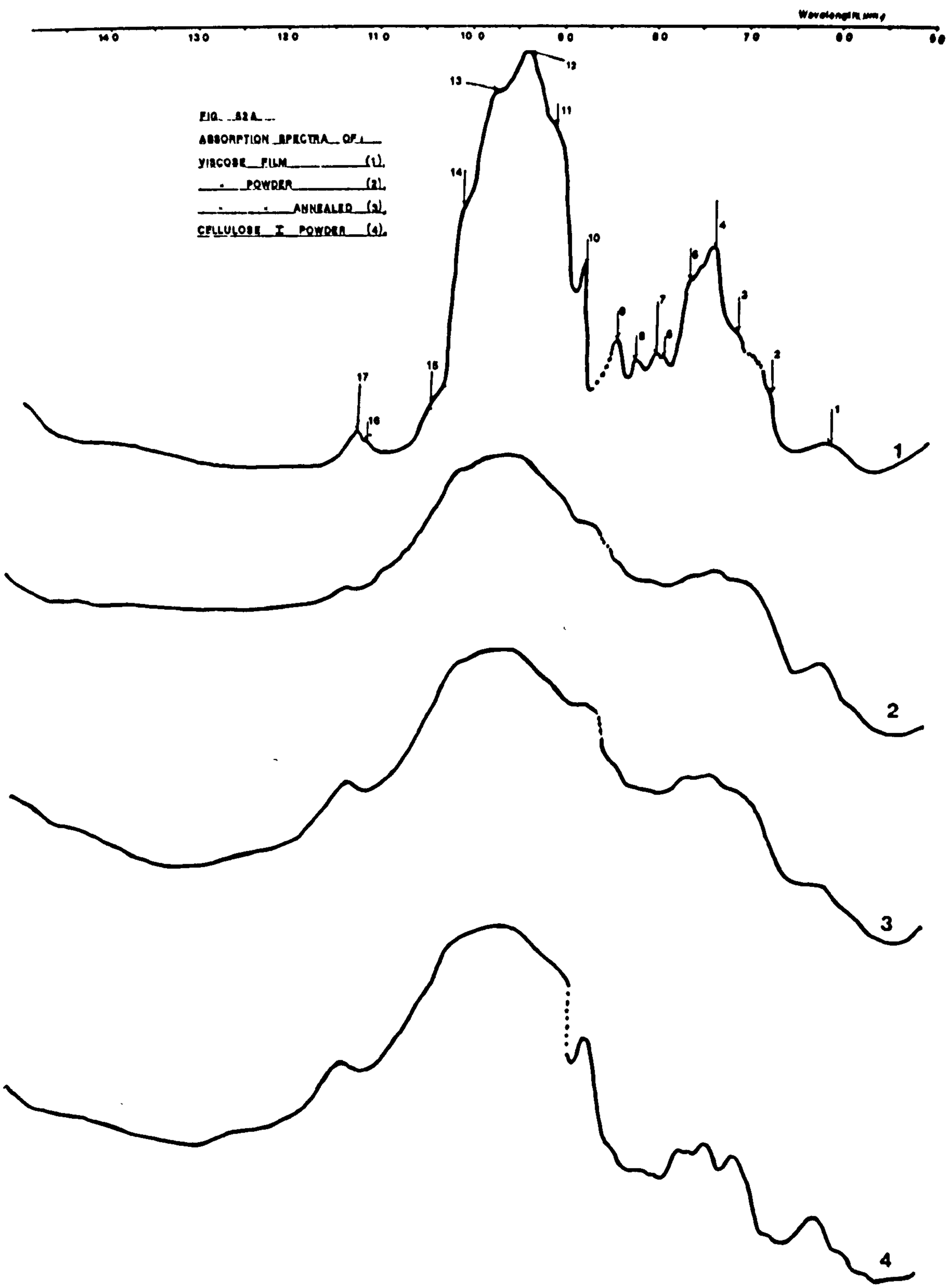

FIG. 82A.

ABSORPTION SPECTRA OF :—

VISCOSE FILM ——— (1).

" POWDER ——— (2).

" " ANNEALED (3).

CELLULOSE II POWDER (4).

FIG. 52 B.

DERIVATIVE SPECTRA OF :-

VISCOSE FILM (1).

" POWDER (2).

" " ANNEALED (3).

CELLULOSE I POWDER (4).

TABLE XX (Viscose)

Peak	Wavelength (μm)	Wavenumber ($cm.^{-1}$)	New Peak at (in)	Previous Interpretation	Present Interpretation	Code
1	5.825	1717	-	-	Water with an 'Ice Type Structure	w
1a	5.985	1671	-	Absorbed Water (80)	Absorbed Water, Strongly Bound	w
1b	6.140	1629	-	-	" "	w
1c	6.310	1585	-	-	Water with an 'Ice Type' Structure	w
1d	6.470	1546	-	-	" "	w
1e	6.625	1509	-	-	Fairly Strongly Bound Water	w
2	6.805	1470	-	Cellulosic OH In Plane Bending (80)	Same as Previous Interpretation and Also Bound Water	II Mh Ma and w
2a	6.835	1463	-	" "	" "	III 1i Cc and w
2b	6.895	1450	159°C.	-	Transient OH species	III Mh Ma
3	7.080	1412	-	CH_2 Bending Vibration (80)	Same as Previous Interpretation	II 6vi Bc
4	7.365	1358	-	-	Possibly OH In Plane Bending Vibration	I 2i Ac
4a	7.440	1344	-	OH In Plane Bending (80)	OH In Plane Bending Vibration	III Mh Cc
5	7.665	1305	-	-	OH Bending Vibration	II 2vi Bc*
6	7.955	1257	-	Observed By Marchessault (80) - Not Assigned	Stretching Vibration of C-O-C groups.	III 2i Cc*
7	8.175	1223	-	-	" "	II 2vi Bc

TABLE XX (Continued)

Peak	Wavelength (μm.)	Wavenumber ($cm.^{-1}$)	New Peak at (in)	Previous Interpretation	Present Interpretation	Code
8	8.365	1195	-	OH In Plane Bending (80)	Same As Previous Interpretation	II 2vi Bc
9	8.665	1154	-	Stretching of Bridge Oxygen Bonds in Glucose Residues	" "	I 2i Ac
10	9.040	1106	-	Ring Stretching ν_{ai}	" "	II 2vi Bc
11	9.335	1069	-			II Mh Ma
12	9.440	1059	-	C-O Stretching Vibrations (80)	" "	III 2vi Cc
13	9.840	1016	-			II 2vi Bc
14	10.075	993	-			I 2vi Aa
15	10.445	957	-	-	Possibly C-O Vibration of Cellulose I	I 3iv Ab
16	10.885	919	-	-	" "	II 2ii Bb
17	11.225	891	-	C_1 Group Vibration	Same As Previous Interpretation	I 2i Aa

SECTION B

3B.1.1 Results For Viscose

The results in this section are discussed as before, for viscose, dicel and tricel respectively. The absorption and derivative spectra of viscose films are shown in Figs. 51A and 51B respectively, and of viscose powder and Cellulose I powder in Figs. 52A and 52B respectively. Absorption spectra are shown for comparison, but designations (following the scheme in List I) and assignments shown in Table XX were again based upon derivative spectra. Powder spectra were used mainly to confirm existing assignments.

3B.1.2 Discussion of Results for Viscose

A comparison of the absorption and derivative spectra of viscose film (Figs. 51A and 51B) shows that differentiation has not produced a large number of new peaks by resolving existing absorption peaks except in the 6 μm. (1667 $cm.^{-1}$) absorbed water region. However, differentiation has produced peaks which are better resolved and of much higher intensity than corresponding parent absorption peaks. This is important, since it enables small changes which occur in heated or annealed samples, not observed in absorption spectra, to be observed. It also enables any changes in absorption spectra to be more clearly studied in the derivative mode.

(a) Water Peaks (Due to OH Bending in Water)

The derivative spectrum of viscose film recorded at 44 ^{o}C. contains several peaks (1, 1a, 1b, 1c, 1d and 1e) which can be assigned to OH banding modes of absorbed water, from a comparison of structural assignment tables (3-5) and the derivative spectra of water and ice (Figs. 72 & 73). The water present is strongly bound to the cellulose structure, since it is not removed by drying the viscose samples over P_2O_5.

The effect of hydrogen bonding on OH stretching modes has been discussed in detail in section A, but the basic trend which emerges for OH stretching modes (as with all other stretching modes) is that the strongest hydrogen bond (previously ascribed to intermolecular hydrogen bonding from section A) produces corresponding OH spectral peaks which occur at the lowest frequencies (highest wavelengths). However, it has been shown (201, 202) that when a particular stretching mode shifts in frequency, there is a corresponding but opposite frequency shift of proportional magnitude in the bending mode(s). Thus in the case of OH bending modes, it can be shown that the strongest hydrogen bonding is associated with spectral peaks which occur at the highest frequencies (lowest wavelengths).

Although peaks 1a and 1b occur at low wavelengths and thus represent OH bending modes of strongly bound water, they disappear in the heated and in the annealed sample spectra. This behaviour can be explained if these peaks arise from water present in 'crystallizable' regions, since the structures of such regions are less stable and have weaker hydrogen bonds than crystalline structures. At the same time, 'crystallizable' regions will allow water to be more readily lost upon heating than 'crystalline' regions. An alternative explanation is that these peaks represent individual water molecules in 'crystalline' and/or 'crystallizable' regions, which aggregate into groups of water molecules on heating, thus accounting for the decrease in the intensity of these peaks at elevated temperatures. The aggregation of such molecules may be preceded by transference of water to 'crystalline' regions at high temperatures as described in Explanation 1 of Section A (page 68).

Peaks 1a and 1b may thus be assigned to OH bending modes of water for which OH stretching mode peaks (peaks 9, 10 and 12 Fig. 44B) were assigned in section A, since the OH stretching mode peaks show a similar behaviour to peaks 1a and 1b at high temperatures.

Peak 1 has been assigned to water with an 'ice type' structure, since there is a corresponding peak in the derivative spectrum of water and the derivative spectrum of ice (Figs. 72 and 73). The occurrence of this peak at the lowest wavelength either indicates that there is strong hydrogen bonding within the groups of water molecules which constitute the 'ice type' structure and give rise to peak 1, or that there is very strong hydrogen bonding between such groups of water molecules and cellulosic OH and other groups. Peaks 1c and 1d have also been assigned to water with an 'ice type' structure since these peaks have corresponding peaks in the derivative spectra of water and ice. The increase in the intensity of peaks 1, 1c and 1d in heated or annealed sample spectra may be explained by either of the explanations for OH stretching modes of such water, given in section A (Explanation 1 page 68, Explanation 2 page 69). Although it is not possible at this stage to decide which of the two explanations is correct, the first is the most acceptable since the second cannot easily account for the retention of water by 'crystallizable' regions at high temperatures.

The shift of peak 1c to a lower wavelength in heated and annealed sample spectra is difficult to interpret, since this indicates an increase in the strength of hydrogen bonding between the water from which this peak originates and cellulosic OH groups (or other groups, e.g. C-O groups). An increase in the strength of such bonding is unexpected, since annealing causes an increase in the total amount of crystalline material within the viscose film so that there are fewer 'free' (non hydrogen bonded) or weakly hydrogen bonded OH groups (or C-O groups) available to form strong hydrogen bonds with such absorbed water. It is possible, however, that the dissociation of such groups of water molecules from cellulosic OH groups at high temperatures, may induce water migration and hence facilitate the formation of stronger hydrogen bonds.

Peak 1e, which increases in intensity in heated and annealed sample spectra, does not correspond to water with an 'ice type' structure, since there is no corresponding peak in the derivative spectrum of ice, although there is such a peak present in the derivative spectrum of water. However, such a band which is stable at high temperatures may arise from the OH bending mode of bound water, of intermediate binding energy in both 'crystalline' or 'crystallizable' regions of the viscose film. Further water molecules not strongly bound may be transferred to this state on heating and thus account for the increase in the intensity of peak 1e at 220^{o}C.and in the annealed sample spectrum.

The behaviour of small amounts of absorbed water in viscose in this region thus shows a similar pattern to that discussed in the 2.5 - 5 μm. (4000 - 2000 cm.$^{-1}$) region and thus provides further evidence for the aggregation of some of the absorbed water into 'ice type' structures and substantiates the use of Hearle's modified fringed fibril model as a basis for the structure of viscose.

(b) Hydroxyl Peaks

The 5 - 15 μm.(2000 - 667 cm.$^{-1}$) region of the derivative spectrum of viscose contains peaks which arise from OH bending modes. The origins of some of these modes have been previously assigned from absorption spectra by Marchessault (80).

Present Peak		Corresponding Peak quoted previously (80)	
2	(6.805 μm, 1470cm.$^{-1}$)	(6.8027 μm, 1470 cm.$^{-1}$)	
2a	(6.835 μm, 1465cm.$^{-1}$)		
4a	(7.440 μm, 1344cm.$^{-1}$)	(7.4901 μm, 1335 cm.$^{-1}$)	
8	(8.365 μm, 1195cm.$^{-1}$)	(8.33 μm, 1200 cm.$^{-1}$)	

However, we have also

assigned peaks 2 and 2a to the OH bending modes of absorbed water in addition to cellulosic OH bending modes, since corresponding peaks occur in the derivative spectrum of water. Similarity of OH bonded modes is thus indicated. The single absorption peak at 6.8027 μm.(1470 $cm.^{-1}$) which corresponds to these two derivative peaks was assigned by Marchessault (80) to the bending mode of C_2 or C_3 OH groups (of glucose residues constituting Cellulose II molecules), which are involved in intramolecular hydrogen bonding. However, such an assignment does not account for the effect of hydrogen bond strength on OH bending frequencies.

In the case of bending modes, it has been shown that the strongest hydrogen bonding results in corresponding spectral peaks which occur at the highest frequencies, i.e. lowest wavelengths. Peaks 2 and 2a, which correspond to Marchessault's peak at 6.8027 μm.(1470 $cm.^{-1}$), were thus assigned to the OH bending mode resulting from C_6 OH groups, since these groups are involved in the strongest (intermolecular) hydrogen bonding. This is in contradiction to Marchessault's suggestion that this peak corresponds to C_2 or C_3 OH groups intramolecularly hydrogen bonded. Such an explanation is also upheld by the behaviour of peaks 4 and 5, assigned from structural assignment charts (3-5), to OH bending modes. These peaks show 'crystalline' and 'crystallizable' behaviour respectively. On the basis of the above explanation, it is expected that OH bending peaks which correspond to 'crystalline' material (strongly hydrogen bonded) will occur at lower wavelengths than OH bending peaks which correspond to 'crystallizable' (more weakly hydrogen bonded) material, and thus is in accord with the results for peaks 4 and 5. Peak 8, which also shows a 'crystallizable' behaviour, (more weakly hydrogen bonded material) also occurs at a higher wavelength.

(c) CH and CH_2 Stretching and Bending Peaks

Peak 3 (7.080 μm, 1412 $cm.^{-1}$) has been assigned to the CH_2 bending vibration quoted by Marchessault at 7.0621 μm. (1416 $cm.^{-1}$). Since CH_2 groups occur only at C_6 positions of glucose residues in viscose, peak 3 must correspond to C_6, CH_2 groups. This peak does not change significantly in wavelength in the spectra of heated or annealed samples, but does decrease slightly in intensity and has thus been defined as a 'crystallizable' peak (Table XX). The fact that this peak shows a 'crystallizable' behaviour indicates that there is a difference between CH_2 groups in 'crystalline' and 'crystallizable' regions. This difference may be accounted for in terms of hydrogen bonded CH_2 groups of different hydrogen bond strengths in 'crystalline' and 'crystallizable' regions of the structure. This thus provides further evidence for the involvement of CH or CH_2 groups in hydrogen bonding.

(d) C-O Peaks

Peak 6 (7.995 μm. 1257 $cm.^{-1}$) was observed by Marchessault (80) at the same wavelength. This peak has been tentatively designated to the C-O stretching vibration of a C-O-C group in the work discussed here. This designation is based upon assignment tables (3-5) and on the fact that the corresponding peak occurs at a higher intensity in the spectra of dicel and tricel. This peak in viscose thus corresponds to the C-O stretching vibrations of $C_1 - O - C'_4$ groups (the so-called '1-4' glucosidic linkages between glucose residues) or $C_5 - O - C_1$ groups or both, in addition to C-O-C of acetyl groups in dicel and tricel.

Peak 7 (8.175 μm. 1223 $cm.^{-1}$) which has not been previously recorded, has also been similarly assigned to the C-O stretching vibrations of $C_1 - O - C'_4$ or $C_5 - O - C_1$ groups in addition to the C-O-C group of acetyl

groups in dicel and tricel. However, as is observed from Fig.51B, peak 7 shows a 'crystallizable' behaviour and it is probable therefore that the corresponding C-O-C groups are involved in hydrogen bonding which differs in strength from that which occurs in 'crystalline' regions. Thus as more of the 'crystallizable' material is converted to 'crystalline' material upon heating, the number of C-O-C groups hydrogen bonded in the remaining 'crystallizable' material decreases and thus accounts for the decrease in intensity of peak 7 on heating and annealing.

Peak 9 (8.665 μm, 1154 $cm.^{-1}$) in Fig. 51B has been previously assigned from the absorption spectrum by Marchessault to an antisymmetric bridge oxygen stretching vibration (i.e. of $C_1 - O - C'_4$ groups). The 'crystalline' behaviour of this peak confirms that annealing causes an increase in the total proportion of 'crystalline' material in the viscose film. Since the formation of more 'crystalline' material on annealing involves an increase in the amount of material packed into a regular crystalline lattice and involves strong hydrogen bonding, the increase in the intensity of peak 9 also confirms that bridge oxygen atoms are involved in strong hydrogen bonding.

Peaks 11 - 14 have previously been assigned to various C-O stretching vibrations by Marchessault. We have also tentatively assigned two other peaks, not previously reported, to C-O stretching vibrations; namely peaks 15 (10.445 μm.,957 $cm.^{-1}$) and 16 (10.885 μm.,919 $cm.^{-1}$).

The fact that some of these peaks show a 'crystalline' behaviour (peaks 14 and 15), whereas other peaks show a 'crystallizable' behaviour (peaks 11 and 13), also confirms that annealing causes an increase in the total proportion of 'crystalline' structure present in the viscose film. The increase in the wavelength of peak 14 in the annealed sample also indicates that annealing causes an increase in the degree of perfection of at least one crystalline state within the viscose film. However, another

'crystalline' peak, peak 15, shows a decrease in wavelength in the annealed sample spectrum, indicating that a decrease in the degree of perfection of at least one crystalline state within the viscose film has occurred.

These results substantiate the earlier proposals put forward in Section A of the co-existence of more than one crystalline state within the viscose film structure; that is the possibility that small amounts of Cellulose I exist together with large amounts of Cellulose II within the viscose film structure. Since peak 15 is of a much lower intensity than peak 14, it is probable that peak 15 arises from the small amount of Cellulose I present in the structure.

(e) Other Peaks

Peak 10 (9.040 μm., 1059 $cm.^{-1}$) was previously assigned by Marchessault to antisymmetric in phase ring stretching from absorption spectra (and quoted by him at 9.0334 μm, 1107 $cm.^{-1}$), shows a 'crystallizable' behaviour and also shifts to a lower wavelength in the annealed sample spectrum. This indicates that changes in crystallinity which occur on annealing affect the frequency and intensity of ring stretching absorptions.

(f) Results from Powder Spectra

The derivative spectra of powder samples of viscose and Cellulose I in KBr discs were used mainly to confirm assignments made from the spectra of viscose film, for the reasons discussed previously. The derivative spectrum of Cellulose I powder (Fig. 52B) does, however, contain a peak (peak 15) which corresponds to peak 15 in the spectrum of viscose (Cellulose II) film. This peak is not, however, present in the spectrum of viscose powder (Fig. 52B) recorded at 44°C. but it is present in the spectrum of annealed viscose powder (Fig.52B), also recorded at 44°C.. These results support the previous assignment of peak 15 in the derivative spectrum of viscose film (Cellulose II) to small quantities of Cellulose I. The fact that peak 15 is also observed in the derivative spectrum of annealed viscose powder also

FIG. 53A.

ABSORPTION SPECTRA OF DICEL FILM

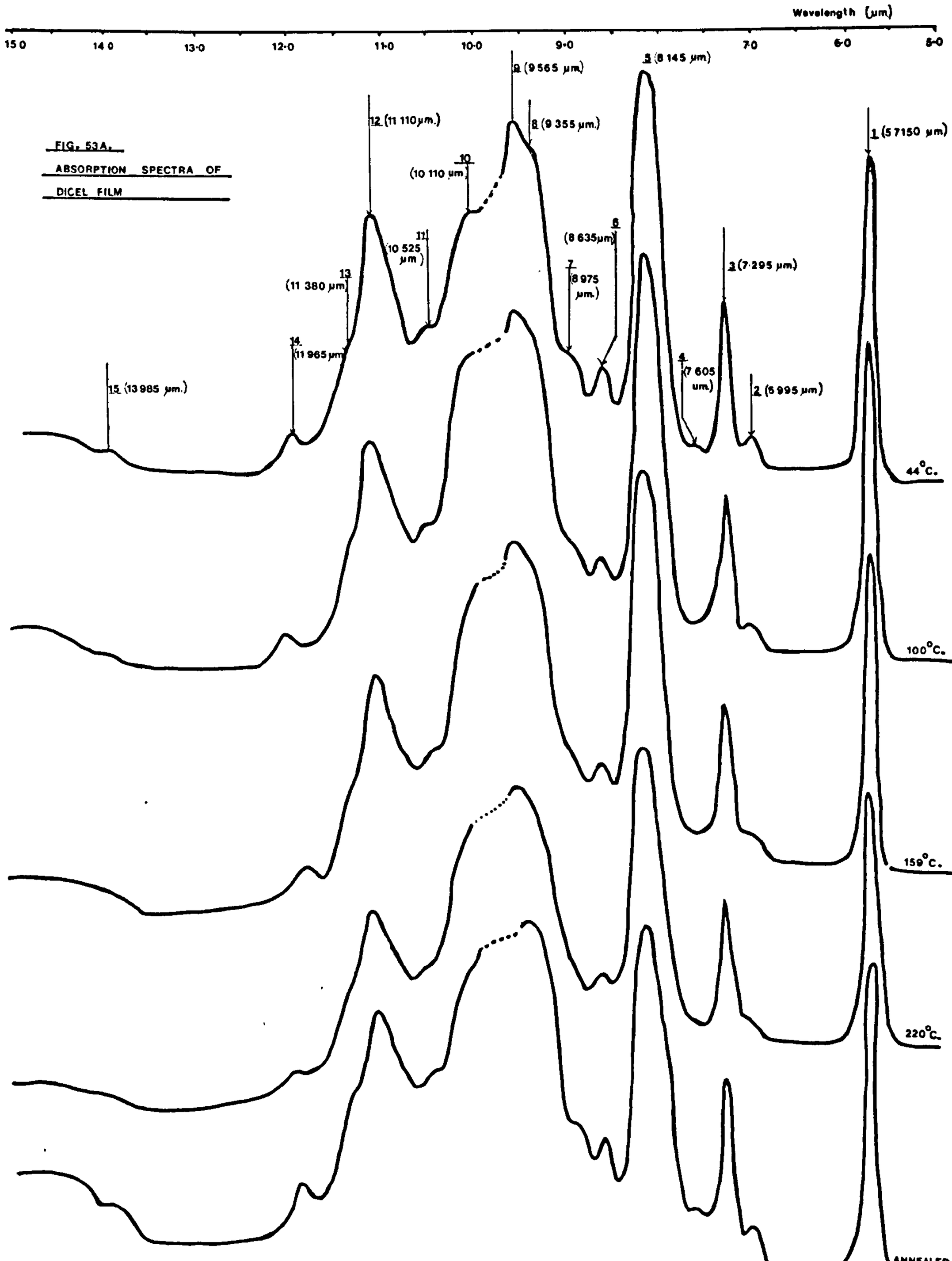

FIG. 53 B.

DERIVATIVE SPECTRA OF DICEL FILM.

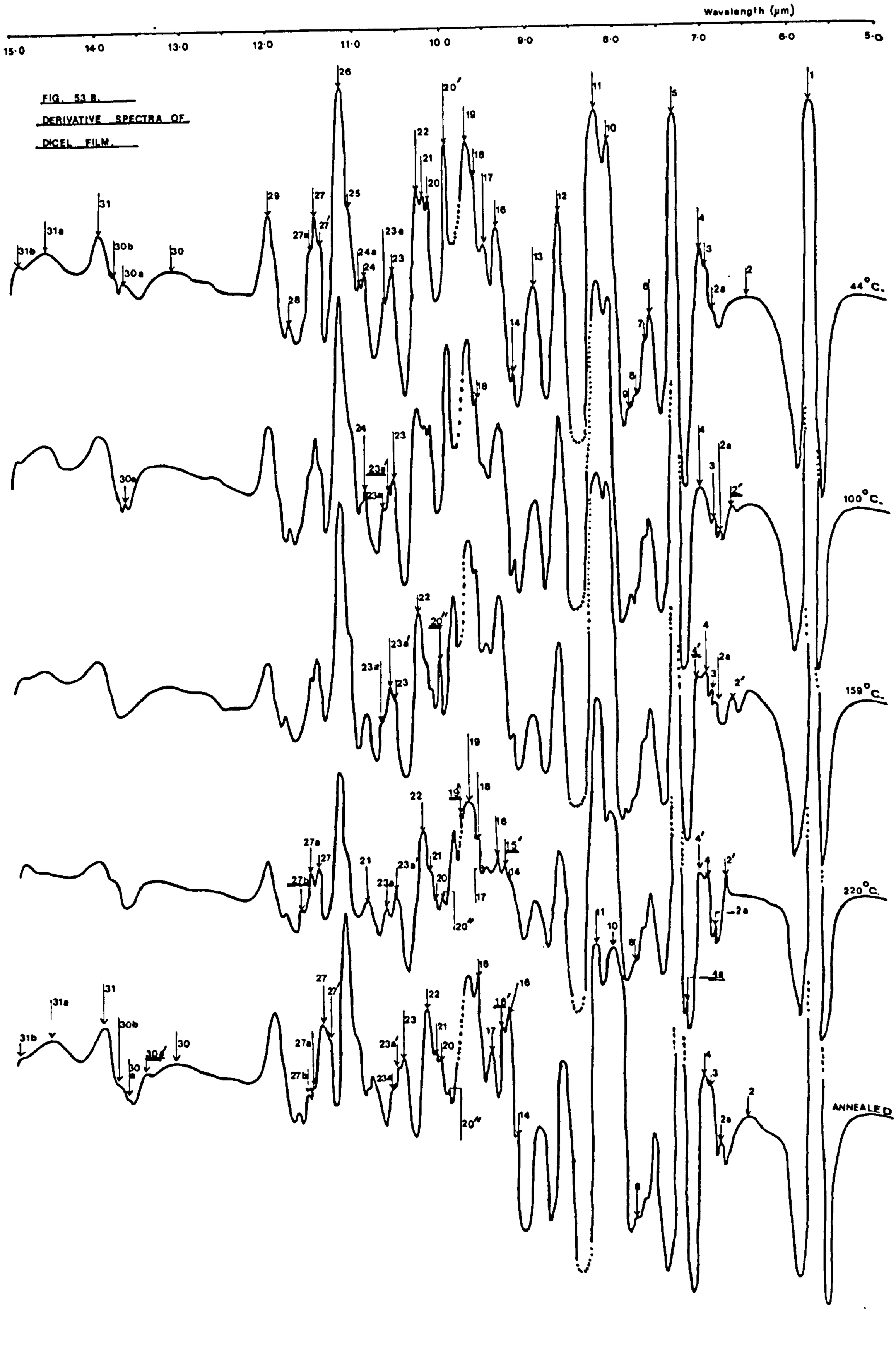

FIG. 54A.

ABSORPTION SPECTRA OF :—

DICEL FILM (1).

" POWDER (2).

" " ANNEALED (3)

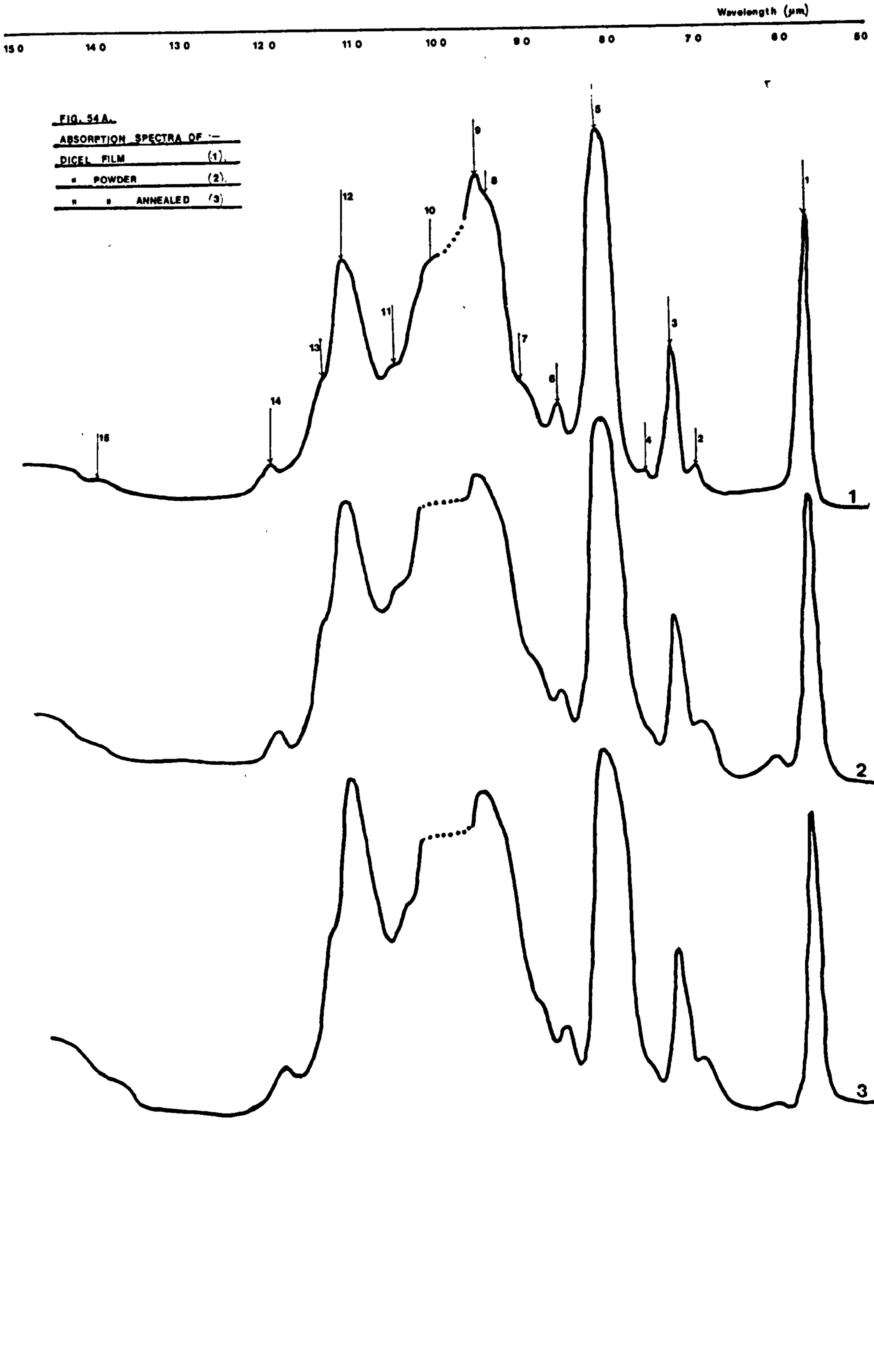

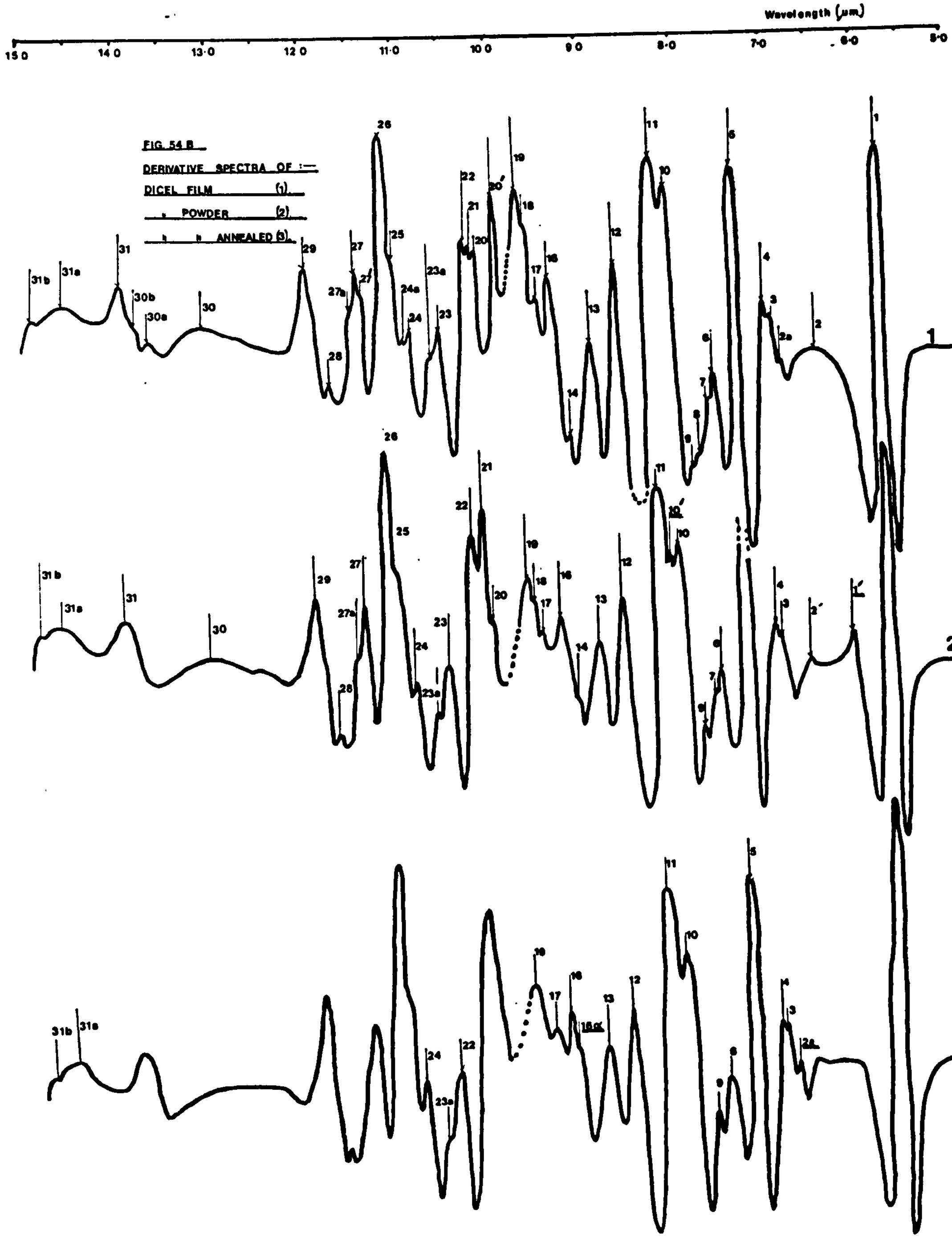
Wavelength (μm)
15·0
14·0
13·0
12·0
11·0
10·0
9·0
8·0
7·0
6·0
5·0
FIG. 54 B
DERIVATIVE SPECTRA OF :—
DICEL FILM (1).
" POWDER (2).
" " ANNEALED (3).
1
2
3

FIG 55 A.

ABSORPTION SPECTRA OF TRICEL FILM

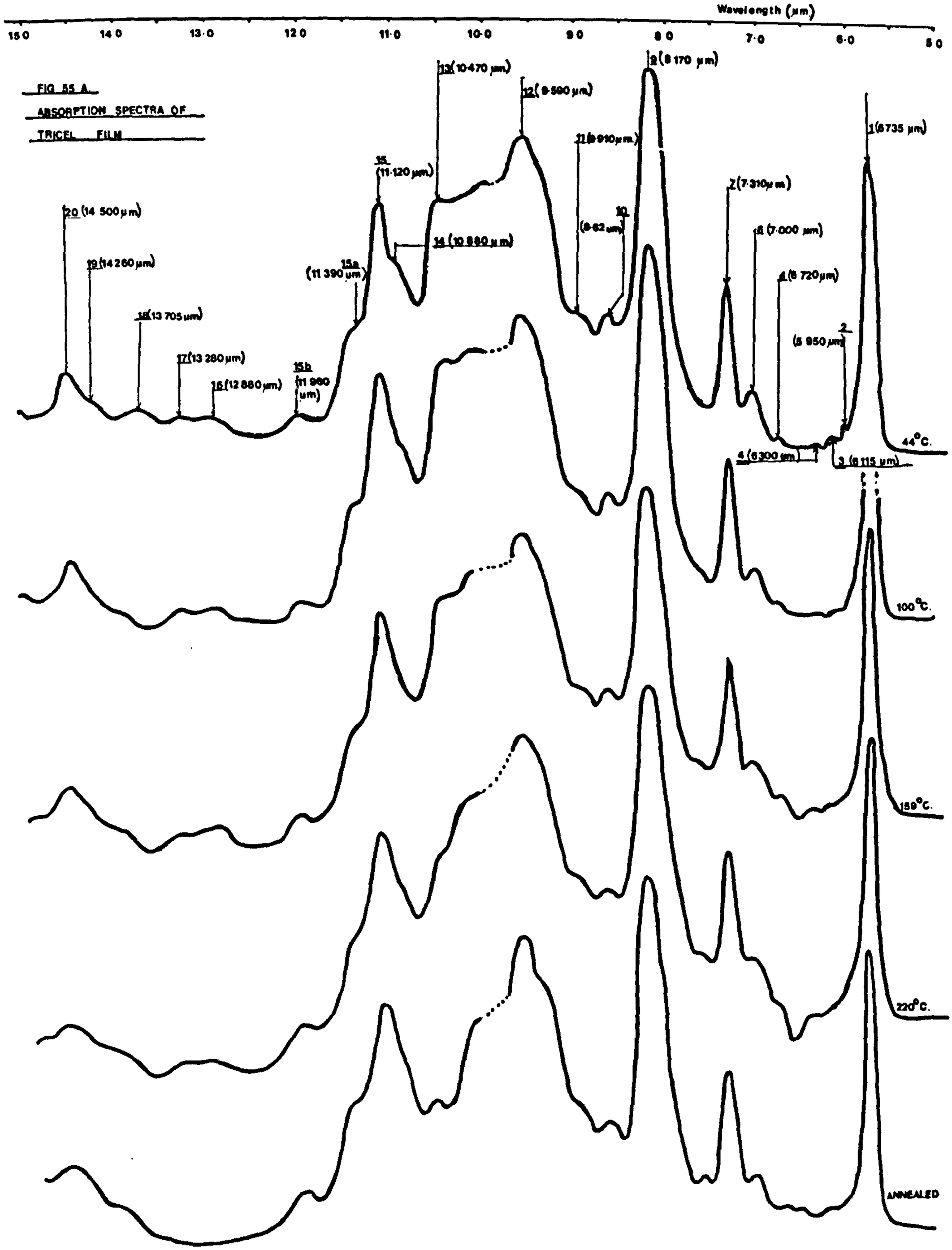

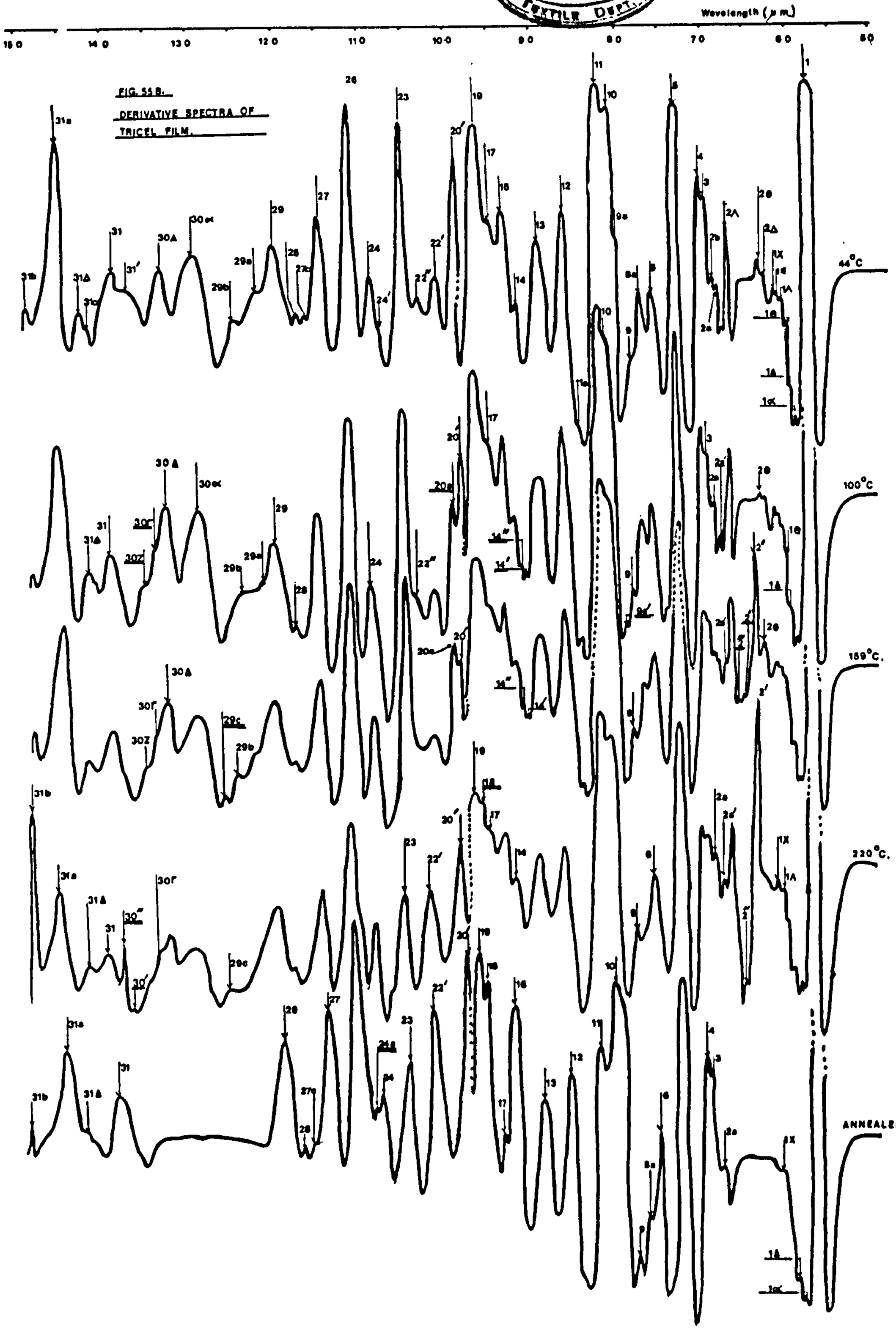

FIG. 55 B.

DERIVATIVE SPECTRA OF TRICEL FILM.

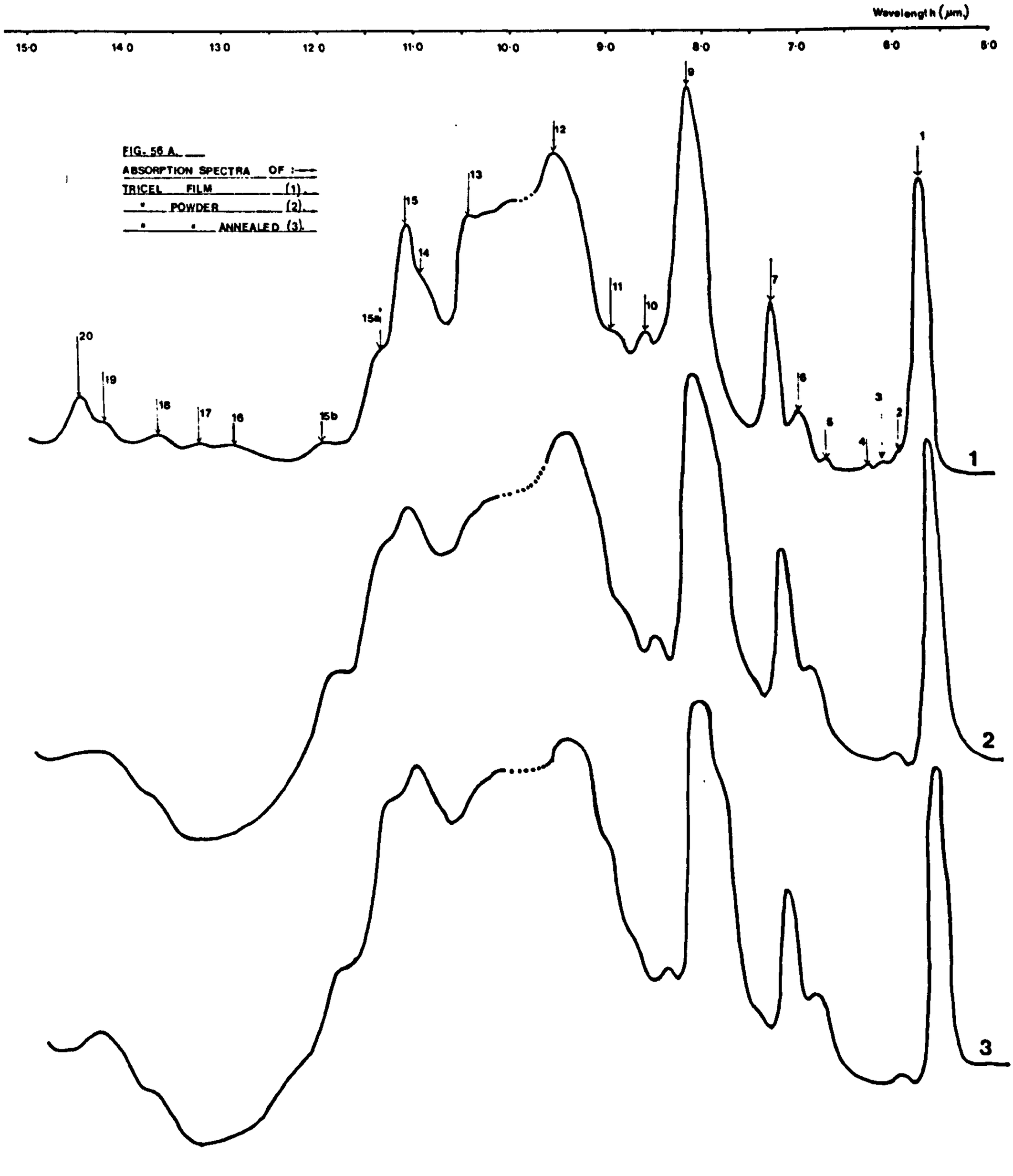
Wavelength (μm.)
15·0
14·0
13·0
12·0
11·0
10·0
9·0
8·0
7·0
6·0
5·0
FIG. 56 A.
ABSORPTION SPECTRA OF :—
TRICEL FILM (1).
" POWDER (2).
" " ANNEALED (3).
20
19
18
17
16
15b
15a
15
14
13
12
11
10
9
8
7
6
5
4
3
2
1
1
2
3

FIG 56 B

DERIVATIVE SPECTRA OF :—

TRICEL FILM (1)

" POWDER (2)

" " ANNEALED (3)

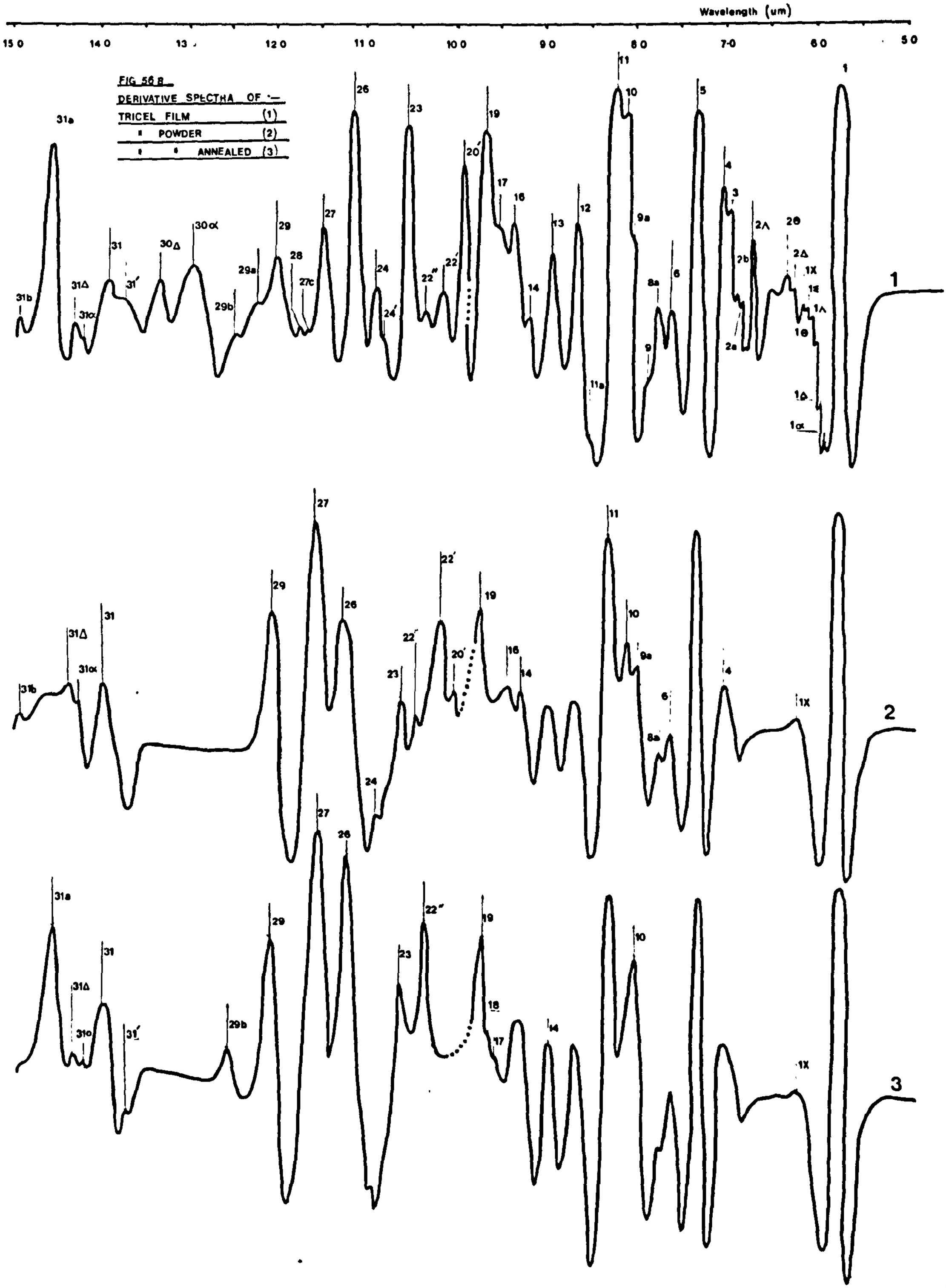

FIG 87

DERIVATIVE SPECTRA OF

VISCOSE FILM (1),

DICEL . (2),

TRICEL . (3),

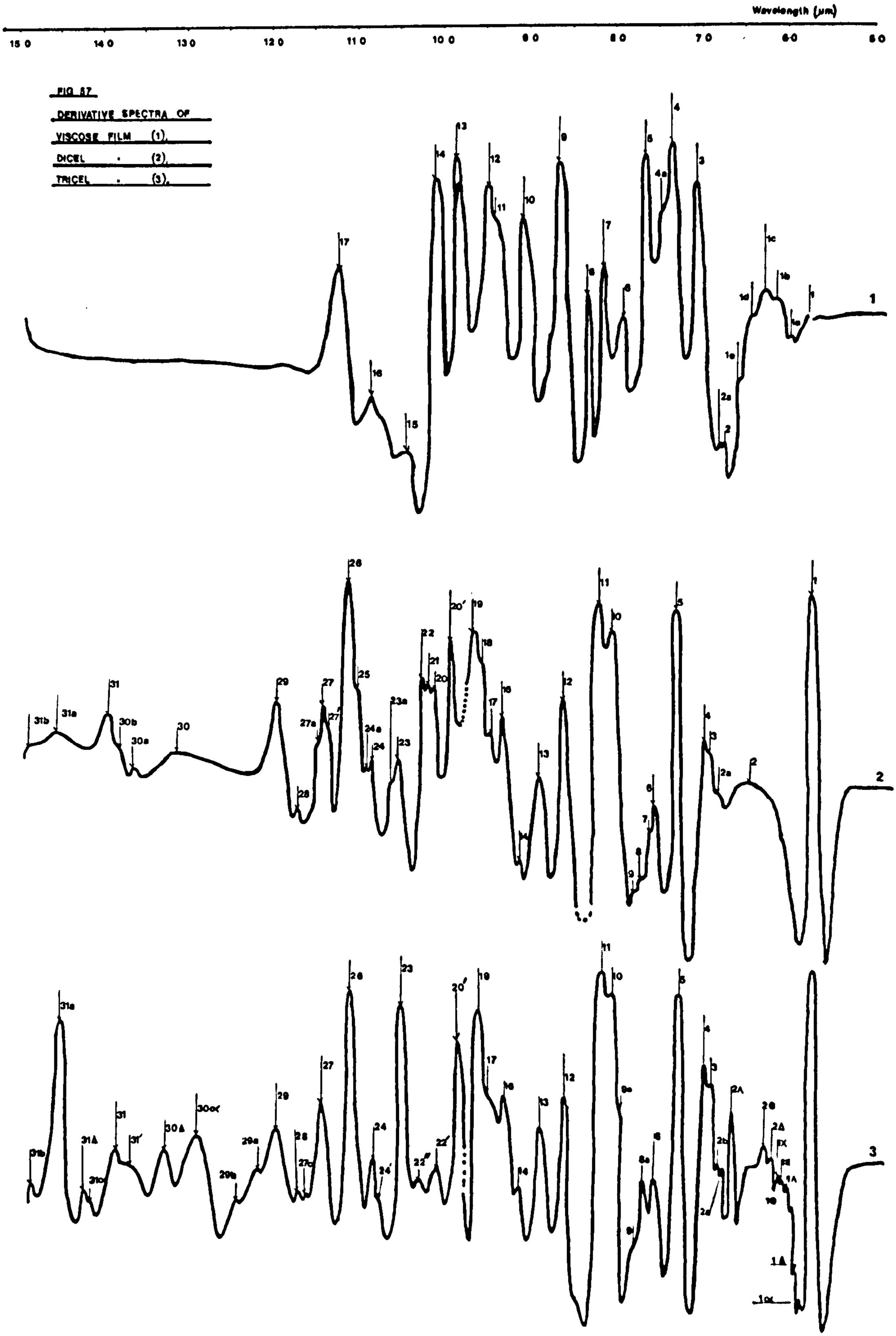

TABLE XXI (Dicel)

Peak	Wavelength (μm)	Wavenumber ($cm.^{-1}$)	New Peak at (in)	Corresponding Peak In Viscose (μm)	Corresponding Peak In Tricel (μm)	Interpretation	Code
1	5.730	1745	-	-	1 (5.735)	C=O Stretching Vibration (3)	III 6vi Cc
2	6.485	1542	-	1c (6.310)	2e(6.315)	Cf. Viscose. Water with an 'Ice Type' Structure	w
2′	6.660	1502	100°C.	-	2′ (6.410)	Water Species	w
2a	6.855	1459	-	2 (6.805); 2a (6.835)	2a(6.865)	Cf. Viscose, Water, and OH in plane bending Vibration	w and Il i Ab
3	6.985	1432	-	-	3 (6.980)	CH_2 bending Vibration of Acetyl Group	III Mh Cb
4	7.015	1426	-	3 (7.080)	4 (7.025)	Cf. Viscose, CH_2 Bending Vibration	I 2 ii Ab
4′	7.065	I4I5	159°C.			OH bending vibration	III Mh Ma
5	7.310	1368	-	-	5 (7.325)	Tentatively assigned to a CH_2 vibration of Acetyl Groups	III 6vi Cc
6	7.630	1311	-	4 (7.365)	6 (7.600)	Cf. Viscose, OH In Plane Bending Vibration	I 1 vi Ac
7	7.680	1302	-	4a (7.440)	-	" "	III 6vi Cc
8	7.770	1287	-	-	-	OH In Plane Bending Vibration	III 6vi Cc
9	7.8500	1274	-	5 (7.6650)	9 (7.8300)	Cf. Viscose, OH Bending Vibration	II, Mh,Ma
10	8.0700	1239	-	6 (7.9550)	10(8.100)	Cf. Viscose, Stretching Vibration of Cellulosic C-O-C but also Acetyl C-O-C groups.	I 2i Ac

TABLE XXI (Continued)

Peak	Wavelength (μm)	Wavenumber ($cm.^{-1}$)	New Peak at (in)	Corresponding Peak in Viscose (μm)	Corresponding Peak in Tricel (μm)	Interpretation	Code
11	8.2500	1212	-	7 (8.1750)	11 (8.250)	Cf. Viscose, Stretching Vibration of Cellulosic C-O-C but also Acetyl C-O-C groups	III 6vi Cc
12	8.6400	1157	-	9 (8.665)	12 (8.640)	Cf. Viscose, Stretching of Bridge Oxygen bonds in Glucose Residues	II 2vi Cc
13	8.9350	1119	-	10(9.040)	13 (8.020)	Cf. Viscose, Ring Stretching	III 2vi Cc
14	9.1790	1090	-	-	14 (9.2050)		II 3i Ba
15′	9.290	1076	220°C.	-	-		III Mh Ma
16	9.3450	1070	-	-	16 (9.3400)	C-O Stretching Vibrations of Acetyl Group	I 6i Ac
16′	9.3200	1073	Annealed Sample	-	-		I - -
17	9.5150	1051	-	-	17 (9.515)		I 4ii Ab
18	9.640	1037	-	11(9.335)	-	Cf. Viscose, C-O Stretching Vibration	I 3ii Ca
19	9.6900	1032	-	12(9.440)	19 (9.690)	Cf. Viscose, Stretching Vibration of Cellulosic C-O but also of Acetyl C-O groups	III 2vi Cc
19′	9.790	1021	220°C.	-	-	C-O Vibration	III - -
20′	9.950	1001		13(9.840)	20′ (9.895)	Cf. Viscose. Cellulosic C-O Stretching Vibration but also of Acetyl C-O groups	II Mh Ma

TABLE XXI (Continued)

Peak	Wavelength (μm)	Wavenumber ($cm.^{-1}$)	New Peak at (in)	Corresponding Peak in Viscose (μm.)	Corresponding Peak in Tricel (μm.)	Interpretation	Code
20''	10.025	998	159°C.	-	20a(9.925)	C-O Vibration Possibly of Acetyl Group	II 2vi Bc
20	10.145	986		14 (10.075)	22' (10.120)	Cf. Viscose, C-O Stretching Vibrations	II 2ii Bb
21	10.175	983					II 2ii Bc
22	10.270	974			22''(10.340)		II 2vi Bc
23	10.560	947				Cf. Viscose, Cellulosic C-O Stretching But Also of Acetyl C-O groups	II 2vi Bc
23a'	10.585	945	100°C.	15 (10.445)	23 (10.490)	" "	I 3i Ac
23a	10.655	939				" "	III 6vi Cc
24	10.900	917		16 (10.885)	24 (10.890)	Cf. Viscose, CO Stretching	III 3vi Ca
24a	10.945	914				" "	III Mh Cc
25	11.075	903		-	-	C-O Stretching Vibration of Acetyl Group	III 6vi Cc
26	11.165	896			26 (11.140)	CH_2 Bending in Acetyl Groups	II 2vi Ba
27'	11.395	878			27 (11.480)	Cf. Viscose C_1 Group Frequency	III Mh Cc
27	11.450	873		17 (11.225)		" "	II 2vi Ba
27a	11.490	870			27c(11.650)	Possibly C-C Vibration of Acetyl Group	II 2vi Ba
27b	11.635	859	220°C.	-	-	" "	

TABLE XXI (Continued)

Peak	Wavelength (μm.)	Wavenumber ($cm.^{-1}$)	New Peak at (in)	Corresponding Peak in Viscose (μm)	Corresponding Peak in Tricel (μm.)	Interpretation	Code
28	11.750	851	-	-	28(11.760)	Possibly C-C or CH Vibration of Acetyl Group	III 2i Cc
29	11.990	834	-	-	29(12.020)	Possibly CH Vibration of Acetyl Group	III 2i Cc
30	13.115	762	-	-	-		III 4i Cc
30a	13.695	730	-	-	-	Possibly CH_2 Vibrations (mainly rocking modes) of Acetyl Groups	II Mh Bc I - -
30a'	13.500	741	-	-	-		I - -
30b	13.790	725	-	-	-		III 4vi Cc
31	13.975	716	-	-	31(13.880)		III 2vi Cc
31a	14.610	684	-	-	31a(14.520)	Possibly Skeletal Vibration	III 2vi Cc
31b	14.925	670	-	-	31b(14.860)	Possibly Skeletal Vibration	III 2vi Cc

TABLE XXII (Tricel)

Peak	Wavelength (μm)	Wavenumber ($cm.^{-1}$)	New Peak at (in)	Corresponding Peak in Viscose (μm)	Corresponding Peak in Dicel (μm)	Interpretation	Code
1	5.7350	1744	-	-	1 (5.7450)	Cf. Dicel, C=O Stretching Vibration	I 6vi Cc
1α	5.9050	1693				Water with an 'Ice Type' Structure	w
1Δ	5.9900	1669		1a (5.985)		Cf. Viscose, Strongly Bound Water	w
1e	6.050	1653				Cf. Viscose, Fairly Strongly Bound Water	w
1Λ	6.0950	1641				Cf. Viscose, Strongly Bound Water Fairly	w
1$\leq$	6.1200	1634		1b (6.140)		" "	w
1x	6.1600	1623				Water with an 'Ice Type' Structure	w
2Δ	6.2850	1591				Less Strongly Bound Water	w
2e	6.3150	1584		1c (6.310)	2 (6.485)	Cf. Viscose and Dicel, Water with an 'Ice Type' Structure	w
2'	6.4100	1560	159°C.		2' (6.660)	Cf. Dicel, Water	w
2	6.5000	1538				Water	w
2''	6.5800	1520	159°C.			Water	w
2'''	6.6200	1511	159°C.			"	w
2Λ	6.7100	1490				Water with an 'Ice Type' Structure	w

TABLE XXII (Continued)

Peak	Wavelength (μm.)	Wavenumber ($cm.^{-1}$)	New Peak at (in)	Corresponding Peak in Viscose (μm.)	Corresponding Peak in Dicel (μm.)	Interpretation	Code
2a'	6.805	1470	100° C.			Possibly OH Bending Vibration	III 1 vi Ma
2a	6.8650	1457		2 (6.805) 2a(6.835)	2a (6.855)	Cf. Viscose and Dicel: OH In Plane Bending and Absorbed Water	I 4vi Ac and w
2b	6.9100	1447	-	-	-	OH In Plane Bending or water	II Mh Ma or w
3	6.9800	1433	-	-	3 (6.9800)	Cf. Dicel, CH_2 Bending Vibration of Acetyl Groups	III 3vi Co
4	7.025	1423	-	3 (7.080)	4 (7.015)	Cf. Viscose and Dicel, CH_2 Bending Vibration	III 2i Co
5	7.3250	1365		-	5 (7.310)	Cf. Dicel, CH_2 Vibration of Acetyl Groups	III 6vi Cb
6	7.6000	1316		4 (7.365)	6 (7.630)	Cf. Viscose and Dicel, OH In Plane Bending Vibration	I 6vi Ab
8a	7.7400	1292		-	-	CH or CH_2 Deformation Mode of Acetyl Groups	II Mh Bc
9	7.8300	1277		5 (7.665)	9 (7.850)	Cf. Viscose and Dicel, OH Bending Vibration	I 1 iii Ab
9a'	7.9400	1259		-	-	CH or CH_2 Vibration	III Mh Ma
9a	8.020	1247	-	-	-	CH or possibly CH_2 vibration of Acetyl Groups	II Mh Ma
10	8.1000	1235		6 (7.955)	10(8.070)	Cf. Viscose, Stretching Vibration of Cellulosic C-O-C but also Cf. Dicel, Stretching Vibration of Acetyl C-O-C	I 4i Ab

TABLE XXII (Continued)

Peak	Wavelength (μm.)	Wavenumber ($cm.^{-1}$)	New Peak at (in)	Corresponding Peak in Viscose (μm.)	Corresponding Peak in Dicel (μm.)	Interpretation	Code
11	8.2500	1212		7 (8.175)	11 (8.250)	Cf. Viscose, Stretching Vibration of Cellulosic C-O-C but also Cf. Dicel, Stretching Vibration of Acetyl C-O-C	II 4vi Bb
12	8.6400	1157		9 (8.665)	12 (8.6400)	Cf. Viscose and Dicel, Stretching of Bridge Oxygen bonds in Glucose Residues.	III 2vi Cc
13	8.9200	1121		10(9.040)	13 (8.935)	Cf. Viscose and Dicel, Ring Stretching	I 2vi Aa
14′	9.1000	1099	100°C.	-	-	Possibly C-O Vibration of Acetyl Group	II Mh Ma
14″	9.1450	1093	100°C.	-	-	" "	II Mh Ma
14	9.2050	1086	-	-	14 (9.175)		II 2vi Ma
16	9.3400	1071	-	-	16 (9.345)	Cf. Dicel, C-O Stretching Vibration of Acetyl Group	I 2vi Ab
17	9.5150	1051	-	-	17 (9.515)		I 2vi Ab
18	9.6400	1037	159°C.	-	-	C-O Stretching of Acetyl Group	I -- Ac
19	9.6900	1032		12(9.440)	19 (9.690)	Cf. Viscose, Stretching Vibration of Cellulosic C-O but also Cf.Dicel, Stretching Vibration of Acetyl C-O	I 2i Ac
20′	9.8950	1011		13(9.840)	20 (9.950)	" "	I 2ii Ac
22′	10.1200	988		14 (10.075)	20, and 21	Cf.Viscose and Dicel,Cellulosic	I 4i Aa
22″	10.3400	967			22 (10.270)	C-O Stretching Vibrations	II Mh Ma

TABLE XXII (Continued)

Peak	Wavelength (μm)	Wavenumber (cm^{-1})	New Peak at (in)	Corresponding Peak in Viscose (μm.)	Corresponding Peak in Dicel (μm.)	Interpretation	Code
23	10.4900	953		15 (10.445)	23, 23a and 23a'	Cf. Viscose, Cellulosic C-O Stretching but also Cf. Dicel, of Acetyl C-O Groups	II 6ii Bc
24'	10.7900	927				Possibly Acetyl C-O or Skeletal Vibration	II Mh Ma
24	10.8900	918		16 (10.885)	24 (10.900)	Cf. Viscose and Dicel, C-O Stretching Vibration	II 2vi Bb
24a	10.9100	917	Annealed	-	-	Possibly Acetyl CO Stretching Vibration	I - -
26	11.140	898			26 (11.165)	Cf. Dicel, CH_2 Bending of Acetyl Groups	III 3i Cc
27	11.480	871		17 (11.225)	27 (11.450)	Cf. Viscose and Dicel, C_1 Group Frequency	I 3i Ac
27c	11.650	858			27a(11.490)	Cf. Dicel, Possibly C-C Vibration of Acetyl Group	III Mh Cc
28	11.760	850			28 (11.750)	Cf. Dicel, Possibly C-C or CH Vibration of Acetyl Groups	III 6vi Cc
29	12.020	832			29 (11.990)	Cf. Dicel, Possibly CH Vibration of Acetyl Groups	III Mh Ma
29a	12.215	819			-	Possibly CH_2 Rocking Vibration of Acetyl Groups	III Mh Ma
29b	12.470	802			-	" "	II 2vi Bc

TABLE XXII (Continued)

Peak	Wavelength (μm.)	Wavenumber ($cm.^{-1}$)	New Peak at (in)	Corresponding Peak in Viscose (μm.)	Corresponding Peak in Dicel (μm.)	Interpretation	Code
29c	I2. 730	786	T_3	-		Possibly CH_2 Rocking Mode of Acetyl Group	II 2vi Ma
30α	12.885	776		-	30a' (13.540)	Cf. Dicel, CH_2 Rocking Mode of Acetyl Group	II 3i Ma
30Δ	13.310	751		-	30b (13.790)	" "	II 3ii Ma
30Γ	13.470	742	T_2	-			II Cc Ma
30z	13.585	736	T_2	-		Possibly CH_2 Rocking Modes of Acetyl Groups	II Cc Ma
30'	13.720	729	T_4	-			II-- Ma
30''	13.820	724	T_4	-			II -- Ma
31'	13.735	728		-		Possibly CH_2 Rocking of Acetyl Groups	II Mh Ma
31	13.880	720		-	31 (13.975)	Cf. Dicel, CH_2 Rocking Mode of Acetyl Groups	III 2i Cc
31α	14.190	705		-		Possibly CH_2 Rocking of Acetyl Groups	II Mh Ma
31Δ	14.260	701		-			II 3vi Ma
31a	14.520	689		-	31a (14.610)	Cf.Dicel,Possibly Skeletal Vibration	II 2vi Bc
31b	14.865	673		-	31b (14.925)	" "	II 1i Bb

confirms that annealing causes an increase in the amount of crystalline Cellulose I within the viscose (Cellulose II) film.

3B.2.1 Results For Dicel and Tricel

The absorption and second derivative spectra of dicel film are shown in Figs. 53A and 53B respectively, and of dicel powder in Figs. 54A and 54B respectively. The absorption and second derivative spectra of tricel film are shown in Figs. 55A and 55B respectively, and of tricel powder in Figs. 56A and 56B respectively. The derivative spectra of viscose, dicel and tricel films recorded at 44°C.are compared in Fig.57. The absorption spectra are included for comparison, but designations (following the scheme shown in List I) and assignments were again based upon derivative spectra, as for viscose. The designations and assignments are shown for dicel in Table XXI and for tricel in Table XXII. Powder spectra were again used mainly to confirm previous assignments.

3B.2.2 Discussion of Results for Dicel and Tricel

(a) Water Peaks (Due to OH Bending in Water)

In the derivative spectrum of dicel, recorded at 44°C., there is only a single broad unresolved peak which we could assign entirely to OH bending modes of absorbed water, namely peak 2 (6.485 μm., 1542 cm^{-1}). Peak 2a (6.885 μm., 1459 cm^{-1}) in the spectrum of dicel and its counterpart in the spectrum of tricel, namely peak 2a (6.865 μm., 1457 cm^{-1}) correspond to peaks 2 (6.805 μm., 1470 cm^{-1}) or 2a (6.835 μm., 1463 cm^{-1}) in the spectrum of viscose film. Peak 2a in the spectra of dicel and tricel was thus similarly assigned to an OH bending mode of cellulosic OH groups in addition to the OH bending mode of absorbed water.

The fact that there are only two peaks in the spectrum of dicel which are assignable to absorbed water, whereas there are many peaks in the spectra

of viscose (1, 1a, 1b, 1c, 1d, 1e, 2 and 2a) and tricel (1α, 1Δ, 1Λ, 1Ξ, 1x, 2Δ, 2e, 2, 2', 2Λ, 2a and 2b), also confirms that in terms of energy difference and stability, there is a smaller difference between 'crystalline' and 'crystallizable' regions in dicel than in viscose or tricel. The occurrence of a large number of water peaks in viscose and tricel may be explained on the basis of well defined regions of crystalline structure which give rise to specific structural environments surrounding bound water molecules; each specific environment giving rise to one or more water peaks, which may be resolved.

In dicel, however, which is basically non crystalline, a range of environments are present for absorbed water molecules, thus accounting for the broad band of water absorption peaks in which only two peaks are resolved.

Since there are a greater number of water peaks in tricel than in viscose in this region, it is indicated that there are a larger number of discrete 'crystalline' states in tricel than in viscose and this is in accord with the results and explanation for 'mixed response' peaks in tricel from Section A (page 80).

Peaks 2Δ and 2Λ in the derivative spectrum of tricel do not have any corresponding peaks in the spectra of viscose or dicel. However, peak 2Δ has been assigned to water, since there is a corresponding peak in the derivative spectrum of water (Figs. 72 and 73). Peak 2Λ has been similarly assigned to the presence of water with an 'ice type' structure, since there is a corresponding peak in both the derivative spectra of water and ice (Figs. 72 and 73). However, all the peaks (1α , 1x , 2e and 2Λ) which correspond to groups of water molecules with an 'ice type' structure in tricel either decrease in intensity or disappear in heated and annealed sample spectra and confirm that the binding of such groups of water molecules to remaining cellulosic OH (or other cellulosic groups, e.g. C-O

groups) is very weak. This is in accord with the results for 'ice type' water peaks in tricel in the 2.5 - 5 μm. (4000 - 2000 $cm.^{-1}$) region (peaks 2a, 3b, 3c and 3d from Fig. 48B).

Peak 2′ in the derivative spectrum of dicel film (6.600 μm. 1502 $cm.^{-1}$) and the corresponding peak 2′ in the spectrum of tricel film (6.410 μm. 1560 $cm.^{-1}$), which appear at 100°C. in the spectrum of dicel and 159°C. in the spectrum of tricel, increase considerably in intensity at 220°C. Since these peaks are not present in the annealed sample spectra, it is thus possible that they represent a water species which only exists at high temperatures, but which possesses stronger hydrogen bonding in tricel, since the peak in tricel occurs at a lower wavelength.

The much higher intensity of this peak in the spectrum of tricel may be accounted for if this peak corresponds to water present in 'crystalline' regions, since tricel has been shown to be a much more crystalline polymer than dicel.

A more probable explanation for the behaviour of peak 2′ in the spectra of dicel and tricel is that this peak does not represent bound water, but represents OH groups of degradation products formed during the heating of samples within sample cells. It has already been shown that tricel film is more susceptible to degradation by heating in the atmosphere than dicel and the large increase in peak 2′ in tricel at 220°C., compared to dicel, could thus be accounted for by the larger quantity of degradation products which are produced in tricel. The fact that peak 2′ is not apparent in the derivative spectra of annealed dicel and tricel film samples may be accounted for by the fact that the annealing process was carried out under an inert nitrogen atmosphere, which greatly reduces the total amount of degradation occurring by eliminating oxidative degradation.

(b) Hydroxyl Peaks

The main peaks which arise from OH bending modes in the derivative spectrum of viscose recorded at 44°C.(Fig.51B) have some corresponding peaks in the spectra of dicel and some which do not correspond, as is seen from the following list:-

Peak in Viscose	Corresponding Peak in Dicel	Corresponding Peak in Tricel
2 (6.805 μm, 1470 $cm.^{-1}$)	2a (6.855 μm, 1459 $cm.^{-1}$)	2a(6.865 μm, 1457$cm.^{-1}$)
2a(6.835 μm, 1463 $cm.^{-1}$)		
- -	- -	2b(6.910 μm, 1477$cm.^{-1}$)
2b(6.895 μm, 1450 $cm.^{-1}$)	- -	- -
4 (7.365 μm, 1358 $cm.^{-1}$)	6 (7.630 μm, 1311 $cm.^{-1}$)	6(7.600 μm, 1316$cm.^{-1}$)
4a(7.440 μm, 1344 $cm.^{-1}$)	7 (7.680 μm, 1302 $cm.^{-1}$)	- -
- -	8 (7.770 μm, 1287 $cm.^{-1}$)	- -
5 (7.665 μm, 1305 $cm.^{-1}$)	9 (7.850 μm, 1274 $cm.^{-1}$)	9(7.830 μm, 1277$cm.^{-1}$)
8 (8.365 μm, 1195 $cm.^{-1}$)	- -	- -

The most notable feature of peaks which correspond to OH bending modes in the spectra of dicel and tricel is that they occur at higher wavelengths than any similar peaks in the spectra of viscose. Since weak hydrogen bonding has been shown to produce bending mode peaks at low frequencies (high wavelengths) (201, 202), the results for such peaks in dicel and tricel clearly show that the hydrogen bonding of OH groups is weaker in dicel and tricel than in viscose. This is in accord with the results for OH stretching modes in viscose, dicel and tricel, reported in Section A.

The occurrence of the OH bending mode which corresponds to peak 2a in tricel at a lower frequency (higher wavelength) than the equivalent peak 2a in dicel also confirms the interpretation of the results from Section A (of OH stretching modes), which suggest the occurrence of weaker hydrogen

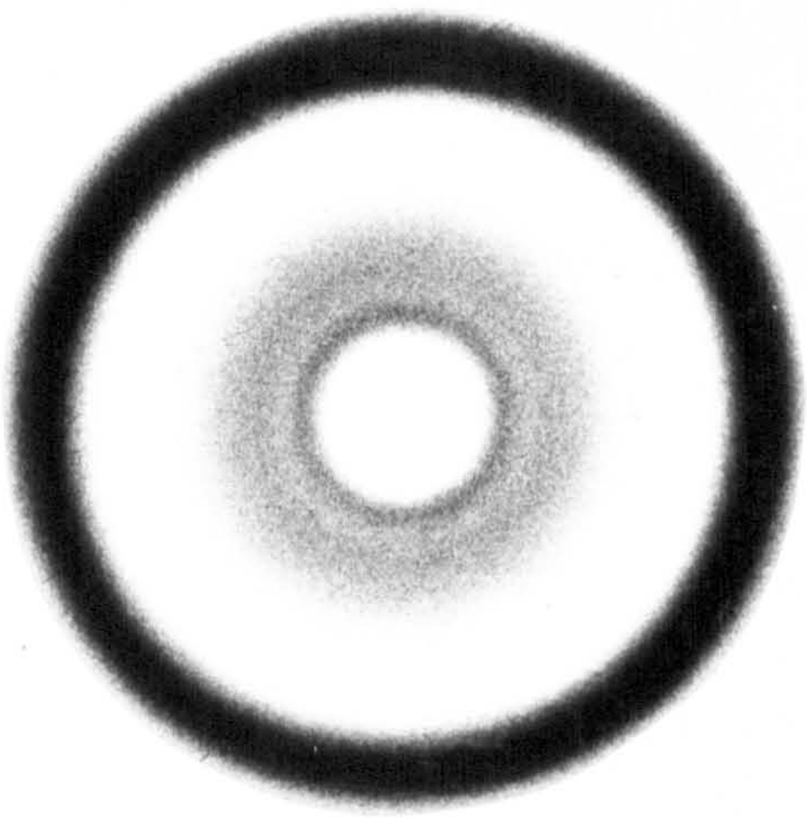

Viscose

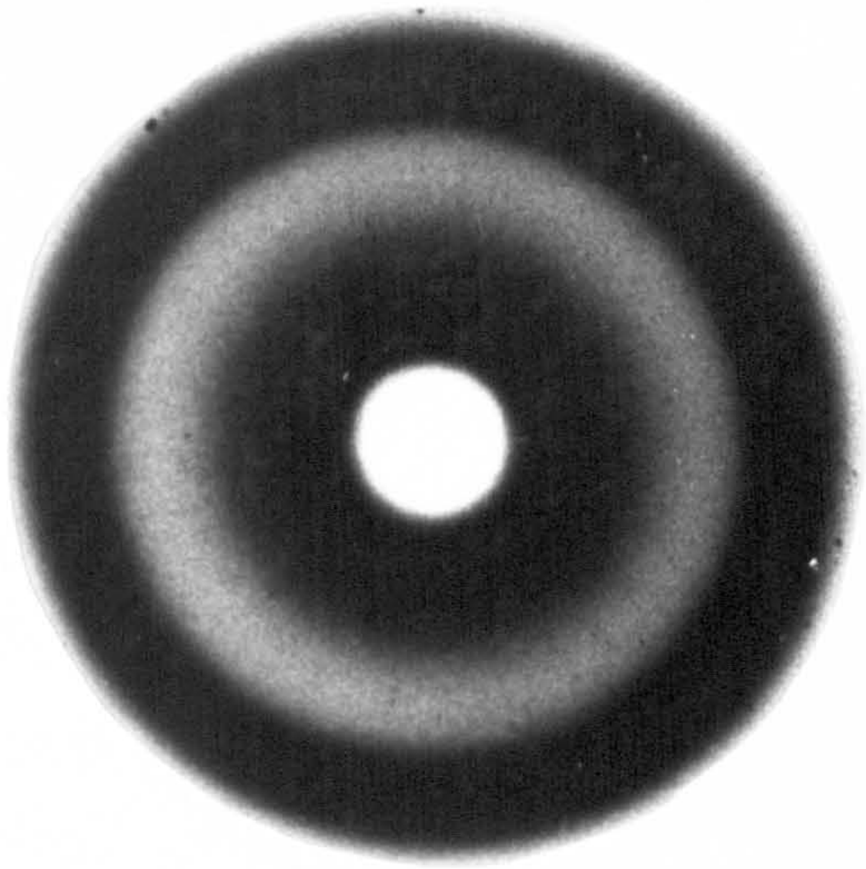

Viscose Annealed

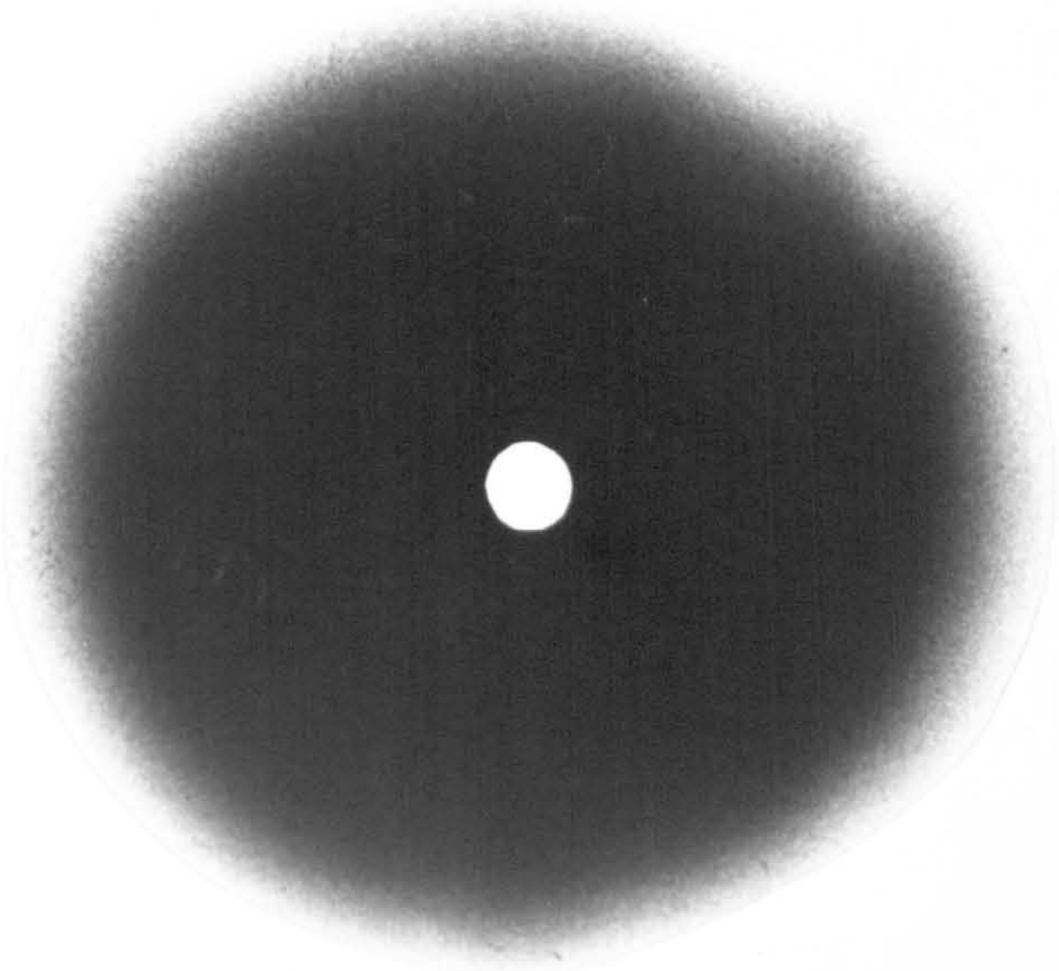

Dicel

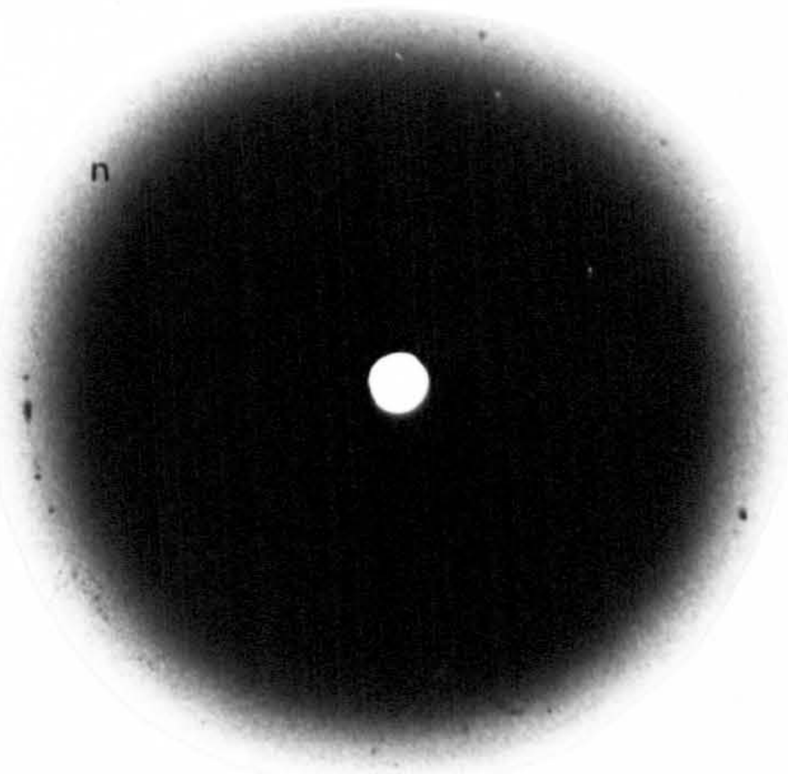

Dicel Annealed

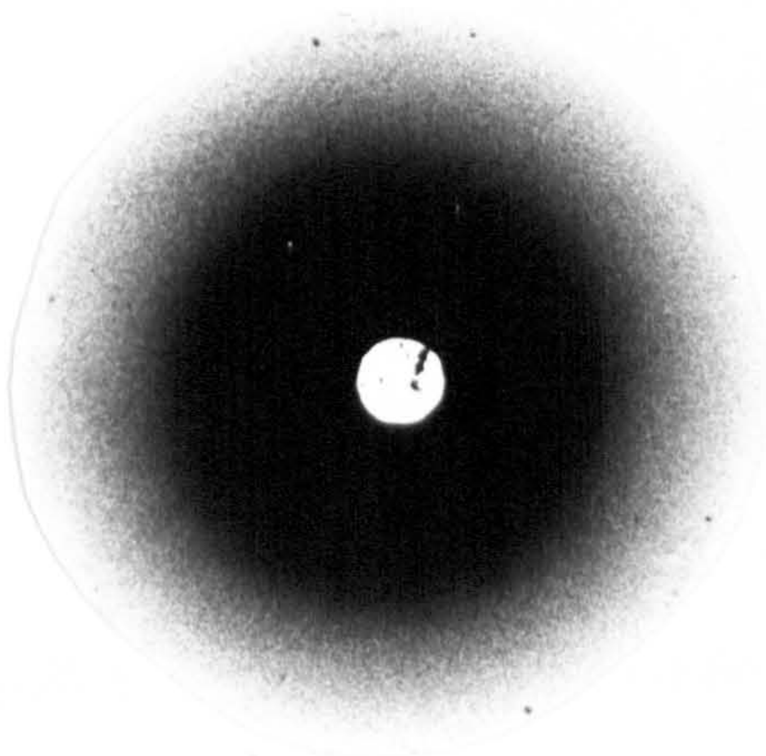

Tricel

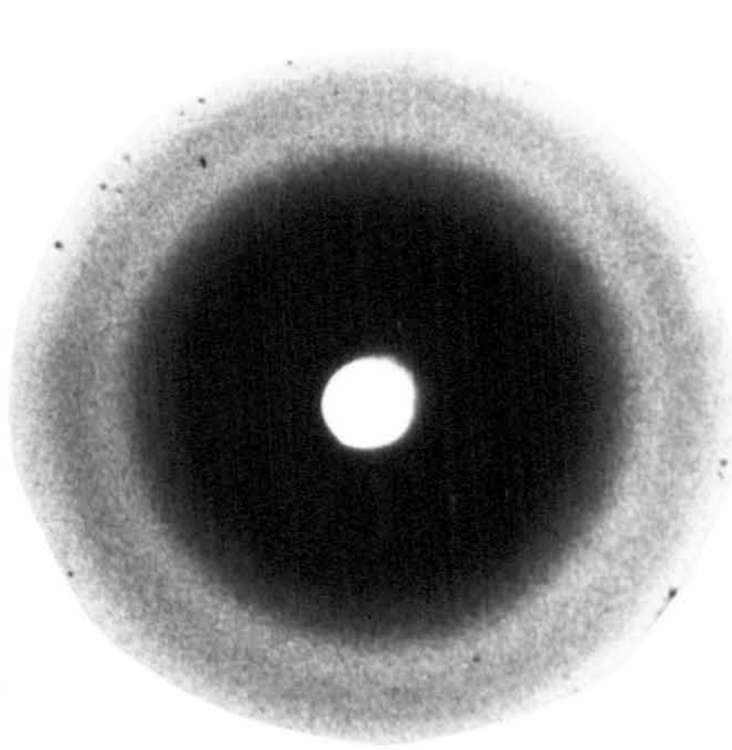

Tricel Annealed

FIG.58

bonding in tricel than in dicel. However, an anomaly occurs in that peaks 6 and 9 in dicel, also assigned to OH bending modes, occur at lower wavelengths than the corresponding peaks in tricel (peaks 6 and 9), which suggests stronger hydrogen bonding in dicel than in tricel.

The fact that some OH bending mode peaks show a 'crystalline' behaviour (peaks 2a and 6 in dicel and tricel, peak 9 in tricel) and other peaks show a 'crystallizable' behaviour (peak 9 in dicel) also shows that annealing causes an increase in the total amount of crystalline material present in dicel and tricel. The fact that such 'crystalline' and 'crystallizable' peaks occur at all in dicel shows that there is some differentiation of material in 'crystalline' and 'crystallizable' regions. However, this differentiation is not as marked as in viscose and tricel, as is seen from previous results.

Fig. 58 shows the X-ray diffraction photographs of viscose, dicel and tricel films before and after annealing. These show the presence of rings due to unoriented crystallites in both viscose and tricel, but dicel gives a broad diffuse pattern, typical of disordered material. The increase in the intensity and number of these rings in viscose and tricel in annealed sample photographs also confirms that annealing causes an increase in the total proportion of crystalline material present within the viscose and tricel films.

(c) CH and CH_2 Bending and Stretching Peaks

Peak 3 in viscose (7.080 μm., 1412 $cm.^{-1}$) corresponds to peak 4 in dicel (7.015 μm., 1426 $cm.^{-1}$) and peak 4 in tricel (7.025 μm., 1422 $cm.^{-1}$) and has been assigned to a CH_2 bending vibration. This must be due to CH_2 groups at the C_6 position of glucose residues, since the C_6 position is the only position in Cellulose II where CH_2 groups occur.

The different wavelengths at which this peak occurs in viscose, dicel and tricel must be due to different interactions involving C_6 methylene (CH_2) groups, in viscose, dicel and tricel. Such interactions are possibly hydrogen bonds, so that if hydrogen bonding of CH_2 groups is involved, the fact that the CH_2 bending mode peak occurs at the lowest wavelength in dicel indicates the presence of the strongest CH_2 hydrogen bonding in dicel. This may be accounted for by suggesting that C_6 methylene groups in dicel and tricel form strong intermolecular hydrogen bonds with acetyl C=O groups, whereas CH_2 groups in viscose form weaker hydrogen bonds with C-O groups of glucose residues which constitute the viscose molecules. The increase in the intensity of the peak in tricel compared to dicel can be attributed to the increased number of acetyl groups in tricel available for hydrogen bond formation with C_6,CH_2 groups.

Since peak 4 in tricel occurs at a higher wavelength than in dicel, the hydrogen bonding in tricel must be weaker than in dicel. This may also be due to the fact that the more crystalline structure of tricel prevents acetyl C=O groups and C_6 CH_2 groups in neighbouring chains from approaching each other as closely as in the irregularly structured dicel. Thus in tricel, the formation of very strong hydrogen bonds between C_6 CH_2 groups and acetyl groups is prevented.

Peak 3 in dicel (6.985 μm, 1432 $cm.^{-1}$) and peak 3 in tricel (6.9800 μm, 1433 $cm.^{-1}$) have also been assigned to a CH_2 bending mode of acetyl groups, since there is no equivalent absorption in viscose and this peak is of highest intensity in tricel, in which a greater number of acetyl groups are present.

(d) <u>C-O Peaks</u>

The main C-O stretching frequencies of viscose assigned to peaks 6 (7.995 μm., 1257 $cm.^{-1}$), 7(8.175 μm., 1223 $cm.^{-1}$) and 9(8.665 μm, 1154 $cm.^{-1}$) have corresponding peaks in dicel, which have been assigned to the same

origins: namely peaks 10 (8.070 um, 1239 $cm.^{-1}$), 11 (8.250 um, 1212 $cm.^{-1}$) and 12 (8.6400 um, 1157 $cm.^{-1}$) respectively and in tricel, peaks 10 (8.1000 um, 1235 $cm.^{-1}$), 11 (8.2500 um, 1212 $cm.^{-1}$) and 12 (8.6400 um, 1157 $cm.^{-1}$) respectively.

Since peaks 10 and 11 in dicel and tricel occur with higher intensities, it is probable that these peaks also arise from C-O stretching vibrations of acetyl groups in addition to other C-O groups present.

Another set of C-O stretching bands in the spectra of viscose (peaks 11 - 16) have corresponding peaks in dicel (peaks 18, 19, 20′, 20 - 24a) and in tricel (various peaks between 20′ and 24). The peaks in dicel all occur at higher wavelengths than the corresponding peaks in viscose and most of the peaks occur at a higher wavelength in dicel than the corresponding peaks in tricel. It is possible that this may be due to the formation of stronger hydrogen bonds at the carbonyl groups in dicel than in viscose or tricel. The stronger hydrogen bonding in dicel may be accounted for in the previous manner in which the non-crystalline structure of dicel allows neighbouring molecules to pack more closely and form strong hydrogen bonds. Since some of these peaks occur with greater intensity in dicel and tricel, they have similarly been assigned to vibrations of acetyl C-O groups in addition to main chain C-O groups.

Of the C-O peaks so far considered, a greater number of peaks in viscose and tricel show 'crystalline' or 'crystallizable' behaviour than peaks in dicel, and the magnitude of the effects noted (as seen from relative increases or decreases of peak intensity in annealed sample spectra) is in addition greater in viscose and tricel than in dicel. This also confirms that in terms of energy levels and stability, there is a much smaller difference in structure between 'crystalline' and 'crystallizable' regions in dicel than for viscose and tricel, confirming previous interpretations in this thesis.

A further group of peaks occurs in dicel (14, 15′ , 16, 16′ , 17, 18, 25 and 26) and in tricel (14, 14′ , 14″ , 16, 17, 18, 20a, 22″ , 24a and 26) which have been tentatively assigned to C-O vibrations on the basis of structural assignment charts (3-5) and from increased intensity measurements of tricel spectra. However, no significant trends in intensity or frequency differences between peaks in dicel and tricel have been found except that peaks 16 and 17 in tricel show a more definite 'crystalline' behaviour than the corresponding peaks in dicel.

(e) Other Peaks

(i) C=O Peaks

Peak 1 in dicel (5.730 μm, 1745 cm^{-1}) corresponds to peak 1 in tricel (5.735 μm, 1744 cm^{-1}) and has previously been assigned from structural assignment charts (3-5) to a C=O stretching vibration. This peak remains unchanged in frequency and intensity in both high temperature and annealed sample spectra, and can thus be classified as 'non crystallizable'. This result is anomalous, however, since it suggests that C=O groups are not involved in hydrogen bonding. It is also anomalous that no other peaks were detected which can also be assigned to the C=O group. It is possible, however, that the high intensity of peak 1 in both dicel and tricel may obscure such small peaks. However, no evidence for the existence of such peaks has been obtained from the derivative spectra recorded.

(ii) Ring Stretching Peaks

The antisymmetrical ring stretching frequency assigned in viscose to peak 10 corresponds to peak 13 in dicel (8.935 μm, 1119 $cm.^{-1}$) and peak 13 in tricel (8.9200 μm, 1121 $cm.^{-1}$). The decrease in wavelength of this peak from viscose → dicel → tricel indicates that acetylation of C_6 OH groups causes ring stretching vibrations to occur at higher frequencies (i.e. higher

energies) so that peak maxima of infra-red absorption bands occur at lower wavelengths.

This occurs because substituent acetyl groups are electron donors for the glucose ring with the net result that band characteristics are changed to induce a higher frequency of vibration.

(iii) Peaks from 11.5 - 15 μm. (870 - 667 $cm.^{-1}$)

The spectra of dicel and tricel contain many peaks not observed in the spectrum of viscose in the region from 11.5 - 15 μm. (870 - 667 $cm.^{-1}$). We have tentatively assigned these peaks to C-C, C-H or CH_2 stretching vibrations, and CH_2 rocking vibrations, mainly of acetyl groups since such peaks were not present in the spectra of viscose. However, peaks 31a and 31b in the spectra of dicel and tricel have been tentatively assigned to skeletal vibrations. In all cases, the assignments were based upon structural assignment charts.

Many more of these peaks in tricel show a 'crystalline' or 'crystallizable' behaviour than in dicel. This also confirms the often stated contentions of a greater difference between 'crystalline' and 'crystallizable' regions in tricel than in dicel in terms of energy difference and stability.

3.3 Conclusions (Sections A and B)

The main conclusions to be drawn from the work presented in this chapter can be best discussed in six different sections which will be considered in turn:-

(1) Derivative spectra are much better resolved than corresponding absorption spectra, especially in the 2.5 - 5 μm. (4000 - 2000 $cm.^{-1}$) region. Many new peaks not previously observed appear in the derivative spectra of viscose, dicel and tricel films and these have been assigned to absorbed water or to the vibrations of cellulosic groups and acetyl groups in dicel and tricel. Derivative spectra also enable changes in structure which occur

in heated and annealed sample spectra to be much more clearly observed than in the absorption spectra. Also, many changes not observed in absorption spectra are observed in the derivative spectra.

(2) Derivative spectra of samples of viscose, dicel and tricel powders, examined in the form of KBr discs, contain many peaks, which are due to absorbed water (which cannot be removed by drying samples over P_2O_5) and also to interactions between the KBr matrix and the sample.

(3) The derivative spectra of viscose, dicel and tricel films discussed in sections A and B of this chapter contain peaks assigned to absorbed water, which has not been removed by extensive drying. Peaks assigned to OH stretching modes of weakly bound water occur at low wavelengths and disappear in the spectra of heated film samples. Some peaks have been assigned to water with an 'ice type' structure since they have corresponding peaks in the derivative spectra of water and ice.

In viscose, the majority of the peaks assigned to water with an 'ice type' structure increase in intensity on heating and annealing. This effect may be explained on the basis of the transfer of water molecules from 'crystallizable' to 'crystalline' regions at high temperatures, followed by the aggregation of these water molecules into groups which possess an 'ice type' structure. Hearle's fringed fibril model of structure is very useful in this interpretation since it postulates the presence of weak points along the boundaries of crystalline regions at which water molecules may penetrate at high temperatures.

Alternatively, the increase in the intensity of peaks assigned to 'ice type' water may be accounted for if it is assumed that some of the water molecules which dissociate from cellulosic OH and other groups at high temperatures then aggregate in groups of molecules with an 'ice type' structure in both the 'crystalline' and 'crystallizable' regions. However, the retention of such groups of water molecules by 'crystallizable' regions

at high temperatures can only be explained if it is also assumed that there is some hydrogen bonding between such groups of water molecules and cellulosic OH (or possibly C-O) groups, and for this reason the first explanation is more acceptable.

In dicel, many of the peaks assigned to water with an 'ice type' structure and which correspond to peaks in viscose, show a similar behaviour. Thus the increase of intensity of such peaks in dicel in heated and annealed sample spectra may be similarly accounted for by assuming that aggregation of water molecules occurs at high temperatures in either 'crystalline' or in both 'crystalline' and 'crystallizable' regions to produce groups of water molecules with an 'ice type' structure.

In tricel, peaks which correspond to water with an 'ice type' structure are not present in the spectra of annealed samples and disappear in heated sample spectra. This indicates that the binding of such water by hydrogen bonding is weak and that little penetration of water to crystalline regions has occurred on heating.

In dicel, many peaks assigned to absorbed water (OH stretching modes) occur at higher wavelengths than the corresponding peaks in the derivative spectra of viscose and tricel. This effect may be accounted for, however, in terms of the structures of viscose, dicel and tricel. The lack of regular crystalline structure in dicel, due to the irregular (atactic) structure of chain molecules, indicates that there is a greater number of free (non hydrogen bonded) or weakly hydrogen bonded OH groups than in viscose or tricel, which form strong hydrogen bonds with absorbed water. Such strong hydrogen bonding tends to substantially increase the length of OH bonds of individual water molecules and hence produce weaker OH bonds which require less energy to cause them to stretch. In consequence, interactions between the electric vector of infra-red radiation and the dipole moment of the OH bonds of water occur at lower energies for OH stretching vibrations (i.e.

higher infra-red wavelengths). Peak maxima corresponding to such OH bonds of water thus occur at higher wavelengths.

In viscose and tricel, the more regular structure of chain molecules (greater tacticity) and larger proportion of material packed into a regular crystalline lattice results in fewer 'free' or weakly hydrogen bonded OH groups being available to form strong hydrogen bonds with the absorbed water. Any water molecules bonded to the cellulosic OH groups in viscose or tricel will thus be less strongly bound so that OH stretching bands detected from absorbed water in viscose and tricel will be detected at higher frequencies (lower wavelengths) than those in dicel.

(4) Evidence which shows that the differences in structure between 'crystalline' and 'crystallizable' regions in terms of energy levels and stability is greater in viscose and tricel than in dicel, and that annealing causes more significant structural changes to occur in viscose and tricel than in dicel, is summarised below:-

(i) In the 6 μm.(1667 $cm.^{-1}$) region there are only two peaks which correspond to absorbed water in the derivative spectrum of dicel, whereas in viscose and tricel there are many peaks.

(ii) A greater number of peaks in the spectra of viscose and tricel show a 'crystalline' or 'crystallizable' behaviour than peaks in the spectra of dicel. Where peaks in dicel do show a 'crystalline' or 'crystallizable' behaviour, any corresponding peaks in viscose or tricel often show the same behaviour but to a more marked degree, so that greater increases or decreases in intensity are observed from annealed sample spectra.

(iii) X-ray photographs of viscose, dicel and tricel film and annealed film samples clearly show the presence of rings due to unoriented crystalline material in viscose and tricel, but dicel exhibits a diffuse scatter, characteristic of disordered material. Furthermore, these rings increase in intensity in the photographs of annealed samples of viscose and tricel, indicating an increase in the proportion of crystalline material; but no

significant change was observed in the photograph of an annealed sample of dicel film.

(5) In viscose, the shift of some OH or C-O peaks (attributed to stretching vibrations) to higher wavelengths and other OH or C-O peaks to lower wavelengths in annealed sample spectra, indicates that annealing causes an increase in the degree of structural order (perfection) of at least one crystalline state, concurrently with a decrease in the degree of perfection of at least one other crystalline state, within the viscose film. The existence of at least two crystalline states in viscose film has been attributed to the existence of small amounts of Cellulose I within the viscose (Cellulose II) film. Two peaks have been assigned to Cellulose I in the derivative spectra of viscose film and confirmed from the spectra of KBr disc samples of viscose (Cellulose II) powder and cotton (Cellulose I) powder. Such findings are in accord with the results of Manjunath and Peacock (73) who have shown the existence of small amounts of Cellulose I in samples of viscose rayon (Cellulose II) from X-ray work.

(6) On hydrogen bonding, OH bending modes, as all other bending modes, exhibit : an increase in frequency, so that a band shift occurs to lower wavelengths (201, 202). The results for OH bending modes in viscose are consistent with this since a 'crystalline' peak (involving strongly hydrogen bonded OH groups), assigned to OH bending, occurs at a lower wavelength than a 'crystallizable' peak (involving more weakly hydrogen bonded OH groups) also assigned to an OH bending mode.

However, the OH bending modes, which correspond to peaks 2 and 2a (Fig. 51B), occur at the lowest wavelength, and in theory corresponding OH groups involve the strongest hydrogen bonding. However, Marchessault assigned his corresponding single absorption peak to intramolecularly hydrogen bonded C_2 or C_3 OH groups. This assignment is questioned, since the strongest (intermolecular) hydrogen bonds were shown by Marchessault and in

this work to be formed by C_6 OH groups. Peaks 2 and 2a (Fig. 51B) were thus assigned here to OH bending modes of C_6 OH groups.

The occurrence of OH bending modes in dicel and tricel at a higher wavelength than corresponding peaks in viscose also confirms the results from OH stretching modes of weaker hydrogen bonding involving OH groups being present in dicel and tricel.

CHAPTER 4

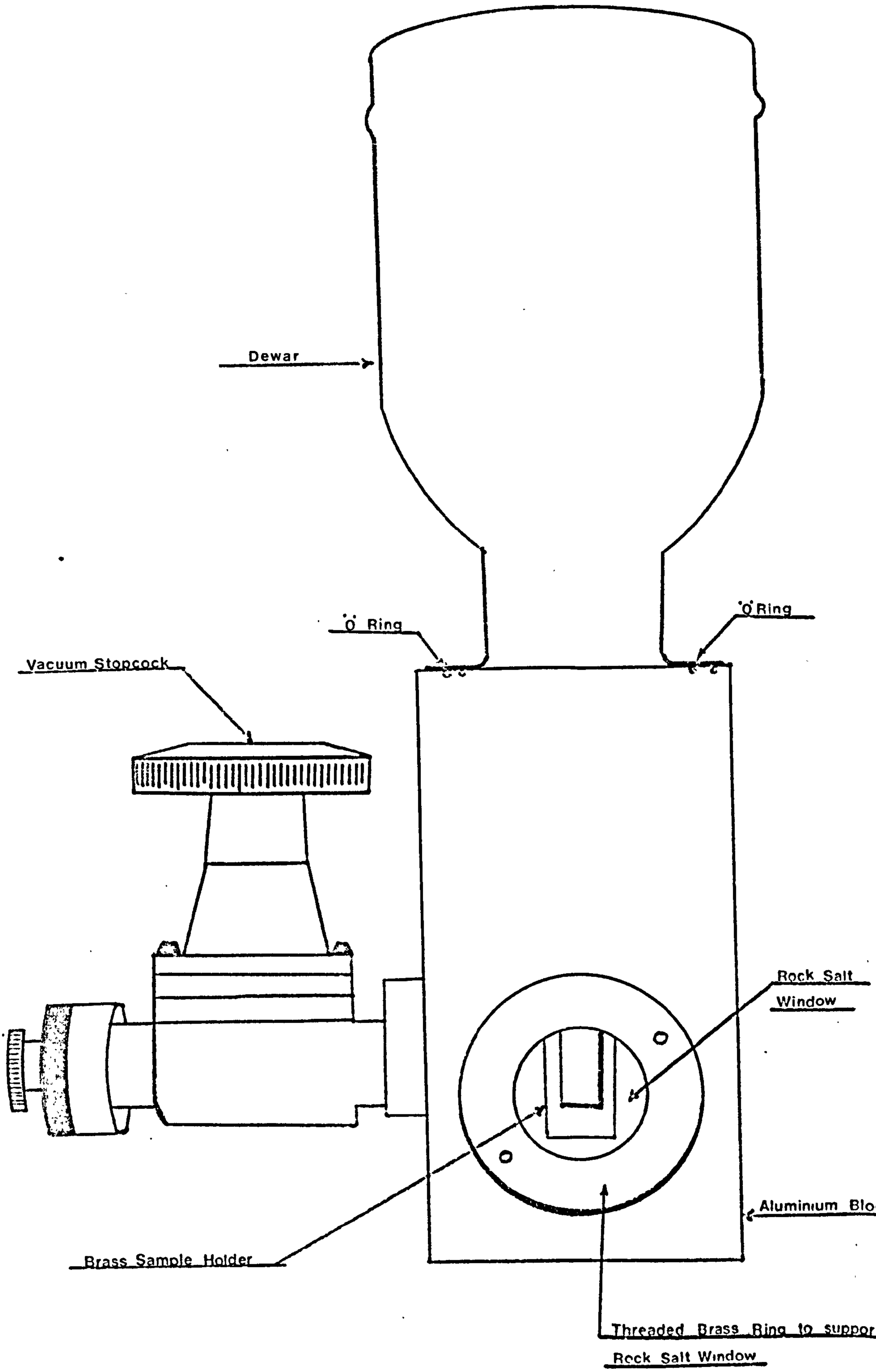
Dewar
O Ring
O Ring
Vacuum Stopcock
Rock Salt
Window
Brass Sample Holder
Aluminium Block
Threaded Brass Ring to support
Rock Salt Window

FIG. 59 A

CHAPTER 4

SPECTRA OF VISCOSE DICEL AND TRICEL AT LOW TEMPERATURES

4.1 Introduction

Absorption and derivative spectra of viscose, dicel and tricel films were obtained at 0°C. and -196°C. (boiling point of liquid nitrogen). A detailed analysis of the results obtained in this chapter was not undertaken, since spectra were only obtained at two low temperatures. It was not possible to obtain a large number of spectra at various low temperatures, due to the large amount of time required, although the techniques involved have been established. It is also possible that anomalies occur in the spectra due to the loss of strongly bound water from viscose and tricel at low temperatures and pressures, but not from dicel. The presence of such water, as ice at low temperatures, may induce peak changes in the spectra of dicel which are not apparent in the spectra of viscose or tricel and which cannot be easily distinguished from other peak changes which occur in the spectra of viscose and tricel at low temperatures. For these reasons, the results in this chapter are discussed in more general terms than the results in Chapter 3.

4.2 Method

Spectra of film samples were obtained by means of a low temperature cell (Fig. 59A) previously designed to obtain infra-red spectra of film samples at low temperatures (172). The cell system consists of a rectangular aluminium block with a cylindrical cavity cut into it, and connected to a vacuum stopcock. Two circular holes in opposite faces of the block enable infra-red radiation to pass through via supported NaCl windows and the sample holder, also suspended in the cavity. The windows are cushioned and vacuum sealed below the surface of the block by means of 'O' rings, and a threaded groove enables the windows to be screwed in tightly with a threaded brass ring to produce a vacuum tight seal.

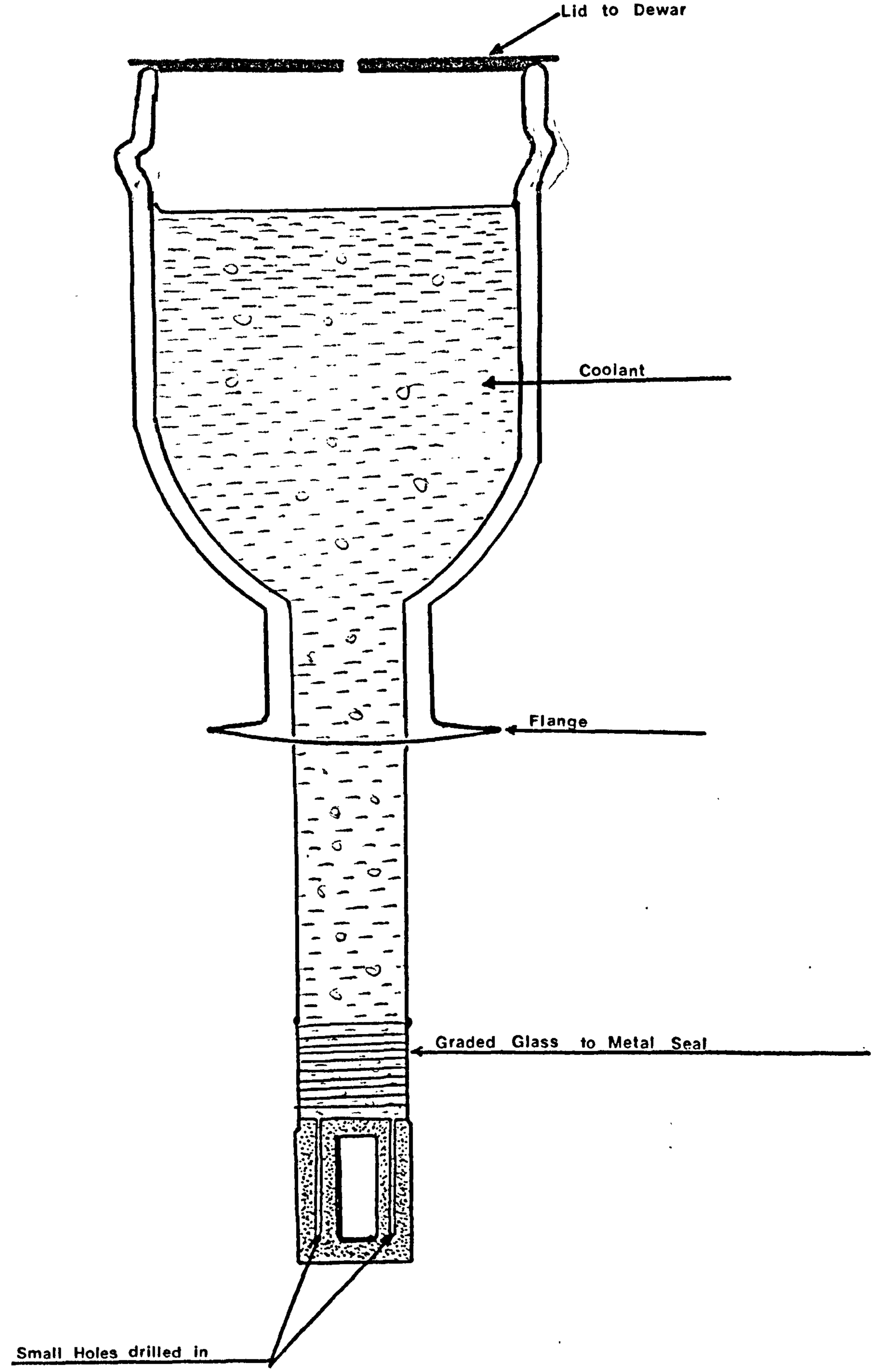
Lid to Dewar
Coolant
Flange
Graded Glass to Metal Seal
Small Holes drilled in
Sample Holder to enable Solvent to Penetrate

FIG 59 B

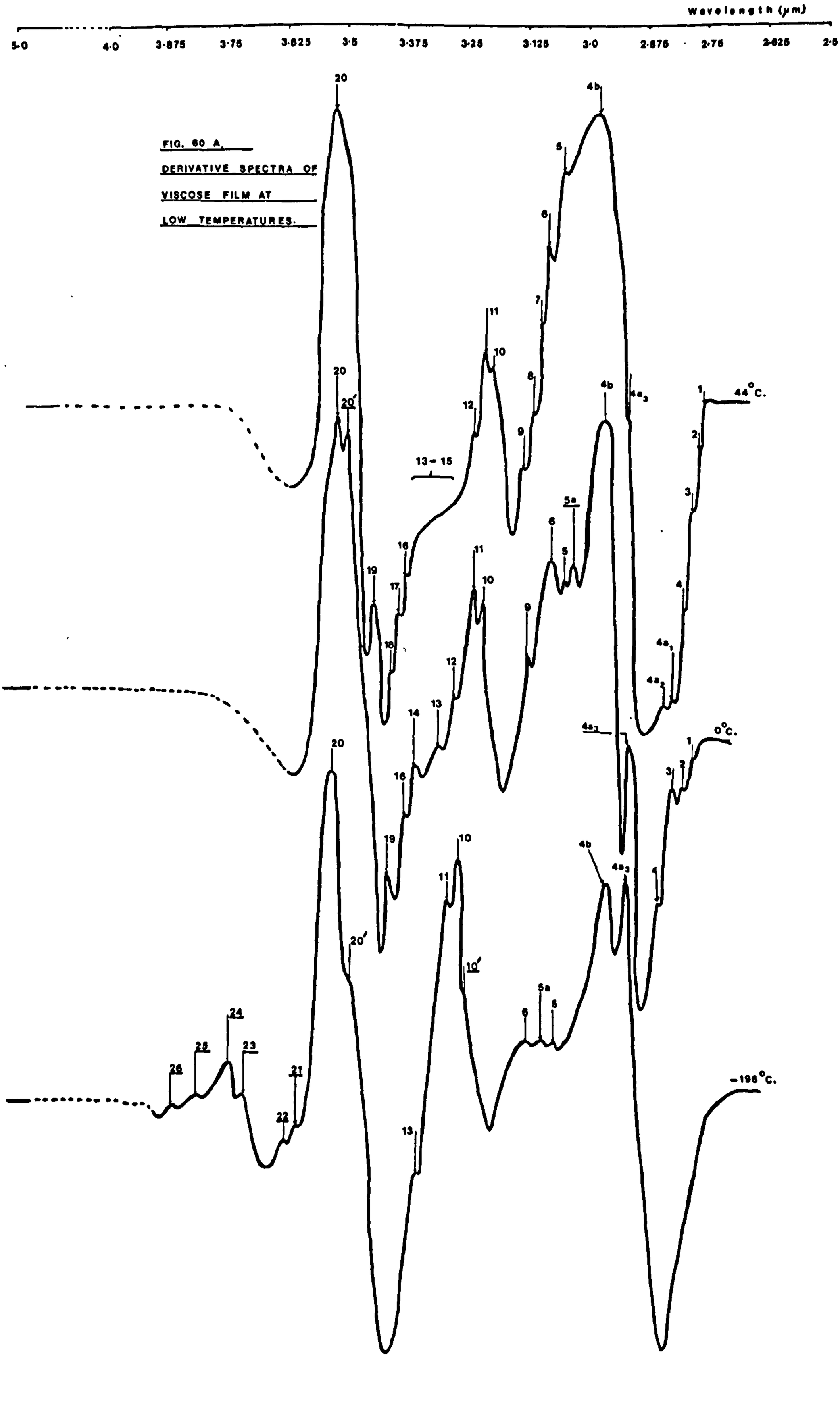

FIG. 60 A.

DERIVATIVE SPECTRA OF VISCOSE FILM AT LOW TEMPERATURES.

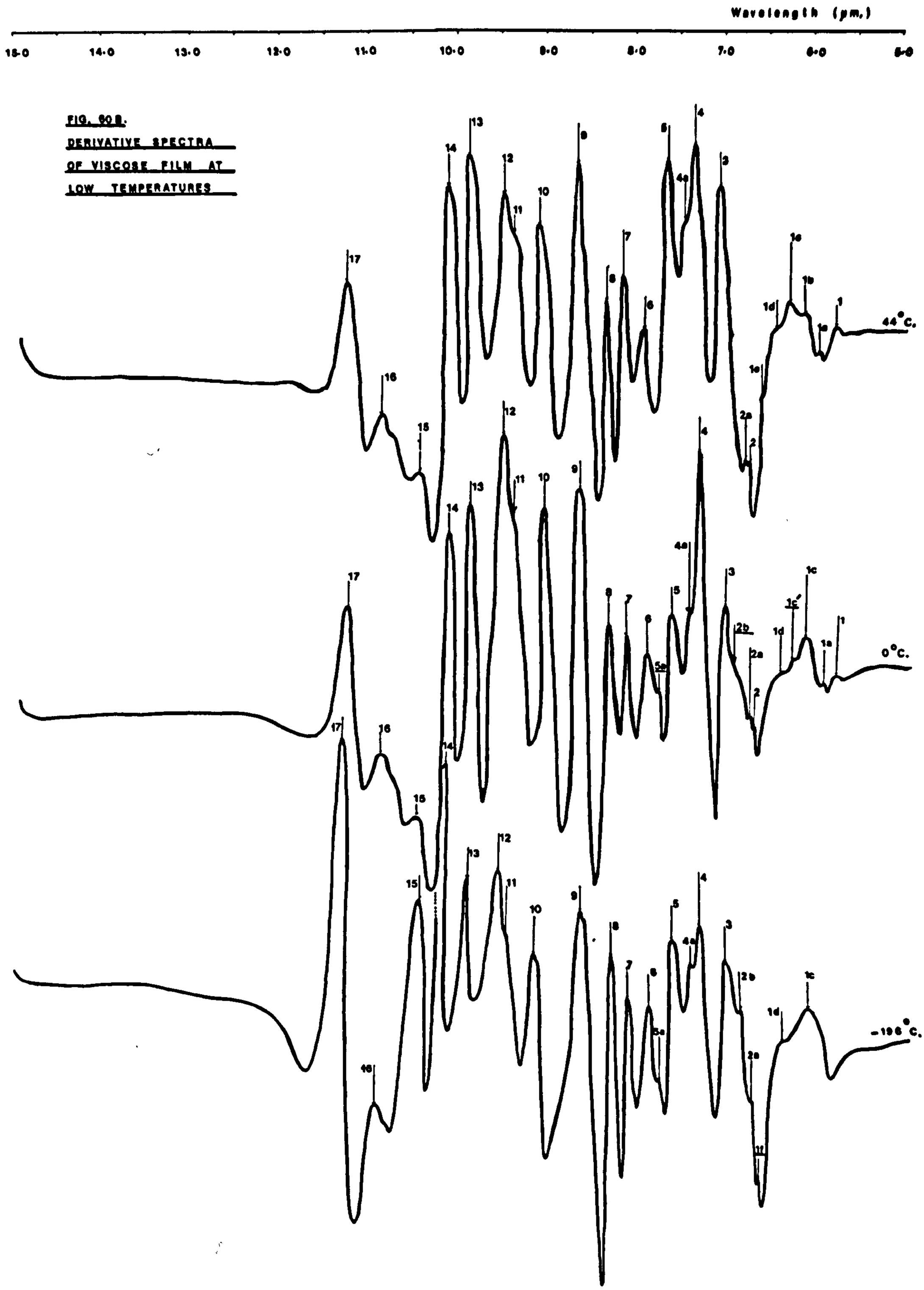

FIG. 90 B.
DERIVATIVE SPECTRA OF VISCOSE FILM AT LOW TEMPERATURES

FIG. 61A

DERIVATIVE SPECTRA OF DICEL FILM AT LOW TEMPERATURES

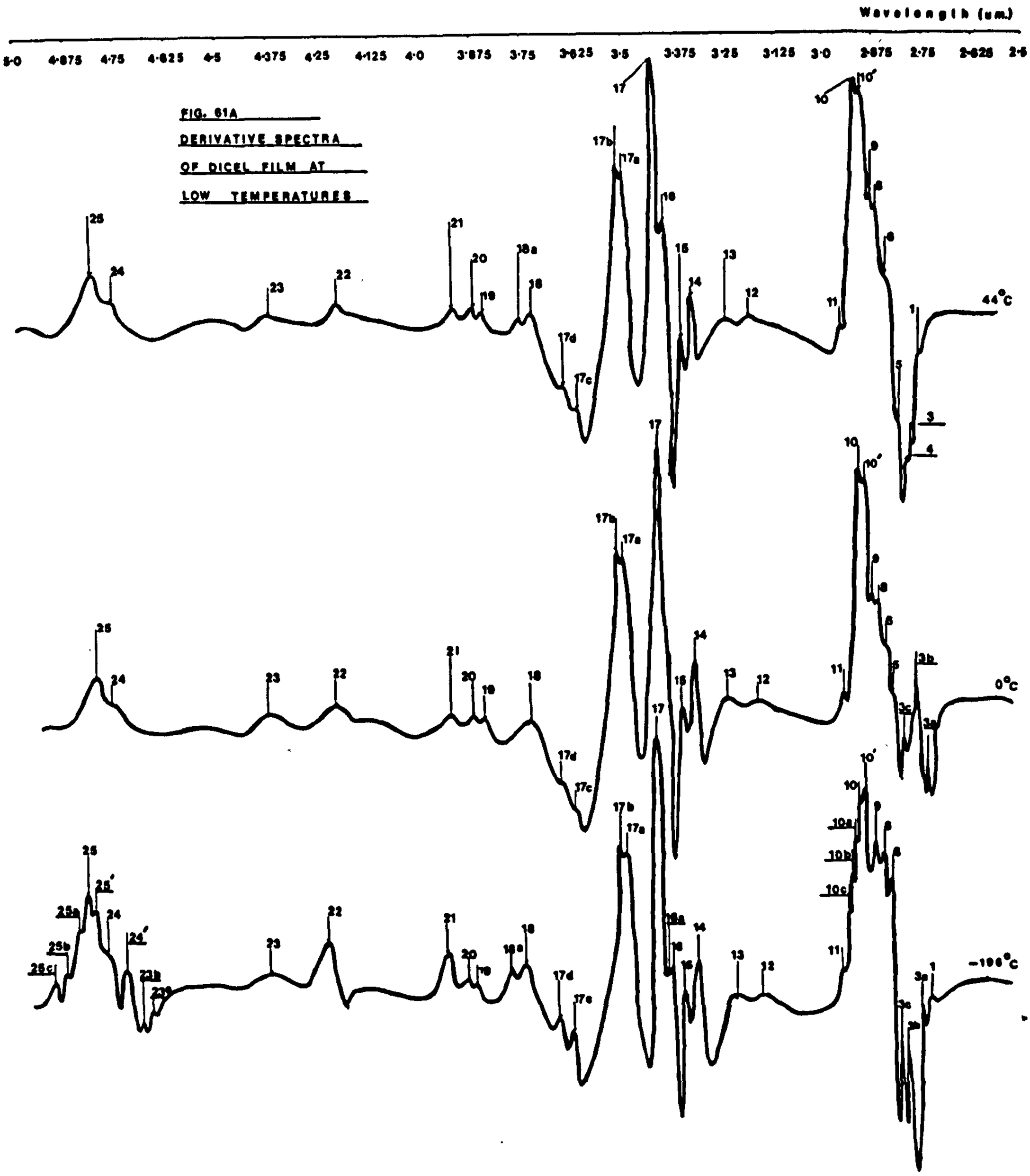

FIG. 61B.
DERIVATIVE SPECTRA OF DICEL FILM AT LOW TEMPERATURES

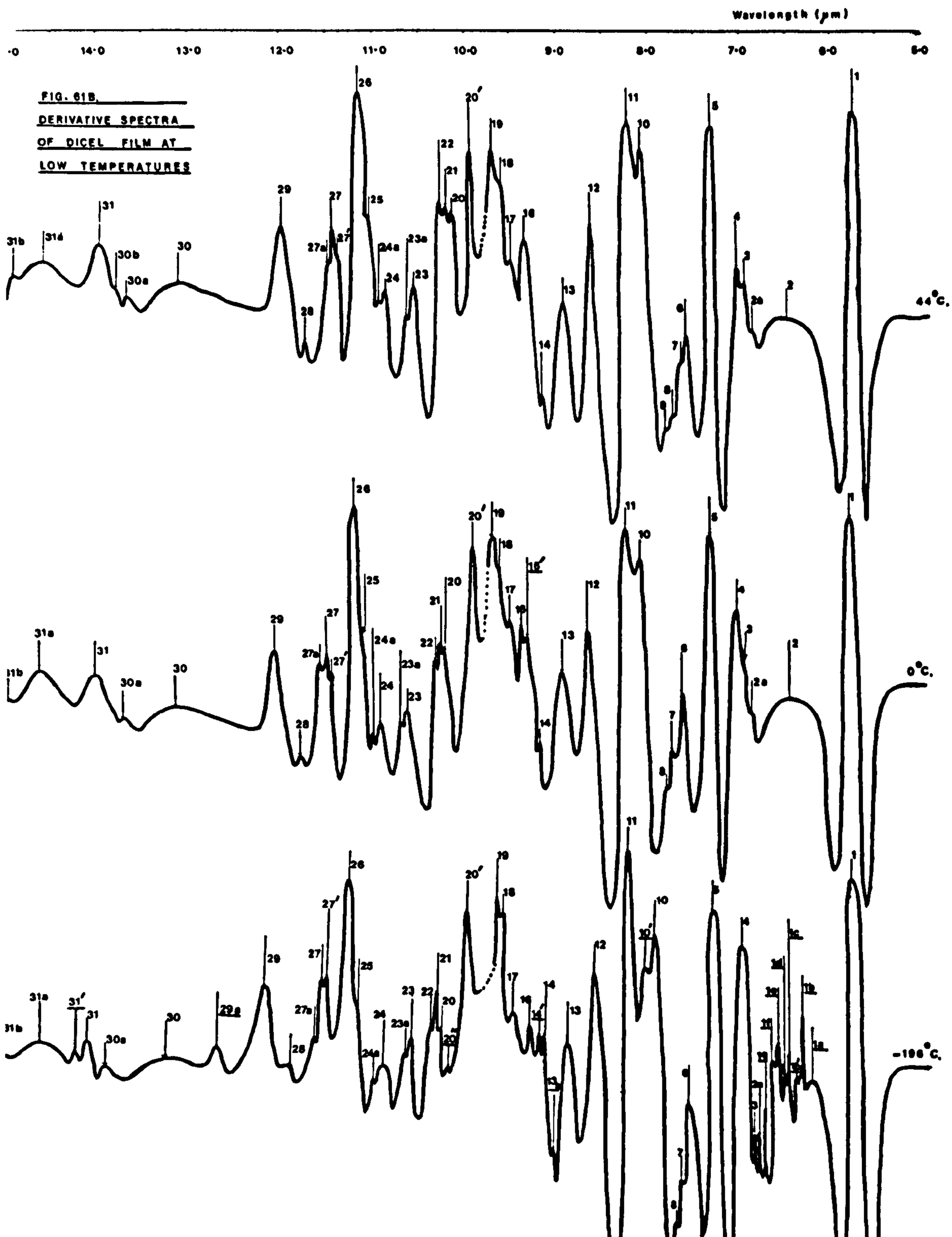

FIG. 62 A.

DERIVATIVE SPECTRA OF TRICEL FILM AT LOW TEMPERATURES

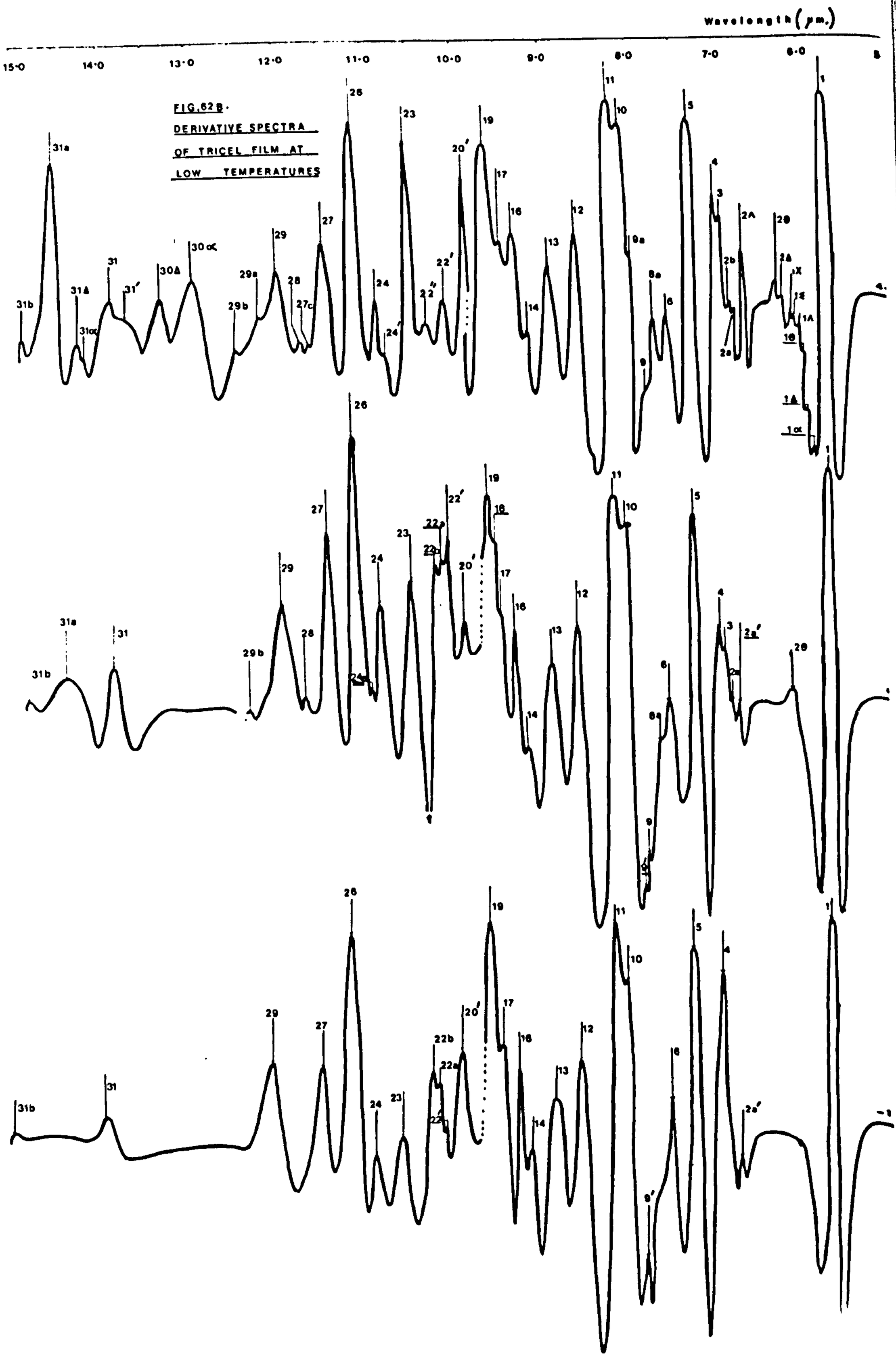
Wavelength (μm.)
15·0
14·0
13·0
12·0
11·0
10·0
9·0
8·0
7·0
6·0
5
FIG.62B.
DERIVATIVE SPECTRA
OF TRICEL FILM AT
LOW TEMPERATURES

TABLE XXIII

Spectrum	Changes in Peak Intensity	Changes in Peak Wavelength	New Peaks
60A (viscose)	1,2,3,4,17 & 18 disappear at 0°C.		5a, 20′ at 0°C.
	16 & 19 " " -196°C.		
	5 decreases at 0°C.	5 increases at 0°C.	10′, 21 24 at -196°C.
	6 increases at -196°C.	6 decreases at -196°C.	
	12 & 14 clearly resolved at 0°C. but disappear at -196°C.		
	13 clearly resolved at 0°C. & -196°C.	13 increases at T_6	
	10 & 11 increase at 0°C. & -196°C.	10 & 11 increase at 0°C. & -196°C.	
60B (viscose)	1a,1b,1e disappear at 0°C.	1c decreases at 0°C.	1e, 2b, 5a at 0°C.
	1c′ disappears at -196°C.	14 increases at -196°C.	1f at -196°C.
	4, 9-14 increase at 0°C. decrease at T_6	15, 16 decreases at -196°C.	
	15 & 17 increase at -196°C.		
61A (dicel)	3b,3c,21,22,25 increase at T_6	3c increases at -196°C.	3a,3b,3c at T_5
	10 decreases at -196°C.	11 decreases at -196°C.	10a,10b,10c,16a,23a
	18a disappears at 0°C., re-appears -196°C.		23b,24′,25′,25a,25b
			25c at -196°C..

TABLE XXIII (Continued)

Spectrum	Changes in Peak Intensity	Changes in Peak Wavelength	New Peaks
61B (dicel)	4,24,24a increase at -196°C.	7,16,20,20′ increase at 0°C.	16′ at 0°C.
	23,23a,26,27′,27,27a decrease at -196°C.	10 & 17 decrease at -196°C.	1a,1b,1b′,1c,1d,1e, 1f,1g 13a,14′,20″,29a,31′ at -196°C.
	31a increases at 0°C. decreases at -196°C.		
62A (dicel)	3b,3c,3d disappear at 0°C.		
	1a,1b,1c,1α,3a,8a,8b,9′,9c	9,9e,9f decrease at 0°C. but	1α,8a,8b
	disappear at -196°C.	increase at -196°C.	9c′,9c″,9e′,9e″ at 0°C.
	6,7,8 decrease at T_5 but increase at 196°C.	6 & 7 increase at -196°C.	
	9c,9g,10a,10b,10c decrease at 0°C.		
	9e increases at -196°C.		
62B (tricel)	1α - 2Δ , 2Λ , 2b,22″,24′,27c		2a′,9′,18,22a,22b
	29a,30α,30Δ,31′,31α,31Δ		24a at 0°C.
	disappear at 0°C.		
	2e,3,8a,9,18,24a,28,29a,	8a, 8b decrease at 0°C.	
	31a disappear at -196°C.	6 decreases at -196°C.	
	4,6,20′ decrease at 0°C. but increase at -196°C.	10 increases at -196°C.	

TABLE XXIII (Continued)

Spectrum	Changes in Peak Intensity	Changes in Peak Wavelength	New Peaks
62B (tricel) continued	24 & 27 increase at 0°C. decrease at -196°C.		
	10, 22a, 22b, 23 decrease at -196°C.		
	14 & 29 increase at -196°C.		
	16 increases at 0°C. & -196°C.		

The sample holder (Fig. 59B) consists of a brass rod with a rectangular hole cut through it and a ridge halfway in to allow samples to be supported. The rod is fixed to a Dewar system by means of a graded glass seal. Two small holes drilled in the brass rod enable the coolant to penetrate the brass block so as to ensure that the sample temperature reaches the coolant temperature. During operation (Fig. 59A) the flange of the Dewar system is mounted on 'O' rings on the top of the block so that the sample holder is located between the windows. A sealedcell system in which the Dewar can operate as such is produced by pumping down the cavity with a vacuum pump and closing the stopcock before placing the cell in the spectrometer cavity.

Absorption and second derivative spectra of composite samples of viscose, dicel and tricel films were obtained over the whole of the spectral range from 2.5 - 15 μm. (4000 - 667 $cm.^{-1}$) (Figs. 60A - 62B). Spectra were obtained at $0^{o}C.$ by using an ice/water mixture in the Dewar, and at $-196^{o}C.$ by using liquid nitrogen. Care was necessary when using liquid nitrogen to ensure that the cold heavy vapour from the boiling liquid nitrogen in the Dewar did not sink into the sample cavity of the spectrometer and cause condensation to occur on the rock salt windows or the spectrometer mirrors. This was prevented by placing large sheets of paper at the top of the Dewar and temporarily sealing them to the flange of the Dewar with plasticine.

4.3 Results

The derivative spectra of viscose, dicel and tricel films recorded at $0^{o}C.$ and $-196^{o}C.$ were compared with the corresponding spectra recorded at $44^{o}C.$ in Figs. 60, 61 and 62. Changes which occurred in peak wavelength or intensity at $0^{o}C.$ or $-196^{o}C.$ are listed in Table XXIII. Peak changes were assessed by comparing spectra recorded at $0^{o}C.$ with spectra recorded at $44^{o}C.$, and by comparing spectra recorded at $-196^{o}C.$ with those at $0^{o}C.$ New peaks which were detected at $0^{o}C.$ or $-196^{o}C.$ were designated as previously by

underlined labels. The wavelengths and frequencies of these peaks are shown in Appendix (i).

Absorption spectra are not shown since they are poorly resolved and are not involved in the discussion.

4.4 Discussion

An analysis of the derivative spectra of viscose, dicel and tricel films at 0°C. and -196°C., as shown in Table XXIII, indicates that a larger number of changes occur with change of temperature in the spectra of viscose and tricel than in the spectra of dicel. This confirms the previous results which suggest that in terms of energy levels and stability there is a considerably smaller difference in structure between 'crystalline' and 'crystallizable' regions in dicel than in viscose or tricel.

In the derivative spectra of viscose (Figs. 60A and 60B) and tricel (Figs. 62A and 62B) film, the number and intensities of peaks attributable to absorbed water decreases at 0°C., and at -196°C. most of such peaks have disappeared. It is probable that this situation arises from the sublimation of ice from viscose and tricel polymer films at the low temperatures and the low pressures present in the cell. In the case of dicel, however, peaks attributable to absorbed water increase in number at -196°C. in both the 2.5 μm. ($4000\ cm.^{-1}$) and 6 μm. ($1667\ cm.^{-1}$) regions of the spectrum. At -196°C. peaks 3a, 3b, 3c, 10a, 10b and 10c appear in the 2.5 μm. ($4000\ cm.^{-1}$) region (Fig. 61A) and peaks 1a - 1g appear in the 6 μm. ($1667\ cm.^{-1}$) region (Fig. 61B). It is thus likely that these peaks are due to one or more forms of ice structure within the dicel film.

The fact that such peaks are not present in viscose or tricel spectra, and that it is necessary for water to be present in the dicel film structure (before cooling) for such peaks to occur, substantiates the earlier findings that the binding of water by dicel is much stronger than by viscose or tricel.

An examination of the results from Table XXIII and reference to the

assignment tables given in Chapter 3 (Tables XVII - XXII) show that in the spectra of viscose and tricel, many more peaks assigned as 'crystallizable' decrease in intensity at 0°C. and -196°C. than do 'crystallizable' peaks in the spectra of dicel. This indicates that cooling from 44°C. to -196°C. causes a temporary increase in the total amount of 'crystalline' material present in viscose and tricel films, but only a slight increase (if any) in the amount of 'crystalline' material present in dicel film. It is likely that cooling below 0°C. also causes changes in the 'crystalline' form in both viscose and tricel; however, no attempt has been made to define all the changes which occur, since spectra were only recorded at 0°C. and -196°C. and temporary structural changes which occur below 0°C. are not fully understood nor widely documented.

One effect which is difficult to explain is the appearance of a group of peaks near peaks 24 (4.7245 μm., 2116 $cm.^{-1}$) and 25 (4.7670 μm., 2098 $cm.^{-1}$) at -196°C. in the spectra of dicel (Fig. 61A). These two peaks were previously tentatively assigned to C-O group vibrations of acetyl groups (Chapter 3) and together with the new peaks (23a, 23b, 24′, 25′, 25a, 25b, 25c) they form a cluster of peaks with a profile very similar to that which occurs in the spectrum of tricel recorded at 44°C.. It is possible, however, that these peaks arise as a result of increased resolution at low temperatures.

The changes observed in the spectra of viscose are most marked between 44 and 0°C. and it is probable that this is due in part to the second order transition at 25°C. previously described by Ramiah and Gording (88) and Mahba (86) (Chapter 1). These workers assigned the transition to the formation of a set of intramolecular hydrogen bonds between C_3 OH and O_5' atoms, but it is more probable that the transition is due to the formation of a set of intermolecular hydrogen bonds for the following reasons:-

(i) The results of Chapter 3 show that although intermolecular hydrogen bonds are in theory stronger than intramolecular hydrogen bonds (for hydrogen bonds resulting from cellulosic OH groups), the intermolecular

hydrogen bonds are more easily broken at increasing temperatures. The second order transition which occurs in viscose (Cellulose II) when the temperature is raised above 25°C. (i.e. from 0 to 44°C. in this case) is thus probably due to the breakage of intermolecular hydrogen bonds, rather than intramolecular hydrogen bonds.

(ii) A new peak, peak 5a occurs in the spectrum of viscose recorded at 0°C. (Fig. 60A). This peak is very close to peak 5, previously assigned to intermolecularly hydrogen bonded OH groups. The assignment of peak 5a to intermolecularly hydrogen bonded OH groups is thus more probable than the assignment to intramolecularly hydrogen bonded OH groups. The appearance of peak 5a may thus be due to the formation of a set of intermolecular hydrogen bonds at 25°C.

(iii) Peak 11 (Fig. 60A), also assigned to intermolecularly hydrogen bonded OH groups, increases in intensity between 44 and -196°C, and this may be due in part to an increase in the number of intermolecular hydrogen bonds as the temperature is decreased from 44 to -196°C.

CHAPTER 5

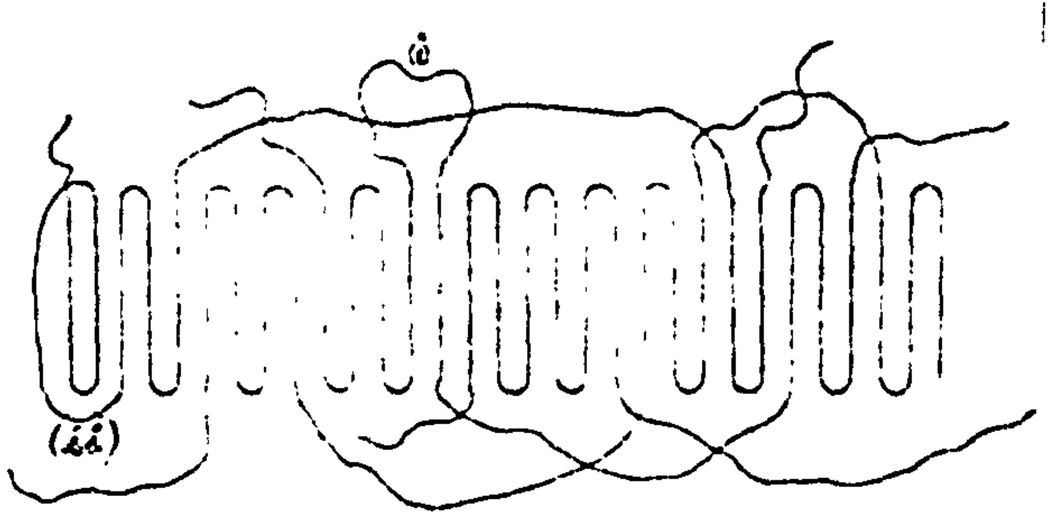

Schematic representation of a composite fold surface consisting of adjacently re-entrant sharp folds and various elements of surface looseness(i) 4(ii)

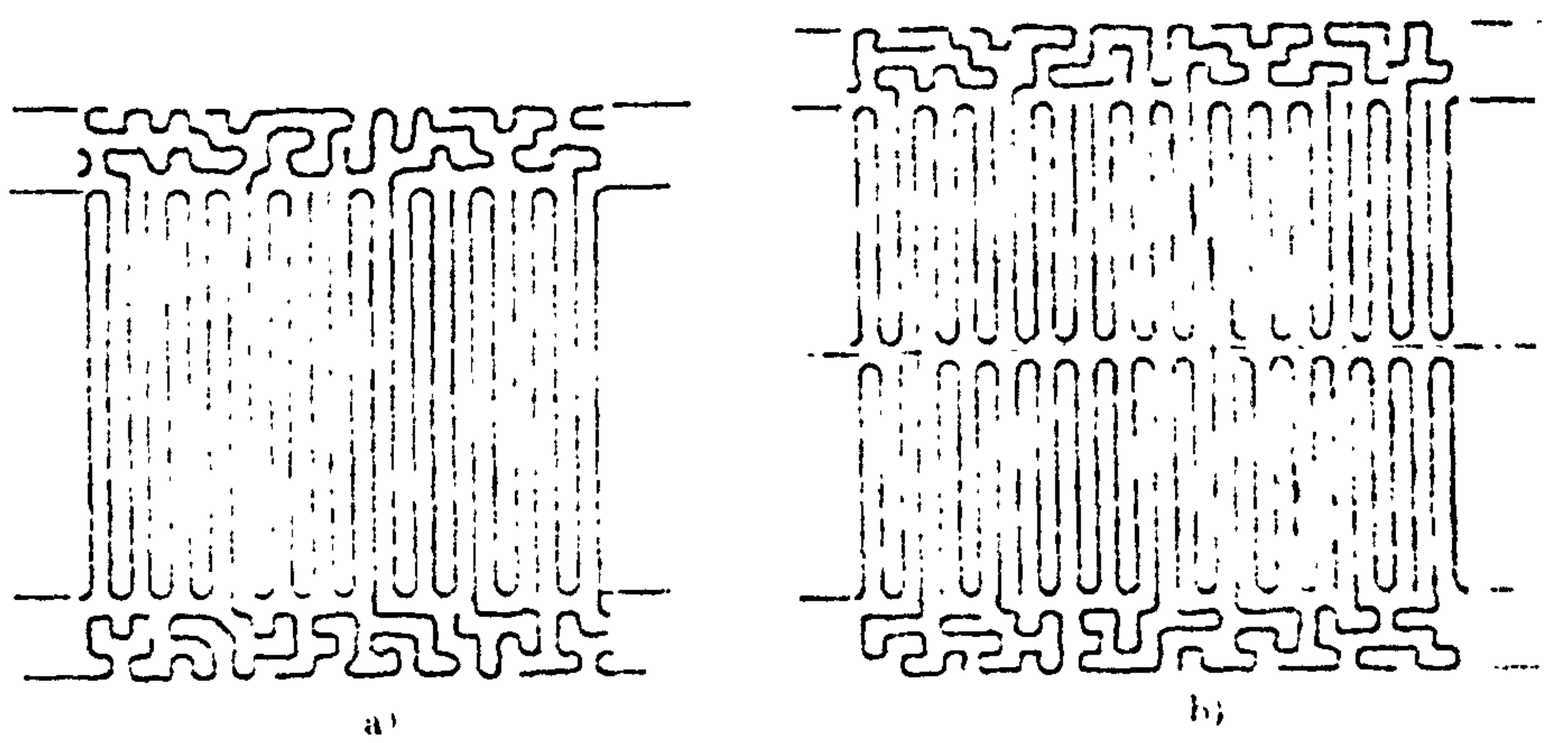

Structure models for crystals of poly(ethylene oxide) - polystyrene (PEO-PS) two block copolymers. a) Single layer crystals. b) Doublet layer crystals

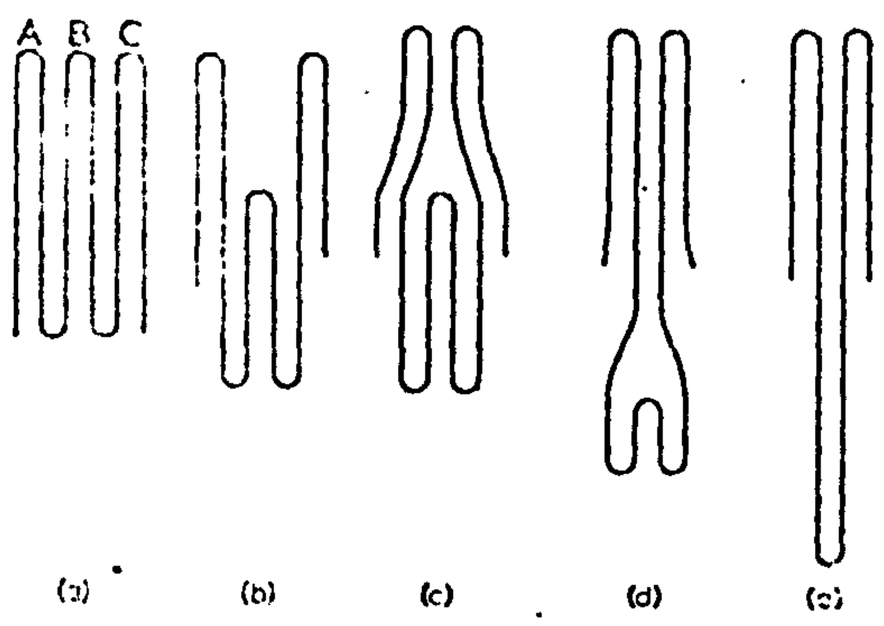

Schematic representation of various stages of the fold length increase to a doubled fold length by the present scheme.

FIG. 63

CHAPTER 5

CHAIN FOLDING IN VISCOSE, DICEL AND TRICEL

5.1 Introduction

The existence and nature of chain folding in many man made fibre forming polymers, such as polyamides, has been established using infra-red spectroscopic methods (173 - 177). However, until recently, little information concerning chain folding in natural fibrous polymers had been obtained, due to the high scattering of such polymers and the poorly resolved and complex spectra recorded. Rhodes (12) was able to largely overcome these problems with keratin utilising derivative spectroscopy to detect the unresolved peaks present. Using nylon 6 as a model compound for keratin, Rhodes was thus able to show the existence of bands arising from chain folding structures in keratin.

Some of the main aspects of chain folding are reviewed by Keller (178) and Keller and Dreyfus (179). A main point of contention is whether the fold is 'loose' or 'sharp' (180) and examples of various fold structures proposed to explain the properties of different crystalline polymers or crystallization processes are shown in Fig. 63. Spectroscopic evidence suggests a 'sharp' fold, since this will produce structural groups which are essentially different from others in terms of bond strain, hydrogen bonding and structural environment. Such differences are necessary to influence vibrational frequencies of such groups and hence induce characteristic infra-red absorption peaks. Since such peaks have been observed, the concept of 'sharp' chain folds is supported. It is considered that 'loose' chain folds will produce a structure which is little different from the rest of the 'crystallizable' material and as such would be spectroscopically indistinguishable from it.

There has been much speculation concerning the existence of helical chain folded structures in cellulose (181 - 186), but little convincing evidence

had been obtained at the outset of this work, in spite of the fact that X-ray diffraction techniques should provide such information. Such evidence should in theory be obtainable from theoretical X-ray analyses of atomic and molecular models and compared with practical X-ray diffraction photographs; as was effected for αkeratin (187) (based on models by Pauling and Corey (188 - 195)).

The method employed by Rhodes (12) to determine which derivative spectral peaks of nylon 6 (as a model compound for keratin) were due to chain folding, involved partial hydrolysis of samples of nylon in increasing concentrations of formic acid at the same temperature and for the same period of time. Samples were then washed and dried, prior to recofding their spectra. Rhodes assumed that if chain folds occurred, they represented weak or exposed points which were much more susceptible to hydrolysis than the rest of the molecule. He maintained that in the spectra of a series of samples of nylon treated with increasing concentrations of formic acid, a critical concentration would be reached where hydrolysis at chain folds only would occur. Thus at this critical concentration, peaks corresponding to the chain fold would decrease markedly in intensity, whereas other peaks would not decrease markedly in intensity.

However, it is probable that some main chain hydrolysis occurs at the critical concentration, but if Rhodes' contentions are correct, 'crystalline' peaks which are characteristic of the remainder of the chain will only show a small decrease in intensity. The method employed by Rhodes also assumes that the partial hydrolysis technique does not cause any permanent large scale structural changes, other than hydrolysis at chain folds and that if any temporary changes in structure occur, that these are reversed when the polymer is washed and dried.

Rhodes (12) was able to confirm the existence of chain folding in nylon 6 by observing the derivative spectra of samples cold drawn to an extension of 300%. As expected, peaks previously assigned to chain folding decreased

markedly in intensity or disappeared in the spectra of such samples. A similar stretching technique could not, however, be applied to viscose, dicel or tricel films, since these ruptured at low extensions before any significant change in absorption or derivative spectra could be observed.

An alternative method of γ- irradiating samples of viscose, dicel and tricel films was thus employed in an attempt to confirm the existence of chain fold structures. The effects of γ radiation on polymers are complex, but one basic effect involves the formation of high energy electrons which then induce the formation of free radicals by chain scission or displacement of atoms from chains. After the initial production of free radicals, a series of reactions usually ensues, which includes the formation of cross-links by the combination of two radicals in adjacent chains or by the displacement of atoms (e.g. hydrogen atoms) from one chain by the radical in another chain. Another series of reactions involves the 'quenching' of these radicals by reaction with atmospheric oxygen or water and the elimination of O•, •OH or H• radicals, which then react to form oxygen, hydrogen, water or hydrogen peroxide.

E.S.R. studies (196) on cellulosic materials have shown that stable free radicals are formed at C_5 and C_6 positions of glucose residues which constitute the cellulosic molecules, as shown in Fig.68 for cellulose.

FIG. 68

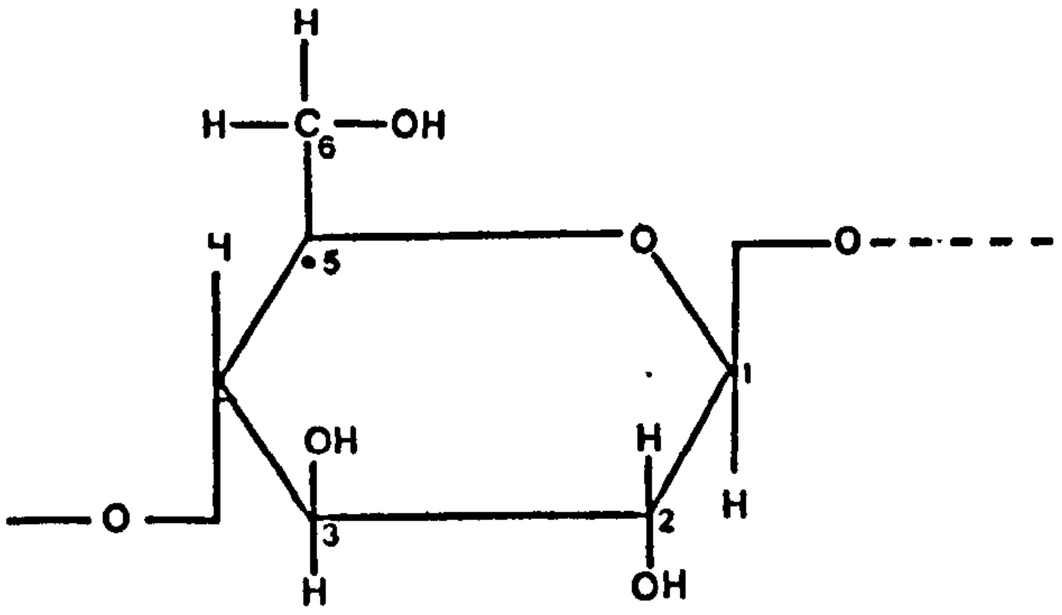

Stable free radical at C_5 position of glucose residues.

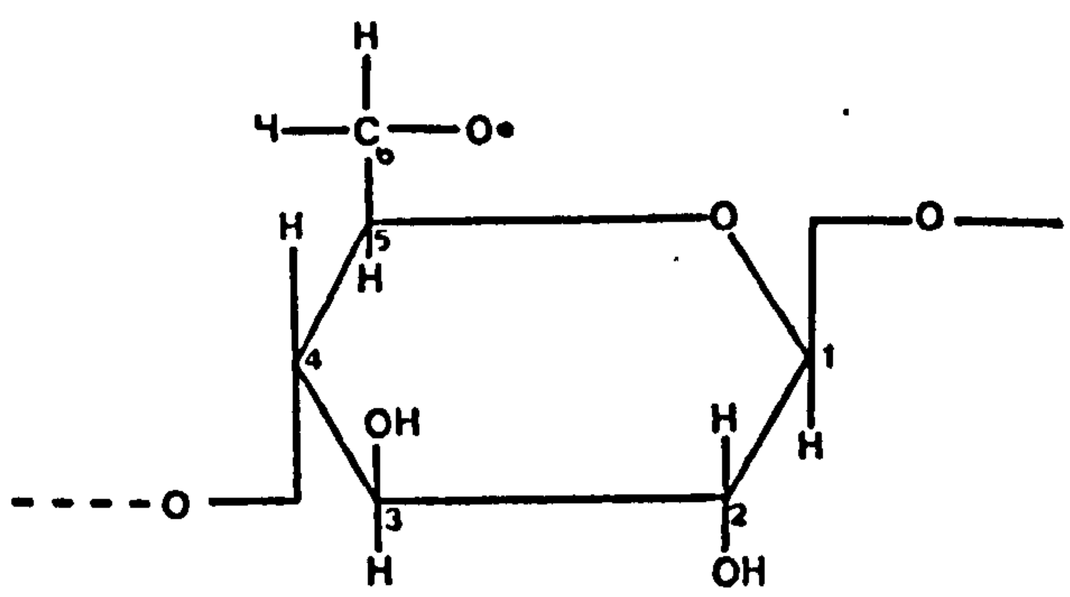

Stable free radical at C_6 position of glucose residues.

A more recent E.S.R. study by Barkakaty (197) on cellulose and cellulose γ- irradiated in both aerobic and anaerobic conditions, has shown that the radicals at C_5 and C_6 positions of glucose residues shown in Fig.68. are the only radicals present. However, since γ- irradiation of cellulosic materials causes a decrease in the length of chain molecules, chain scission involving the formation of free radicals at positions other than those at C_5 or C_6 positions of glucose residues must clearly occur.

The fact that radicals formed by chain scission are not observed in the E.S.R. spectra of cellulosic materials can be adequately explained by Keighley's theory of charge transfer (198) whereby the unpaired electrons which constitute free radicals can effectively move along chain molecules to the positions of greatest stability. Free radicals formed by chain scission in cellulosic materials can thus effectively move to C_5 or C_6 positions of glucose residues and form stable free radicals. The details of the mechanism of charge transfer are as yet unclear, but the theory has been successfully applied by McKinnley and Keighley (199) to explain the types of radicals observed in keratin from E.S.R. spectra.

If chain folds represent regions of instability (high energy) due to bond strain or steric hindrance or the presence of unstable repeat unit conformations (e.g. the boat conformation of glucose residues), and if it is further assumed that charge transfer can occur over fairly large sections of cellulosic chain molecules, then it is not unreasonable to suggest that free radicals formed by chain scission can move along chains to points where chain folding occurs, since under such circumstances the maximum amount of free energy would be yielded from the system resulting in the greatest stability. The points of chain scission may thus be effectively moved to chain folded regions and further stabilization can then occur by further charge transfer and the formation of stable free radicals at C_5 or C_6 positions of glucose residues, as in Fig.68.

Hence it is proposed that Y- irradiation of chain folded materials (in which the fold represents regions of instability) provides a means of selective chain scission at chain folds so that the spectral peaks which correspond to such folds will decrease more markedly in intensity than other peaks. This thus provides a method of confirming the assignment of chain folded peaks from partial hydrolysis experiments.

5.2 Method

Annealed samples of viscose film and untreated samples of dicel and tricel film were partially hydrolysed by exposure to hydrochloric acid solutions at 20^{o}C. for a period of 12 hr. and experiments were carried out at increasing acid concentrations. The samples were then thoroughly washed in distilled water and dried over P_2O_5 for 24 hr., prior to recording their absorption and derivative spectra in sealed sample cells with P_2O_5 at a temperature of 44^{o}C. In the case of viscose, annealed samples were used in order to increase the total amount of crystalline material present, since it was considered that the bonding in crystalline regions was likely to act as a barrier to the penetration of H Cl between chains, whereas dislocations between chains provided by chain folds were thought to be more accessible to the acid. Such a method was viewed as an attempt to induce preferential hydrolysis at chain folds and hence cause a larger decrease to be observed in the intensity of spectral peaks which correspond to chain folds. In the case of dicel and tricel, untreated samples were used, since annealed samples proved to be impenetrable to H Cl.

Samples of viscose, dicel and tricel film were Y- irradiated in a cobalt 60 Y ray source for periods of 5 days (strength of source 10,000 Curies, giving a dose rate of 2×10^{4} J.h.$^{-1}$ kg.$^{-1}$ of sample and hence a total dose rate of 2.4×10^{6} J. kg.$^{-1}$ of sample), when significant changes in the absorption and derivative spectra of these materials became observable. Spectra were again recorded with the samples dry in sealed sample cells with

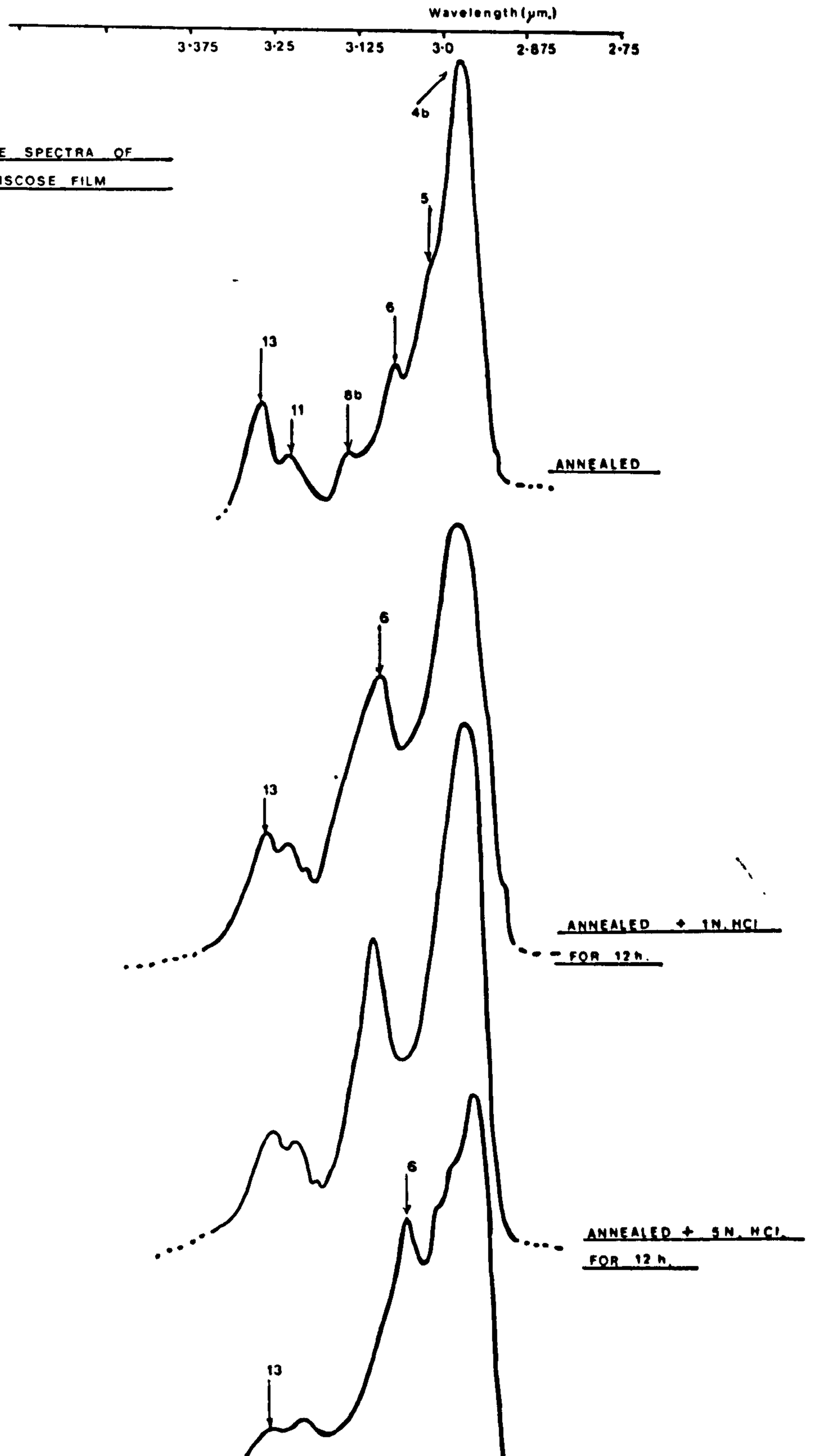

FIG 64

DERIVATIVATIVE SPECTRA OF TREATED VISCOSE FILM

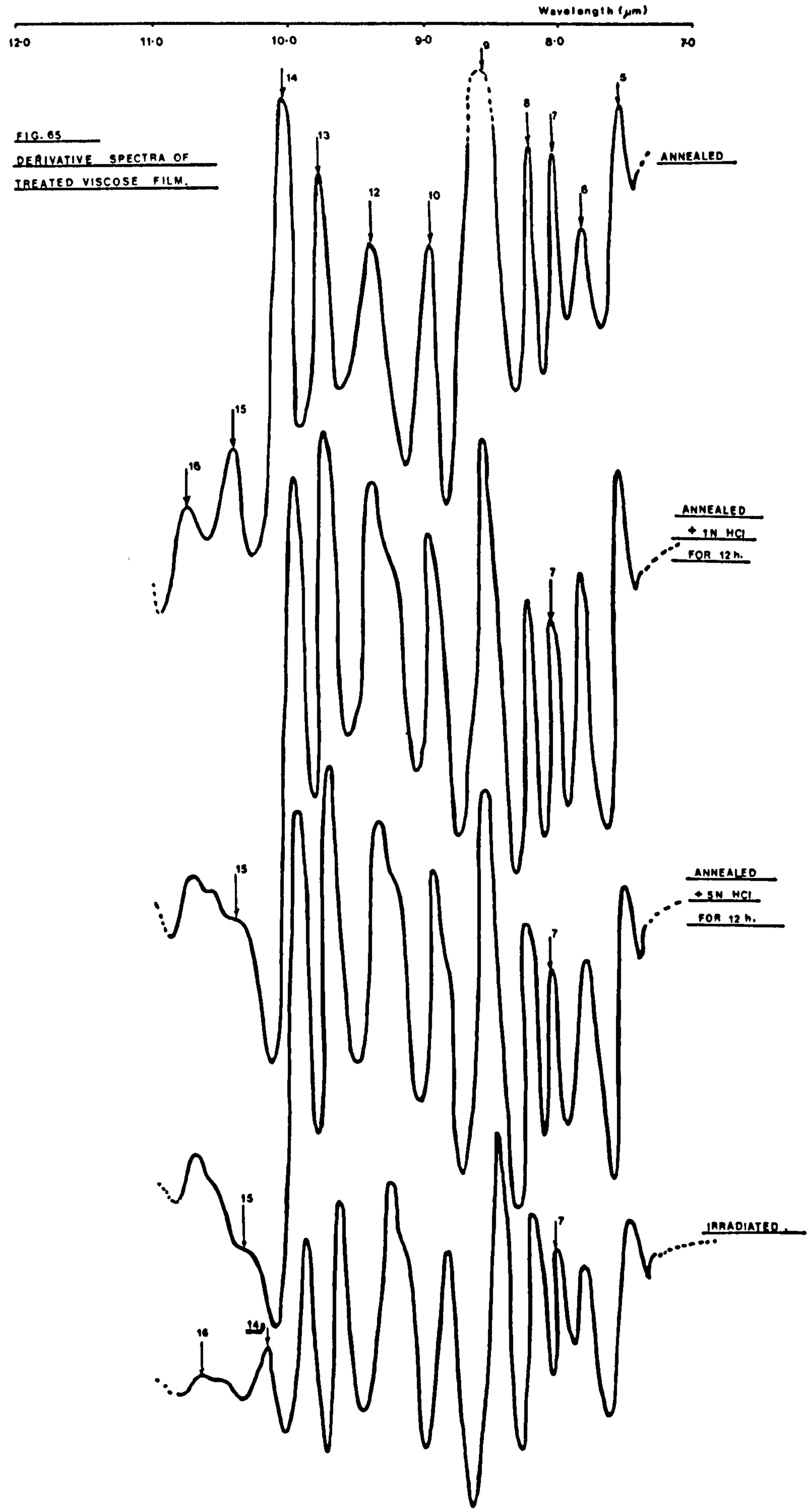

FIG. 65
DERIVATIVE SPECTRA OF
TREATED VISCOSE FILM.

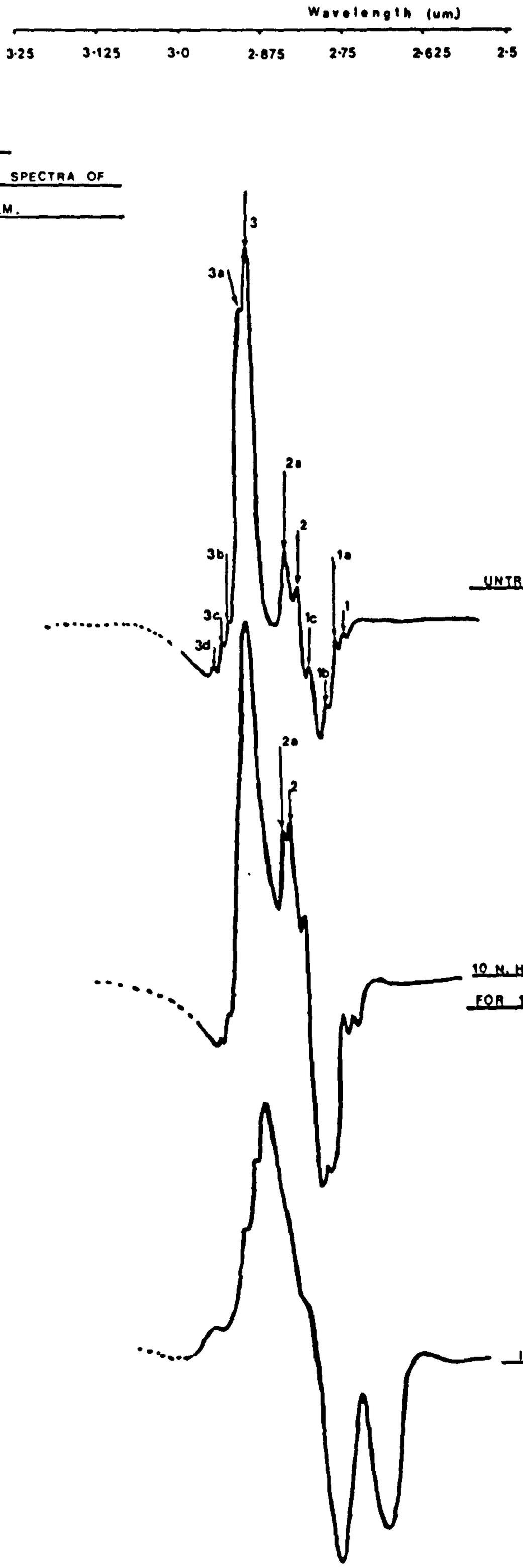

FIG. 66

DERIVATIVE SPECTRA OF TRICEL FILM.

FIG. 67

DERIVATIVE SPECTRA OF TREATED TRICEL FILM

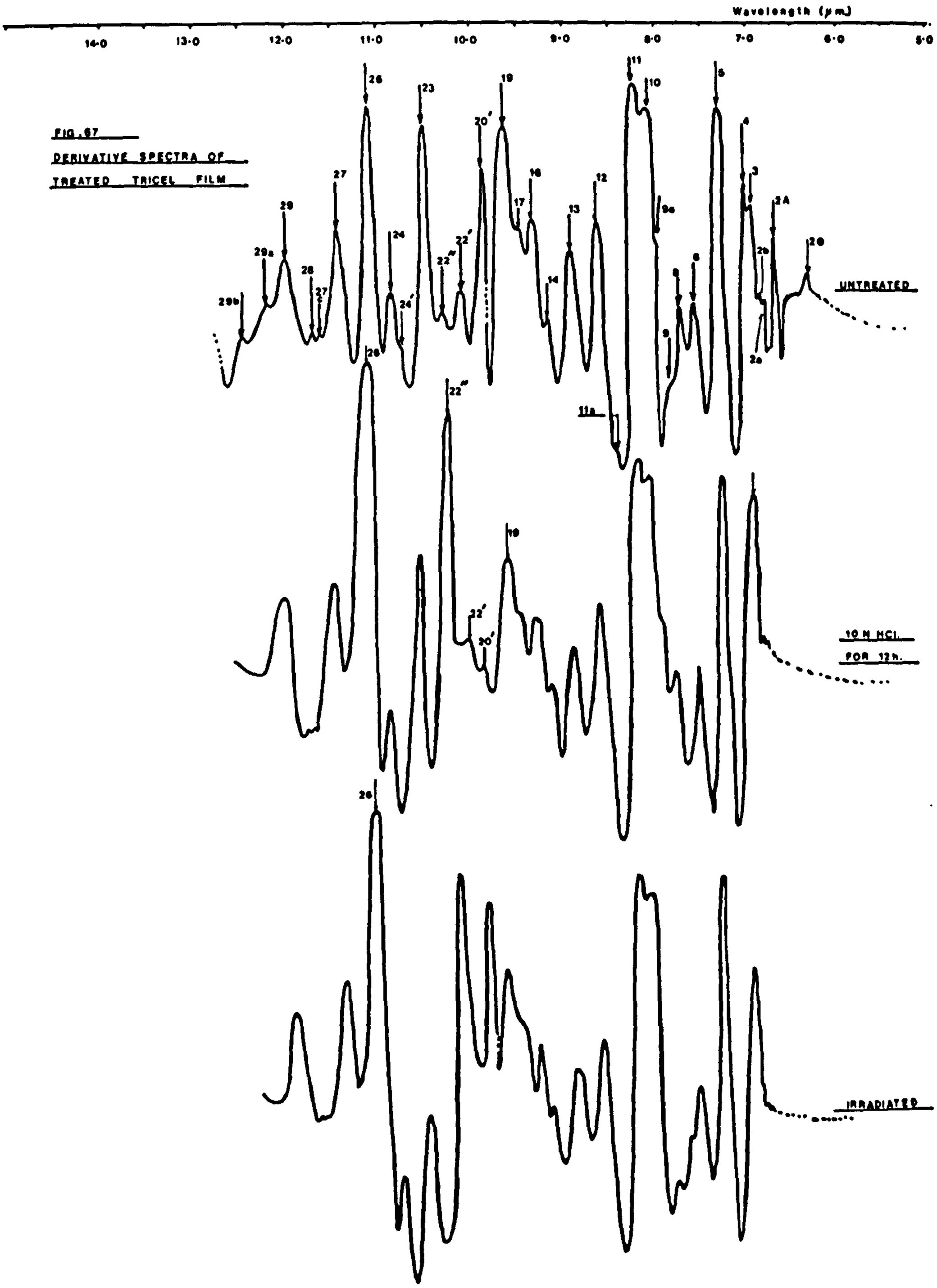

P_2O_5 and at a temperature of 44 °C.

5.3 Results

The derivative spectra of samples of acid treated and γ- irradiated viscose films are shown in Figs. 64 and 65. Derivative spectra of samples of tricel film similarly treated are shown in Figs. 66 and 67. The concentrations of H Cl used indicate the concentration (or concentration range) at which significant changes in the derivative spectra of viscose or tricel occurred. Lower concentrations of H Cl did not have any significant effect on the spectra of viscose or tricel and those spectra are thus not shown, whilst higher concentrations caused samples to disintegrate. The spectra of dicel are not shown, since few significant changes occurred in the spectra of dicel up to a concentration of 10 N. H Cl, when disintegration of the film occurred.

5.4 Discussion

In the derivative spectra of viscose in the 2.5 - 5 μm. (4000 - 2000 $cm.^{-1}$) region (Fig.64), peak 13 shows a decrease in intensity due to partial acid hydrolysis. This crystalline hydrogen bonded OH peak (Chapter 3 Section A), is thus assigned to chain folded regions of Cellulose II molecules. This assignment is upheld by the fact that a marked decrease in the intensity of this peak also occurs in the derivative spectrum of an irradiated sample of viscose.

Peak 6, previously assigned to strongly bound water (Chapter 3 Section A), also increases in intensity in the spectra of both partially hydrolysed and γ - irradiated samples of viscose (Fig.64), and this indicates that both partial acid hydrolysis and γ-irradiation of viscose cause some structural changes to occur which enable more atmospheric water to be strongly bound by the viscose. Such structural changes may include an increase in the total number of OH groups present in the viscose due to chain scission, although

the increase is not significant enough to cause any large increases in the intensities of derivative peaks which correspond to OH groups in viscose in this spectral region (2.5 - 5 μm. 4000 - 2000 cm.$^{-1}$).

A further structural change in viscose caused by partial acid hydrolysis and γ- irradiation is a decrease in the total amount of crystalline material present. Such a decrease is borne out by a decrease in the intensity of the 'crystalline' peak 13 just assigned to chain folded material, as well as by decreases in the intensities of other 'crystalline' peaks in the 5 - 15 μm. (2000 - 667 cm.$^{-1}$) region. A decrease in the total amount of crystalline material present in the viscose film means that the film structure is more accessible to atmospheric water, so that a greater amount of such water can penetrate the film, some of which will be strongly bound. The increase in the intensity of peak 6 in spectra of partially acid hydrolysed and γ - irradiated samples of viscose is thus accounted for.

In the derivative spectra of viscose in the 5 - 15 μm. (2000 - 667 cm.$^{-1}$) region (Fig. 65), peak 7 previously assigned to 'non crystallizable' C-O-C groups and peak 15 previously assigned to crystalline C-O groups (Chapter 3 Section B) decrease markedly in intensity in the derivative spectra of partially acid hydrolysed samples. These peaks are thus also tentatively assigned to chain folded regions and this assignment is confirmed by equivalent decreases in the intensities of these peaks in the irradiated sample spectrum.

In dicel, the fact that there are no significant decreases in derivative peak intensities of partially hydrolysed samples up to acid concentrations where sample disintegration occurred, indicates, as expected, that dicel is not significantly chain folded. This lack of chain folding may also be attributed to the irregular (atactic) nature of dicel molecules.

In the spectrum of partially hydrolysed tricel in the 2.5 - 5 μm. (4000 - 2000 cm.$^{-1}$) region (Fig.66), there are very few significant changes, except that peak 2 previously assigned (Chapter 3 Section A) as a

'crystallizable' OH peak involving OH groups intramolecularly hydrogen bonded increases in intensity. However, this peak decreases in intensity in the irradiated sample spectrum. In the 5 - 15 μm. (2000 - 667 $cm.^{-1}$) region, however, (Fig.67) peaks 19, 20′, 22′ and 23 ('crystalline' C-O peaks) and peaks 29a and 29b (non crystallizable CH_2 peaks) all decrease markedly in intensity or disappear in the partially acid hydrolysed sample spectrum. Furthermore, all these peaks except peak 20′ decrease in intensity in the irradiated sample spectrum .

A tentative assignment of these peaks to chain folded material is thus possible, but certain factors not present in the case of viscose make such an assignment more tentative. In the case of tricel, all the peaks assignable to a chain fold are CO or CH_2 peaks, which are due to both the basic cellulosic chain and also to the substituted acetyl groups. Unfortunately, hydrochloric acid does not specifically attack 1-4 β D glucosidic linkages of the chains, but also attacks the ester linkages of some side chain acetyl groups, producing acetic acid and OH groups on the main chain. The decrease in the intensity of peaks 19, 20′, 22′ and 23 could thus be due to the removal of some acetyl groups from the tricel molecules. Similarly, it is possible the decrease in intensity of most of these peaks in the irradiated sample spectrum could be due to the removal of some acetyl radicals which then form acetaldehyde, acetic acid etc.

For these reasons it is not possible to conclude that chain folding occurs in tricel, but this problem may be resolved if a reagent can be found which is specific for the hydrolysis of 1-4 β D glucosidic linkages, and this is discussed further in Chapter 8. The existence of chain folding in viscose (Cellulose II) films is, however, suggested, and a possible structure for the fold is discussed in Chapter 8.

CHAPTER 6

CHAPTER 6

SPECTRA OF VISCOSE, DICEL AND TRICEL FILMS OVER A RANGE OF RELATIVE HUMIDITIES

6.1 Introduction

This chapter deals with the derivative spectra of viscose, dicel and tricel films over a range of humidities from 0 to 75.1% Relative Humidity (R.H.). Spectra obtained were analysed in terms of the state of bound water with increasing humidity, i.e. increasing amounts of absorbed water, and also in terms of the effect on structure of increasing amounts of absorbed water. Such effects on film structure were assessed from changes which occurred in the intensities or wavelengths (frequencies) of structural peaks at increasing humidities and the disappearance of some of these peaks or the appearance of new peaks at increasing humidities. Absorption and deriviative spectra of water and ice are also included in this chapter, to assist in the assignment of water peaks.

6.2 Method

Composite samples of viscose, dicel and tricel films were prepared as described previously (Chapter 3) so as to cover the whole of the spectral range from 2.5 - 15 μm. (4000 - 667 $cm.^{-1}$). Samples were then mounted in sample cells containing saturated solutions of various salts in contact with small amounts of the pure undissolved salt in the small tubes supported by the brass sample disc. Rock salt windows were then fitted to the cells which were then sealed with apiezon sealing compound and fixed in the heated block mounted on the spectrometer bed so that the sample beam passed through the sample in the cell. A 'blank' cell humidified to the same conditions was placed in the reference beam so as to nullify any absorptions due to atmospheric water vapour within the sample cell. Sample and reference cells were maintained at a constant temperature of $44^{\circ}C.$ for 12 - 24 hr. prior to the

recording of spectra in order to allow a saturated atmosphere to be produced within the cells and to allow the sample to equilibrate with this atmosphere.

Four saturated salt solutions were chosen so as to give a range of humidities from 11.5 - 75.1% R.H., namely those of LiCl, $MgCl_2$, $MgNO_3$ and NaCl. The estimated R.H.'s of the saturated atmospheres produced by these solutions inside the sealed cells at 44°C. were estimated from tables given by Wexler (200) and are shown below in table XXIV. Such estimates vary from the

TABLE XXIV

Estimated Relative Humidity of Saturated Salt Solution at 44°C.

LiCl	$MgCl_2$	$MgNO_3$	NaCl
11.5%	31.8%	47.7%	75.1%

true R.H.'s since they do not take into account variations in atmospheric pressure etc. However, accurate measurements of the R.H.'s of the atmosphere inside the sample cell are not necessary, since it is not possible to accurately correlate sample regain at a particular R.H. with the intensities of derivative peaks which correspond to water absorbed by the sample, due to slight variations which occur in derivative peak intensities (though not in frequencies) between consecutive spectra, recorded under the same conditions.

Although the R.H.'s of the atmospheres within the sample cells were not measured, it was, however, necessary to ensure that the R.H. varied as little as possible for a particular salt solutions in order to ensure the greatest possible reproducibility of spectra. Thus accurate comparisons could be made between the spectra of conditioned samples of viscose, dicel and tricel.

This was achieved by recording all the spectra as rapidly as possible and during a period in which large fluctuations in external atmospheric pressure were not experienced.

In the case of samples whose spectra were recorded using saturated NaCl solution to provide a conditioning atmosphere of approximately 75.1% R.H., it was found to be necessary to provide greater thermal insulation of the rock salt windows from ambient temperature conditions, in order to prevent water vapour condensation on the inner faces of the rock salt windows. This was achieved by a reduction of the path length of each cell, so that each window was located closer to the cell centre and its temperature was effectively raised, thus alleviating the condensation problem. In practice, condensation could not be entirely prevented and measurements could not be made at R.H.'s in excess of 75.1%.

Samples of thin films of liquid water were prepared by exposing a cool CaF_2 disc to a stream of steam and rapidly sandwiching the resultant thin film of water with a further CaF_2 disc. The two discs were then sealed at the edges with apiezon sealing compound and the small sealed cell thus produced was then placed inside a heated cell. The apsorption and derivative spectra of the film of water were then recorded at a temperature of 44^{o}C. in both the 3 μm. (3333 $cm.^{-1}$) and 6 μm. (1667 $cm.^{-1}$) regions.

The absorption and derivative spectra of a thin film of ice at -80^{o}C. were recorded by utilising the cold cell described in Chapter 4. A mixture of 'dry ice' (solid CO_2) and acetone was used as a coolant in the Dewar part of the cell and a thin rock salt plate placed inside the cooled sample holder at the base of the Dewar. The Dewar was suspended inside the aluminium block fitted with rock salt windows and which contained a small dish of P_2O_5 to produce a dry atmosphere within the cell.

The Dewar part of the cell was removed from the block for just sufficient time for a thin film of ice to be deposited on the rock salt plate from the

FIG. 69A.

DERIVATIVE SPECTRA OF VISCOSE FILM AT INCREASING HUMIDITIES

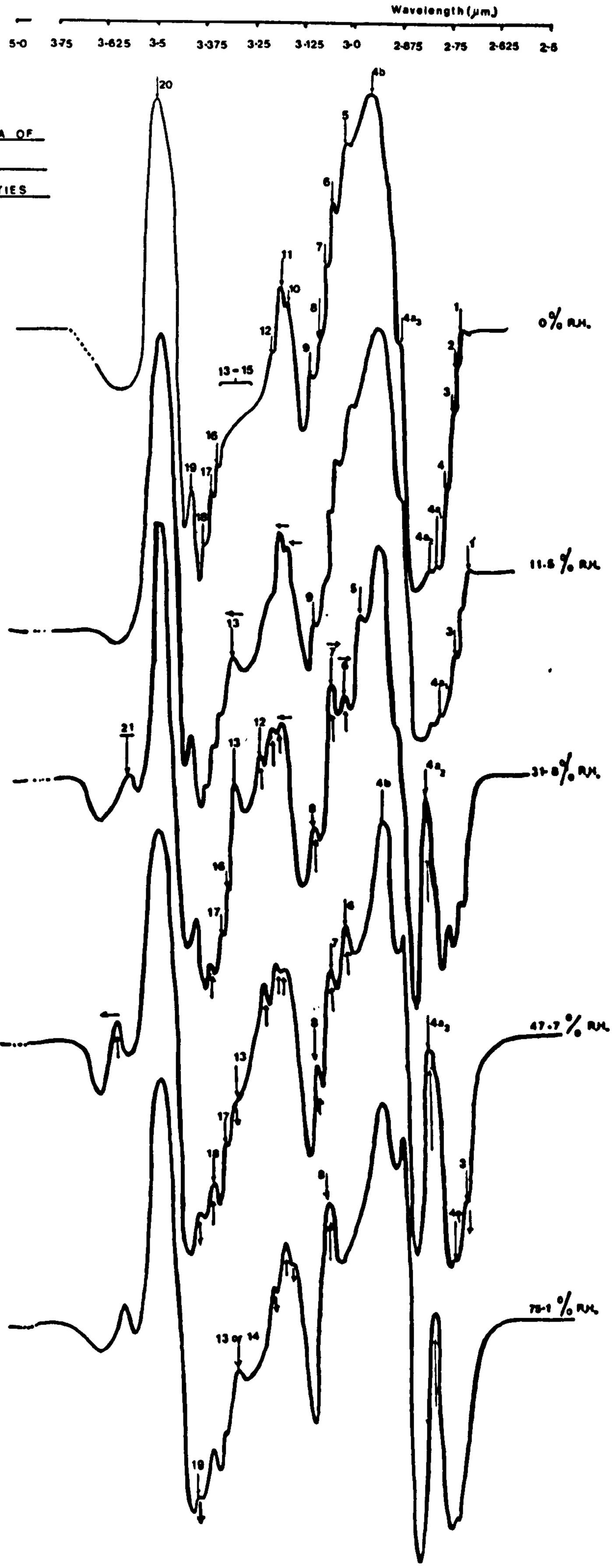

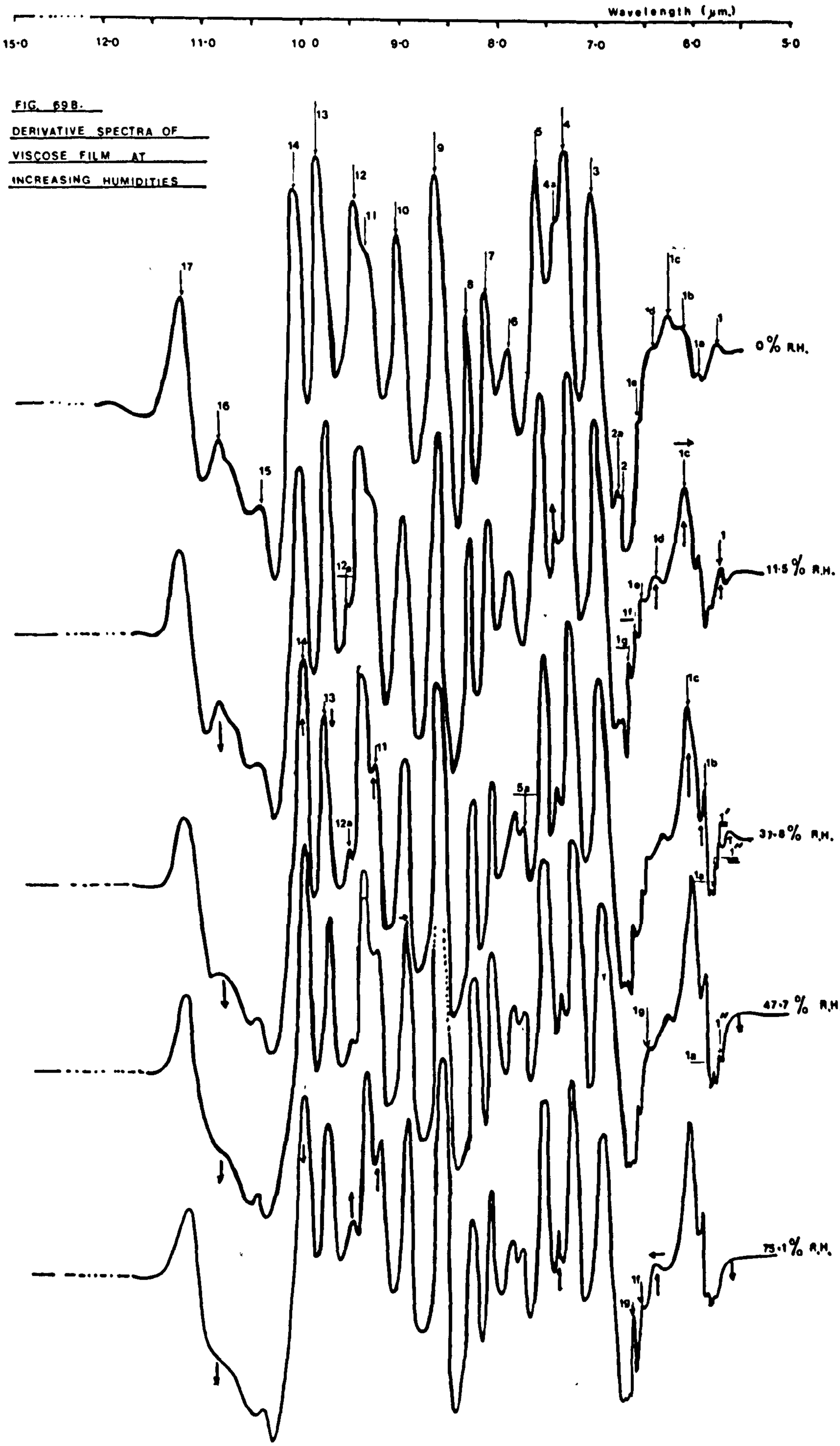

FIG. 69B.

DERIVATIVE SPECTRA OF VISCOSE FILM AT INCREASING HUMIDITIES

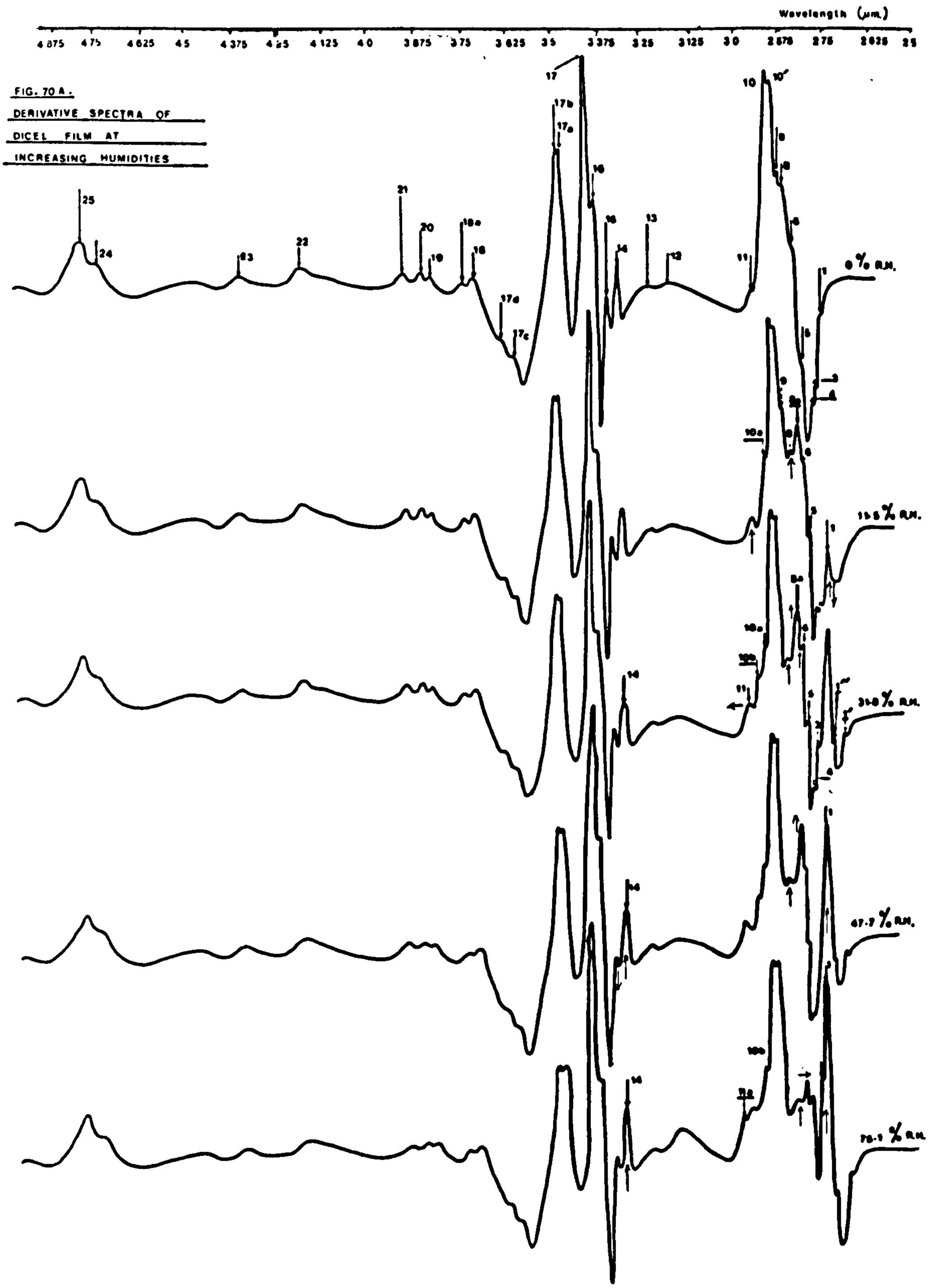
Wavelength (μm.)
4.875 4.75 4.625 4.5 4.375 4.25 4.125 4.0 3.875 3.75 3.625 3.5 3.375 3.25 3.125 3.0 2.875 2.75 2.625 2.5
FIG. 70 A.
DERIVATIVE SPECTRA OF DICEL FILM AT INCREASING HUMIDITIES
0 % R.H.
11.5 % R.H.
31.0 % R.H.
47.2 % R.H.
72.1 % R.H.

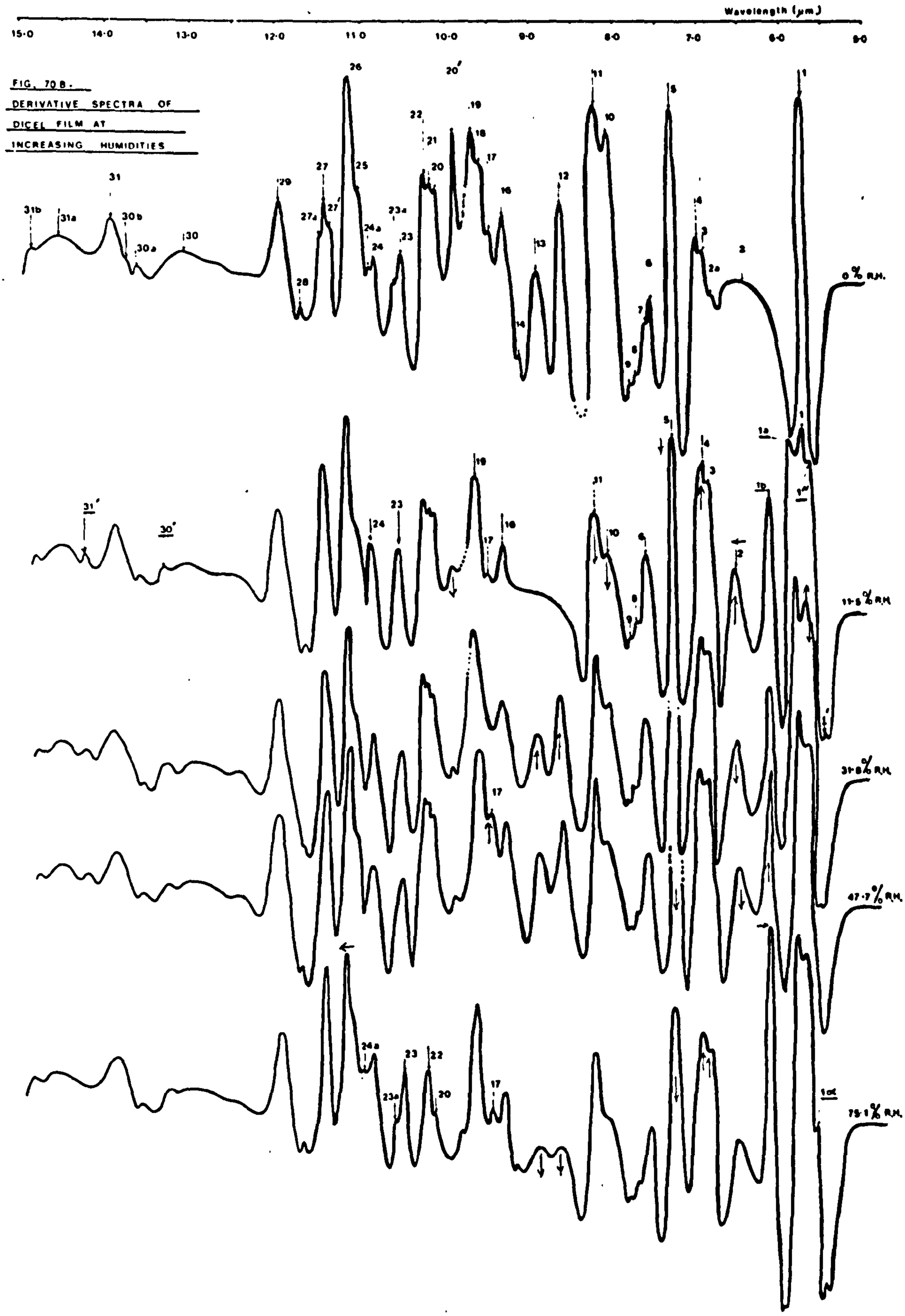

FIG. 70 B.

DERIVATIVE SPECTRA OF DICEL FILM AT INCREASING HUMIDITIES

FIG. 71 A.

DERIVATIVE SPECTRA OF TRICEL FILM AT INCREASING HUMIDITIES

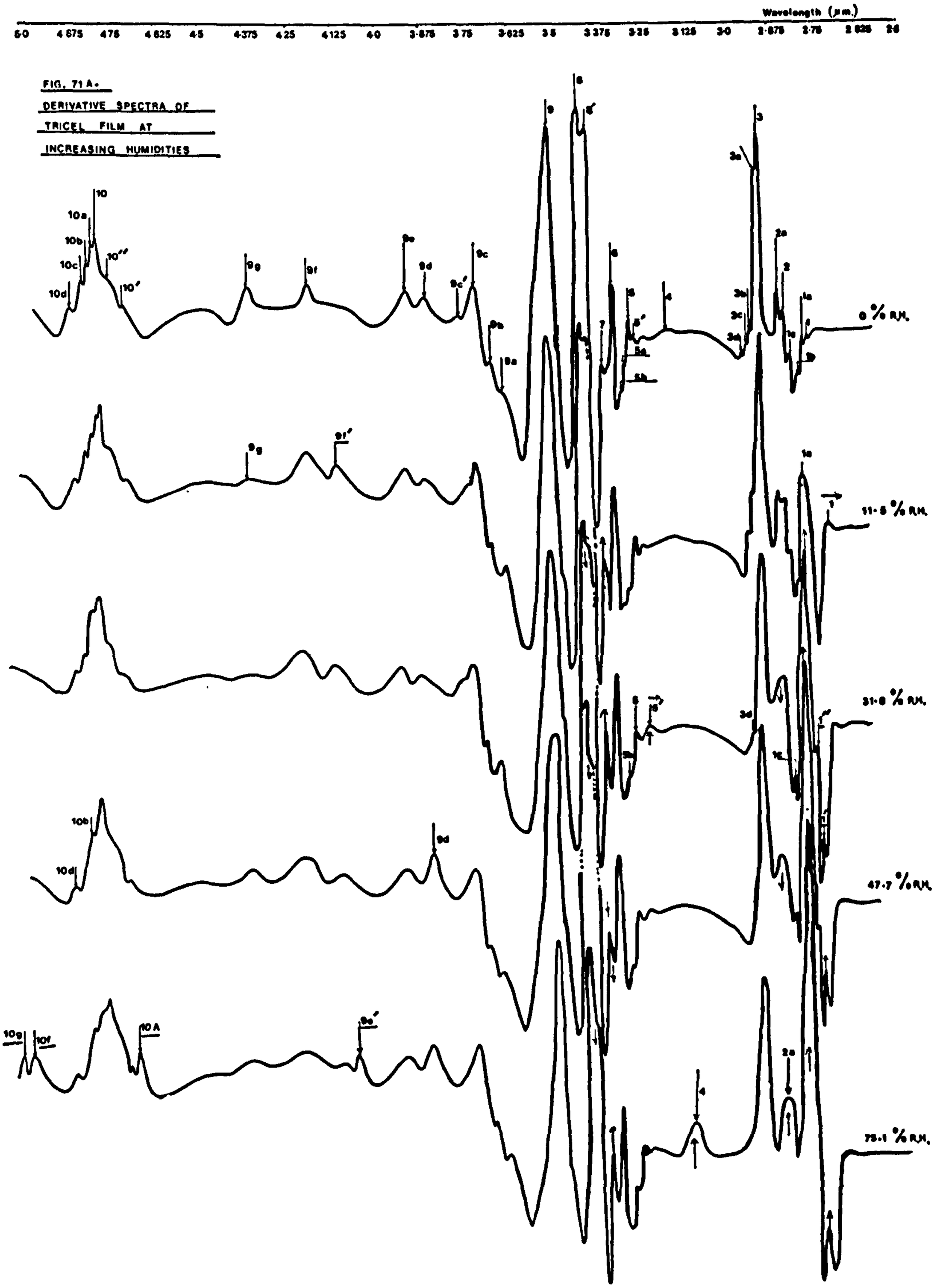

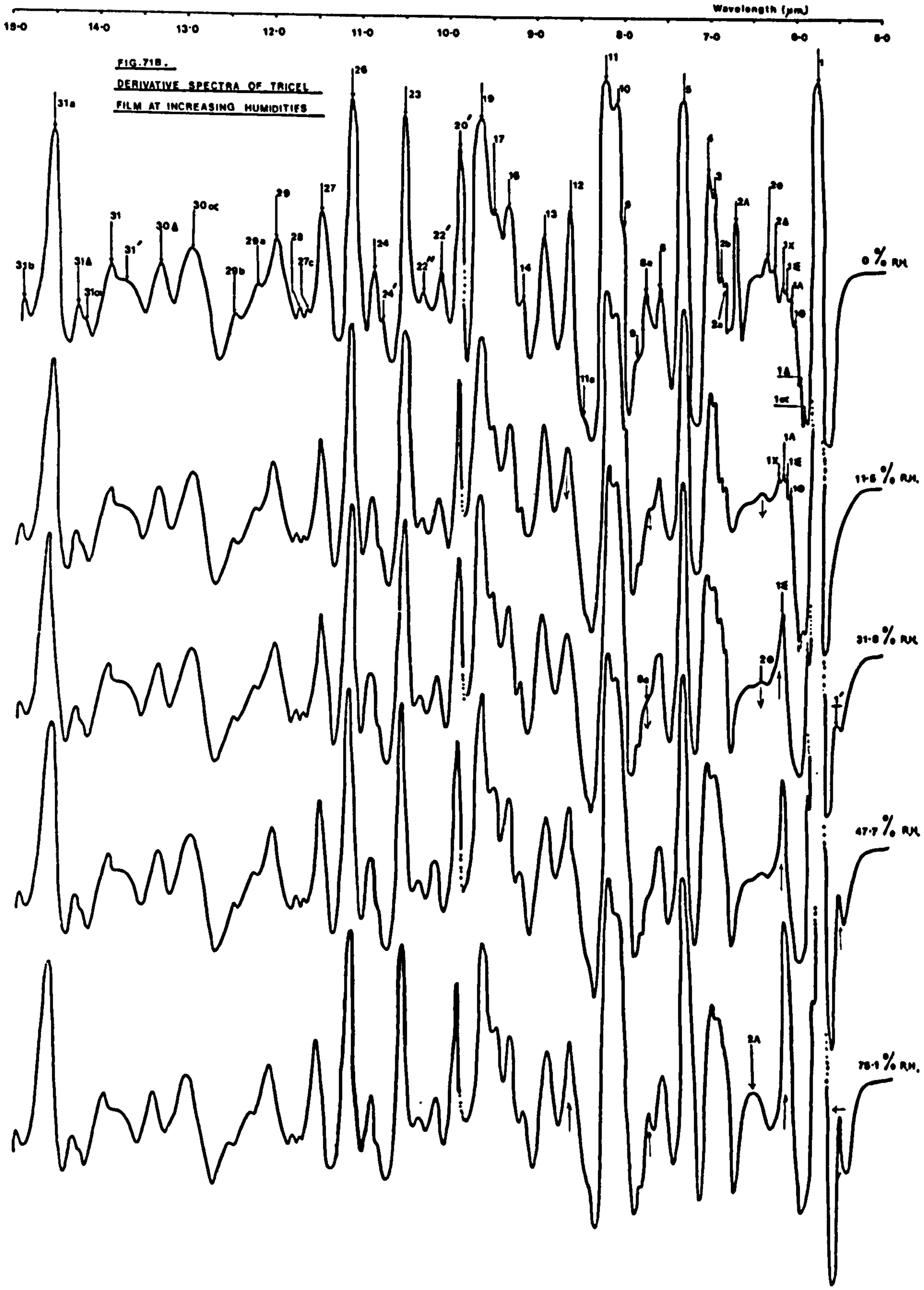
Wavelength (μm)
15·0
14·0
13·0
12·0
11·0
10·0
9·0
8·0
7·0
6·0
5·0
FIG.71B.
DERIVATIVE SPECTRA OF TRICEL FILM AT INCREASING HUMIDITIES
0 % R.H.
11·6 % R.H.
31·8 % R.H.
47·7 % R.H.
78·1 % R.H.

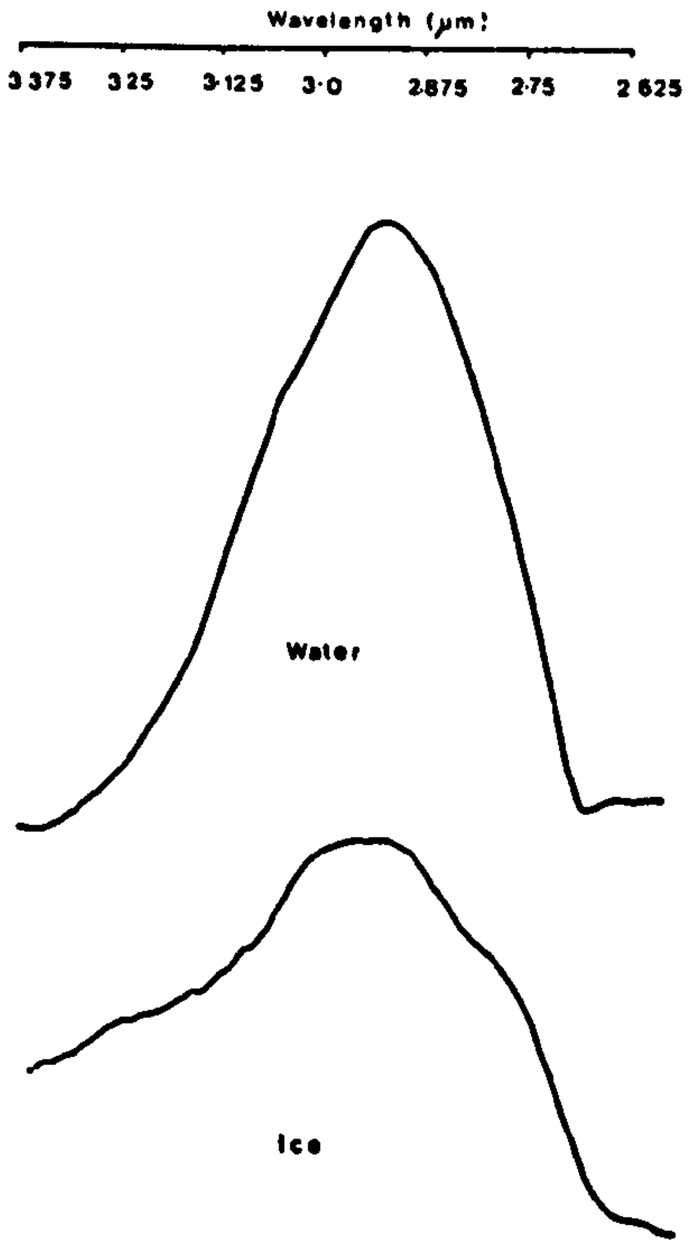

ABSORPTION SPECTRA

FIG. 72.

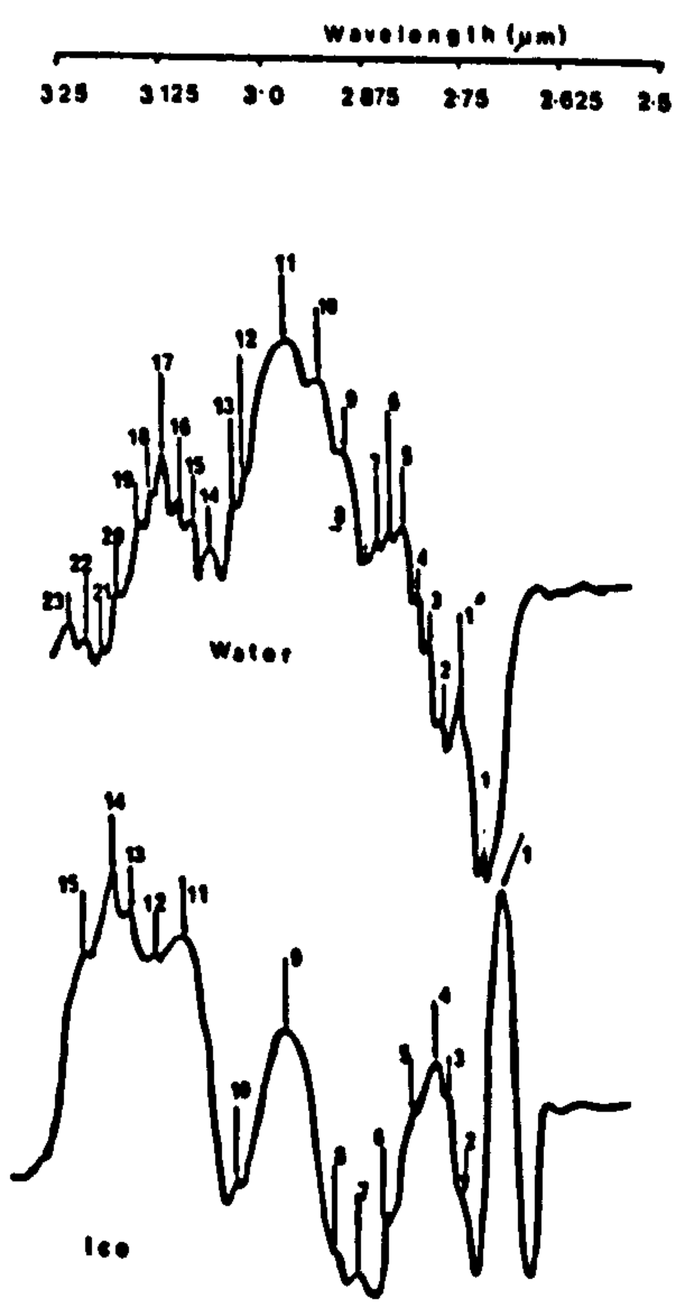

DERIVATIVE SPECTRA

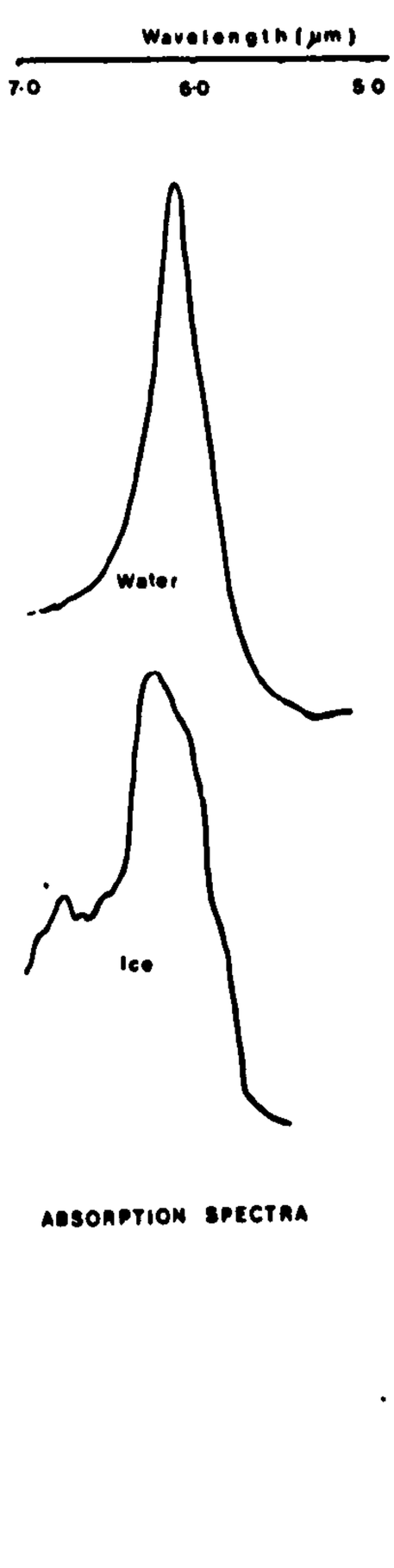

ABSORPTION SPECTRA

FIG. 73.

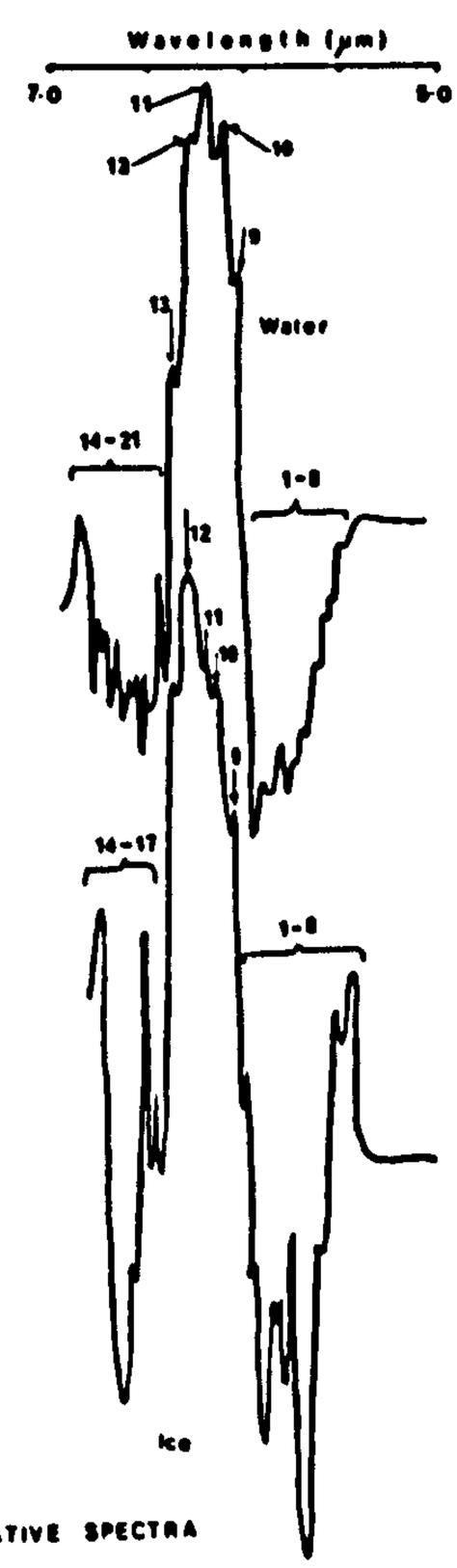

DERIVATIVE SPECTRA

TABLE XXV New Peaks

Fig.	Peak	Wavelength (μm.)	Wavenumber ($cm.^{-1}$)	Fig.	Peak	Wavelength (μm.)	Wavenumber ($cm.^{-1}$)	Fig.	Peak	Wavelength (μm.)	Wavenumber ($cm.^{-1}$)
69A(viscose)	21	3.557	2811	69B	1′	5.840	1712	71B	1′	5.535	1806
70A(dicel)	1′	2.6942	3712	(viscose)	1″	5.895	1696	(tricel)			
"	1″	2.7292	3664		1f	6.660	1502				
"	8a	2.8042	3566		1g	6.735	1485				
"					5a	7.850	1274				
	10a	2.9180	3427		12a	9.555	1047				
	10b	2.9355	3407								
	11a	2.9880	3347	70B							
				(dicel)							
71A(tricel)	1′	2.7090	3691		1′	5.455	1833				
	1″	2.7260	3668		1α	5.615	1781				
	9e′	4.0630	2461								
	9f′	4.090	2445		1″	5.635	1774				
	10∧	4.6695	2142		1a	5.890	1698				
	10f	4.9658	2014		1b	6.150	1620				
	10g	4.9883	2005		30′	13.365	748				
					31′	14.330	698				

TABLE XXVI

Fig.	Spectrum of:-	Peak	Wavelength (μm.)	Wavenumber ($cm.^{-1}$)	Fig.	Spectrum of:-	Peak	Wavelength (μm.)	Wavenumber ($cm.^{-1}$)
72	Water	1	2.7232	3672	73	Water	1	5.525	1810
		1′	2.7482	3639			2	5.585	1791
		2	2.7720	3608			3	5.620	1779
		3	2.7895	3588			4	5.650	1770
		4	2.8042	3566			5	5.695	1756
		5	2.8270	3537			6	5.760	1736
		6	2.8407	3520			7	5.840	1712
		7	2.8557	3502			8	5.940	1684
		8	2.8682	3487			9	6.030	1658
		9	2.8970	3452			10	6.075	1646
		10	2.9307	3412			11	6.150	1626
		11	2.9720	3365			12	6.275	1594
		12	3.0158	3316			13	6.360	1572
		13	3.0333	3297			14	6.440	1553
		14	3.0645	3263			15	6.530	1531
		15	3.0820	3245			16	6.575	1521
		16	3.0970	3229			17	6.615	1512
		17	3.1245	3201			18	6.680	1497
		18	3.1358	3189			19	6.735	1485
		19	3.1482	3176			20	6.760	1479

TABLE XXVI (continued)

Fig.	Spectrum of:-	Peak	Wavelength (μm)	Wavenumber (cm^{-1})	Fig.	Spectrum of:-	Peak	Wavelength (μm)	Wavenumber (cm^{-1})
72	Water	20	3.1707	3154	73	Water	21	6.845	1461
		21	3.1895	3135					
		22	3.2157	3110					
		23	3.2450	3082					
72	Ice	1	2.7070	3694	73	Ice	1	5.4700	1828
		2	2.7570	3626			2	5.5700	1795
		3	2.7808	3596			3	5.6550	1768
		4	2.7908	3583			4	5.8100	1721
		5	2.8132	3555			5	5.8650	1705
		6	2.852	3506			6	5.9050	1693
		7	2.8908	3459			7	5.9950	1668
		8	2.9170	3428			8	6.0250	1660
		9	2.9582	3380			9	6.1000	1639
		10	3.0358	3294			10	6.1850	1617
		11	3.1045	3221			11	6.2150	1609
		12	3.1385	3186			12	6.3150	1584
		13	3.1670	3157			13	6.4150	1559
		14	3.1870	3137			14	6.5150	1535
		15	3.2245	3101			15	6.5555	1525
							16	6.6150	1512
							17	6.7950	1472

atmosphere. The Dewar was then returned to the block so as to produce a closed cell system. The sample cavity was not evacuated to produce a perfectly sealed system on this occasion, since this would induce the sumblimation of ice from the surfaces of the rock salt plate. The complete cell was then placed in the sample cavity of the spectrometer and the absorption and second derivative spectra of the thin films of ice on either side of the rock salt plate recorded, in both the 3 μm.(3333 $cm.^{-1}$) and 6 μm. (1667 $cm.^{-1}$) regions of the spectrum.

6.3 Results

The second derivative spectra recorded at 44°C. within the range 0 - 75.1% R.H. are shown for viscose film in Figs. 69A and 69B, for dicel film in Figs. 70A and 70B and for tricel film in Figs. 71A and 71B. The absorption and second derivative spectra of water and of ice (under these conditions thought to be a mixture of hexagonal, I_h and cubic I_c ices, by Beaumont (139) are shown in the 3 μm. region in Fig. 72 and in the 6 μm. (1667 $cm.^{-1}$) region in Fig. 73.

In the spectra of viscose, dicel and tricel films, (Figs. 69A - 71B) any new peaks which occurred at increasing humidities were denoted as before by underlined labels e.g. peak 21 at 31.8% R.H. in Fig. 69A. The wavelengths and frequencies of these peaks are given in Table XXV. Spectra recorded at increasing humidities were compared, and any significant intensity changes which occurred were denoted by arrows ↑ for intensity increases and arrows ↓ for intensity decreases. Any increase or decrease in peak wavelength was similarly noted by arrows ← or → respectively.

The wavelengths and frequencies of all the peaks in the derivative spectra of water and ice are shown in Table XXVI. Any water or 'ice type' water peaks in the derivative spectra of viscose, dicel and tricel films which correspond to peaks in the derivative spectra of water and ice (Figs. 72 or 73) (or which are thought to be due to a state of absorbed water but not

TABLE XXVII

Peak (μm.,cm.$^{-1}$) in spectrum of Viscose film (Fig.69A)	Corresponding Peak (μm.,cm.$^{-1}$) in spectrum of Dicel film (Fig.70A)	Corresponding Peak (μm.,cm.$^{-1}$) in spectrum of Tricel film (Fig.71A)	Corresponding Peak (μm.,cm.$^{-1}$) in spectrum of Water (Fig.72)	Corresponding Peak (μm.,cm.$^{-1}$) in spectrum of Ice (Fig.72)
1 (2.7320,3660)	-	-		
-	1′(2.6942, 3712)	1′(2.7090, 3691)	-	1 (2.7070, 3694)
-	1″(2.7292, 3664)	1″(2.7260, 3668)	1 (2.7232, 3672)	
2 (2.7406, 3649)	1 (2.7455, 3669)	1 (2.7392, 3651)	1′(2.7482, 3639)	-
3 (2.7520, 3634)	3 (2.7680, 3613)	1a(2.7517, 3634)	-	-
4 (2.7720, 3620)	4 (2.7717, 3608)	1b(2.7642, 3618)	2 (2.7720, 3608)	-
4′ (2.7795, 3597)	-	-	possibly 2 (2.7720, 3608)	-
$4a_1$(2.7870, 3588)	-	-	3 (2.7895, 3588)	3 (2.7808, 3596)
4″ (2.7995, 3572)	8a(2.8042, 3566)	-		
$4a_2$(2.8158, 3551)	8 (2.8442, 3516)	2a(2.8217, 3544)		5 (2.8132, 3555)
4b (2.9120, 3434)	10′(2.8830,3469)	3 (2.8767, 3476)	9 (2.8970, 3452)	7 (2.8908, 3459)
	10 (2.8892,3461)	3a(2.8830, 3469)		
6 (3.0470, 3282)	-	-	possibly 13(3.033, 3297)	possibly 10(3.0358, 3294)
-	-			
	10a(2.9180,3427)	3b(2.9092, 3438)		possibly 8 (2.9170, 3428)
	10b(2.9355,3407)		possibly 10(2.9307,3412)	-
8 (3.0858, 3240)	11 (2.9292, 3414)	3c(2.9155, 3430)	13(3.0333,3297)	10(3.0358, 3294)
8b (3.0920, 3234)	-	-	16(3.0970,3229)	possibly 10(3.0358, 3294)

TABLE XXVII (continued)

Peak ($\mu m., cm.^{-1}$) in spectrum of Viscose film (Fig.69A)	Corresponding Peak ($\mu m., cm.^{-1}$) in spectrum of Dicel film (Fig.70A)	Corresponding Peak ($\mu m., cm.^{-1}$) in spectrum of Tricel film (Fig.71A)	Corresponding Peak ($\mu m., cm.^{-1}$) in spectrum of Water (Fig.72)	Corresponding Peak ($\mu m, cm^{-1}$) in spectrum of Ice (Fig.72)
-	-	3d(2.9242, 3420)	13(3.0333, 3297)	possibly 10(3.0358, 3294)
9 (3.1020, 3224)	-	-		
10 (3.1632, 3162)	12(3.1467, 3178)	4 (3.1492, 3176)	19(3,1482, 3176)	-
12 (3.1467, 3178)	-	-	possibly 19(3.1482, 3176)	-

TABLE XXVII (continued)

Peak (μm., cm.$^{-1}$) in spectrum of Viscose film (Fig.69B)	Corresponding Peak (μm., cm.$^{-1}$) in spectrum of Dicel film (Fig.70B)	Corresponding Peak (μm., cm.$^{-1}$) in spectrum of Tricel film (Fig.71B)	Corresponding Peak (μm., cm.$^{-1}$) in spectrum of Water (Fig.73)	Corresponding Peak (μm., cm.$^{-1}$) in spectrum of Ice (Fig.73)
	1′(5.455, 1833)	1′(5.535, 1806)	-	1 (5.4700)
	1α(5.615, 1781)	-	-	
	1″(5.635, 1774)		possibly 4 (5.650, 1770)	possibly 3 (5.6550, 1768)
1′ (5.840, 1712)			7 (5.840, 1712)	
1″ (5.895, 1696)	1a(5.890, 1698)		possibly 6 (5.9050, 1693)	-
		1α(5.9050, 1693)		6 (5.9050, 1693)
1a (5.985, 1671)		1A(5.9900, 1669)		-
		1e(6.050, 1653)		-
1b (6.140, 1629)		1Λ(6.0950, 1641)	possibly 10(6.075, 1646)	-
		1≤(6.1200, 1634)		-
possibly 1d (6.470, 1546)	1b(6.150, 1620)	1X(6.1600, 1623)	11(6.150, 1626)	possibly 10(6.1850, 1617)
		2A(6.2850, 1591)	12(6.275, 1594)	-
1c (6.310, 1585)	2 (6.485, 1542)	2e(6.3150, 1584)	possibly 13(6.360, 1572)	12(6.315, 1584)
1d (6.470, 1546)			possibly 14(6.440, 1553)	13(6.4150, 1559)
	2′(6.660, 1502)	2′(6.410, 1560)	-	-
		2 (6.5000, 1538)	15(6.5300, 1531)	possibly 14(6.515, 1535)
1e (6.625, 1509)			17(6.615, 1512)	-
1f (6.660, 1502)			possibly 18(6.680, 1497)	-
1g (6.735, 1485)			19(6.735, 1485)	-
2 (6.805, 1470) } 2a (6.835, 1465) }	2a(6.855, 1459)	2a(6.865, 1457)	possibly 21(6.845, 1461)	-
		2Λ(6.7100, 1490)	possibly 2I (6.845, 1461)	I7(6.7950, 1472)

present in the derivative spectra of water or ice) are shown in Table XXVII.

6.4 Discussion

The results of this chapter are discussed in two parts. Part I deals with all the peaks assigned to absorbed water in the derivative spectra of conditioned samples of viscose, dicel and tricel films (Figs. 69A - 71B), together with corresponding water peaks in the derivative spectra of water and ice (Figs. 72 and 73). Part II is concerned with the spectral changes which occur with increased humidity as a consequence of changes in the structure of viscose, dicel and tricel films and which are considered in terms of changes in intensity and wavelength of structural peaks.

6.4.1 Part I

6.4.1.1 Water Peaks in the Spectra of Viscose (Fig. 69A & 69B)

6.4.1.1.1 The 3 μm. (3333 $cm.^{-1}$) Region

In the spectra of viscose (Fig. 69A) in this region, certain water peaks, namely peaks 1 - 4 and 9, decrease in intensity throughout the humidity range or disappear at some point within the range. Peaks 1 - 4 were previously assigned to loosely bound water whereas peak 9 was previously assigned to more strongly bound water (Chapter 3). However, peaks $4a_2$ and 8, previously assigned to water with an 'ice type' structure, increase in intensity throughout the humidity range.

These results thus suggest that an increase in the R.H. (i.e. an increase in the amount of absorbed water) causes a reduction in the proportion of weakly bound water with a consequent decrease in the intensity or disappearance of peaks assigned to this state. A concomitant increase in the proportion of water with an 'ice type' structure also occurs. It is possible to explain these results if it is assumed that at low R.H.'s, a large proportion of the water present in viscose is present in the form of small groups of water molecules and these are associated with peaks 1 - 4 and 9. At higher

R.H.'s, however, more water molecules are absorbed and can associate with the water molecules already present to form larger clusters of water molecules, some of which have an 'ice type' structure. The number of water molecules present in viscose as individual or small groups of water molecules thus decreases and hence accounts for the decrease in the intensity or disappearance of peaks 1 - 4 and 9. As the number of groups of water molecules with an 'ice type' structure increases at higher R.H.'s, the increase in the intensity of peaks $4a_2$ and 8 which correspond to such water is thus accounted for.

Peaks 6 and 7 also previously assigned to strongly bound water increase in intensity up to 31.8% R.H. and this shows that some absorbed water goes into a strongly bound state up to 31.8% R.H. However, in the spectrum of visoose recorded at 47.7% R.H., these two peaks have disappeared. One possible explanation for this is that at a given R.H. between 31.8 and 47.7%, large numbers of cellulosic hydrogen bonds involving cellulosic OH and other cellulosic groups are broken. This allows large numbers of water molecules to penetrate the structure and form large groups of water molecules by associating with individual or small groups of water molecules already bound to the cellulose structure. This association thus reduces the number of individual or small groups of water molecules present in the viscose and hence accounts for the disappearance of peaks 6 and 7, which represent such individual or small groups of water molecules.

The breakage of cellulosic hydrogen bonds involving cellulosic OH groups is supported by the behaviour of peak 13. This crystalline peak represents cellulosic OH groups involved in hydrogen bonding and it decreases markedly in intensity as the R.H. is increased from 31.8 to 47.7%.

An alternative explanation for the behaviour of peaks 6 and 7 has however, been formulated. As the R.H. increases, further absorbed water molecules form hydrogen bonds with the cellulosic OH groups which are not involved (or only weakly involved) in hydrogen bonds with other cellulosic OH (or other cellulosic) groups, and a point is reached where saturation of

all the available cellulosic OH groups has occurred. At still higher humidities, further absorbed water molecules will tend to associate by hydrogen bonding to the cellulose bound water already present. Such association will tend to reduce the strength of cellulosic OH - bound water hydrogen bonds as is seen from the shift of peaks 6 and 7 to a lower wavelength between 11.5 and 31.8% R.H. However, a critical point is reached between 31.8 and 47.7% R.H. where the attraction between recently absorbed water molecules and cellulose bound water molecules becomes greater than the strength of cellulosic OH - bound water hydrogen bonds. The strongly cellulose bound water molecules may thus dissociate from the cellulosic OH groups at this point and associate with the newly absorbed water molecules to form larger groups of water molecules, some of which may have 'ice type' structures and correspond to peaks $4a_2$ and 8.

However, if this theory is correct, one would expect a shift to lower wavelength to be observed in some cellulosic OH peaks at R.H.'s above 11.5%, when hydrogen bonds between cellulosic OH groups and bound water become weaker and are eventually broken: but no such shift was observed. On the contrary, many cellulosic OH peaks, including peaks 4b, 11 and 13, shifted to a higher wavelength at higher R.H. 's. Furthermore, the first explanation can account for the bonding of 'ice type' groups of water molecules to cellulosic OH groups, discussed in Chapter 3 (page 68) whereas the second explanation cannot easily account for this. For these reasons the first explanation is the one which is most acceptable.

6.4.1.1.2 <u>The 6 μm. (1667 $cm.^{-1}$) Region</u>

In this region, the behaviour of water peaks in viscose (Fig.69B) is similar to that which occursin the 3 μm. (3333 $cm.^{-1}$) region, although some anomalies are noted in the 6 μm region. Peaks 1c and 1d, assigned to water with an 'ice type' structure, increase in intensity throughout the humidity range as do equivalent 'ice type' peaks in the 3 μm. (3333 $cm.^{-1}$) region. Of the new water peaks which occur in the 6 μm. (1667 $cm.^{-1}$) region, (1', 1", 1f

and 1g), peaks 1' and 1" are assigned to strongly bound water whereas peaks 1f and 1g are assigned to more weakly bound water. These new peaks appear between 0 and 31.8% R.H. but peaks 1' and 1f, together with peaks 1 and 1e, disappear between 31.8 and 75.1% R.H., in accord with the behaviour of corresponding peaks in the 3 μm.region. However, peaks 1b and 1g, which are also assigned to absorbed water, are anomalous in their behaviour in that they increase in intensity throughout the humidity range. It is possible that these peaks are associated with water which binds to water molecules already present in the cellulose structure.

6.4.1.2 Water Peaks in the Spectra of Dicel (Figs. 70 & 70B)

6.4.1.2.1 The 3 μm. (3333 $cm.^{-1}$) Region

In this region, the spectra of dicel do not show the same tendency of becoming simpler at increasing humidities as do the spectra of viscose (Fig.69A), where most peaks which correspond to loosely or strongly bound water disappear and several 'ice type' water peaks increase in intensity. However, peak 4 in the spectrum of dicel, previously assigned to loosely bound water, shows a similar behaviour to the corresponding peak, peak 4 in the spectrum of viscose (Fig.69A), which disappears at higher humidities, although in the case of dicel this peak does not disappear until a R.H. of 47.7% has been exceeded. Peak 10a, which is assigned to more strongly bound water (possibly water with an 'ice type' structure), also disappears above 47.7% R.H. The most notable features of the spectra are the large and steady increase of peak 1 assigned to loosely bound water throughout the humidity range, and the appearance of two new peaks: peak 1' (water possibly with an 'ice type' structure) and peak1"(loosely bound water). There are also small increases in the intensities of peaks 8 and 11 between 31.8 and 75.1% R.H. and these peaks were previously assigned to water with an 'ice type' structure. The different behaviour of dicel in this region may be due in part to the much lower regain of dicel compared with viscose and to the fact that at

higher humidities there are fewer new water molecules absorbed to compete with water molecules already present. It is also probably due in part to the fact that at very low regains some water molecules which are present in dicel are more strongly bound by hydrogen bonding to cellulosic OH groups than corresponding water molecules present in viscose. (This feature has been attributed to the atactic structure of dicel in Chapter 3 (page 75)). It is thus more difficult for water molecules which are absorbed by dicel at higher humidities to associate with water molecules already present by causing existing cellulosic OH - bound water hydrogen bonds to be broken. However, water molecules absorbed at higher humidities may associate by water - water hydrogen bonds with bound water already present by forming groups of bound water molecules, some with an 'ice type' structure, represented by peaks 1', 8 or 11.

6.4.1.2.2 The 6 μm. (1667 $cm.^{-1}$) Region

In this region, the unresolved group of water peaks which surround peak 2 (Fig. 70B) become more resolved with increasing R.H., i.e. increasing amounts of absorbed water, and many new peaks appear, namely peaks 1', 1", 1a, 1b and 1α, which represent OH bending modes of water. This higher resolution may be due in part to the disappearance of some bound water states which are reflected by the disappearance of some OH stretching mode peaks (e.g. peak 4 in Fig. 70A) in the 3 μm. (3333 $cm.^{-1}$) region.

Peak 2, which was previously assigned to water with an 'ice type' structure, becomes more clearly resolved in the spectrum recorded at 11.5% R.H. but decreases steadily in intensity between 11.5 and 75.1% R.H. It is possible that this intensity decrease is due to the transformation of the 'ice type' water which corresponds to peak 2 into a different 'ice type' structure at higher humidities, since peak 1b which also corresponds to water with an 'ice type' structure increases in intensity throughout the humidity range.

6.4.1.3 Water Peaks in the Spectra of Tricel (Figs. 71A & 71B)

6.4.1.3.1 The 3 μm. (3333 $cm.^{-1}$) Region

In the case of tricel, the behaviour of water peaks in this region is similar to viscose in that the spectrum becomes simpler due to the disappearance of many water peaks at increasing humidities. However, many 'ice type' water peaks, namely peaks 3a, 3b, 3c and 3d disappear, in addition to peaks assigned to loosely bound water, i.e. peaks 1, 1b and 1c.

The fact that many of the 'ice type' water peaks disappear at increasing humidities, i.e. when increasing amount of water are absorbed, may be attributed in part to the fact that the hydrogen bonding to cellulosic OH (or other cellulosic) groups by groups of water molecules which possess an 'ice type' structure, and which correspond to peaks 3a - 3d; is weaker than any hydrogen bonding between such 'ice type' groups of water molecules and cellulosic OH (or other) groups in viscose or dicel. It is thus possible that further water molecules absorbed by tricel at increasing humidities are able to break the hydrogen bonds between such groups of 'ice type' water molecules and cellulosic OH (or other) groups and form new groups of water molecules,.some of which may correspond to the 'ice type' water peak 1', since this peak increases in intensity at increasing R.H.'s.

The considerable increase in the intensity of peak 1a previously assigned to loosely bound water, with increasing humidity, is difficult to explain; but it is possible that this peak represents 'free' (i.e. non hydrogen bonded to cellulosic groups) water, which increases in amount with increasing R.H., since there are very few OH groups available in tricel to form strong hydrogen bonds with absorbed water. This assignment is also upheld by Whitaker (162), who found an equivalent non bound water peak in the derivative spectra of sections of horn keratin and wool fibres, conditioned at high R.H.'s.

Peak 2a was previously assigned to strongly bound water and also to

cellulosic OH groups involved in intramolecular hydrogen bonding. This peak decreases in intensity between 11.5 and 31.8% R.H., but increases in intensity between 31.8 and 75.1% R.H. The initial decrease in intensity may be attributed to a breakage of some intramolecular hydrogen bonds between cellulosic OH (and other) groups, whereas the later increase in intensity may be attributed to an increase in the amount of water with an 'ice type' structure and represented by peak 2a. An increase in the amount of 'ice type' water at higher R.H.'s is substantiated by the appearance of a new 'ice type' water peak, peak 1', (which corresponds to peak 1' in dicel). This peak also increases in intensity with increasing humidity, i.e. with increasing amounts of absorbed water.

Peak 4 was previously assigned to strongly bound water and increases in intensity between 47.7 and 75.1% R.H. It is possible that the breakage of cellulosic hydrogen bonds at a critical R.H. between 47.7 and 75.1%, (i.e. when a critical amount of water has been absorbed), allows water to penetrate the tricel structure, including 'crystalline' regions, and become strongly bound in the same state as other water molecules which correspond to peak 4. This accounts for the increase in the intensity of peak 4 between 47.7 and 75.1% R.H.

From the behaviour of all the water peaks in tricel in this region, it is clear that the ratio of the amount of water with an 'ice type' structure: 'free' or bound water is greater in viscose than in tricel.

6.4.1.3.2 <u>The 6 μm. (1667 $cm.^{-1}$) Region</u>

In this region, the behaviour of water peaks which correspond to OH bending modes is very similar to that of the OH stretching modes of water in the 3 μm. (3333 $cm.^{-1}$) region. Spectra again become simpler as more water is absorbed at higher R.H.'s, and many water peaks disappear. Peaks 1α and 1Δ associated which correspond to 'ice type' water and strongly bound water respectively disappear between 11.5 and 31.8% R.H. and between 0 and 11.5% R.H. respectively; while peaks 1θ, 1Λ and 2Δ, associated with slightly

less strongly bound water disappear between 11.5 and 31.8% R.H. Peak 1X, which also represents water with an 'ice type' structure, also disappears between 11.5 and 31.8% R.H., whereas the 'ice type' water peak 2θ disappears between 47.7 and 75.1% R.H.

A further 'ice type' water peak, peak 2Λ , disappears between 0 and 11.5% R.H., but re-appears at 75.1% R.H. This behaviour is difficult to explain, but since this peak occurs at such a high wavelength it is possible that it represents groups of water molecules which are not bound, or only loosely bound, to cellulosic OH groups. As water molecules are absorbed at increasing R.H., they are able to interact with groups of water molecules represented by peak 2Λ to form new 'ice type' groups of molecules possible represented by peak 1', a new 'ice type' water peak which appears at 31.8% R.H. and which increases in intensity at higher R.H.'s. The disappearance of peak 2Λ between 0 and 11.5% R.H. is thus accounted for. The re-appearance of this peak between 47.7 and 75.1% R.H. is, however, more difficult to explain, but it is possible that when a critical amount of water has been absorbed, some reorganisation of the states of bound water occurs, possibly as a result of some structural changes occurring within the tricel, so that groups of water molecules with an 'ice type' structure represented by peak 2Λ re-appear.

Peak 1≤ , representing strongly bound water, is most significant in that its intensity increases enormously between 11.5 and 75.1% R.H. It is thus probable that the simplification of spectra observed at increasing R.H.'s is due to a large proportion of the water already present at 0% R.H. and absorbed at higher R.H.'s going into the bound state represented by peak 1≤ .

6.4.2 Part II

6.4.2.1 Structural Peaks in the Spectra of Viscose (Figs. 69A & 69B)

6.4.2.1.1 The 2.5 - 5 μm. (4000 - 2000 $cm.^{-1}$) Region

In this region, the most significant change is the disappearance of peak 5 on changing the R.H. from 31.8 to 47.7%. This peak has been previously assigned to a stretching mode of OH groups involved in intermolecular hydrogen bonding, and its disappearance upholds the proposal of Part I concerning the large scale breakage of hydrogen bonding at a critical humidity between 11.5 and 31.8% R.H., i.e. when a critical amount of water has been absorbed.

However, peak 11, which was also assigned to intermolecularly hydrogen bonded OH groups (C_6 OH..oxygen bridge), does not show a similar behaviour to peak 5, but shows a slight intensity increase within this humidity range. It is possible to explain the behaviour of peak 11 if it is associated with a stretching vibration of C_6OH groups which are strongly hydrogen bonded, i.e. after formation of a 'double' hydrogen bond or an inter chain hydrogen bond with other cellulosic OH groups. This is contrary to the suggestion of Marchessault (78-80) that this peak represents C_6OH groups intermolecularly hydrogen bonded with oxygen bridge atoms of neighbouring chains. The possibility of 'double' hydrogen bonding was in fact suggested by Marchessault, but was not attributed by him to any particular peak. The assignment of peak 11 to strongly hydrogen bonded OH groups is also upheld by the fact that peak 11 occurs at a much higher wavelength than peak 5.

Peak 13 was also attributed to intermolecularly hydrogen bonded OH groups, and is similar to peak 5 in its behaviour in that it almost disappears between 31.8 and 47.7% R.H., although it had previously increased in intensity between 0 and 31.8% R.H. Since this peak represents OH groups primarily of 'crystalline' material, it is possible that the initial increase in the intensity of this peak may be caused by the addition of further water to the viscose to allow the reorganisation of some 'crystallizable' material to a 'crystalline' structure. However, above 31.8% R.H., many of the cellulosic hydrogen bonds involving OH groups which correspond to peak 13 may be broken due to competition from large numbers of water molecules, (as described in

section I in the context of water peaks 6 and 7), thus accounting for the decrease in intensity of peak 13 above 31.8% R.H.

The crystallization of some 'crystallizable' material into 'crystalline' material is upheld by the fact that the 'crystalline' peak 18, previously assigned to CH or CH_2 stretching vibrations, increases in intensity at increasing R.H.'s, whereas peak 19, which is a 'crystallizable' CH peak, decreases in intensity at increasing humidities . Such a possibility is upheld by the role of water in the crystallization of polyamides studied recently by Hallos (173).

A new peak, peak 21 (3.557 μm, 2811 $cm.^{-1}$) has been assigned to a CH stretching vibration from structural assignment tables (3 - 5). It is probable that this peak represents a state in which CH groups are strongly hydrogen bonded to absorbed water, and this is supported by the fact that this peak occurs at a higher wavelength than any other CH stretching peaks in this region. The fact that this peak only becomes apparent in the spectra recorded at 31.8% R.H. and higher humidities may be attributed to the fact that absorbed water has a greater affinity for OH and CO groups, and only when most of the available OH or CO groups have been saturated by hydrogen bonding to absorbed water can further water molecules absorbed at higher R.H.'s begin to bind by hydrogen bonding to CH groups.

6.4.2.1.2 <u>The 5 - 15 μm. (2000 - 667 $cm.^{-1}$) Region</u>

In this region, there are fewer changes in structural peaks than in the 3 μm. (3333 $cm.^{-1}$) region. However, peak 4a, which was previously assigned to the OH bending mode of 'non crystallizable' material, shows a steady intensity increase throughout the humidity range. It is possible to explain this behaviour in terms of increasing amounts of water in the viscose film which enable structural changes to occur so that the structure typified by peak 4a is present, although on the basis of annealing treatments the

material represented by peak 4a was classified as 'non crystallizable'. This explanation may also apply to the new peaks 5a and 12a, which can be assigned to C-O stretching vibrations from structural assignment charts.

The increase in the intensity of the 'crystalline' C-O peak, peak 14, and the decrease in the intensity of peak 16, a 'crystallizable' C-O peak, also upholds the proposal that some 'crystallizable' material is converted into 'crystalline' material at increasing R.H.'s, i.e. when increasing amounts of water are absorbed. However, peak 11 exhibits an anomalous behaviour in that it has been classed as a 'crystallizable' C-O peak and yet increases in intensity from 11.5 to 75.1% R.H.

6.4.2.2' Structural Peaks in the Spectra of Dicel (Figs. 70A & 70B)

6.4.2.2.1 The 2.5 - 5 μm. (4000 - 2000 $cm.^{-1}$) Region

In this region there are, as expected, fewer significant changes in structural peaks than in the spectra of viscose (Fig.69A). However, peak 5 disappears between 47.7 and 75.1% R.H. and peak 9 disappears between 11.5 and 31.8% R.H., both bands being assigned to intramolecularly hydrogen bonded OH groups. Peaks 10 and 10', which also represent intramolecularly hydrogen bonded OH groups, also decrease in intensity between 47.7 and 75.1% R.H. The changes in these four peaks indicate that absorbed water does cause some hydrogen bonds to be broken at critical humidities (or over critical humidity ranges), i.e. when critical amounts of water have been absorbed, as in the case of viscose. However, in the case of dicel, intramolecular hydrogen bonds are broken, whereas in viscose, intermolecular hydrogen bonds were broken.

The fact that some intramolecular hydrogen bonds involving cellulosic OH groups are broken by absorbed water in dicel, but not in viscose, may be accounted for in part by the atactic structure of dicel. This structure prevents a regular sequence of strong intramolecular hydrogen bonds from

being formed, so that any intramolecular hydrogen bonds formed by OH groups are weaker than the equivalent hydrogen bonds in viscose.

The 'non crystallizable' peaks 14 and 15, which represent stretching modes of acetyl CH_3 groups, increase and decrease in intensity respectively between 31.8 and 47.7% R.H. This behaviour can be explained if one assumes that peak 14 represents acetyl CH_3 groups which are not involved in hydrogen bonding with cellulosic OH (or CO) groups, whereas peak 15 represents acetyl CH_3 groups which are involved in such hydrogen bonding. This assumption is upheld by the fact that peak 15 occurs at a higher wavelength than peak 14. As further water molecules are absorbed by dicel at increasing humidities up to 47.7% R.H., they become attached to cellulosic OH or CO groups by hydrogen bonding and effectively reduce the number of hydrogen bonds between cellulosic CH_3 and OH groups, thus producing more 'free' (non hydrogen bonded to cellulosic OH) CH_3 groups. Hence peak 15, which arises from CH_3 groups hydrogen bonded to cellulosic OH (or CO) groups, decreases in intensity, whereas peak 14, which is associated with non hydrogen bonded ('free') CH_3 groups, increases in intensity.

When considering all the dicel spectra in this region, the fact that there are no significant increases in the intensities of 'crystalline' peaks or decreases in the intensities of 'crystallizable' peaks at higher R.H.'s suggests that increasing amounts of absorbed water do not cause the conversion of some 'crystallizable' material to 'crystalline' material to occur. This is as expected, since it has already been shown that the energy difference (i.e. difference in structure) between 'crystalline' and 'crystallizable' regions is much smaller in dicel than in viscose or tricel.

6.4.2.2.2 <u>The 5 - 15 μm. (2000 - 667 $cm.^{-1}$) Region</u>

In this region, there are a few changes in structural peaks which are of significance (Fig.70B). Peaks 3 and 4, which are assigned to CH_2 bending vibrations, increase in intensity markedly between 0 and 11.5% R.H.

It is possible to explain this increase by attributing these peaks to 'free' (non hydrogen bonded to cellulosic OH) CH_2 groups, which increase in number at increasing humidities, (cf. the explanation for peak 14, Fig.70A). Similarly, it is possible to explain the decrease in the intensity of peak 5 at increasing humidities, by suggesting that this band is associated with hydrogen bonded CH_2 groups, although the occurrence of peak 5 at a higher wavelength than peaks 3 and 4 is then anomalous.

Peaks 10 and 11, previously assigned to CO stretching vibrations, decrease markedly in intensity between 0 and 11.5% R.H., and this suggests that these two peaks arise from CO groups which are not hydrogen bonded to absorbed water. As further water molecules are absorbed between 0 and 11.5% R.H., the number of CO groups which correspond to peaks 10 and 11 and which are not hydrogen bonded to absorbed water decreases, thus accounting for the decrease in the intensity of these peaks. The fact that there is no subsequent increase in the intensity of these peaks at higher R.H.'s shows that the strength of hydrogen bonding between water and these CO groups is strong enough to resist competition from further water molecules absorbed at higher humidities. However, such competition is probably effective in the case of the CO groups assigned to peaks 23a and 24a (also not involved in hydrogen bonding to absorbed water), since although these peaks disappear between 0 and 11.5% R.H., they re-appear in the spectrum recorded at 75.1% R.H. Peak 19 may be assigned to CO groups which are strongly involved in hydrogen bonding to absorbed water, since this peak shows a steady intensity increase throughout the humidity range.

The sudden disappearance of peaks 12 and 13, which are assigned to bridge oxygen atom stretching (C - O - C stretching) and ring stretching respectively, and their appearance with varying intensities at subsequent humidities, is very difficult to explain. However, it is possible that this behaviour is due to variations in bonding with OH groups, which occur at different humidities.

6.4.2.3 Structural Peaks in the Spectra of Tricel (Figs.71A & 71B)

6.4.2.3.1 The 2.5 - 5 μm. (4000 - 2000 $cm.^{-1}$) Region

In this region, increasing the R.H. produces many more changes in the structural peaks of tricel (and viscose) than in dicel. This is expected, since the difference in energy (structure) between 'crystalline' and 'crystallizable' regions is greater in tricel (and viscose) than in dicel. In the spectra of tricel, peaks 2 and 3a disappear between 11.5 and 31.8% R.H. and between 0 and 11.5% R.H. respectively. Since these peaks represent stretching modes of OH groups involved in intermolecular and intramolecular hydrogen bonding respectively, their disappearance shows that increasing amounts of absorbed water cause the disruption of some hydrogen bonds, of cellulosic OH groups, within the tricel structure.

Peak 5a ('crystallizable' CH, CH_2 or CH_3 groups) and peaks 8' and 8 ('crystallizable' CH groups) disappear or decrease in intensity throughout the humidity range. Since these peaks represent 'crystallizable' material, it is possible to explain their behaviour by suggesting that some 'crystallizable' material is converted into 'crystalline' material at increasing humidities.

Another explanation for the nature of these bands is that they represent CH, CH_2 or CH_3 groups involved in hydrogen bonding to cellulosic OH (or CO) groups. The behaviour of these bands may be explained in terms of a greater number of water molecules being absorbed at higher humidities as they hydrogen bond to cellulosic OH (or CO) groups and thus break the weaker hydrogen bonds between CH, CH_2 or CH_3 groups and cellulosic OH (or CO) groups. Hence the peaks which correspond to CH, CH_2 or CH_3 groups hydrogen bonded to cellulosic OH (or CO) groups i.e. peaks 5a, 8' and 8, decrease in intensity or disappear at increasing humidities.

However, as hydrogen bonds between CH and OH (or CO) groups are broken

at higher humidities, more 'free' groups (non hydrogen bonded to cellulosic OH or CO groups) are formed. The increase in the intensity of peak 7 with increasing R.H. could thus be accounted for if this peak corresponds to vibrations of 'free' CH groups (of acetyl groups). However, it could also be argued that the increase in the intensity of peak 7 at increasing humidites is due to an increase in the amount of 'crystalline' material, since peak 7 was previously classed as a 'crystalline' peak.

Either or both of the explanations given for peaks 5a, 8' and 8 could also apply to peaks 10a and 10e, which represent CO stretching vibrations of acetyl groups and which disappear between 11.5 and 31.8% R.H. and between 31.8 and 47.7% R.H. respectively. It is not possible at this point to decide which of the two explanations is the most probable, since in the case of tricel both processes of breakage of weak CH .....cellulosic OH (or CO) hydrogen bonds or the crystallization of some 'crystallizable' material could occur concurrently. However, the second explanation involving the breakage of weak CH .....cellulosic OH (or CO) hydrogen bonds by absorbed water also applies to the case of dicel, i.e. to peaks 14 and 15 (Fig.70A), in the spectra of dicel recorded at increasing humidities in the 2.5 - 5 μm. (4000 - 2000 $cm.^{-1}$) region. The first explanation involving the crystallization of some 'crystallizable' material cannot be applied to these peaks in dicel.

Several new peaks (9e', 10$\wedge$ and 10g) appear in the spectrum of tricel recorded at 75.1% R.H. and a single new peak, peak 9f', occurs in the spectrum recorded at 11.5% R.H. These peaks may be attributed to the appearance of one or more new states of acetyl CH groups hydrogen bonded to absorbed water in the case of peaks 9e' and 9f', or to one or more new states of acetyl CO groups, hydrogen bonded to absorbed water, in the case of peaks 10$\wedge$, 10f and 10g. The fact that no equivalent peaks are found in the spectra of dicel also supports the contention that more structural changes occur in tricel than in dicel at increasing humidities.

6.4.2.3.2 The 5 - 15 μm. (2000 - 667 $cm.^{-1}$) Region

In this region, there are fewer changes in the structural peaks with increasing humidity than in the 2.5 - 5 μm. (4000 - 2000 $cm.^{-1}$) region. However, peaks 2a and 2b, which are assigned to bending modes of cellulosic OH groups (intermolecularly hydrogen bonded in the case of peak 2a, not specified for peak 2b), disappear between 31.8 and 47.7% R.H.. This indicates that some hydrogen bonds involving cellulosic OH groups are disrupted when a critical amount of water has been absorbed as in the case of viscose and dicel.

Peak 8a, which represents a bending mode of CH_2 groups of 'crystallizable' material, decreases in intensity between 11.5 and 31.8% R.H., and this indicates that the structure is in part converted from 'crystallizable' to 'crystalline' when more water molecules are absorbed by the tricel as the humidity increases, although this peak does increase slightly in intensity between 47.7 and 75.1% R.H. Peak 10 behaves similarly to peak 10 of the dicel spectra (Fig.70B) and decreases in intensity throughout the humidity range. This peak thus represents a stretching vibration of CO groups, and the decrease in its intensity may be similarly accounted for by assigning the peak to CO groups not involved in hydrogen bonding with absorbed water.

CHAPTER 7

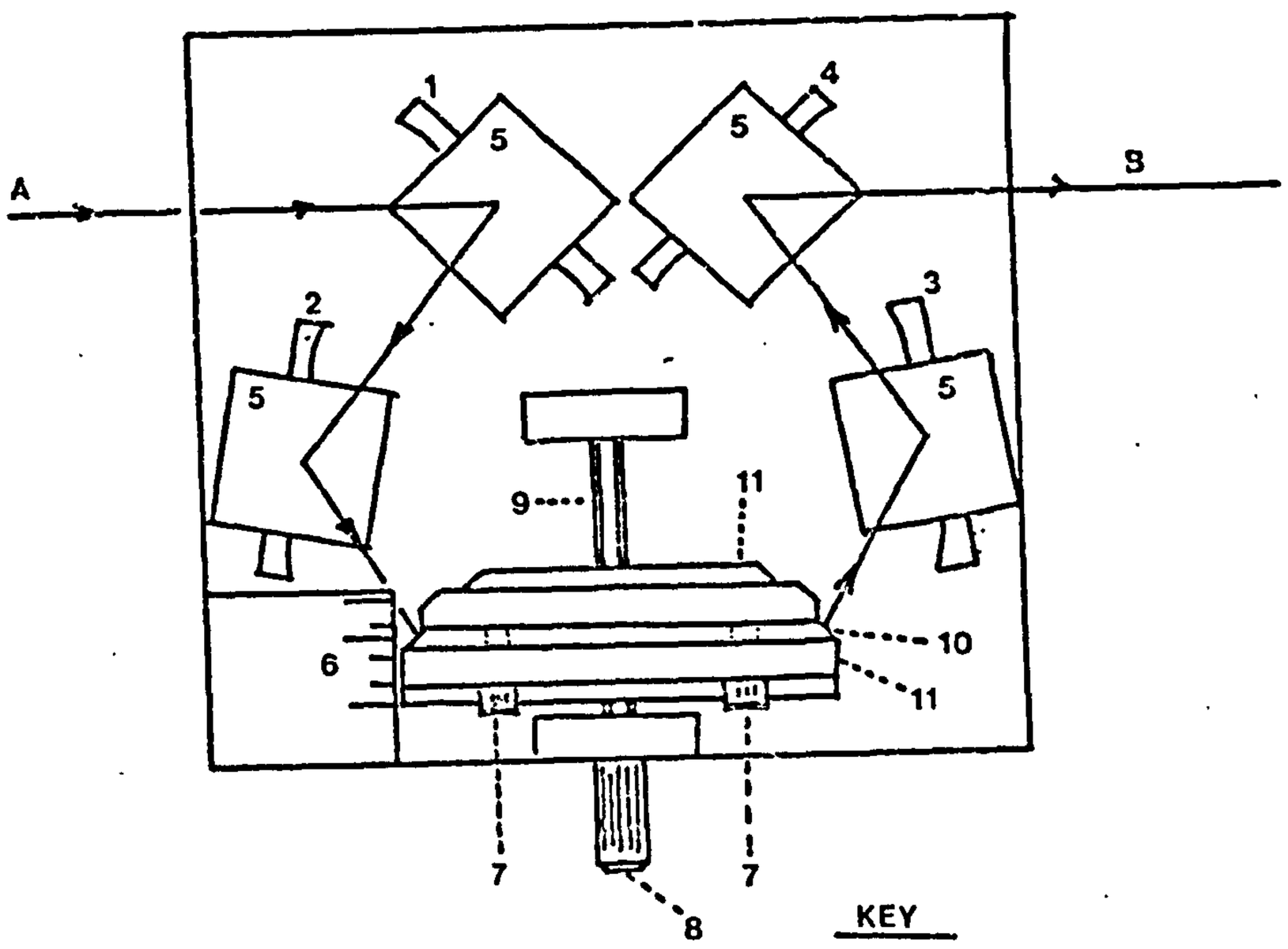

KEY

1 - 4 :- Face Silvered Concave Mirrors

5 :- Rotatable Mountings

6:- Scale

7:- Screws Holding Crystal Between Metal Plates

8:- Screw to Adjust Position of Crystal

9:- Threaded Track.

10:- Crystal

11 :- Metal Plates

A ⟶ B :- Path of Infrared Radiation

FIG. 74

CHAPTER 7

A.T.R. SPECTRA OF VISCOSE, DICEL AND TRICEL FILMS

7.1 Introduction

Using the technique of attenuated total reflection spectroscopy (A.T.R.), the surface structures of viscose, dicel and tricel films have been examined. Differences were assessed where possible, on comparison with derivative spectra (i.e. of all the material in a particular film) previously recorded and where possible these were related to direct observations of the surface topography of viscose, dicel and tricel films obtained from the use of scanning electron microscopy.

7.2 Method

The method and principles of A.T.R. spectroscopy are well documented (201, 202) and will not be discussed in detail here. However, a diagram of the A.T.R. unit used is shown in Fig.74. An identical unit was used in the reference beam during the recording of spectra to equalise the path length of sample and reference beams.

Samples of viscose film, conditioned in the atmosphere (approximately 50% R.H.) were placed on either side of the KRS sample crystal, with the mirrors adjusted so as to give maximum transmission through the sample crystal. Attempts were then made to record absorption spectra of the film in both the 2.5 - 5 μm. (4000 - 2000 $cm.^{-1}$) and 5 - 15 μm. (2000 - 667 $cm.^{-1}$) regions, but in both cases no spectrum was obtained, due to the large reduction in the intensity of the infra-red beam by the A.T.R. units. However, increasing the spectrometer gain caused the spectrometer performance to be regained. Unfortunately, the spectra produced under such 'high gain' conditions were 'noisy' and only the major peaks were reproducible. Such a high 'noise' level was also unacceptable to the differentiator, so that it was not

FIG. 75

DERIVATIVE SPECTRUM OF VISCOSE FILM (1).

A.T.R. " " " SURFACE (2)

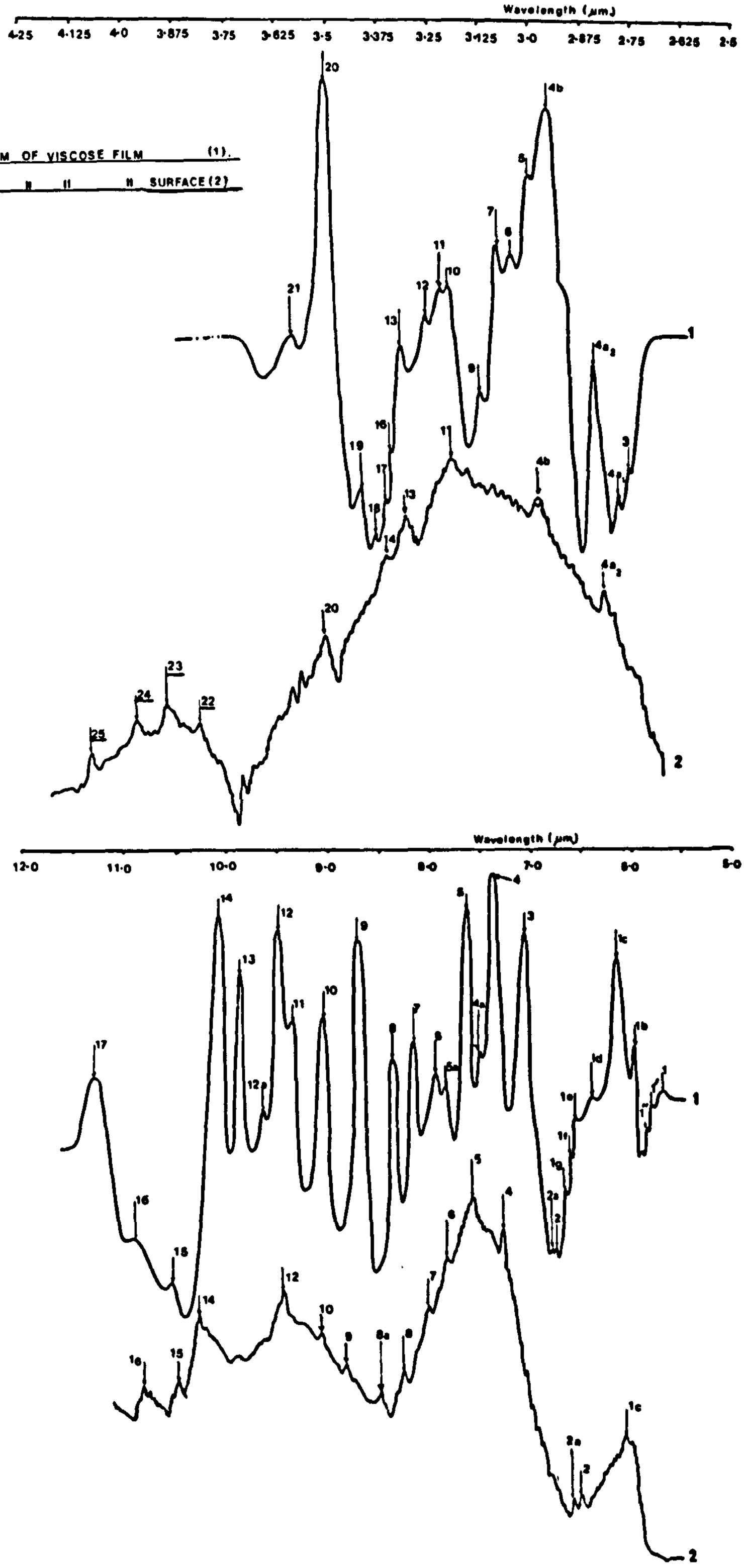

FIG. 76

DERIVATIVE SPECTRUM OF DICEL FILM (1)

A.T.R. " " " " SURFACE (2)

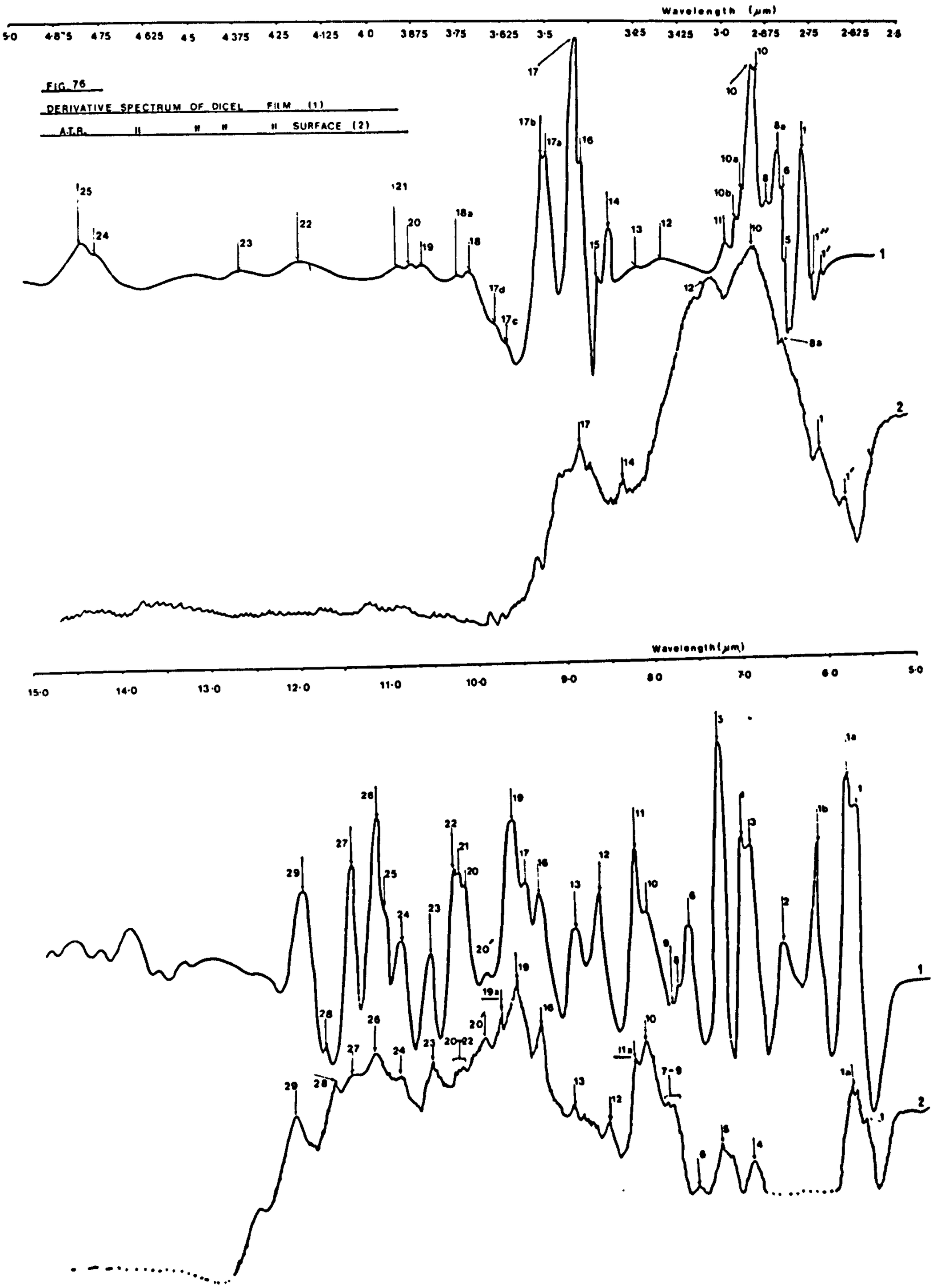

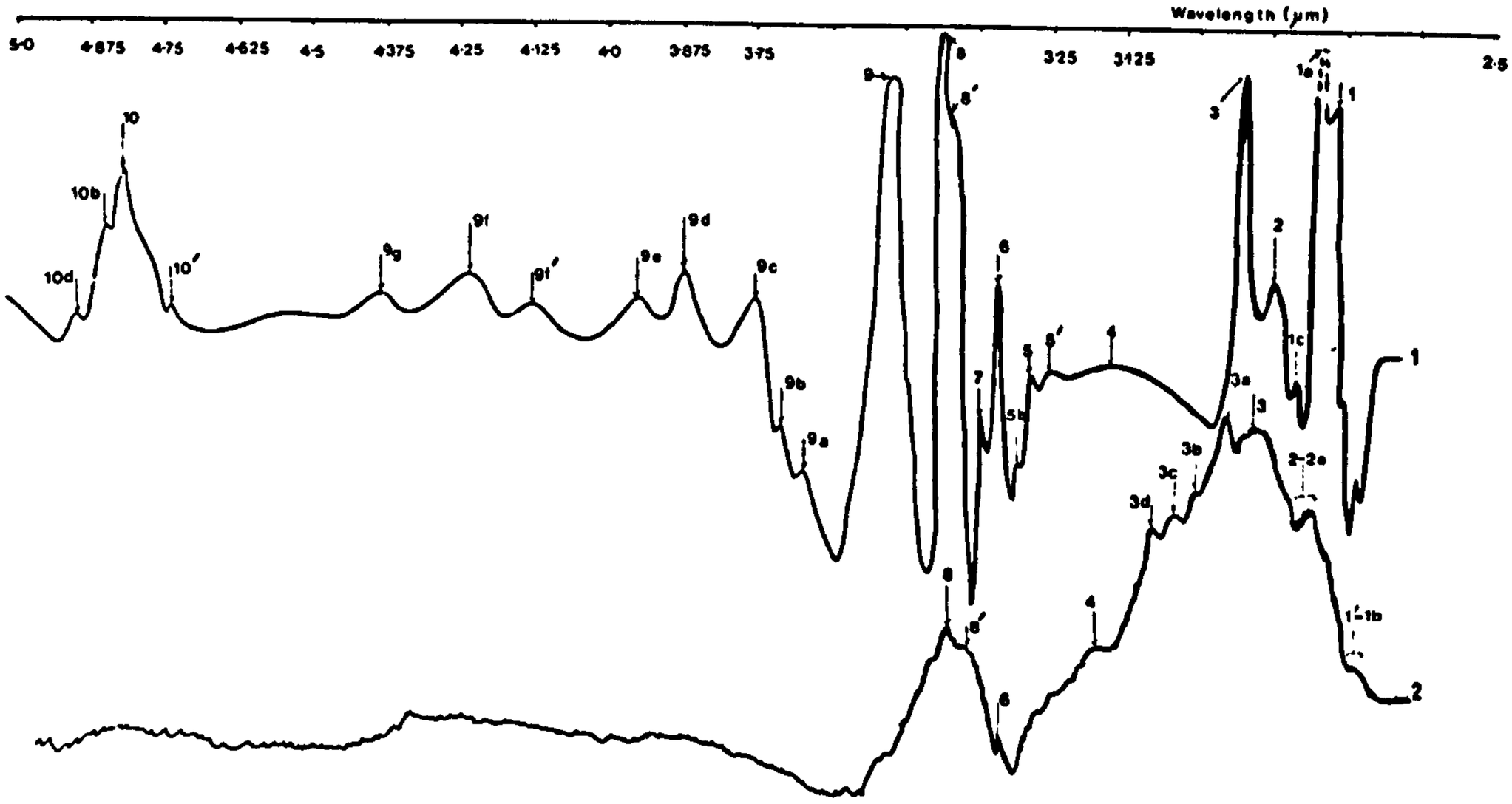

FIG. 77

DERIVATIVE SPECTRUM OF TRICEL FILM (1)

A.T.R. " " " " SURFACE (2)

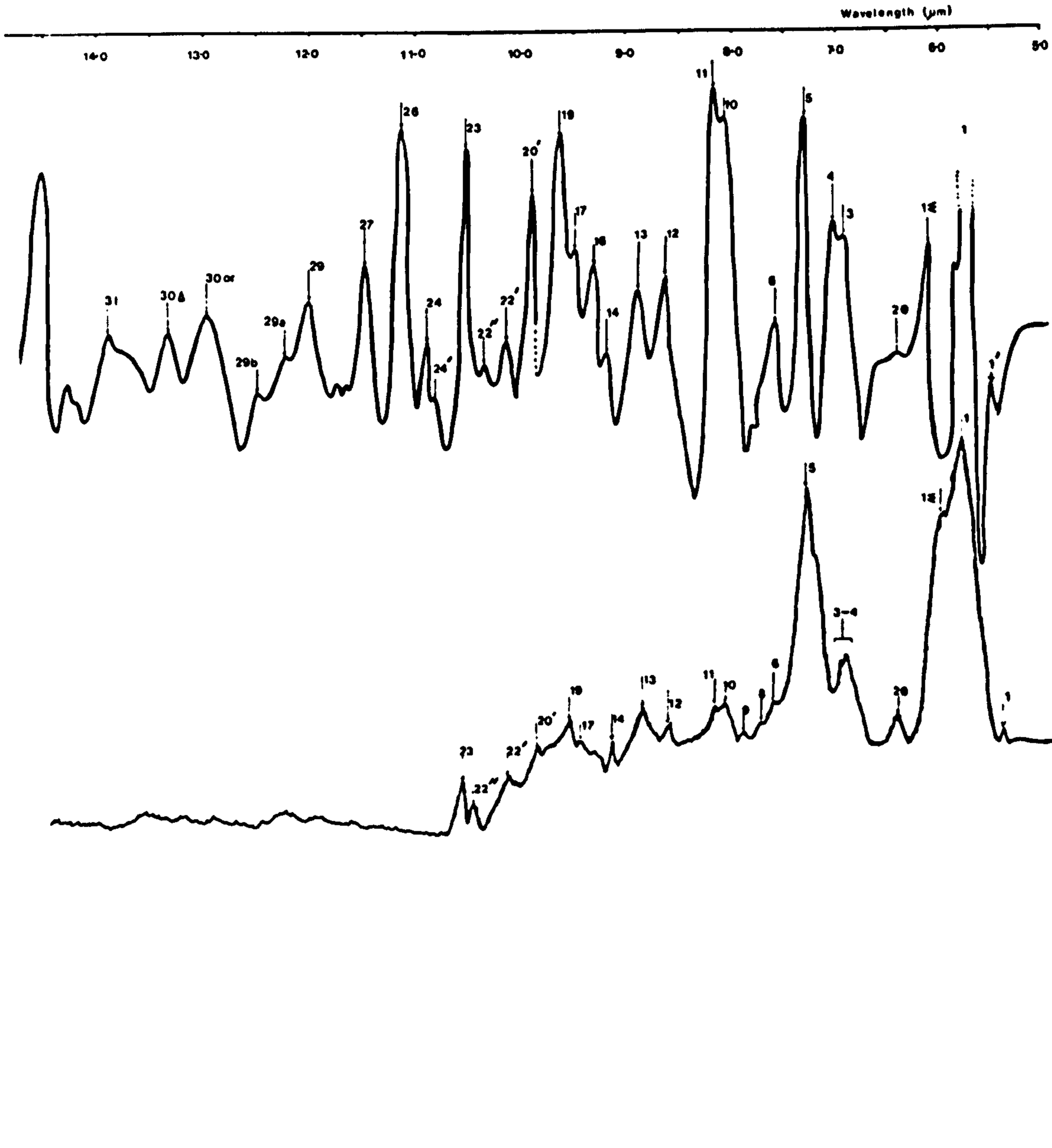

FIG. 80

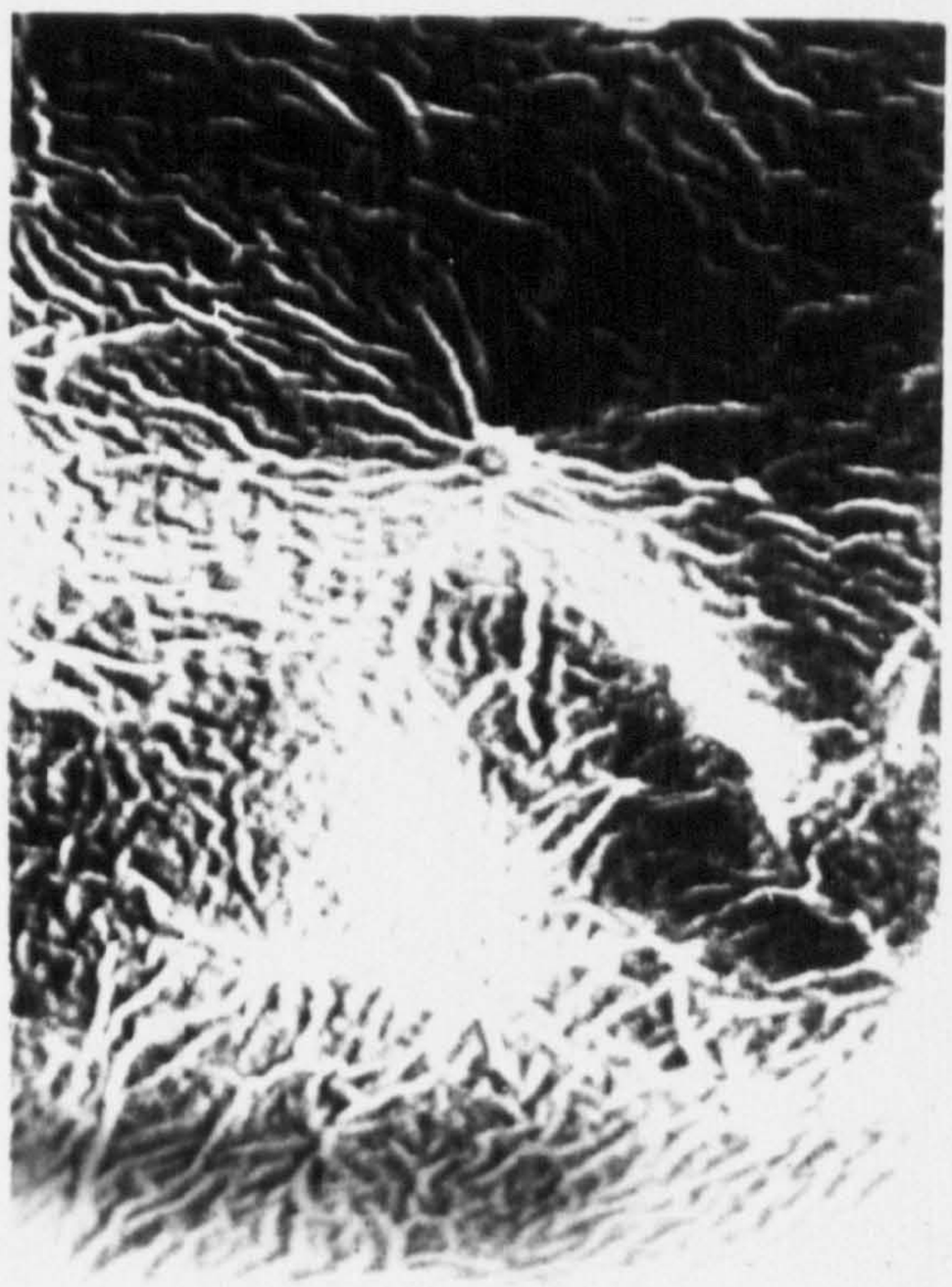

FIG. 79

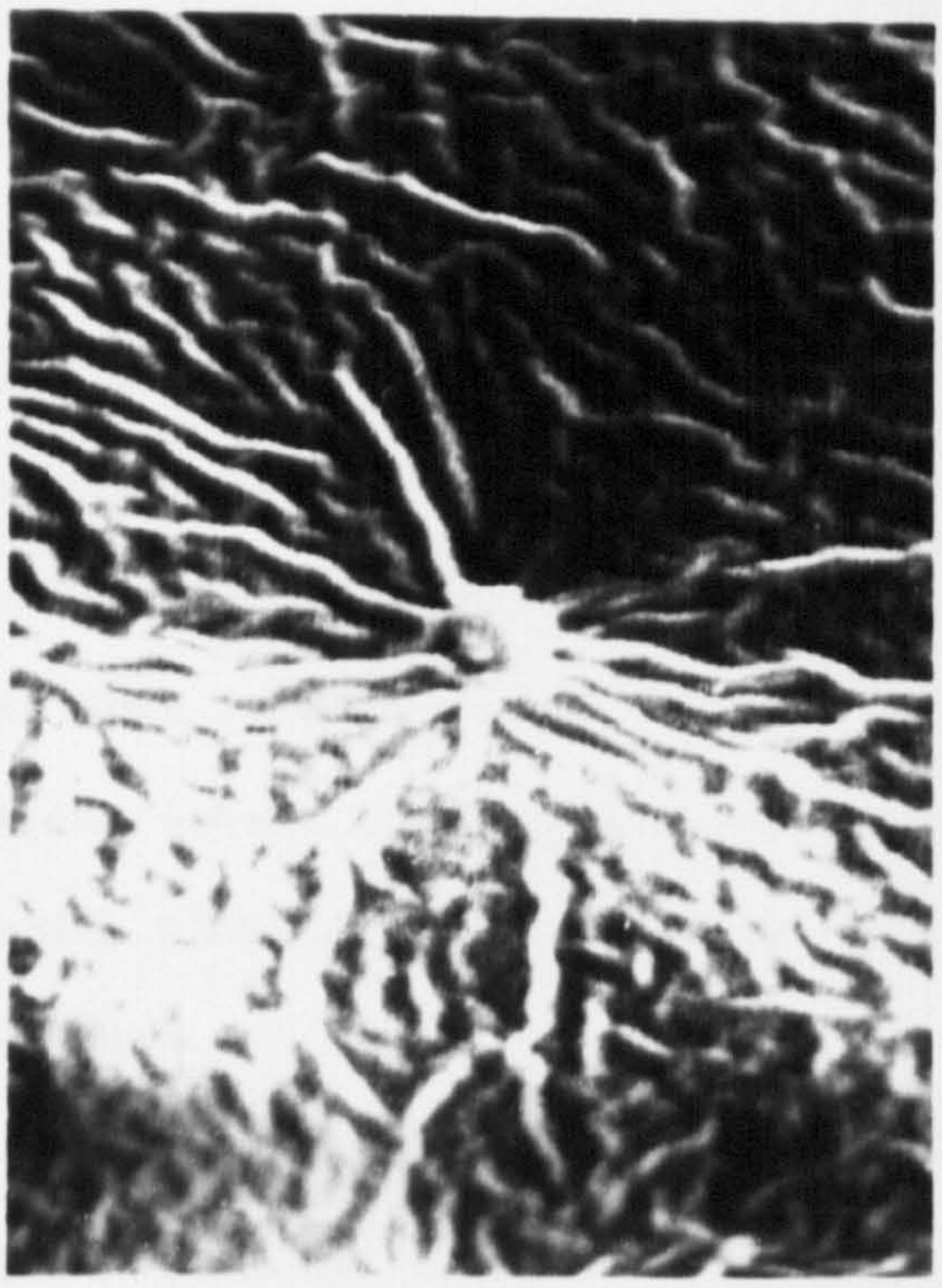

FIG. 79

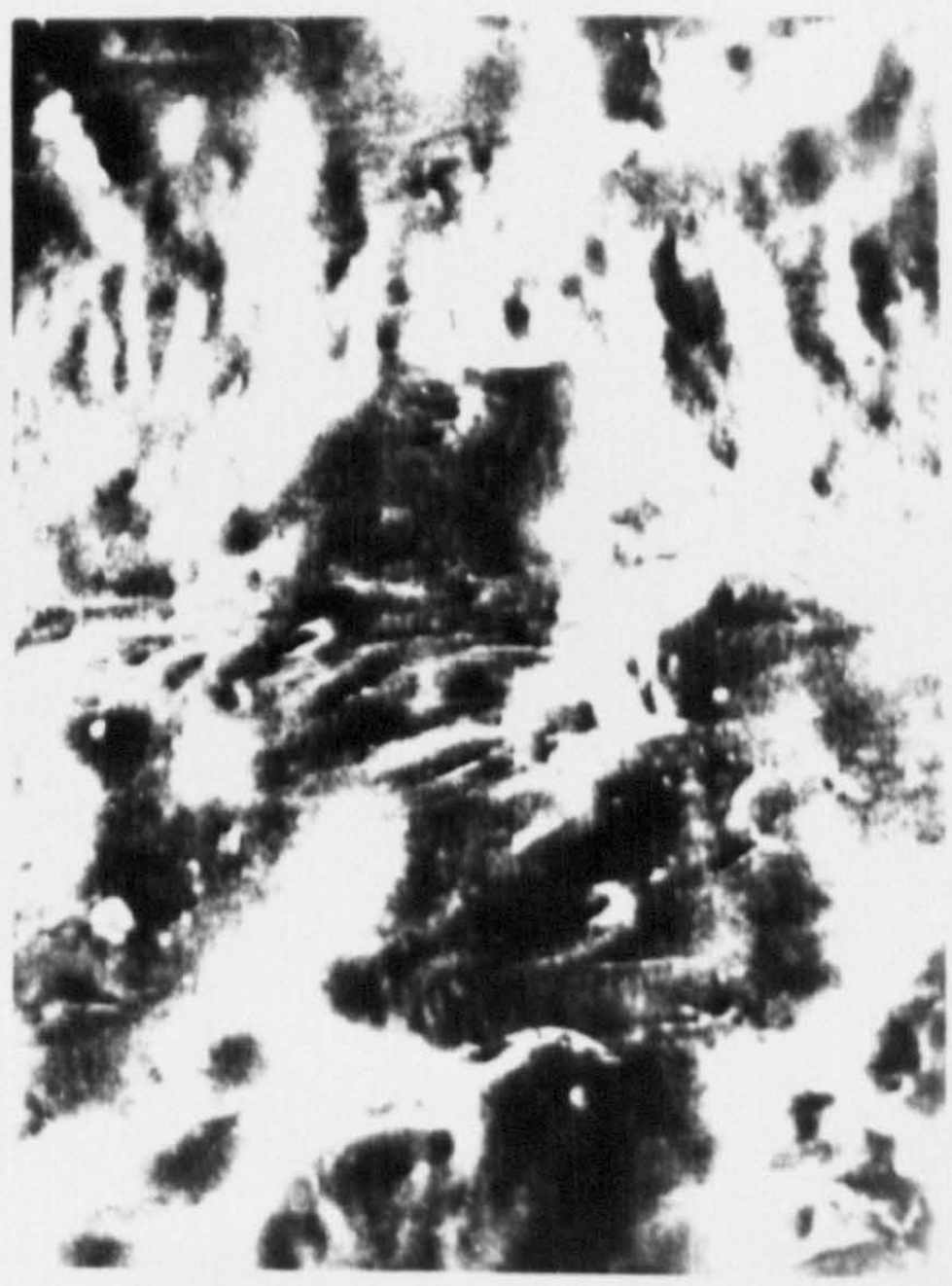

FIG. 78

possible to obtain second derivative A.T.R. spectra.

Similar problems were experienced with both dicel and tricel film samples, but in all cases it was necessary to use varying amounts of viscose, dicel or tricel film on the sample plate in different regions of the spectrum in order to record acceptable spectra and also to obtain maximum sensitivity in each region.

7.3 Results

A.T.R. spectra of viscose, dicel and tricel film surfaces compare favourably with derivative spectra of these materials. They are thus shown together with the derivative spectra recorded at approximately the same R.H. (47.7%) as the A.T.R. spectra - in Fig. 75 for viscose, Fig.76 for dicel and Fig.77 for tricel. Prints of the stereoscan tracings of the surface topography of viscose, dicel and tricel films are shown in Figs. 78, 79 and 80 respectively.

7.4 Discussion

Figs. 75 - 77 indicate the difficulties in the interpretation of changes which occur in structural and water peaks arising from material or water at the surfaces of viscose, dicel or tricel films, due to the high 'noise' level and poor resolution of A.T.R. spectra. Errors also arise due to the fact that derivative spectra were recorded at a constant temperature of 44°C, whereas A.T.R. spectra were recorded at a varying room temperature. However, despite these difficulties, interpretations which could be made are as follows:-

In the A.T.R. spectrum of viscose film recorded in the 2.5 - 5 μm. (4000 - 2000 $cm.^{-1}$) region (Fig.75), several peaks occurred (peaks 22 - 25) which had not been previously observed in absorption or derivative spectra of the whole film. It is possible that these peaks represent CH or CH_2 stretching vibrations present at the surface of the viscose film, but not

present in the material inside the film. This indicates the possibility of some re-organisation of viscose molecules at the surface of the film to produce CH or CH_2 groups which are involved in different inter- or intra-molecular interactions, e.g. hydrogen bonding. These different interactions, associated with peaks 22 - 25, represent CH or CH_2 stretching vibrations which occur at lower frequencies (higher wavelengths) than any other CH or CH_2 stretching vibration peaks in this region present in the derivative spectrum. This indicates that interactions such as hydrogen bonding are stronger at the surface of the viscose film than inside it.

It is thus proposed that the surface of the viscose film differs in structure from the material inside the film, and this is upheld by the results in the 5 - 15 μm. (2000 - 667 $cm.^{-1}$) region in which the CO stretching peaks 12 and 14 have shifted considerably in the A.T.R. spectrum. Since peak 14 shows a 'crystalline' behaviour, the shift of this peak to a higher wavelength (lower frequency) may be due to an increase in the degree of crystalline perfection of the surface of the viscose film compared to the material inside the film, although this is not confirmed by the shift of any other band.

The stereoscan photographs of the surface topography of the viscose film (Fig.78) indicate the presence of an undulating surface, but no large cracks. Such an observation does not indicate the presence or absence of any specific crystalline structures at the surface of the film.

In the case of dicel (Fig.76), the A.T.R. spectrum is very poorly resolved in the 2.5 - 5 μm. (4000 - 2000 $cm.^{-1}$) region. This may be due in part to the very cracked surface of the film, as observed from the stereoscan photograph (Fig.79), which prevents a good contact between the sample crystal and the dicel film from being achieved. In the 5 - 15 μm. (2000 - 667 $cm.^{-1}$) region, the appearance of a new peak, peak 11a (CO stretching vibration), in the A.T.R. spectrum, indicates that a structural

change has occurred at the surface of the dicel film, but this is not confirmed by the presence of any new peaks nor by shifts in peak wavelength (frequency).

The A.T.R. spectrum of tricel (Fig.77) in the region from 2.5 - 3.5 μm. (4000 - 2857 $cm.^{-1}$), is slightly better resolved than the corresponding region in the A.T.R. spectrum of dicel. This may be due in part to the much smoother surface of the tricel film, as observed from the stereoscan photograph, Fig.80 , which enables a better contact to be established between the sample crystal and the tricel film. The appearance of peaks 3b, 3c and 3d in the A.T.R. spectrum (water with an 'ice type' structure) suggests that such water is present only at the surface of the film at Relative Humidities between 45 and 55% and not inside the film, since such peaks are not present in the derivative spectra recorded in this humidity range. At lower R.H's, however, the derivative spectra do show the presence of these water peaks. These observations suggest that the water with an 'ice type' structure is bound more strongly to the material present at the surface of the tricel film than the material inside it.

CHAPTER 8

CHAPTER 8

GENERAL DISCUSSION

8.1 Introduction

Most of the work presented in this thesis has been discussed in detail at the end of each Chapter and it is thus unnecessary to repeat these discussion in detail. However, some aspects of the work could not be fully discussed and it is thus pertinent to consider these further here.

The work and the conclusions drawn, and some points which emerge from several Chapters can be considered under the following headings:-

8.1.1 Chain Folding in (a) Viscose (b) Tricel

and 8.1.2 The Involvement of C-H bonds of CH, CH_2 and CH_3 groups in Hydrogen Bonding.

Any further experiments which were suggested in the experimental Chapters and any other experiments which now appear necessary to confirm existing results or provide further information are also considered here, together with any new experiments which are based upon different physical or chemical treatments of viscose, dicel or tricel. All these experiments are considered under the general heading:-

8.2 Further Work to be Carried Out.

8.1.1 Chain Folding in (a) Viscose (b) Tricel

The results of Chapter 5 suggest that chain folding does occur in viscose (Cellulose II) and that folded regions involve:-

(i) OH groups (peak 13, Fig.64),

(ii) C-O-C groups (peak 7, Fig.65),

(iii) C-O groups (peak 15, Fig.65).

a.

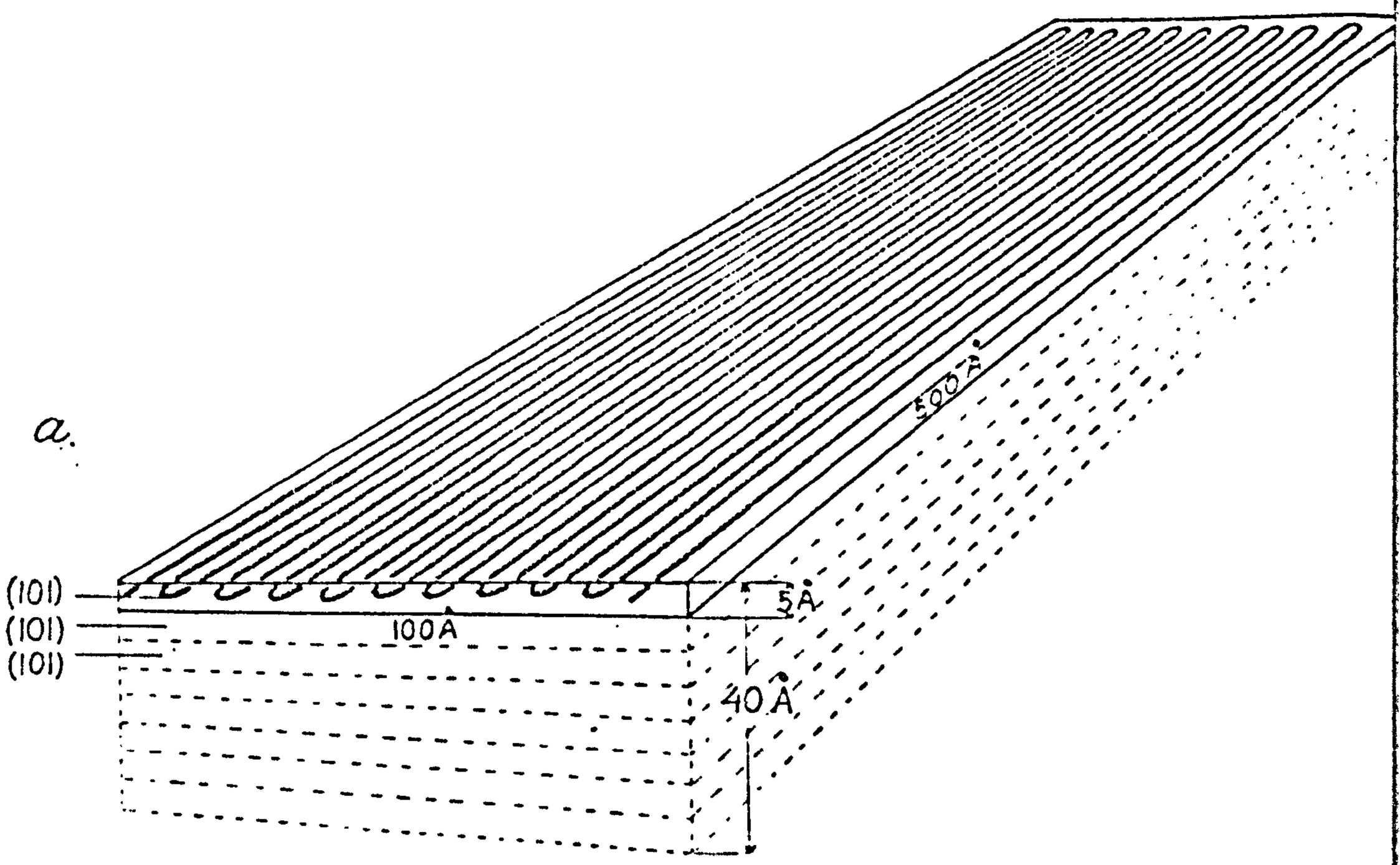

b.

FIG 81.

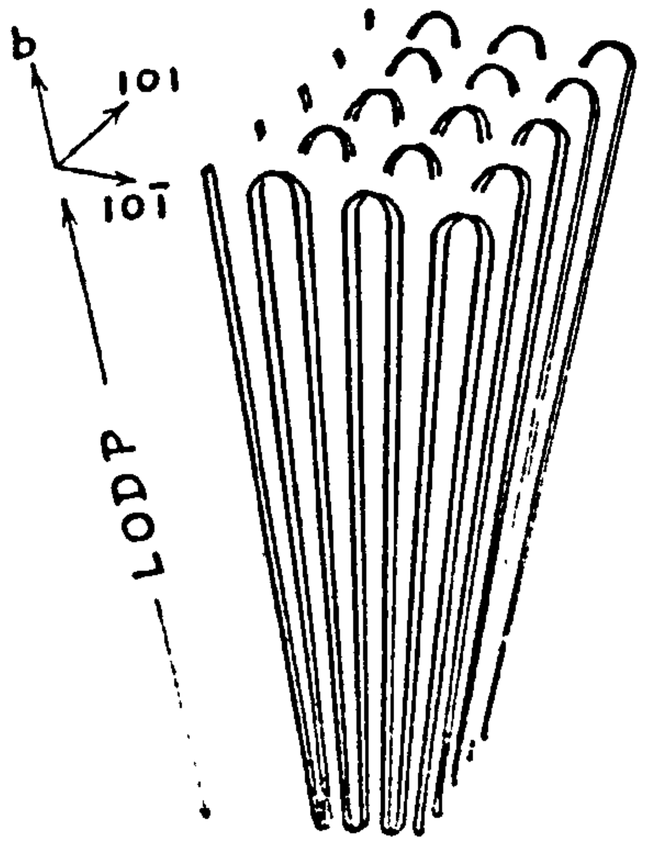

FIG 82 Perspective view of a cellulose crystallite according to the Chang model.

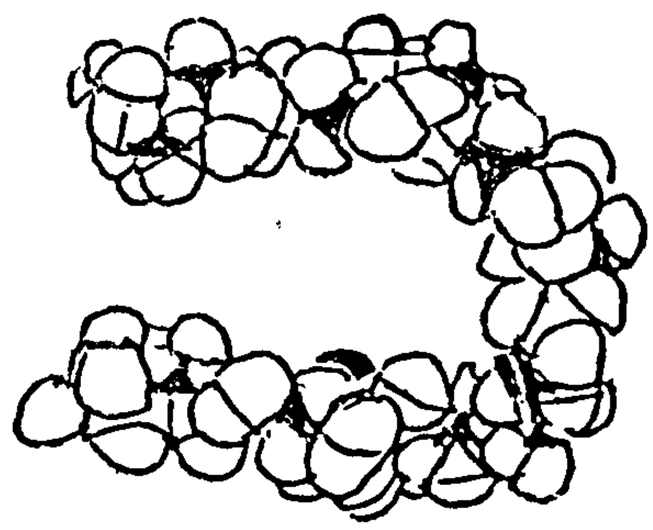

FIG.84 Cellulose fold involving 3 successive β_L bonds.

The fact that spectroscopic peaks have been detected in viscose which are characteristic of the folded regions supports the previous contentions of Dreyfus and Keller (179) that the folds are 'sharp', since only 'sharp' folds will produce structural groups which are essentially different from others in terms of bond strain and hydrogen bonding, and can hence induce infra-red absorption peaks characteristic of the folded regions. There has been much discussion and speculation about the presence and nature of chain folding in natural celluloses (Cellulose I) (181-186), but there has been very little discussion concerning chain folding in regenerated celluloses (Cellulose II), despite the fact that thermodynamic studies have shown that chain folding in regenerated cellulose is probable. (203, 204).

However, Kiessig's (205) experiments on viscose swollen with hydrochloric acid or water at high temperatures showed that up to 100h. treatment, certain spacings in X-ray diffraction photographs increased from approximately 14 to 17 nm, but then decreased to 15.6 nm. upon heat treatment for between 100 and 800 h. This decrease was attributed by Kiessig to the occurrence of folded chains in the viscose, but no model was proposed for these folds, nor for the structure of viscose containing them.

A recent paper presented by Chang (206) has, however, reviewed various models proposed for the structure of cellulose containing folded chains. Chang concluded that Ellefsen's model (207) (Fig.81) was the only one which was compatible with both the measurements of the lengths of crystallites from hydrolysed cellulose and with Manley's measurements of the lengths of protofibrils in regenerated celluloses (Cellulose II) (208). Ellefsen's model was refined by Chang, and a general model was proposed for the structure of both natural (Cellulose I) and regenerated cellulose (Cellulose II) crystallites in which weak linkages occurred at folded regions (Fig.82). The weak linkages were attributed by Chang to the rotation of glucose residues about C_1 - oxygen linkages to form 1-4 β L linkages as opposed to

the normal 1-4 β linkage (Fig.83).

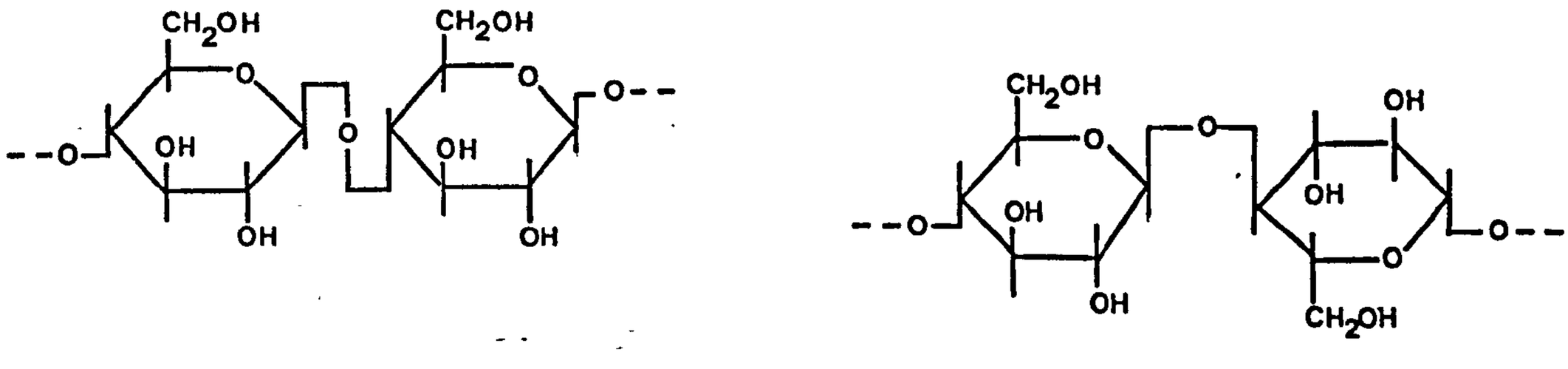

1 - 4 β L linkage 1 - 4 β Linkage

FIG. 83

Rees and Skerret's (209) calculations of the relative amounts of 1-4β and 1-4 β L linkages showed that 98.5% of the linkages were of the 1-4 β type and 1.5% of the 1-4 β L type, the latter being present at folds. Chang (206) showed that these figures were consistent with the Ellefsen model of the structure of cellulose and his modifications of it (Fig.82) and also that the oxygen atoms which link glucose residues in the cellulose chain were forced into a more exposed position in the 1-4 β L linkages present at the folds. Chang argued that the exposure of these oxygen atoms made the 1-4 β L linkages present at the folds weaker, i.e. more susceptible to chemical attack by hydrolysing reagents, than 1-4β linkages present in the rest of the cellulose molecules.

The model proposed by Chang (Fig.82) shows cellulose crystallites to be composed of a network of looped molecules in $10\bar{1}$ planes, which form a network of platellites in $10\bar{1}$ planes, with a sheet-like structure. The sheet-like structure of cellulose proposed by Warwicker (47-49) also coincides with the present platellite system proposed. The model proposed by Chang was also used as a basis for describing the changes which occur when Cellulose I is converted to Cellulose II. This model was thus compatible with the twisting of glucosidic rings relative to the $10\bar{1}$ plane from approximately

45° to approximately 90° and also with the compression of molecules in the $10\bar{1}$ plane, which occur when Cellulose I is converted to Cellulose II.

Chang also proposed a model for the structure of the fold itself in Cellulose I, in which 2 monomer units (i.e. glucose residues) and 3 β L linkages were involved (Fig.84). This model produces a 180° loop without any substantial strain on the backbone and also produces adjacent chains whose spacing is compatible with unit cell dimensions. A model for the structure of the fold in Cellulose II was not proposed, however, but clearly the fact that some compression of adjacent molecules in the $10\bar{1}$ plane has occurred necessitates that the folds in Cellulose II are tighter than in the parent Cellulose I. It is thus probable that the folded regions of Cellulose II molecules contain a single glucose residue with 2 β L linkages, one at either end of this residue. Such a fold in Cellulose II would, however, be highly strained, but it is possible that some of this strain could be relieved if the single glucose residue involved in the fold were to take up the 'boat' (cis) conformation rather than the 'chair' (trans) conformation normally present in the rest of the glucose residues of the Cellulose II molecule.

In conclusion, it should be said that although the Chang model for the structure of Cellulose (Fig.82) is compatible with the dimensions of unit cells proposed by Sponsler and Dore (210) and by Ellis and Warwicker (211) (based upon modifications of the Meyer-Misch (43) and Andress (45) unit cells), in the case of Cellulose I, certain X-ray reflections may only be indexed in terms of a super lattice in which a and c have twice the values of the Meyer-Misch unit cell dimensions (203,212-213).

(b) Tricel

As was pointed out in Chapter 5, the existence of chain folding in tricel could not be confirmed due to the fact that in tricel, both 1-4 glucosidic linkages and also acetyl C-O linkages are attacked by hydrolysing reagents, such as hydrochloric acid. Also, the literature published has not as yet provided a way of solving this problem by suggesting a reagent which only

attacks the 1-4 glucosidic linkages in tricel.

One way of confirming the existence of chain folds in tricel would be to devise a method for stretching tricel films, which did not cause the films to rupture. Stretching removes many of the chain folds according to Rhodes (12), with the result that spectral peaks which are characteristic of the fold decrease markedly in intensity. It may be possible to achieve this stretching by keeping the tricel film in a controlled atmosphere of acetone vapour and water vapour, since acetone vapour causes tricel film to swell and soften.

8.1.2 The Involvement of CH, CH_2 and CH_3 Groups in Hydrogen Bonding

Many of the results of Chapters 3-7 have shown that CH groups (also CH of CH_2 and CH_3 groups) of viscose, dicel and tricel are involved in hydrogen bonding with cellulosic OH (or CO) groups or with OH groups of absorbed water. The observation of the hydrogen bonding of C-H groups was based upon shifts in the intensities or frequencies of derivative peaks which represent CH, CH_2 or CH_3 groups in spectra of viscose, dicel or tricel films, recorded at increasing temperature or humidity or in annealed samples. These spectral changes were usually quite small and are not detected in the absorption spectra.

Evidence for the involvement of CH groups in hydrogen bonds has been previously suggested and it is thus relevant to discuss this here. The possibility of this involvement was reviewed in 1960 by Pimmentel and McClellan in 'The Hydrogen Bond' (161) and they concluded that CH groups could be involved in hydrogen bonding with strong bases, provided the CH group was activated by adjacent electrophilic atoms or groups. One of the earliest examples of the involvement of CH groups in hydrogen bonding was detected in the chloroform/triethylamine system (214-215) by a shift to a higher wavelength and an increase in the intensity of the CH stretching mode peak of chloroform. The fact that the CH group in chloroform could form a hydrogen bond was attributed to the presence of electrophilic chlorine

atoms adjacent to it. (Fig.85). The high electronegativity of chlorine atoms

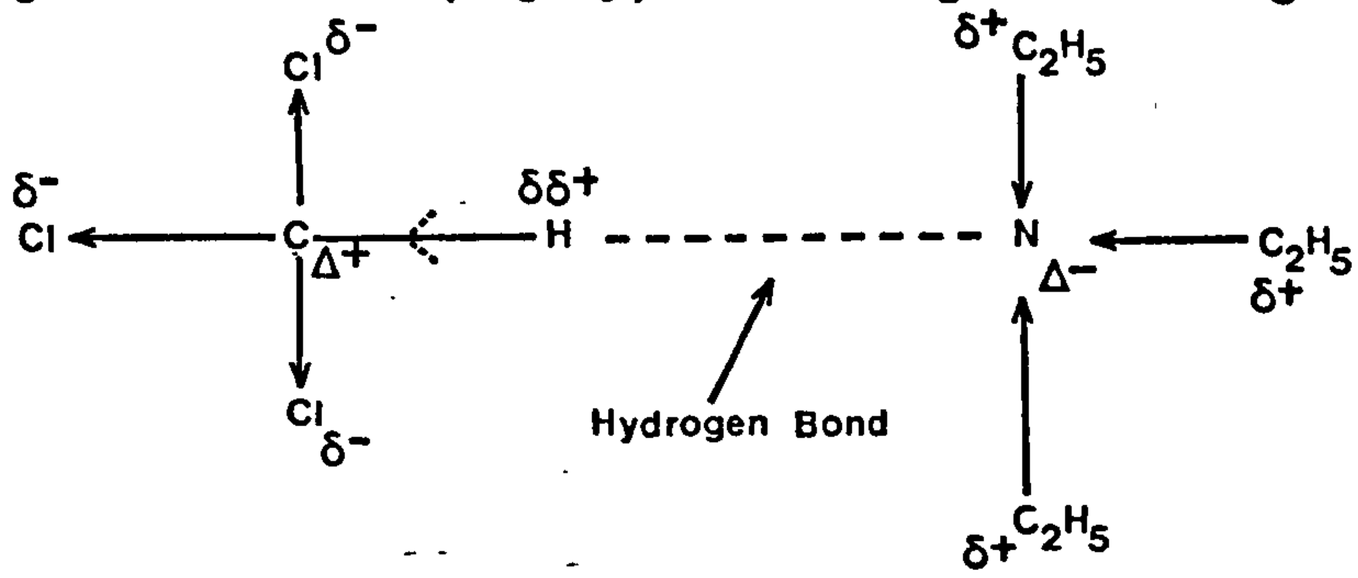

Arrows indicate the displacement of an electron pair (displacement of charge).

FIG. 85

induces the electron pairs which constitute C-Cl σ bonds to be displaced towards the chlorine atoms so that these acquire a small negative charge (δ⁻) and the carbon atom acquires a small δ+ charge. However, since there are three C-Cl bonds in chloroform molecules, the total charge at the carbon atom is 3 x δ+ = Δ+. This large Δ+ charge at the carbon atom will induce a slight displacement of the electron pair in the C-H bond towards the carbon atom, so that Δ+ decreases slightly in magnitude and a small δδ+ charge is induced at the hydrogen atom. It is thus possible for this 'activated' hydrogen atom which possesses a small δδ+ charge to form a hydrogen bond with a strongly basic group which possesses a large Δ- charge, such as triethylamine.

Proton magnetic resonance studies by Huggins et al. (216) have given spectra which show the characteristics of hydrogen bond formation between chloroform and acetone or trimethylamine. The hydrogen bonding between acetone and chloroform has also been substantiated by Kearns (217) from measurements of the heat of mixing.

In the case of aldehydes, there has been some uncertainty concerning the existence of hydrogen bonds between C-H groups and C=O groups of other aldehyde molecules. Schneider and Bernstein (218) have found no evidence for such hydrogen bond formation from the infra-red spectra of solid

formaldehyde and acetaldehyde, but Pinchas and Fregmann (219, 220) have cited infra-red data as evidence of such hydrogen bonding in aldehydes (Fig.86).

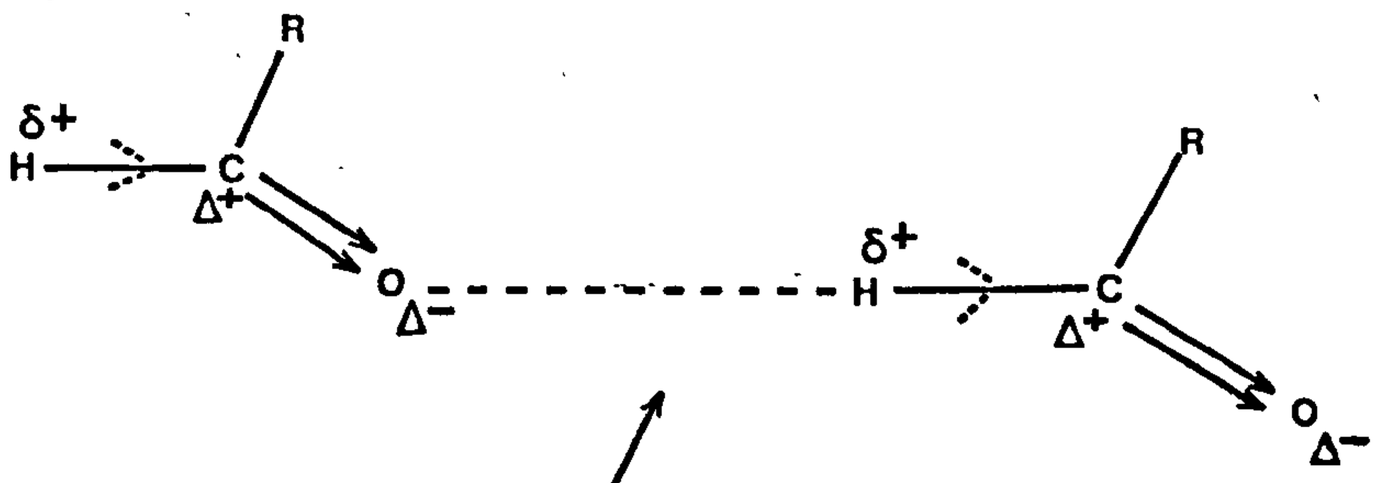

Arrows indicate the displacement of an electron pair (displacement of charge).

FIG. 86.

A large Δ- charge is present at the oxygen atom of the aldehyde C=O group due to the displacement towards the oxygen atom of two electron pairs in both the C-Oπ and C-Oσ bonds which constitute the C=O double bond. This large Δ- charge is also due in part to the shorter carbon-oxygen distance present in the C=O double bond, since in shorter bonds the displacement of an electron pair produces a larger charge separation, i.e. a larger Δ- charge at the oxygen atom and a larger Δ+ charge at the carbon atom in this case. Hydrogen bond formation by C-H groups attached to aldehyde C=O groups could occur if the large Δ+ charge present at the carbonyl (C=O) carbon atom induces the electron pair of the aldehyde C-H bond (hydrogen atom also attached to the aldehyde C=O group) to shift towards the carbon atom so that a small δ+ charge occurs at the hydrogen atom, thus 'activating' it and enabling it to form a weak hydrogen bond with the carbonyl oxygen atom of another aldehyde molecule. (Fig.86).

Evidence has also been presented to suggest that CH groups attached to acetylenic C≡C groups can also be involved in hydrogen bonding. Standford and Gordy (221) found systematic shifts of the acetylinic C-H stretching mode

of phenyl acetylenes dissolved in bases, and more recently Kreevoy et al. (222) have shown that intermolecular hydrogen bonding takes place in the case of the vinyl acetylene, 2 - ene but- 3 yne:- (Fig.87.)

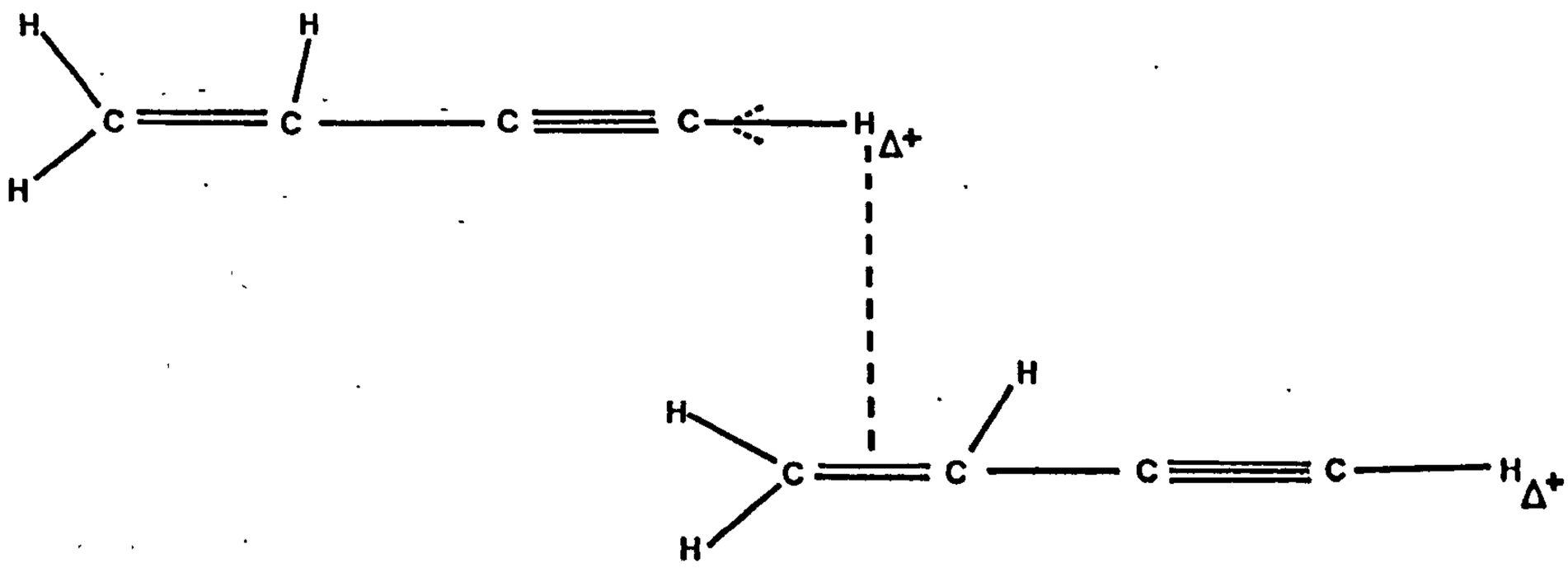

FIG.87

In these cases, the hydrogen bonding may be attributed to the 'activation' of the hydrogen atom of the CH groups attached to the acetylenic C≡C group by the presence of a large Δ+ charge at the hydrogen atom. This charge is induced by the presence of the C≡C acetylenic triple bond; the induction of this charge is discussed by Morrison and Boyd (223).

Another series of hydrogen bonds has been shown to occur between CH groups which are 'activated' by being attached to a benzene ring and a series of alcohols. This type of hydrogen bonding occurs, for example, between hexamethylbenzene and alcohols such as phenol, n butanol, heptanol and benzyl alcohol (224).

The cases so far discussed of CH groups being involved in hydrogen bonding have all been for fairly simple molecules which are 'activated' by adjacent groups. In the case of polymers, however, no conclusive evidence has been presented from infra-red spectra to suggest the involvement of CH groups in hydrogen bonding. The main reason for this is that the very complex nature of polymer absorption spectra masks any small changes which occur in the absorption spectra due to changes in very weak CH hydrogen bonds when the temperature or moisture content of the polymer are changed.

The much greater resolution of derivative spectroscopy has, however, enabled many of these small changes to be observed in the derivative peaks which correspond to CH, CH_2 or CH_3 groups of viscose, dicel and tricel films when temperature or water content of the polymer are changed. These changes are discussed in detail in Chapters 3-7. The observation of such changes has led to the conclusion that CH bonds of CH, CH_2 or CH_3 groups of viscose, dicel and tricel films are involved in hydrogen bonding with cellulosic OH (or CO) groups or with absorbed water.

At this point, it is necessary to examine how CH bonds are associated with other atoms and groups in viscose, dicel and tricel molecules, and also how H atoms of CH groups can acquire a small $\delta+$ charge, which is a necessary 'activation' prerequisite to the formation of CH hydrogen bonds. The following theory is thus proposed to account for the small $\delta+$ charge at hydrogen atoms of CH bonds (of CH, CH_2 or CH_3 groups) in viscose, dicel and tricel. The carbon atom of every CH group in viscose, dicel or tricel

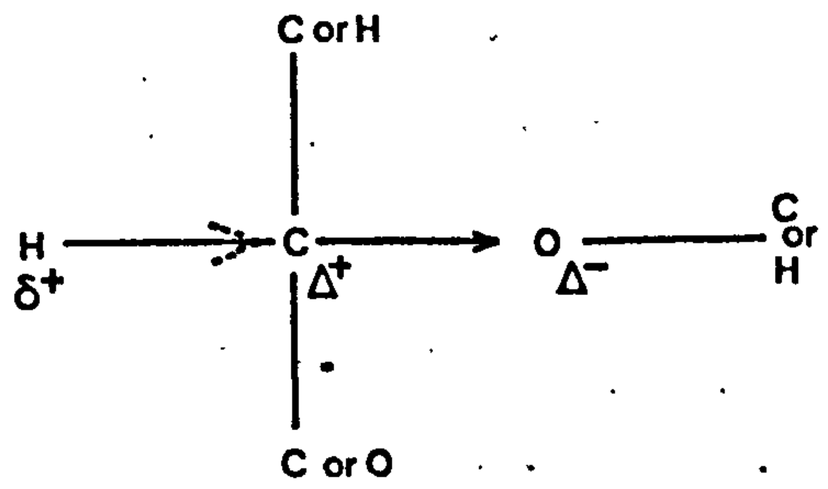

FIG.88

(except those CH groups of the acetyl groups in dicel and tricel), is also bonded to an oxygen atom (Fig.88) by a σ bond. The high electronegativity of the oxygen atom will cause the electron pair which constitutes the C-O σ bond to be shifted towards the oxygen atom, thus producing a $\Delta-$ charge at the oxygen atom and a $\Delta+$ charge at the carbon atom. This $\Delta+$ charge can in turn induce a slight movement of the electron pair which constitutes the CH bond towards the carbon atom, so that a small $\delta+$ charge is induced at the hydrogen atom. CH hydrogen atoms 'activated' by the presence of

this small δ+ charge may then form very weak hydrogen bonds with cellulosic OH (or CO) groups, or with absorbed water.

Hydrogen atoms of CH groups of acetyl CH_3 groups may be 'activated' by the carbonyl group present in the acetyl group (Fig.89), due to the relatively large Δ+ charge present at the carbonyl carbon atom. In this

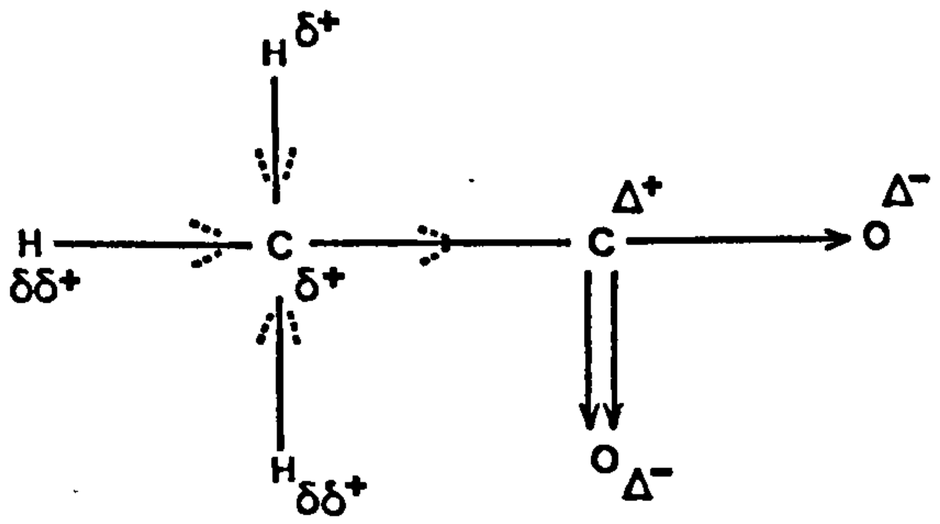

FIG.89

case, however, the CH groups are not attached to the carbonyl carbon atom, but are linked indirectly by a C-C σ bond. This separation of the CH groups from the Δ+ charge at the carbonyl carbon atom causes the Δ+ charge to have a much smaller inductive effect on the electron pairs which constitute the CH bonds so that only a very small charge, δδ+, is induced at each of the hydrogen atoms of the three CH groups. The charge is also made smaller at the hydrogen atoms because the inductive effect of the Δ+ charge is distributed between 3 CH groups.

If the very small δδ+ charge present at the CH hydrogen atoms enables hydrogen bonds to be formed with other cellulosic OH (or CO) groups or with absorbed water, then these hydrogen bonds will be very weak indeed. This may in part account for the fact that the hydrogen bonding of CH groups is weaker in dicel than in viscose and is weaker still in tricel.

8.2 Future Work to be Carried Out

8.2.1 Chapter 3

One of the most interesting features to emerge from the work carried out in Chapter 3 was that viscose films (Cellulose II) contain small amounts

of Cellulose I, and the amount of Cellulose I present increases with annealing. This increase in the amount of Cellulose I present in viscose (Cellulose II) with annealing was in fact predicted by Chang (206), and these results thus substantiate his predictions. As was pointed out in Chapter 3, it would be very useful to produce a film of Cellulose I which could be examined by derivative spectroscopy, since this would enable previous results to be confirmed, and also enable the properties of Cellulose I and Cellulose II to be compared by repeating all the experimental work carried out on viscose film (Cellulose II) in Chapters 3-7 with a Cellulose I film.

However, an extensive search of the literature has not as yet revealed a way of preparing Cellulose I film of sufficiently low scatter to enable reproducible spectra to be produced over the whole of the spectral range, as in the case of the Cellulose II films used in the work presented in this thesis. One report of well resolved absorption spectra of Cellulose I has, however, been published, but details of sample preparation were not given (78).

8.2.2 Chapters 3 and 4

The work carried out on viscose, dicel and tricel films at increasing temperatures from 44°C. in Chapter 3 and at decreasing temperatures from 44°C. in Chapter 4, could undoubtedly be extended by recording derivative spectra at much narrower temperature intervals. This would provide much more information concerning structural changes which occur at increased or decreased temperatures, and enable the temperatures or temperature ranges in which significant structural changes occur to be much more accurately defined. Time precluded such a study here.

8.2.3 Chapter 5

In Chapter 5 the existence of chain folding in viscose was confirmed by exposing viscose films to γ radiation for 5 days (total dose 2.4 x 10^6 $J.h.^{-1}$ kg^{-1} sample) prior to recording the spectra of such films. This irradiation technique could be applied to viscose, dicel and tricel films by irradiating film samples for 6 or 12 hour periods and recording derivative spectra between each period, up to a point where the films disintegrated. Such an examination would be useful as part of a study of the effects of γ radiation on cellulosic materials, since derivative spectra are much better resolved than parent absorption spectra, and hence much more information concerning the changes in structure which occur due to γ-irradiation could be obtained.

8.2.4 Chapter 6

One of the main effects to be observed from the recorded derivative spectra of viscose, dicel and tricel films (originally dry) at increasing R.H's was the 'temporary' conversion of some 'crystallizable' material to 'crystalline' material in viscose and tricel. It would thus be useful to examine the spectra of viscose and tricel films at decreasing R.H's (samples originally 'wet' i.e. in an atmosphere of 100% R.H.) in order to determine how the reversion of some 'crystalline' material to 'crystallizable' material was related to the hysteresis regain curves. A study of the water peaks present in these spectra, and similar spectra also recorded for dicel, would also be useful in ascertaining how the state of absorbed water changes at decreasing R.H's with samples originally conditioned from the 'wet' state.

The observation of the spectra of viscose, dicel and tricel films at R.H's in excess of 75.1% would also provide further information on structural changes which occur, and also on the state of absorbed water. However, such spectra cannot be observed with the present cell and heated block system, due to the condensation of water vapour on the inside of the rock salt windows of both the sample and reference cells. An alternative heated block

and cell system would thus be required to ensure that the outer face of the windows was thermally insulated from the atmosphere. Such a system would require the construction of cells which are similar to the original ones, but incorporating heated and double rock salt windows which contain the humidity chamber. A wider heated block would also be required to accommodate the increased size of these cells.

The study of the spectral peaks of absorbed water in viscose, dicel and tricel films has been hampered to some extent by the presence of large cellulosic structural peaks, especially those peaks which correspond to cellulosic OH groups, since these often occur near and are sometimes coincident with water peaks.

The elimination of cellulosic peaks could be achieved by the construction of separate sample and reference cells, each with their own temperature and R.H. control systems. By using a sample conditioned to a given R.H. in the sample beam and a 'dry' sample in the reference beam, the position of the reference cell could be adjusted so that the reference sample balanced out any cellulosic peaks of the sample beam sample. This would hence produce a spectrum containing no cellulosic peaks, but only peaks due to absorbed water present in the sample beam sample.

However, such a spectrum does not take into account the fact that it is impossible to remove all the water from the reference sample, and peaks which correspond to this residual water are thus eliminated from such spectra. Also, the process of elimination of cellulosic peaks of a high intensity may reduce spectral sensitivity so much that any water peaks which occur near the maxima of these peaks may also be eliminated from such spectra.

For these reasons, the spectra of absorbed water in viscose, dicel or tricel, with the cellulosic peaks eliminated, cannot be used to ascertain the total state of absorbed water present in viscose, dicel or tricel films. These spectra are thus only useful in confirming previous spectral assignments.

8.2.5 Chapter 7

The results obtained from A.T.R. spectra of the surfaces of viscose, dicel and tricel films were very poor, due mainly to the very low intensity of the transmitted radiation in the sample and reference beams due to the multiple reflection of radiation by the A.T.R. units, and the high noise level which was thus incurred when the spectrometer gain was increased to amplify the output. However, some differences in spectral peaks were noticed when A.T.R. spectra of film samples were compared with derivative spectra. These differences suggest that some structural changes at the surface of viscose and tricel films occur but the evidence for such changes at the surface of dicel film was more tentative.

One possible way of confirming these changes in the case of dicel and tricel films would be to record the spectra of samples of dicel and tricel films swollen according to the method described by Jeffries (225), so that they contain a large number of cavities. In these samples, the total amount of surface material being observed is greater than in an ordinary sample, so that spectral peaks which are characteristic of surface structure may increase in intensity. This method does, however, assume that the material present at the surfaces of the cavities is of the same structure as the material present at the surface of the film. Also, it is not known what effect the presence of a large number of cavities would have upon the scattering of infra-red radiation and hence the quality of spectra produced.

8.2.6

The deuteration of samples of cellulose in both the vapour and liquid phases has been classically used by Mann and Marinan (58-59) to determine the 'crystalline'/'amorphous' ratio. However, the method is not very reliable

since it assumes that D_2O vapour cannot penetrate 'crystalline' regions of the structure, and this is contrary to the results of Hermans (63-66), and Jeffries (75) and is also contrary to the results for viscose presented in this thesis. This assumption also accounts for the discrepancy between the 'crystalline'/'amorphous' ratios quoted by Mann and Marinan and the ratios obtained by other methods (67-71).

However, bearing these points in mind, vapour and liquid phase deuterations of viscose film were undertaken prior to recording spectra, in order to attempt to confirm previous assignments of derivative OH peaks as 'crystalline' or 'crystallizable'. Unfortunately, in both cases of vapour and liquid phase deuteration, consecutive derivative spectra recorded under the same conditions varied so much that it was impossible to state how individual OH peaks behaved. A preliminary investigation of many consecutive spectra does, however, suggest that some 'crystallizable' OH peaks decrease in intensity more than some 'crystalline' peaks, which confirms that OH groups of 'crystallizable' regions are more accessible to D_2O (and water) than OH groups of 'crystalline' regions.

The reason for this large variation between consecutive spectra is not yet understood, but it may be associated with 'back' exchange of deuteration with small amounts of water vapour present in the sample cells, or with water vapour during transfer to the sample cells. This problem may in future be overcome by observing the spectra of samples which have been deuterated inside sealed sample cells; but again, this would require a cell system with four windows in each cell and a larger heated block to prevent the condensation of D_2O vapour on the inner faces of the rock salt windows.

8.2.7 Treatment of Viscose Film with Liquid Ammonia or Glycerine

The treatment of viscose film (Cellulose II) with liquid ammonia (52,53) or with glycerine at 300°C. (54) will result in the production of films of

Cellulose III_{II} and Cellulose IV_{II} respectively. These two materials could thus be used to repeat all the experimental work carried out on Cellulose II and discussed in Chapters 3 - 7. Such a study would enable a comparison with Cellulose II to be made, and also enable many of the structural and water absorption properties of these materials to be determined.

APPENDIX (i)

Spectrum	Peak	Wavelength (μm)	Wavenumber ($cm.^{-1}$)
60A	5a	2.9895	3345
	10′	3.2170	3108
	20′	3.4558	2894
	21	3.5583	2810
	22	3.5858	2789
	23	3.6745	2721
	24	3.7108	2695
	25	3.7670	2655
	26	3.8245	2614
60B	1c′	6.2900	1590
	1f	6.715	1489
	2b	6.9200	1445
	5a	7.8300	1277
61A	3a	2.7380	3652
	3b	2.7667	3614
	3c	2.8005	3571
	10a	2.9193	3425
	10b	2.9330	3409
	10c	2.9475	3393
	16a	3.4017	2940
	23a	4.6020	2173
	23b	4.6270	2161
	24′	4.6595	2146
	25′	4.7395	2110
	25a	4.7745	2094
	25b	4.8070	2080
	25c	4.8370	2067

APPENDIX (i) Continued

Spectrum	Peak	Wavelength (μm.)	Wavenumber ($cm.^{-1}$)
61B	16′	9.325	1072
	1a	6.2500	1600
	1b	6.3500	1575
	1b′	6.4250	1556
	1c	6.5100	1536
	1d	6.5750	1521
	1e	6.6300	1508
	1f	6.7100	1490
	1g	6.7850	1474
	13a	9.1100	1098
	14′	9.2450	1082
	20″	10.080	992
	29a	12.500	800
	31′	14.070	711
62A	1α	2.7405	3649
	8a	3.4555	2894
	8b	3.4730	2879
	9c″	3.7695	2653
	9e′	3.9770	2514
	9e″	4.0458	2472
62B	2a′	6.8580	1458
	9′	7.9630	1255
	18	9.6280	1038
	22a	10.2600	974
	22b	10.313	969
	24a	11.038	906

LIST OF REFERENCES

1. Rao, C.N.R., — Ultra-Violet and Visible Spectroscopy Butterworths (1967).
2. Herzberg, G., — Molecular Spectra and Molecular Structure, Volume I. Van Nostrand (1950).
3. Jones, N.R., — Infra-red Spectra of Organic Compounds, Principal Group Frequencies. National Research Council Ottawa (1959).
4. Colthrup, N.B., — J. Opt. Soc. Amer. 148, 183 (1944).
5. Flett, M.St.C., — Physical Aids to the Organic Chemist. Elsevier (1962)
6. Liang, C.Y. and Krimm, S., — J. Chem.Phys. 25, 563 (1956).
7. Zbinden, R., — Infra-red Spectroscopy of High Polymers Academic Press (1964).
8. Krimm, S., — Fortschrift Hochpolymforch, 2, 51 (1960).
9. Nielson, J.R., and Holland R.F., — J. Mol. Spectrosc. 6, 394 (1961).
10. Krimm, S., — J. Chem.Phys. 22, 567 (1954).
11. Snyder, R.G., — ibid 47, 1316 (1967)
12. Rhodes, P., — Ph.D. Thesis, Leeds University (1971).
13. Miyazawa, T., — J. Chem. Phys. 32, 1647 (1960)
14. Miyazawa, T. and Blout, E.R., — J.A.C.S. 83, 712 (1961)
15. Higgs, P.W., — Proc.Roy.Soc. A220, 472 (1953)
16. Tadokaro, H., — J. Chem.Phys. 33, 1558 (1960)
17. Miyazawa, T., — in Polyamino Acids, Ed. Stahman, Wisconsin Univ (1962).
18. Schachtschneider, J.H. and Snyder, R.G., — J. Pol.Sci. C7, 99 (1964)
19. Nägeli, — Original Papers, printed as "Ostwald's Klassiker", No.227, Edited by Frey, A. (1928).
20. Herrmann, K. and Gerncross, O., — Kautschuk.8, 181 (1932)
21. Kratky, O., and Mark, H., — Z. Physik.Chem. B36, 129 (1937)
22. Hengstenberg, J., and Mark, H., — Z. Kristallogr. 69, 271 (1928)
23. Staudinger, H., — 'Die Hochmolekularen Organischen Verbindungen'. Springer-Verlag (1932).

24. Abitz, W., Gerncross, O., and Herrmann, K., — Naturwiss, 18, 754 (1930)

25. Gerncross, O., Hermann, K., and Abitz, W., — Biochem.Z. 228, 409 (1930)

26. Hearle, J.W.S., — J. Pol.Sci. 28, 432 (1958)

27. Keller, A., — ibid 17, 251 (1955)

28. Keller, A., — ibid 17, 291 (1955)

29. Keller, A., — ibid 17, 445 (1955)

30. Hearle, J.W.S., and Peters, R.H., — Fibre Structure, Butterworths, (1963)

31. Hosemann, R., — Polymer 3, 349 (1962)

32. Johnson, D.J., — Private Communication

33. Honeymann, J., — Recent Advances in the Chemistry of Cellulose and Starch. Heywood & Co. (1959)

34. Schultz, G.V., — J.Pol.Sci. 3, 365 (1948)

35. Pascu, E., — ibid 2, 567 (1947)

36. Nishikawa, S., and Ono, S., — Proc.Phys.Math.Soc. Japan, Sept. 20 (1913)

37. Scherrer, P., — 'Kolloidchemie'. Edited by Zsigmondy, R Spommer (1920)

38. Herzog, R.O., and Jancke, W., — Z. Physik. 3, 196 (1920)

39. Polyani, M., — Naturwissen, 9, 288 (1921)

40. Meyer, K.H., and Mark, H., — Z.Physik. Chem. B2, 115 (1929)

41. Gross, S.T., and Clark, G.L., — Z. Kristallogr. 99, 357 (1938)

42. Meyer, K. — Ber. 70, 226 (1937)

43. Meyer, K.H., and Misch, L., — Helv.Chim.Acta 20, 232 (1937)

44. Meyer, K.H., and Lotmar, W., — ibid 19, 68 (1938)

45. Andress, K., — Z. Physik Chem. B4, 190 (1929)

46. Baule, B., Kratky, O., et al., — ibid B50, 255 (1941)

47. Jeffries, R., and Warwicker, J.O., — T.R.J. 39, 548 (1969)

48. Warwicker, J.O., and Wright, C., — J. Appl.Pol.Sci. 11, 659 (1967)

49. Warwicker, J.O., — J.Pol.Sci. 5, 2579 (1969)

50. Manjunath, B.R., T.R.J. 40, 769 (1970)

51. Jeffries, R., and Warwicker, J.O., ibid 40, 770 (1970)

52. Hess, K., Kolloid Z. 98, 148 (1942)

53. Wellard, H.J., J.Pol.Sci. 13, 471 (1954)

54. Meyer, K.H., and Badenhuizen, N.P., Nature 140, 281 (1937)

55. Viswanathan, A., Colourage 17(13), 33 (1970)

56. Ellefsen, O., Norwegian Paper Industry Research Institute, Report No.186 (1964).

57. Ellefsen, O., Norelco.Reporter 7(3), 104 (1960)

58. Mann, J., and Marrinan, H.J., Trans.Farad.Soc. 52, 481 (1956)

59. Mann, J., and Marrinan, H.J., ibid 52, 487 (1956)

60. Rowen, J.W., and Plyer, E.K., J.Nat.Bur.Stand. 39, 133 (1947)

61. Rowen, J.W., ibid 44, 313 (1950

62. Rowen, J.W., ibid 46, 38 (1951)

63. Hermans, P.H., and Weidinger, J., J.Coll.Sci. 1, 185 (1946)

64. Kast, W., and Schwarz, R., Z. Electrochem. 56, 228 (1952)

65. Kast, W., and Kiessig, H., ibid 54, 320 (1950)

66. Kratky, O., and Treiber, E., ibid 55, 716 (1951)

67. Hermans, P.H., and Weidinger, A., J.Appl.Phys. 19, 491 (1948)

68. Klug, H.P., and Alexander, I.E., X-ray Diffraction Procedures J. Wiley (1954)

69. Hessler, L.E., and Power, R.E., T.R.J. 24, 822 (1954)

70. Hermans, P.H., Contributions to the Physics of Cellulose Fibres. Elsevier (1946)

71. Valentine, L., J.Pol.Sci. 27, 313 (1958)

72. Manjunath, B.R., and Peacock, N., J.Appl.Pol.Sci. 16, 1305 (1972)

73. Manjunath, B.R., and Peacock, N. T.R.J. 40, 70 (1969)

74. Knight, J.A., et al., ibid 39, 324 (1969)

75. Jeffries, R., Polymer 4, 375 (1963)

76. Jeffries, R., J.Appl.Pol.Sci. 8, 1213 (1964)

77. Nelson, M.L., and O'Connor R.J., J.Appl.Pol.Sci. 8, 1311 (1964)

78. Marchessault, R.H., and Liang, C.Y., J.Pol.Sci. 27, 385 (1959)

79. Marchessault, R.H., and Liang, C.Y., ibid 39, 269 (1959)

80. Marchessault, R.H., and Liang, C.Y., ibid 45, 71 (1960)

81. Hermans, P.H., Physics and Chemistry of Cellulose Fibres. Elsevier (1949)

82. Burkit, S.C., and Bedger, R.M., J.A.C.S. 72, 4379 (1950)

83. Ramsey, D.A., Proc.Roy.Soc. A190, 562 (1947)

84. Barker, S.A. et al., J.Chem.Soc. page 171 (1954)

85. Jones, D.W., J.Pol.Sci. 32, 371 (1958)

86. Wahba, M., Arkiv For Kemi 29(5), 395 (1968)

87. Claesson, S., and Wahba, M., Svensk.Papperstidn. 9, 366 (1968)

88. Ramiah, M.V., and Goring, R.A.J., J.Pol.Sci. C11, 27 (1965)

89. Zhbankov, R.G., Infra-red Spectra of Cellulose and its Derivatives. Consultant's Bureau (New York)(1966)

90. Wahba, M., and Nashed , S., J.T.I. 48(T1) (1957)

91. Bajaj, P., and Pande, A., Tex.Mfr. 94, 496 (1968)

92. Rowland, S.P., T.R.J. 39, 748 (1969)

93. Goodlet, V.W., et al., J.Pol.Sci. 9(A1),155 (1971)

94. Malm, C.J., et al., J.A.C.S. 72, 2674 (1950)

95. Gardner, J.S., et al., ibid 64, 1539 (1942)

96. Herzog, R.O., J.Phys.Chem. 30, 457 (1926)

97. Hess, K., and Trogus, C., Z.Physik.Chem. B5(3/4), 161 (1929)

98. Hess, K., and Trogus, C., ibid B9, 160 (1930)

99. Hess, K., and Trogus, C., ibid B15, 157 (1932)

100. Naray-Szabo, S., and Susigh, G., ibid B4, 268 (1928)

101. Baker, W.O., Ind.Eng.Chem. 37, 246 (1945)

102. Happey, F., J.T.I. 41, T381 (1950)

103. Howsmon, J.A., and Sisson, W.A., Cellulose Derivatives (High Polymers Volume 5) page 338. Interscience, (1954)

104. Sprague, J.L., et al., T.R.J. 28(4), 275 (1958)

105. Baker, W.O., et al., J.A.C.S. 64, 776, (1942)

106. Stoll, R.G., T.R.J. 25, 650 (1951)

107. Dulmage, W.J., J.Pol.Sci. 26, 277 (1957)

108. Watanaba, S., et al., ibid C23, 825 (1968)

109. Alishoev, V.E., et al., Zh.Fiz.Khim. 39, 200 (1965)

110. Altenu, A.G. et al., J.Gas Chromatog. 3, 96 (1966)

111. Smidsdrød O., and Guillet, J.E., Macromolecules 2, 272 (1969)

112. Lavoie, A., and Guillet, J.E., ibid 2, 443 (1969)

113. Nakamura, S., et al., Polymer Letters 9, 591 (1971)

114. Mandelkern, L., and Flory, P.J., J.A.C.S. 73, 3206 (1951)

115. Nakamura, S., Kobunski Kagaku 13, 47 (1956)

116. Russel, J., and Van Kerpel, R.G., J.Pol.Sci. 25, 77 (1957)

117. Sharples, A., and Swinton, F.L., ibid 50, 53, (1961)

118. Klarman, A.F., et al., ibid A2, 1513 (1969)

119. Hindeleh, A.M., Ph.D. Thesis Leeds University (1970)

120. Walrafen, G.G., J.Chem.Phys. 36, 1035 (1962)

121. Walrafen, G.G., ibid 40, 3249 (1964)

122. Walrafen, G.G., ibid 43, 479 (1965)

123. Walrafen, G.G., ibid 44, 1546 (1966)

124. Walrafen, G.G., ibid 46, 1870 (1967)

125. Walrafen, G.G., ibid 47, 114 (1967)

126. Morgan, J., and Warren, B.E., ibid 6, 666 (1938)

127. Van Pantheon, C.L., et al., Disc.Farad.Soc. 24, 200 (1957)

128. Frank, H.S., Science 169, 3496 (1970)

129. Marten, A.H. et al., Disc.Farad.Soc. 43, 97 (1967)

130. Del Bene, J., and Pople, J.A., J.Chem.Phys. 52(9), 4858 (1970)

131. Eisenburg, D., and Kauzman, W., The Structure and Properties of Water. Clarendon Press, (1969)

132. Bertie, J.E., and Whalley, E., J.Chem.Phys. 40, 1646 (1964)

133. Lonsdale, K., Proc.Roy.Soc. A(247) 424 (1958)

134. Owston, P.G., Adv.Phys. 7, 171 (1958)

135. Sugisaki, M., — Physics of Ice, Edited by Riehl., et al., Plenum Press (1969)

136. Honjo, G., and Shimaka, K., — Acta.Cryst. 10, 710 (1957)

137. Blackman, M., and Liesgarten, N.D., — Proc.Roy.Soc. A(239), 93 (1957)

138. Dowell, L.G., and Rinfret, A.P. — Nature 188, 1144 (1960)

139. Beaumont, R.H., et al., — J.Chem.Phys. 34, 1456 (1961)

140. Giguère, R.A., and Harvey, K.B., — Can.J.Chem. 34, 798 (1956)

141. Hornig, D., and White, H.F., — Spectrochim.Acta 12, 338 (1958)

142. Hornig, D., Haas, C., et al., — J.Chem.Phys. 32, 1763 (1960)

143. Hardin, A., and Harvey, K.B., — Spectrochim.Acta. 20(A) 1130 (1973)

144. Baptiste, J.E., and Whalley, E., — J.Chem.Phys. 40, 1637 (1964)

145. Brunauer, S., — Physical Adsorption of Gases and Vapours. Oxford University Press (1943)

146. Peirce, F.T., — J.T.I. 20, T133 (1929)

147. Hailwood, A.J. and Horrobin, S., — Trans.Farad.Soc. 42B, 84 (1946)

148. Urquhart A.R., and Williams, A.M., — J.T.I. 15, T559 (1924)

149. Ogiwara, Y., — J.Appl.Pol.Sci. 13, 1689 (1969)

150. Ogiwara Y., et al., — ibid 14, 303 (1970)

151. Kimura, M., et al., — J.Appl.Pol.Sci. 16, 1749 (1972)

152. Child, T.F., — Polymer 13, 259 (1972)

153. Feughelman, M., and Haly, A.R., — T.R.J. 32, 966 (1962)

154. Ant-Wuorinen, O., and Visapää, A., — Papper Och. Tra.3, 81 (1963)

155. - — British Cellophane Ltd. Bath Road, Bridgewater, Somerset, G.B.

156. - — Bexford Ltd, Manningtree, Essex, G.B.

157. Truter, E.V., — Unpublished Work, Dept. of Textile Industries, Leeds University.

158. Vandenbelt, J.M., and Henrich, C., — Appl. Spect. 7, 171 (1953)

159. Glasse, A.T., and French, C.S., — ibid 9, 78 (1955)

160. Pemsler, J.P., Rev.Sci.Inst. 28, 274 (1957)

161. Pimmentel C., and McClellan, A.L., The Hydrogen Bond
W.H. Freeman & Co. (1960)

162. Whitaker, A., Private Communication

163. Brook, D.B., Unpublished Results. Dept. of
Textile Industries, Leeds Universit

164. Choppin, G.R., and Downey, J.R. Spectrochim.Acta 30, 43 (1974)

165. Kaye, W., ibid 6, 257 (1954)

166. Seanor, D., and Amberg, C.H., Rev.Sci.Inst. 34(ii), 917 (1963)

167. Vratny, F., and Graves, B., ibid 31, 65 (1960)

168. Sutherland, G.B.B.M., and Tsuboi, M., Proc.Roy.Soc. A239, 446 (1957)

169. Green, D.M., et al., Rev.Sci.Inst. 39, 197 (1968)

170. Neu, T., J.Opt.Soc.Amer. 43, 520 (1953)

171. Hurtubise, F.G., and Krassig, H., Anal.Chem. 32(2), 177 (1960)

172. Gatheral, G., Unpublished Results. Dept. of
Textile Industries, Leeds University

173. Hallos, R.S., Unpublished Results

174. Dreyfus, P., and Keller, A., J.Macromol Sci.(Phys.)B4(4),811
(1970)

175. Koenig, J.L., and Itoga, M., ibid B6(2), 327 (1972)

176. Koenig, J.L., and Agboatwala, M.C., ibid B2(3), 391 (1968)

177. Dismore, P.F., and Statton, W.O., J.Pol.Sci. C13, 133 (1966)

178. Keller, A., Physics Today page 45, (1970)

179. Dreyfus, P. and Keller, A., Polymer Letters 8, 253 (1970)

180. Keller, A., et al., Kolloid. Z. 231 (1969)

181. Manley, R.S.J., Nature 204, 1155 (1964)

182. Manley, R.S.J., Polymer Letters 3, 691 (1965)

183. Manley, R.S.J., J.Pol.Sci. 9(A2), 1025 (1971)

184. Visapää, A., Paper Timber 47(5), 311 (1965)

185. Ahmed, A.U., et al., J.Pol.Sci. 9(A1), 2299 (1971)

186. French, C.M., J.Appl.Pol.Sci. 16, 1579 (1972)

187. Cochran, W., et al., Acta.Crysta. 5, 581 (1952)

188. Corey, R.B., and Donohue, J., J.A.C.S. 72, 2899 (1950)

189. Pauling, L., and Corey, R.B., Proc.U.S.Nat.Acad.Sci. 37, 251 (1951)

190. Pauling, L., and Corey, R.B., ibid 37, 729 (1951)

191. Pauling, L., and Corey, R.B., ibid 37, 205 (1951)

192. Pauling, L., and Corey, R.B., ibid 37, 241 (1951)

193. Pauling, L., and Corey, R.B., ibid 37, 261 (1951)

194. Pauling, L., and Corey, R.B., ibid 37, 282 (1951)

195. Walton, C.J., Ph.D. Thesis, Leeds University (1972)

196. Arthur, J.C. Jr., T.R.J. 36, 630 (1966)

197. Barkakaty, B.C., Ph.D. Thesis, Leeds University (1973)

198. Keighley, J.H., Ph.D. Thesis, Leeds University (1966)

199. McKinnley, M.I., Ph.D. Thesis, Leeds University (1972)

200. Wexler, A., J.Res.Nat.Bur.Stand. 53(1), paper 2512 (1954)

201. Elliot, A., Infra-red Spectra of Organic Long-Chain Polymers. Arnold. E., (1969)

202. Wendlant, W.W., and Hecht, H.C., Reflectance Spectroscopy Interscience, (1966)

203. Sarko, A., et al., 161st Am.Chem.Soc.Nat.Meet. Paper 41 Division of Cellulose Wood and Fibre Chemistry (1971)

204. Fernando, L.D., Ph.D. Thesis, Leeds University (1974)

205. Kiessig, H., Koll.Zeit. 152, 62 (1957)

206. Chang, M., J.Pol.Sci. 36(C), 343 (1971)

207. Ellefsen, O., and Tonnenson, B.A., Norsk.Skogind 7, 226 (1960)

208. Manley, R.St.J., Pulp Paper Rept. 37, 18 (1970)

209. Rees, D.A. and Skerret, R.J., J.Chem.Soc. B, 189 (1970)

210. Sponsler, O.L., and Dore, W.H. — Colloid Symp. Monog. 4, 174 (1936)

211. Ellis, K.C., and Warwicker, J.O. — J. Pol. Sci. 56, 339 (1962)

212. Honjo, G., and Watanabe, M. — Nature 181, 326 (1958)

213. Fisher, D.G., and Mann, J., — J. Pol.Sci. 42, 189 (1960)

214. Lord, R.C. et al. — J.A.C.S. 77, 1365 (1955)

215. Haldpern, E. et al. — ibid 77, 4472 (1955)

216. Huggins, C.M. et al. — J.Chem.Phys. 23, 1244 (1955)

217. Kearns, E.R. — J. Phys.Chem. 65, 314 (1961)

218. Arthur, J.C.Jr. and Blouin, F.A. — T.R.J. 34, 733 (1964)

219. Pinchas, S. — Anal.Chem. 29, 334 (1957)

220. Pinchas, S. et al. — ibid 27, 2 (1955)

221. Standford, S.L. and Gordy, W., — J.A.C.S. 63, 1094 (1941)

222. Kreevoy, M.M. et al., — ibid 83, 1978 (1961)

223. Morrison, R.T. and Boyd, R.N., — Organic Chemistry Allyn and Bacon (1966)

224. Leickman, J.P. et al., — Proc. 4th Int. Meet. Mol.Spec. 2, 858 (1959)

225. Jeffries, R. — J.T.I. 49, 192 (1958)

ACKNOWLEDGEMENTS

I would like to thank the following for all the help and encouragement they have given me during the course of this work :-

Professors C.S. Whewell and P. Grosberg,

Dr. J.H. Keighley (Supervisor),

Mrs. V. Whitehead (Departmental Librarian),

Miss A. Lally,

Mr. D Brook

and especially my wife, Margaret.